Investigation on Distributed Generation Planning Considering Power Quality Issue of Distribution System

Submitted in

fulfillment of the requirements for the degree of

Doctor of Philosophy

by

MANOJ KUMAWAT
ID: 2013REE9030

Under the supervision of

Dr. NITIN GUPTA

DEPARTMENT OF ELECTRICAL ENGINEERING
MALAVIYA NATIONAL INSTITUTE OF TECHNOLOGY JAIPUR, INDIA
March 2018

© Malaviya National Institute of Technology Jaipur - 2018.
All rights reserved.

Certificate

This is to certify that the thesis entitled "**Investigation on Distributed Generation Planning Considering Power Quality Issue of Distribution System"** being submitted by **Manoj Kumawat** (2013REE9030) is a bonafide research work carried out under my supervision and guidance in fulfillment of the requirement for the award of the degree of **Doctor of Philosophy** in the Department of Electrical Engineering, Malaviya National Institute of Technology, Jaipur, India. The matter embodied in this thesis is original and has not been submitted to any other University or Institute for the award of any other degree.

Place:
Date:

(Dr. Nitin Gupta)
Assistant Professor
Department of Electrical Engineering
MNIT Jaipur

DECLARATION

I, **Manoj Kumawat,** declare that this thesis titled, "**Investigation on Distributed Generation Planning Considering Power Quality Issue of Distribution System"** and the work presented in it, are my own. I confirm that:

- This work was done wholly or mainly while in the candidature for a research degree at this university.
- Where any part of this thesis has previously been submitted for a degree or any other qualification at this university or any other Institution, this has been clearly stated.
- Where I have consulted the published work of others, this is always clearly attributed.
- Where I have quoted form the work of others, the source is always given. With the exception of such quotation, this thesis is entirely my own work.
- I have acknowledged all main sources of help.
- Where the thesis is based on work done by myself, jointly with others, I have made clear exactly what was done by others and what I have contribute myself.

Date:

Manoj Kumawat
(2013REE9030)

ACKNOWLEDGEMENTS

This doctoral thesis would not have been possible without the help and support of the wonderful people during my whole doctoral study. I sincerely acknowledge and thank, from the bottom of my heart to the number of individuals who have supported me in every phase of my Ph.D. work.

First and foremost, I would like to express my deepest gratitude and thanks to my research supervisor, ***Dr. Nitin Gupta,*** *Assistant Professor, Department of Electrical Engineering, Malaviya National Institute of Technology Jaipur for his valuable guidance, suggestions, scholarly inputs and consistent encouragement. This work is possible only because of the unconditional moral support provided by him. It was a great opportunity to do Ph.D. under his supervision and to learn a lot from him. I thank him again for all his help and support.*

I heartily extend my gratitude to ***Dr. Vikas Gupta****, Associate Professor & Head of the Department for his humanistic, encouraging and warm personal approach and for the necessary facilities provided to me to carry out my research work.*

I would like to acknowledge my departmental research committee members ***Prof. R. A. Gupta*** *(Prof., EED)****, Dr. H. P. Tiwari*** *(Asso. Prof. & Convener, DPGC, EED),* ***Dr. Dipti Saxena*** *(Asst. Prof., EED), for the inspiring discussions and fruitful suggestions that enhanced the quality of my research work.*

I would like to extend my special gratitude towards ***Prof. K. R. Niazi, Prof. Manoj Fozdar and Dr. Nikhil Gupta*** *for unconditional moral support and suggestions. Their beliefs and trusts made me strong and boosted my positivity in any phase of my whole Ph.D. work. Their invaluable guidance and thoughtful advices were the vital factors in the successful completion of this research work.*

I would like to eloquently put across my deep gratitude to ***Prof. R .C. Bansal,*** *Professor, University of Pretoria and* ***Dr. Naveen Jain****, Assistant Professor, CTAE Udaipur for their valuable suggestions and unconditional support during my research work. Dr. Jain made me to identify my own strength and drawbacks, and particularly boosted my self-confidence.*

My heartfelt thanks to my Ph.D. senior colleagues and wonderful friends, ***Dr. Shahbaz Siddiqui, Dr. Vinay Kr. Jadoun, Dr. Gulshan, Dr. Neeraj Kanwar, Dr. Nandkishore Gupta, Dr. Kailash, Dr. Narayanan K., Mr. Ajeet Kumar Singh, Mr. Nandkishor Meena, Mr. Saurabh Ratra, Mr. Pankaj Kumar, Mr. Vijaykumar Gali, Mr. Soumyadeep Ray, Mr. Ajay Kumar*** *and other fellow researchers for their cooperation and memorable association. It was an immense pleasure to work alongside with them.*

I thankfully acknowledged the precious financial support provided by Ministry of Human Resource Development ***(MHRD)****, without which it would be difficult to carry out the research work up to this stage.*

Last but not the least, I would like to express my deep gratitude to my family members for all they have undergone to bring me up to this stage. I wish to express gratitude to my parents, ***Mrs. Bhagwati Devi*** *and* ***Mr. Shyam Babu Kumawat*** *and younger brother* ***Dr. Dishant Kumawat*** *for their kind support, the confidence and the love they have shown to me. My special thanks to my wife,* ***Mrs. Shweta Kumawat****, for being a pillar of support, and to my son* ***Dherya Kumawat*** *whose prayer has showered and other family members to their patience, cooperation and understanding during the course of my Ph.D. work.*

At the end of my thesis, it is a pleasant task to express my thanks to all those who contributed directly or indirectly in many ways to the success of this study and made an unforgettable experience for me.

For any glitches or inadequacies that may remain in this work, the responsibility is entirely my own.

(Manoj Kumawat)

ABSTRACT

An evolutionary growth in energy demand with rectifications of the modular power system is a major challenge in the current scenario. The increasing load demand can be supplied by expanding the existing substation. Moreover, regulatory environment and technological innovations under forthcoming economy have resulted in a renewed interest for the Distributed Energy Resources (DERs). The DERs can compensate the demand of the system at local or end-point level. Therefore, it is required to increase the percentage contribution of the DERs into the radial distribution network. However, the non-optimal allocation of the DERs may increase the losses of the distribution network. It may also cause power quality problems. Therefore, an optimization technique is required to optimize the global solution for the accommodation of the DERs in the radial distribution system.

In this work, heuristic-based approaches are applied to the planning of the DERs to reduce the annual energy losses in the systems. The conventional algorithms take more computational time and less robust in nonlinear optimization problem with the integer variables. Therefore, these algorithms are not suitable for multiple DERs planning in the radial distribution network. The heuristic-based approaches can handle both unconstrained and constrained problem for multivariable function with each equality and inequality constraint. Particle swarm optimization (PSO) algorithm has been used to determine the design variables of the DERs to minimize the energy loss. To consider the realistic nature of the distribution system, time-varying characteristics of electrical load demand have been considered to mimic real load scenario in the power distribution system. The proposed approach is generic and straight forward. It can provide optimal solutions to the distribution utilities to select multiple DERs in stages under various constraints. The effectiveness of the proposed approach is validated on 16, 33 and 69-bus radial distribution networks.

Due to advancement in technology, the utility is required to maintain proper quality of supply from the distribution system. The power quality issue with energy demand growth is a complex problem in the distribution network. Moreover, power electronics apparatus are increasing rapidly due to the high efficiency as well as ease of operation and control. However, the optimal DERs penetration at the proper location can mitigate the harmonic distortions with system energy demand. The

artificial intelligence-based heuristic algorithms are required to solve the optimal allocation problem of the DERs in the distorted medium distribution network. However, some algorithm-specific control parameters must be tuned to find the optimal solution for these issues. Further, optimization method becomes complicated because tuning of the parameter is an additional process to achieve the optimal decision parameter. This process increases the computational time of convergence. Hence, a Modified Group experience of Teaching Learning Based Optimization (MG-TLBO) algorithm is proposed to the allocation problem of the DERs with most efficaciously in the distorted and non-distorted radial distribution networks. The proposed algorithm does not require any specific parameter, and it needs only population size and a maximum number of iterations. The proposed method incorporated some modification such as grouping mechanism, modified teaching, learning factor, mutation, and crossover for diversity to remove the drawbacks of basic teaching learning-based optimization. The effectiveness of the proposed approach is validated on standard 33-bus and 69-bus test systems along with 83-bus (Taiwan Power Company) practical radial non-distorted distribution networks. The results with linear as well as nonlinear loads prove that the proposed strategy can be a robust approach to enhance the system performance towards mitigating increasing load demand within the constraints of the distribution network.

Finally, this thesis considered the realistic nature of distribution because the consumer connection is asymmetrical and unequal in the distribution network. Therefore, the DERs planning according to the assumption of the balanced distribution network is not a realistic approach. The realistic nature of the distribution should be considered for the practical planning of the DERs in the radial distribution system. The optimal solution of the DERs planning for the allocation in multi-phased unbalanced distribution system became a highly complex combinatorial optimization problem with consideration of all practical aspects of the three-phase distribution system. Moreover, MG-TLBO is two-stage algorithm which takes more computational time with all practical consideration of the distribution networks.

A sharp Jaya algorithm is proposed to offer a solution to the allocation problem with most efficaciously in the unbalanced distribution networks. The proposed method is a single stage algorithm-specific control parameter less algorithm. This algorithm has the temptation to achieve the destination in minimum time. Therefore, this approach obtains the optimized solution in less computation time with better

consistency. Moreover, it can also be applied to solve both constrained and unconstrained optimization problem.

The unbalanced three-phase distribution system requires a tool and algorithm to manage the all practical condition of the distribution network. Therefore, the proposed algorithm is interfaced with open source software OpenDSS to obtain the optimal allocation of each type of multiple distributed generators in the unbalanced radial distribution system. The OpenDSS simulator has been used to analyze the three-phase radial distribution network by considering all the working condition of the realistic distribution. Further, the co-simulation framework provides a platform to interface between the proposed algorithm and OpenDSS which is used for optimal allocation of the DERs to minimize the losses of the unbalanced distribution network. The suggested methodologies have been effectively studied on IEEE 13-bus, IEEE 37-bus actual California feeder and IEEE 123-bus three-phase distribution systems and provide the detailed discussion for the realistic planning of the DERs with all practical conditions of the distribution system.

CONTENTS

LIST OF TABLES

LIST OF TABLES (continued...)

LIST OF TABLES (continued...)

LIST OF TABLES (continued...)

LIST OF FIGURES

LIST OF FIGURES (continued...)

LIST OF FIGURES (continued...)

LIST OF FIGURES (continued...)

LIST OF FIGURES (continued...)

LIST OF SYMBOLS

The symbols used in the text have been defined at appropriate places, however for easy reference; the list of principle symbols is given below.

Symbol	Explanation
A_t, B_t	Generalized Matrix Constant for Source Side
$A_{\alpha\beta}^{h}$	Coefficient Vector of the Branch between α and β Buses in Presence of H^{th} Harmonic Order
$As_{\alpha\beta}^{h}$	Coefficient Vector of Harmonics Absorbed by Shunt Capacitor
$Ah_{\alpha\beta}^{h}$	Coefficient Vector of Harmonics Contribute to Presence of Linear and Non Linear Load
A_V^{dd}	Turn Ratio Voltage Matrix in Delta-Delta Type Transformer
A_I^{dd}	Turn Ratio Current Matrix in Delta-Delta Type Transformer
a_t	Transformer Ratio
a	Decision Coefficient of Penalty
B	Branch Current (A)
$B_{\alpha\beta}^{h}$	The Branch Current Vector between α and β Buses
b_t, c_t, d_t	Generalized Matrix Constant for Load Side
C^{best}, C^{worst}	Best Candidate of Child and Worst Candidate of Child, respectively
C_{ryb}	Capacitance Matrix
$Child_m.S_r$	Search Region of M^{th} Child
$Child.S_{itr,\mathrm{d_s},\mathrm{p_s}}^{\mathrm{m'}}$	New Computed Value of M^{th} Child Candidate in Iteration I_{tr}
$Child.S_{itr,\mathrm{d_s},\mathrm{p_s}}^{\mathrm{m}}$	Previous Computed Value of M^{th} Child Candidate in Iteration I_{tr}
c	Number of Child
c_1, c_2	Acceleration Coefficients
D, Dim	Dimensions

LIST OF SYMBOLS (continued...)

Symbol	Explanation
$D_{\Re\aleph}$	Distance between $\Re$ and $\aleph$ Conductor
$D_{\aleph\aleph}^{img}$	Distance of $\aleph$ Conductor and Image of $\Re$ Conductor
D_I^{dd}	Turn Ration Inverse Current Matrix in Delta-Delta Type Transformer
D_V	Relationship Matrix between Line to Neutral and Line to Line Voltage
$Difference, Diff$	Difference Value between Teacher's Score and Mean Value
d_m	Current Number of Dimension D_{im}
E_{loss}	Annual Energy Loss
$E_{loss,b\tau}$	Energy Losses with DERs for Each Load Level
$E_{loss,a\tau}$	Energy Losses without DERs for Each Load Level
E_b^τ , E_a^τ	Energy Losses of the System with and without DER
F	Function of Energy Loss
$F_{\mathrm{Re}sult_i}$	Fitness Value of I^{th} Population
$F_{\mathrm{Re}sult_t}$	Fitness Value of Teacher
G	$0.1609344e^{-3}$ (Ω/Mile)
G_{best}	Global Best
G_{dd}	Generalized Matrix
$GrpMean_{ik}$	Mean Value of Group of I^{th} Population and K^{th} Design Variable
$GMR_\aleph$	Geometric Mean Radius of $\aleph$ Conductor
H_1, H_2, H_3, H_0	High Voltage Transformer Winding Terminal
HA	The Relationship Matrix Between V^h and I^h

LIST OF SYMBOLS (continued...)

Symbol	Explanation
HA_s	The Relationship Matrix Between V_s^h and I^h
HA_{sh}	Harmonics Load Current
HA_h	Harmonics Capacity Current
HLF	Harmonics Load Flow Matrix
h	Harmonic Order
$h_{\min}$	Minimum Order of Harmonics
$h_{\max}$	Maximum Order of Harmonics
I_{ryb}^{line}	Line Segment Current
$I^{\max}$	Maximum Current Capacity of a Conductor
I_{LL}^{ryb}	The Load Side Line to Line Current
I_{ryb}	Line Current at Load Side
i	Current Population
itr	Current Iteration Number
$J_Y^{'}$	New Computed Value of Candidate
J_Y	Previous Computed Value of Candidate
J_Y^{best}	Best Candidate
J_Y^{worst}	Worst Candidate
$K^{\max}$	Total Number of Iteration Permitted
K_{χ}	Total Number of DER
k	Current Design Variable
L_{best}	Local Best

LIST OF SYMBOLS (continued...)

Symbol	Explanation
L_F	Learning Factor
L_L	Lower Limit of Subject
$\mathrm{L}_1, \mathrm{L}_2, \mathrm{L}_3, \mathrm{L}_0$	Low Voltage Transformer Winding Terminal
$L_{\aleph\aleph}$	Self Inductance
$L_{\aleph\Re}$	Mutual Inductance of $\aleph$ Conductor to $\Re$ Conductor
loc	Location of the Candidate
loc_{α}^{DERs}	Site of Each Ders at α^{th} Iteration
loc_{α}^{SCs}	Site of Each Scs at α^{th} Iteration
$Mean$	Mean Value of All Learner's Score
$Mean.S_{z_k}^{Grp}$	Mean Value of DER Size for Group
$Mean.S_{t_k}^{Grp}$	Mean Value of DER Site for Group
m	Number of Shunt Capacitor
N_p	Total Size of Population
N_d	Number of Design Variables
n	Number of Harmonic Source
n_{lv}	Total Number of Load Level
n_n	Count of Nodes Index
n_b	Total Number of Branch
η_t	Transformer Winding Turn Ratio
n_g	Maximum Number of DER
P	Resistivity of Earth (Ω-Meter)

LIST OF SYMBOLS (continued...)

Symbol	Explanation
P_D	Active Power Load Demand of the System (Kw)
P_{best}	Personal Best
PF_D	Power Factor of System Load Demand
PF_{DER}	Power Factor of Distributed Energy Resources
P_{DER}	Active Power from Distributed Energy Sources (Kw)
P_{mic}^{DG}	Micro Distributed Energy Resources
P_{s}^{DG}	Small Distributed Energy Resources
P_{loss}	Total Real Power Loss
P_{med}^{DG}	Medium Distributed Energy Resources
P_{l}^{DG}	Large Distributed Energy Resources
$P_{loss^b}^{\tau}$	Power Losses with DERs for Each Load Level
$P_{loss^a}^{\tau}$	Power Losses without DERs for Each Load Level
P_{Grid}	Total Active Power Supplied by Grid Substation
$P^{\min}$	Lower Bound for Injected Active Power by DER
$P^{\max}$	Upper Bound for Injected Active Power by DER
P_{loss}^{h}	Real Power Loss for H^{th} Harmonics
P_{Grid}^{τ}	Total Active Supplied by Grid Substation of Each Load Level
$P_{\aleph\aleph}$	Self Resistivity of Distribution Line
$P_{\aleph\Re}$	Mutual Resistivity of Distribution Line
$P_{primitive}$	Matrix Representation of Primitive Coefficient
P_{loss}^{b} , P_{loss}^{a}	Power Losses Reduction in Percentage Before and After the Allocation of the DERs

LIST OF SYMBOLS (continued...)

Symbol	Explanation
p_h	Maximum Number of Phases
$Parent.S_r$	Search Region of Parent
$Pop_{new_{ik}}$	New Population Data of I^{th} Population and Kth Design Variable
$Pop_{old_{ik}}$	Old Population Data of I^{th} Population and Kth Design Variable
Pop_r , Pop_{r1} Pop_{r2} , Pop_{r3}	Randomly Selected Population
$Pop_r.result$	Fitness Value of Randomly Selected Population
$Pop_i.result$	Fitness Value of I^{th} Population
Pop_{new_g}	The New Generated Data of Group Population
Pop_g	The Previous Data of Group Population
Pop_g^{best}	The Best Data of Group Population
Pop_{mut}	The Population Data of Mutation Phase
$Pop._{S_z}$	Population Data of DER Size
$Pop._{S_t}$	Population Data of DER Site
P_{CP}, P_{CI}, P_{CC}	Active Power of Line for Constant Power, Constant Current and Constant Impedance, respectively
p_s	Population Size
$S_{DER}^{\max}$	Upper Limit of DER Size (MVA)
$S_{DER}^{\min}$	Lower Limit of DER Size (MVA)
T	Total Hours in a Day
T_F	Teaching Factor
$Teacher$	The Best Learner

LIST OF SYMBOLS (continued...)

Symbol	Explanation
$Teacher.S_z$	The Best Size for DER
Q_D	Reactive Power Load Demand of the System (Kvar)
Q_{SCs}	Reactive Power from Shunt Capacitors (Kvar)
$Q^{\min}$	Lower Bound for Injected Reactive Power by Shunt Capacitor
$Q^{\max}$	Upper Bound for Injected Reactive Power by Shunt Capacitor
Q_a	Reactive Power Supplied by the Capacitor at α^{th} Node
Q_{Grid}	Total Reactive Power Supplied by Grid Substation
Q_{Grid}^{τ}	Total Reactive Supplied by Grid Substation of Each Load Level
Q_{CP}, Q_{CI}, Q_{CC}	Reactive Power of Line for Constant Power, Constant Current and Constant Impedance, respectively
R	Reactance of the Linear Load (Ω)
R_{R}	Reduction Rate
R^h	Resistance for the H^{th} Order of Harmonics
$R_{\alpha\beta}^h$	Resistance of Line Between α^{th} and β^{th} Node
R_{ryb}	Branch Resistance Matrix
R_{CP}, R_{CI}, R_{CC}	Resistance of Line for Constant Power, Constant Current and Constant Impedance, respectively
r_1, r_2	Random Numbers
S	Complex Power (MVA)
S_{Grid}	Total Power Supplied by Grid Substation (MVA)
S_{DER}	Total Power Generated from DER (MVA)
$S_{\alpha\beta}$	Power Flow Capacity of the Branch between Bus α and β

LIST OF SYMBOLS (continued...)

Symbol	Explanation
S_d	Unit Size of the DER
$S^{\max}$	Maximum Permissible Limit of the Distribution Line
$S_{\alpha\beta}$	Power Flow Capacity of Branch between Node α and β
$S_r^{cp}, S_y^{cp}, S_b^{cp}$	The Total Power Flow for Constant Power Load at Phase R, Y and B, respectively
S_{ryb}^{grid}	Total Power Supplied by Grid Substation (MVA)
S_{ryb}^{DERs}	Total Power Injection by DERs (MVA)
S_{ryb}^{load}	Total System Demand (MVA)
S_{line}	Total Power Flow in the Line (MVA)
S_t	Total Number of DER Site
S_z	Total Number of DER Size
$S_{line}^{\max}$	Maximum Permissible Limit of the Distribution Line (MVA)
$Teacher.S_t$	Best Site for DER
THD_v	Total Voltage Harmonic Distortion
THD_v^{bus}	Total Voltage Harmonic Distortion at Each Bus
$THD_v^{\max}$	Maximum Permissible Value for *THD*
t	Present Hour in a Day
t_τ	Time Duration of Each Load Level
U	Identity Matrix
U_L	Upper Limit of Subject
u	Current Position of the Particles

LIST OF SYMBOLS (continued...)

Symbol	Explanation
V	Node Voltage of the Linear Load (Volt)
V_m	Magnitude of Node Voltage (P.U.)
$V_{\min}$, $V_{\max}$	Minimum and Maximum Permissible Limit of Node Voltage
V^h	Bus Voltage Vector for the H^{th} Harmonic Order
V_s^h	Bus Node Voltage Vector with Shunt Capacitor for the H^{th}
V_{rms}	Root Mean Square of Bus Voltage
V_{node}	Node Voltage
$V_i^{(1)}$	Fundamental Magnitude Component of Bus Voltage
$V_{\max}^h$	Maximum Permissible Voltage of Single Harmonic Frequency
V_r , V_y , V_b	Voltage Magnitude for Phase R, Y and B, respectively
V_{RN} , V_{YN} , V_{BN}	Line to Neutral Voltage in Source Side for Phase R, Y and B, respectively
V_{rn} , V_{yn} , V_{bn}	Line to Neutral Voltage in Load Side for Phase R, Phase Y and Phase B, respectively
V_{RY} , V_{YB} , V_{BR}	Phase Voltage between Two Phases at Source End
V_{ry} , V_{yb} , V_{br}	Phase Voltage between Two Phases at Load End
V_{tmr}^{ryb}	Lode Side Voltage Index Across the Transformer Winding
V_{LL}^{RYB}	Line to Line Voltage Index of Phase R, Y, B at High Voltage Side
V_{LL}^h , V_{LL}^l	Source Side Line-Line Voltage and Load Side Line-Line Voltage
V_{LL}^{RY} , V_{LL}^{YB} , V_{LL}^{BR}	Line to Line Voltage at Source End in Delta-Delta Type Transformer
V_{tmr}^{ry} , V_{tmr}^{yb} , V_{tmr}^{br}	Line to Line Voltage Across the Load End Windings in Delta-Delta Type Transformer

LIST OF SYMBOLS (continued...)

Symbol	Explanation
V_{LL}^{ryb}	Line to Line Voltage at Phase R, Y, B in Low Voltage Side
V_{LN}^{ryb}	The Load Side Line to Neutral Voltage
V_{LG}^{ryb}	The Load Side of Line to Ground Voltage
V_{LN}^{RYB}	The Source Side of Line to Neutral Voltage
V_{CP}, V_{CI}, V_{CC}	Voltage of Line for Constant Power, Constant Current and Constant Impedance, respectively
$V_{ryb}^{\min}, V_{ryb}^{\max}$	Minimum/Maximum Load Side Voltage
$\nabla V_{\alpha\beta}^{h}$	The Voltage Drop Vector between α and β Buses
v_{u}	Particle's Velocity
$v_{\max}$	Particle's Maximum Velocity
W_{dd}	Constant Matrix
X	Resistance of the Linear Load (Ω)
X_{u}	Position of Particles
$X_{\alpha\beta}^{h}$	Reactance of Line between α^{th} and β^{th} Node
$X_{capacitor,\alpha}^{h}$	Reactance of the Capacitor at h^{th} Harmonic
x	Function Variable
$Y_{capacitor,\alpha}^{h}$	Admittance of the Capacitor at h^{th} Harmonic
Z	Impedance of Branch for Linear Load (Ω)
$Z_{\alpha\beta}^{h}$	Line Impedance Data Between α and β Buses
Z_{s}	Shunt Capacitor Load Impedance
Z_{s}^{h}	Shunt Capacitor Load Impedance of H^{th} Order

LIST OF SYMBOLS (continued...)

Symbol	Explanation
Z_{α}^{h}	h^{th} Harmonic Equivalent Impedance of the Linear Load at α^{th} Node
$Z_{\alpha\beta}$	Branch Impedance between α and β Node of System
Z_r , Z_y , Z_b	Constant Impedance of the Loads for Phase R, Y and B, respectively
Z_{tmr}^{ryb}	Transformer Winding Impedance Matrix at Load Side
Z_{tmr}^{ry}	Transformer Winding Impedance for Phase R and Y
Z_{tmr}^{yb}	Transformer Winding Impedance for Phase Y and B
Z_{tmr}^{br}	Transformer Winding Impedance for Phase B and R
Z_{t}^{ryb}	Transformer Impedance at Load Side
$Z_{\aleph\aleph}$	Self Impedance of Distribution Line
$Z_{\aleph\Re}$	Mutual Impedance of Distribution Line
Z_{ryb}	Phase Impedance Matrix
α	Present Node Number
β	Present Branch Number
τ	Present Value of Load Level
ρ	Bus Voltage Deviation Penalty Factor
ξ	Susceptance of Capacitor
λ	Total Circulating Flux Across the Conductor
Γ	Conductor Resistance
κ , ϑ	Constant Value
γ	Radius of Conductor (Feet)
θ	Angle Between Image of $\Re$ Conductor Line to Own Image Line of $\aleph$ Conductor

LIST OF SYMBOLS (continued...)

Symbol	Explanation
χ	Inertia Factor (Weight)
ω	System Angular Frequency (Radian Per Second)
$\aleph$, $\Re$	Conductor Lines
ζ_r, ζ_y, ζ_b	Voltage Angle for Phase R, Y and B, respectively
Ψ_r, Ψ_y, Ψ_b	Power Factor Angle for Phase R, Y and B, respectively

LIST OF ABBREVIATIONS

The abbreviations used in the text have been defined at appropriate places, however, for easy reference; the list of abbreviations is given below.

Abbreviation	Explanation
AA	Analytical Algorithm
ABC	Artificial Bee Colony
AC	Alternating Current
AC	Ant Colony
ACO	Ant Colony Optimization
AFC	Alkaline Fuel Cell
AI	Artificial Intelligence
ASD	Adjustable Speed Drive
BFO	Bacterial Foraging Optimization
BFS	Backward/Forward Sweep
BFS	Brute Force Crossover
BSO	Backtracking Search Optimization
CC	Constant Current
CCPSOA	Constriction Coefficient Particle Swarm Optimization Approach
CI	Constant Impedance
COM	Component Object Model
CP	Cone Programming
CP	Constant Power
CS	Cuckoo Search
CT	Combustion Turbine
Chr	Characteristics
DC	Direct Current

LIST OF ABBREVIATIONS (continued...)

Abbreviation	Explanation
DE	Differential Evolution
DERs	Distributed Energy Resources
DGs	Distributed Generations
Dim	Dimensions
DP	Dynamic Programming
Delta-Z	Delta Connected Constant Impedance
Delta-PQ	Delta Connected Constant Power
Delta-I	Delta Connected Constant Current
DSS	Distribution System Simulator
EP	Evolutionary Programming
ES	Exhaustive Search
FM	Firefly Method
GA	Genetic Algorithm
GA-OPF	Genetic Optimal Power Flow
GA-PSO	Genetic Particle Swarm Optimization
GA-TS	Genetic Algorithm-Tapu Search
GMR	Geometric Mean Radius
GP	Goal Programming
GSS	Grid Sub Station
HLF	Harmonic Load Flow
HM	Harmony Memory
HMCR	Harmony Memory Considering Rate
HS	Harmonic Search
IAM	Improved Analytical Method

LIST OF ABBREVIATIONS (continued...)

Abbreviation	Explanation
IEC	International Electro-Technical Commission
IEEE	Institute of Electrical and Electronics Engineers
IMOHS	Improved Multi-Objective Harmony Search
ITLBO	Improved Teaching Learning Based Optimization
KH	Krill Herd
L	Light
LF	Learning Factor
LP	Linear Programming
LSF	Load Scaling Factor
LSFA	Loss Sensitive Factor Approach
MATLAB	Matrix Laboratory
MaxIt	Maximum Iteration
MCFC	Molten Carbonate Fuel Cell
MG-TLBO	Modified Group-experience of Teaching Learning Based Optimization
MILP	Mixed Integer Linear Programming
MINP	Mixed Integer Non-Linear Programming
MN	Multi-Model and Non-Separable
MOPSO	Multi Objective Particle Swarm Optimization
MS	Multi-Model and Separable
MT	Micro Turbine
N	Nominal
NLP	Non-Linear Programming
OPF	Optimum Power Flow

LIST OF ABBREVIATIONS (continued...)

Abbreviation	Explanation
P	Peak
PAFC	Phosphoric Acid Fuel Cell
PAFC	Phosphoric Acid Fuel Cell
PAR	Pitch Adjusting Rate
PC	Personal Computer
PEMFC	Proton Exchange Membrane Fuel Cell
PF	Power Factor
PFDE	Pareto Frontier Differential Evolution
PI	Partial Influence
PM	Proposed Method
POP	Population
PSO	Particle Swarm Optimization
PSO-OPF	Particle Swarm Optimization Optimal Power Flow
pu	Per Unit
QCP	Quadratic Constrained Programming
RDS	Radial Distribution System
Re	Real Number
SC	Shunt Capacitor
SCR	Short Circuit Ratio
SD	Standard Deviation
SI	Swarm Influence
SOFC	Solid Oxide Fuel Cell
SQP	Sequential Quadratic Programming
TF	Teaching Factor

LIST OF ABBREVIATIONS (continued...)

Abbreviation	Explanation
THD	Total Harmonic Distortion
THDv	Total Harmonic Distortion of Voltage
TLBO	Teaching Learning Based Optimization
TS	Tabu Search
US	Unimodel and Separable
UN	Unimodel and Non-Separable
UPF	Unity Power Factor
WECS	Wind Energy Conversion System
Wye-Z	Star Connected Constant Impedance
Wye-PQ	Star Connected Constant Power
Wye-I	Star Connected Constant Current

Chapter – 1

INTRODUCTION

1.1 General

Electrical energy has become an integral part of human life and its use is increasing globally by leaps and bounds to improve the living standards. The ever increasing energy demand and scarcity of electric power have attracted the attention of power engineers/researchers to evolve the methods/techniques for effective utilization of electrical energy. It is estimated that the generation of power may increase by 93% during the period 2010-2040 [1]. The increasing load growth can be supplied by expanding the existing substation. However, most of the already established transmission and distribution systems are about to accomplish their lifespan. These will be substituted either by new construction of the conventional structure or innovative design incorporating the distributed energy resources facilities as an alternate solution to defer not only distribution system expansion but also transmission system expansions [2].

The conventional power system is producing various types of problems such as voltage deviations, high capital cost, static-, dynamic-, and transient-stability problems, overloaded lines, service interruptions, high amount of resistive losses and emissions in the environment [3]. Therefore, the electrical power system has many reforms in last few years. Further, conventional distribution system structures are moving towards the smart distribution system structure to achieve higher economic benefits, better asset utilization, socio and other non-tangible benefits such as peak load shaving, reliability, lesser carbon footprints, improved energy security, efficiency and power quality. Further, several countries like USA, Chile, etc., have already been getting benefits of the restructuring of their power system.

Most of the International and National policies restricted pollutants from a conventional power plant with mitigation of magnifying energy demand and power quality issues that imply the requirement for the more efficient power system. Further, the regulatory commission is focused on environmental issues with an object to reduce the pollutants content in the atmosphere by decreasing the percentage of fossil fuel from the power plant and increase the percentage of renewable sources in the

distribution system [4]. In addition to these issue, technological innovations under upcoming economy introduced the renewed interest in the distributed resources to supply the incremental demand of the distribution network in the deregulated power system.

The construction of next-generation active distribution network requires new technologies of the generation with the exploitation of existing infrastructure and changes in operational practices. The integration of the DERs is pivotal in realizing the smart distribution system. Further, distribution system can accomplish technical, environment and economic benefit [5]. The passive distribution system will progressively convert into the active distribution system with extensive deployment of the distributed energy resources. However, this transformation requires a paradigm shift in the planning of the distribution system. Moreover, an efficient distribution system should be adopted with proper degree of accuracy; otherwise, counterproductive results so obtained may threaten in the planning of the distribution network [6].

In electricity market paradigm, several types of the popular distributed energy resources technologies have been utilized and some are still immature and under developing level [7]. These technologies are small hydropower generation, solar photovoltaic, natural gas engines, reciprocating diesel, micro-turbines, wind turbines, fuel cells, and biomass. This type of power generation when located to load end is called Distributed Generation (DG). Moreover, resources used to provide the energy, are named Distributed Energy Resources [8]. These technologies have their limitations and advantages as enumerated and detailed in the next chapter. However, besides the several restrictions, the DERs contribute in the diversification of energy resources to support for uncertainty in the electricity market, enhance the energy security to have competitive policies, down the operating cost of peak load, increases the potential for service quality, and decreases cost and losses of transmission and distribution [9]. Hence, it is required to increase the penetration of the DERs into the distribution system.

However, the non-optimal allocation of the DERs can increase the losses of the distribution system which could also lead to power quality problems [10]. Therefore, various analytical algorithms, artificial intelligence search algorithms, and meta-heuristic optimization techniques are applied by various researchers to optimize the

global solution for allocation of DERs in the radial distribution system. Moreover, the optimal DERs allocation with proper strategy can attenuate above-cited issues.

1.2 Motivation for the Presented Work

Restructuring of the power system has created several opportunities to produce small-scale power in the distribution system. Though, it also introduces many challenges. The proper integration of the DERs in the distribution system can reduce the power losses. Moreover, the power loss minimization has been one of the principal concerns of the DERs [11]. Although, the DERs planners pointed out the various important issues and proposed different methods for allocation of the DERs. However, energy losses based placement considering time-varying load profile has hardly been addressed as the DERs size and locations were obtained at peak load condition of the distribution system. In a practical scenario, the peak demand will stay for a small period of a whole day load profile. However, such planning of the DERs may lead higher energy loss. Therefore, it causes an important need for DERs planning considering energy loss criterion for variable loading conditions. The energy loss is an important criterion, especially, when the load has significant variation over the whole day. The peak load demand supply is a typical case of the distribution system and advanced infrastructure of digital technology to admonish and manage to transmit electricity from all generators to satisfy the departing load demands in smart grid connected distribution system. It is desirable that all planning for the DERs must address time-varying characteristic of the load for the whole day. Therefore, the load profile of the distribution system demand should be modeled to a good degree of accuracy; otherwise, it may be proved to be counterproductive.

Considering above challenge, the problem of coordinated allocation of the DERs has been addressed to improve the performance of the distribution system. These approaches are solved by various conventional, nature and non-nature inspired heuristic and hybrid techniques [12]. However, the conventional algorithm is a single point conversion method [13]. Therefore, it has not been considered for multiple DERs' planning. The artificial intelligence-based heuristic algorithms have been mostly used for distributed generation planning with any type of constraints [14]. The particle swarm optimization algorithm is very popular algorithm for DERs planning in the radial distribution system. The particle swarm optimization takes less processing

time and less probability to fail to convergence in a practical application [15]. Further, the particle swarm optimization has greater diversity and exploration in a single as well multi-dimensional population. Furthermore, momentum effect on particles can help to achieve the faster convergence. However, tuning is required for algorithm specified parameter to achieve the optimal value of DERs design variable. Therefore, there is stringent need to overcome these limitations to extract their full potential and make them suitable to solve complex DERs' allocation problem accurately and efficiently.

Modern distribution network is required to drive good quality of power supply. However, it is a complicated task to maintain according to the present scenario. Nowadays, non-linear load and power switching apparatus are increasing rapidly due to high efficiency as well as ease of operation and control [16]. Although these power electronics devices/controllers operate on sinusoidal voltage, they inject harmonics and increase reactive power demand in the power system network [17]. Also, the characteristics of these devices are highly nonlinear. Further, application of power electronics devices are dominating, which introduces the harmonic distortion in the electrical distribution system [18]. Different sources of harmonics include AC/DC converters, adjustable speed drives, switching power supplies, AC phase control circuit, cyclo-converters, magnetizing current of the transformer, arc furnaces, welding machines, etc. A major portion of harmonics is generated by nonlinear loads and termed as customer-generated harmonics [19].

It is a well-known fact that harmonic distortion originates some problem in a system like decreasing the life of insulation, more heating loss, reducing power factor and affecting the power plant efficiency [20]. In addition, switchgear protection of the electrical system can also be stuck by the presence of harmonics as protection device is designed for the normal operating condition. In concern with above problems of poor power quality, an effective compensation solution with the defined harmonic limit is required to improve the power quality. Many electrical regulatory commissions and standards as IEEE 519-1992 [21] recommend voltage distortion limits for consumers and utilities at various voltage levels. These guidelines are supportive in promoting better practices in planning and erection of both power system and nonlinear equipment. Further, harmonic distortion becomes a complex problem with its resonance, which is introduced by various components of the power electronics [22]. Therefore, planning is necessary to maintain the system harmonics in

the specified limit; otherwise, there will be the poor quality of power with more energy loss. It is not a desirable situation under competitive energy market scenario.

There is an asset of literature dealing with optimal allocation of the DERs by considering a variety of techno-economic objectives. Furthermore, Shunt Capacitor (SCs) and DGs can separately act and dominate the power flow in the distribution system. However, the optimal accommodation of these modules is not individualistic. Moreover, the existence of one may influence the optimal allocation of the other and vice-versa. Simultaneous allocation strategy of DERs is to be investigated with the different constraints of the distribution system. More realistic formulation for these nonlinear optimization problems is developed keeping in view of realities of the distribution system [23]-[24]. These key technologies can achieve the better solutions by using a heuristic algorithm in harmonics distorted system. The artificial intelligence-based heuristic methods have become a popular choice in searching the global or near to the global solution. However, some algorithm-specific control parameters are required to be tuned for the optimal solution. Therefore, this process becomes complicated and increases the computational time of convergence. However, Teaching–Learning-Based Optimization is parameter-less optimization algorithm, which requires the only number of maximum iteration and population size.

Another issue studied in the thesis is realistic planning of the DERs allocation in the radial three-phase distribution system. Most of the research works have been performed on balanced distribution networks. However, an overhead line of the distribution system is un-transposed unlike the transmission system. The phases of the distribution are unequally distributed. Moreover, loads of the distribution system are also unequally distributed in the whole power system. Therefore, the DERs planning according to a balanced distribution network is not a realistic approach. Further, three types of loads (constant current, constant impedance and constant power), capacitor banks, voltage regulators, overhead and underground distribution lines are present in the actual distribution system. Therefore, all practical conditions should be considered for the realistic planning of the DERs in the radial distribution network.

Such correlate approach should be appropriately customized by suitable addressing of the realities of the distribution system otherwise the optimal solution so obtained may introduce the threat in the planning of the electrical distribution system. The optimal allocation of the DERs problem is highly complex combinatorial nonlinear. Further, the complexity of the problem is increased when more realistic operational

issues of the distribution system have been taken into consideration to obtain the more practical solution. Therefore, the existing parameter fewer heuristic techniques have been required to bring further improvement in already established approaches to solve such complex optimization problems efficiently. In fact, the recent evolution of the active distribution system is inflicting the challenges in the modeling and solution techniques for suitable DERs planning of the modern distribution system.

1.3 Contributions of the Presented Work

The objective of this research work is to attempt all issues and to develop the strategy for allocation of the DERs in the radial distribution system. The main contributions of this thesis are as follows:

1. On the basis of the critical survey of the literature, the proposed approach has depicted the comparison of time characteristic and peak load based planning of the DERs. Further, the proposed allocation strategy of multiple distributed energy resources is very effective to minimize annual energy loss in time-varying real load scenario and to maintain better node voltage profiles of the radial distribution system.
2. The initial part of this thesis work contributes the modified parameter-less algorithm. Therefore, the Modified Group-experience Teaching Learning Based Optimization viz. MG-TLBO approach has been developed successfully to solve complex combinatorial optimization problems. The MG-TLBO method incorporated some modifications as a grouping mechanism, modified teaching, learning factor, mutation, and crossover for diversity to furnish the drawbacks of basic TLBO. It is simple, generic and parameter-less.
3. The energy demand and power quality illness with different constraints of the distribution system are addressed by simultaneous allocation strategy of the DERs in multi-level load pattern of the medium distribution network. Moreover, the proposed method is well tested by respective simulated cases including the realistic system with linear as well as non-linear loads for its reliability and robustness.
4. The realistic constraints-based approach is addressed which appropriately customized the realities of the three-phase radial distribution system. Further, co-

simulation framework is used to obtain the optimal allocation of multiple DERs in the unbalanced radial distribution system.

5. Finally, the Sharp Jaya algorithm is also proposed to solve a highly complex combinatorial optimization problem with consideration of all practical aspects of the three-phase unbalanced distribution system. This algorithm is interfaced with OpenDSS through the component object model. This co-simulation framework obtained the optimum penetration of the multiple distributed generators at the particular places of the unbalanced distribution system.

1.4 Organization of the Thesis

The chapter organization is an essential part of the thesis, which gives an overview of the thesis. The current chapter introduces the issue of the distributed energy resources planning in the radial distribution system. The research gap outline help to understand the motivation for research in the current scenario. Further, this chapter summarizes the contribution of the present thesis. The last section organized the rest of the thesis chapters as follow:

Chapter 2 provides the comprehensive literature review on different technology and approaches of the DERs planning in the radial distribution system with presence of linear as well as non-linear load demand. Further, the applicability of each numerical and mathematical modeling based optimization algorithms regarding the allocation of the DERs are described in point of merit and demerit.

Chapter 3 presents a heuristic approach for the planning of the distributed energy resources to minimize the annual energy loss of the distribution system. The particle swarm optimization based algorithm is applied to optimize the allocation problem considering time-varying characteristics of electrical load demand. The effectiveness of the proposed approach is validated on 16-, 33-, and 69-bus radial distribution networks. The results are compared with already existing methods as suggested in the literature.

Chapter 4 proposes a Modified Group experience of Teaching Learning Based Optimization approach, which can deal the allocation of DERs with most efficaciously in three load level of the radial distribution networks. The proposed method is illustrated through three standards 33-bus and 69-bus test systems along with 83-bus (Taiwan Power Company) practical radial distribution systems. The

application results of the proposed method are compared with the results of two approaches viz. PSO and ITLBO approach.

Chapter 5 covers analysis and mitigation of the power quality issue with energy demand. That issue is simultaneously considered towards the realistic planning of the medium voltage radial distribution system. The proposed parameter less algorithm are applied to deal the allocation of the DERs with most efficaciously in harmonics distorted radial distribution networks. The results are compared with results of the PSO method considering modified 33-bus and 69-bus test systems along with 83-bus (Taiwan Power Company) practical radial distribution systems.

Chapter 6 proposes the Sharp-Jaya algorithm which interfaces with open source software OpenDSS. This platform solves the unbalanced optimal power flow. Further, co-simulation framework is applied to obtain the optimal allocation of multiple distributed energy resources in three phase radial distribution system. The effectiveness of the approach is validated on IEEE-13, IEEE-37 (California system) and IEEE-123 node distribution system. The results are compared with the results of already established methods as suggested in the literature.

Chapter 7 summarizes the conclusion, major contribution of the thesis work. Further, the future scopes in this area are also discussed.

Chapter – 2

LITERATURE REVIEW

2.1 Introduction

The utilities are facing many problems with the conventional power system. Moreover, the electrical demand of the system has exponentially increased since last decade. The traditional framework is not able to address the need of the end user with environmental, technical and economic concern. However, some countries have adopted the liberalization in transmission and distribution system. Therefore, a small power generation could compensate the demand [25]. Further, the modified structure of the power is shown in Figure 2.1.

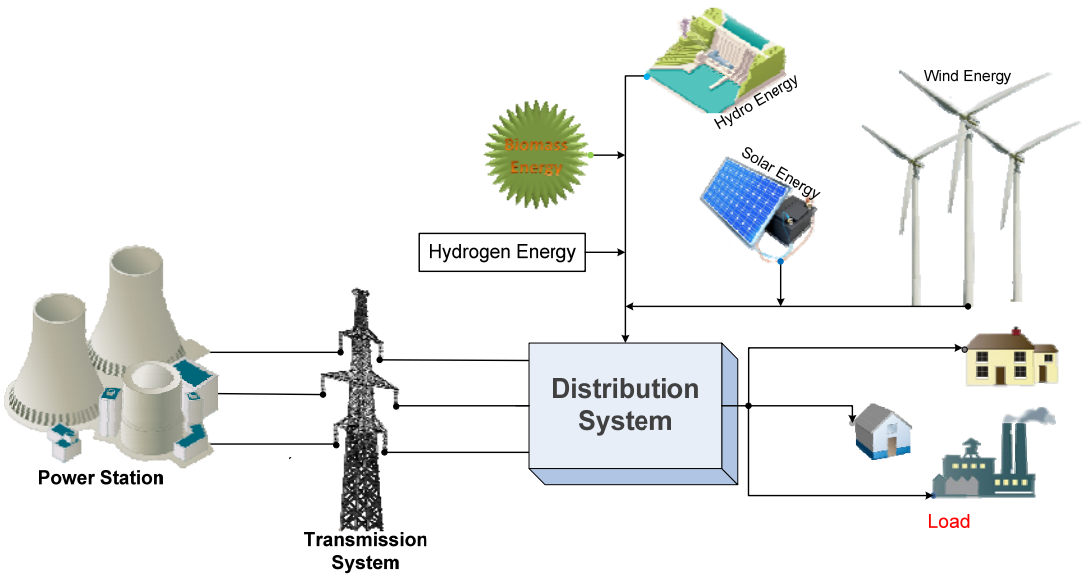

Figure 2.1: Current restructured power system

Several technologies have contributed in the diversification of energy resources to reduce the cost and losses of transmission and distribution, decrease the operating cost of peak load, supports for uncertainty in the electricity market and competitive policies, enhances the energy security, and increases the potential for service quality [26]. Although, the utilities are facing strained operating conditions to meet the expectation in the current competitive liberalization scenario. The smarter distribution system is required to drive the excellent quality of power to the end user. However, it is a complicated task to maintain in the present load scenario. Therefore, the utilities

have to maximize the annual profits of the distribution systems by enhancing the energy efficiencies with the quality of power to customers. A lot of algorithms have been used to maximize the benefit of the distribution system by addressing the proper allocation of DERs. However, each algorithm has a unique application and process to optimize the particular type objective. Therefore, each algorithm finds out the global solution in specific boundaries [27].

This chapter describes a theoretical background and review of the approaches and methods to the allocation of DERs in the radial distribution system. Initially, the classification of various distributed generation technologies is demonstrated which is based on fuel injection. Different methods have been used in the literature for the allocation of DERs which has classified according to the nature of the algorithms. A brief literature survey about these research areas is presented to identify the concerns and issues of current research directions for the smart distribution network. The research gaps about the current research directions are identified. Further, the research objectives of the thesis work have framed on the basis of critical reviews.

2.2 Distributed Energy Resources

The distribution systems of the traditional framework are transformed into active distribution system after the interconnection of the DERs. In last decade, DG was not capable of delivering the reactive power. Therefore, shunt capacitors are placed to supply the reactive power in the system. Further, the innovations have been implemented in that duration to develop the innovative technology in power ststem. Therefore, nowadays the DGs can deliver the active as well as reactive power. However, application of power electronics device is increased with simultaneous innovation in technology. Further, harmonics are being generated in the presence of non-linear load (linear load with power electronics devices) which distorted the power supply. Therefore, DGs (unity power factor) and Shunt Capacitor (SCs) are simultaneously placed in the harmonics distorted radial distribution system [28]. Although DGs and SCs are not independently regulated the active and reactive power flow in the system. Further, one existence could affect to another in the distribution system. Therefore, the allocation of the DERs should be strategical to reduce the feeder energy losses and harmonics distortion with enhancement of node voltage

profile of the network. A brief literature review of the several DERs technologies is presented in the following sections.

2.2.1 Distributed Generation

Distributed Generation referred by several terms as an embedded generation, decentralized generation, and dispersed generation which is defined as the generation of power by small size generators connected near the load or end users in the medium voltage or low voltage distribution network [29]-[30]. The definition of DG is changed according to uses, and region wise. The dispersed generation has been used in the North America. Further, Europe and Asia has used the decentralized generation. Moreover, embedded generation is used in Anglo-America [31]-[32].

In electricity market paradigm, different types of the popular DG technologies have been used, and some are still immature and in developing stage [34]. These techniques are reciprocating engines, gas turbine, electrochemical device, photovoltaic, wind energy conversion system, biomass, small hydropower generation, geothermal, and solar thermal which are exhibited in Figure 2.2. These resources are used to provide the energy and named as distributed energy resources. The energy resources classification according to rating is indicated in Table 2.1.

Table 2.1: Classification of distributed generation according to the rating [33]

S. No.	Classification	Rating
1	Micro distributed energy resources	1 kW $< P_{mic}^{DG} \leq$ 5kW
2	Small distributed energy resources	5 kW $< P_{s}^{DG} \leq$ 5MW
3	Medium distributed energy resources	5 MW $< P_{med}^{DG} \leq$ 50MW
4	Large distributed energy resources	50 MW $< P_{l}^{DG} \leq$ 300 MW

***2.2.1.1. Reciprocating Engines*:** The petrol and diesel engine are being used for a long period as a backup power for residential, commercial and small industrial customers. Reciprocating engines are working on the principle of internal combustion engines. Although, reciprocating engines are fit according to distributed generation definition. Energy station of reciprocating engines is available from 1 to 250 kW [35]. These engines operate with good efficiency and low costs. However, it is operated at large scale due to the significant emission and high maintenance cost.

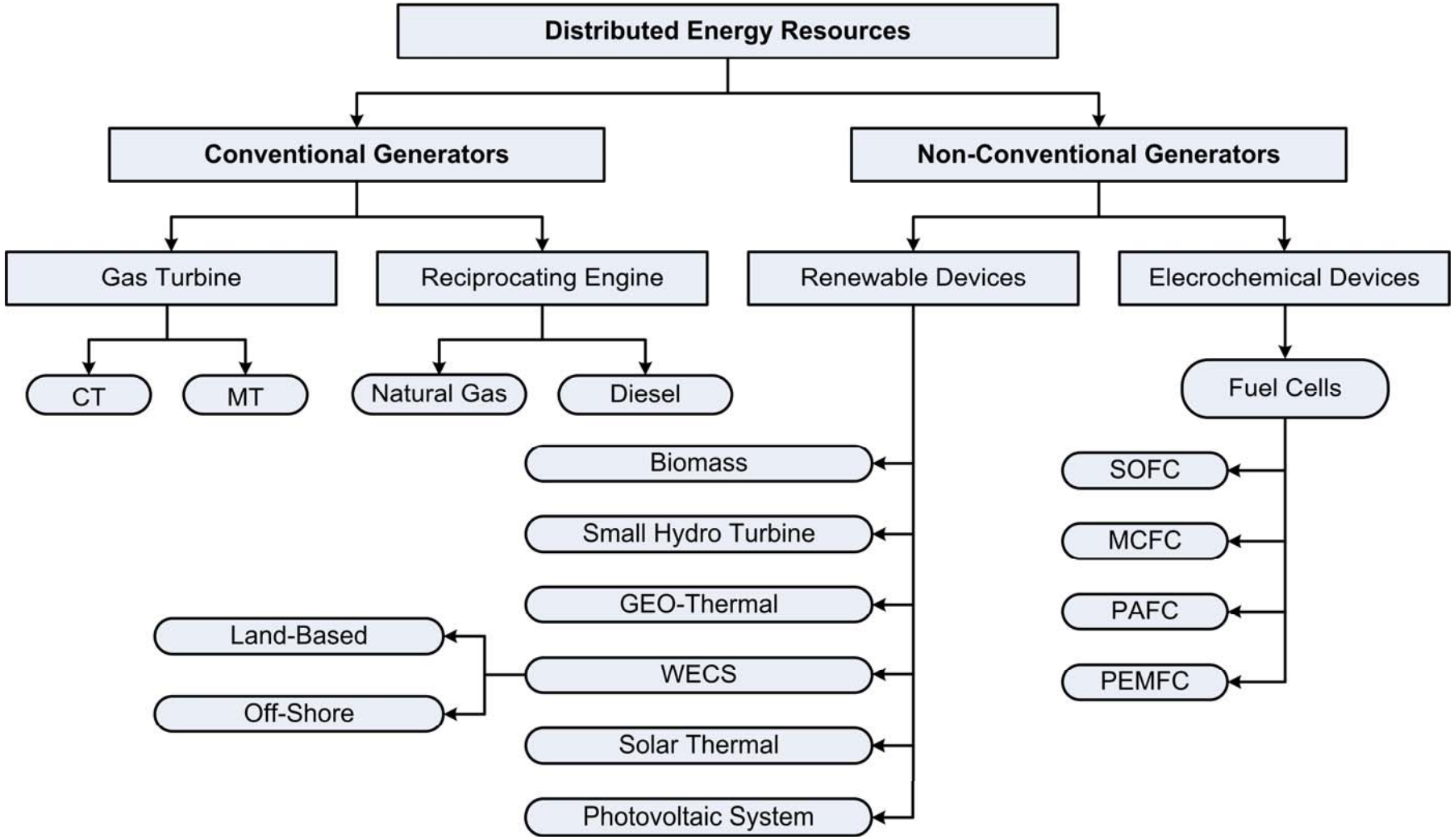

Figure 2.2: Classification of the distributed energy resources [33]

These engines are operating on natural gas with recent advancement of the technology. Moreover, this technique can be used with other energy resources to enhance the reliability and efficiency of the system.

2.2.1.2. Gas Turbine: In the gas turbine, the flow of combustion gas rotates the power shaft. This technology is divided into two parts according to the structure of turbine.

***(i) Micro-Turbine (MT)*:** It is a famous technology for distributed energy resources because it takes very less time to start. Due to starting phenomena, it is also used in the hybrid electric vehicle. In the conventional gas turbine, this technology can produce from 500 kW to 300MW [36]. However, turbine range 30 to 400 kW is used as a distributed energy resources. Innovation in power electronics technology has been enhanced the application of micro-turbine and reduce the moving part. In addition, the efficiency of micro-turbine is approximate 33%, especially with 85% effective recuperator [37]. These turbines exhaust the extremely low emissions. Therefore, micro-turbines are used for reciprocating engines.

***(ii) Combustion Turbine (CT)*:** These were mostly used in the large industrial plant with the rating of 200 kW-250 MW size of per unit [38]. However, this type of technology was used in the last decade. In current perspective, CT is not considered in the distribution system.

2.2.1.3. Electrochemical Device: The fuel cell is an electrochemical device which converts the energy from chemical to heat and electrical energy. These devices generate the direct current by reaction of the oxygen and hydrogen. In this device, two electrodes are made of different material and according to material fuel cell is characterized in five parts as alkaline fuel cell (AFC), proton exchange membrane fuel cell (PEMFC), phosphoric acid fuel cell (PAFC), solid oxide fuel cell (SOFC), and molten carbonate fuel cell (MCFC). The power conditioning device is used to handle the required amount of smooth power supply to the distribution system.

The fuel cells are generating the electrical power with a high efficiency, non-existence of moving part and low emissions. This technology operates in ranges of 50 kW to 3 MW. The effectiveness of the fuel cell is increased by higher conversion energy which is 40% or greater [39]. Further, the utilization efficiency of the cell is approximately 85 %.

***2.2.1.4. Photovoltaic*:** In this technology, solar energy is directly converted into electrical energy via solar panel. The cell of the solar panel is made of two type of material which is poly-silicon and mono-crystalline silicon. The parallel and series connection of the cell is arranged according to the rating of current and voltage. However, the efficiency of the system is relatively low as compared to other that is lying between 10 to 24 % [40]. In the present scenario, much research has been going on the cell material. Further, this system used the power converter to supply the power to the grid. However, the uses of inverters produced the harmonics into the distribution system. Therefore, an investigation is required on the multi-level inverter to reduce the percentage of total harmonics distortion.

2.2.1.5. Wind Energy Conversion System: The kinetic energy of the wind is converted to electrical power by use of wind turbine. The wind range of 4-25m/s is acceptable otherwise the connection is cut off from the mill. Further, power generation from park station of the wind turbine has been increased from 20 kW to 4MW in the recent decade [41]. These technologies are suited for the place where availability of wind speed is constant for the long duration. Consequently, offshore type of power generation most prominent where the large rating of the wind turbine in large number is connected to high voltages of the electrical system. One wind turbine is attached to the grid at 10 to 20 kV voltages level of the distribution system. The power quality problems are introduced in the system with directly connected to the grid.

2.2.1.6. Biomass: Biomass is a renewable energy technology among distributed energy resources in the future. The crops, plant, and a waste of animal are used as a fuel in the biomass plant. The waste of forestry and agriculture can be recycled as fuel which is shown in Figure 2.3. The world's energy production is 11% by biomass plant according to the US International Energy Agency. The poor contraries are driving the 90% of total energy production [42]. The characteristic of this technology is helping to compensate the energy demand of the distribution system. This technology can be used in the hybrid vehicle because of fuel clearness as compared to oil.

2.2.1.7. Small Hydropower Generation - The small capacity of the dam is used to produce the power in the range of 5 kW to 100 MW on the concept of hydropower plant are called small hydropower plant. It is also divided into two parts. First is micro hydroelectric which operate in a power range of 5-100 kW. The second station can

produce the power range of 500 kW to 10 MW that is called mini hydro-power stations [43]. This plant has adopted the electromechanical solutions to construct the station and operations. Therefore, it reduces the possible capital cost and maintains with assuring revert entirely investment.

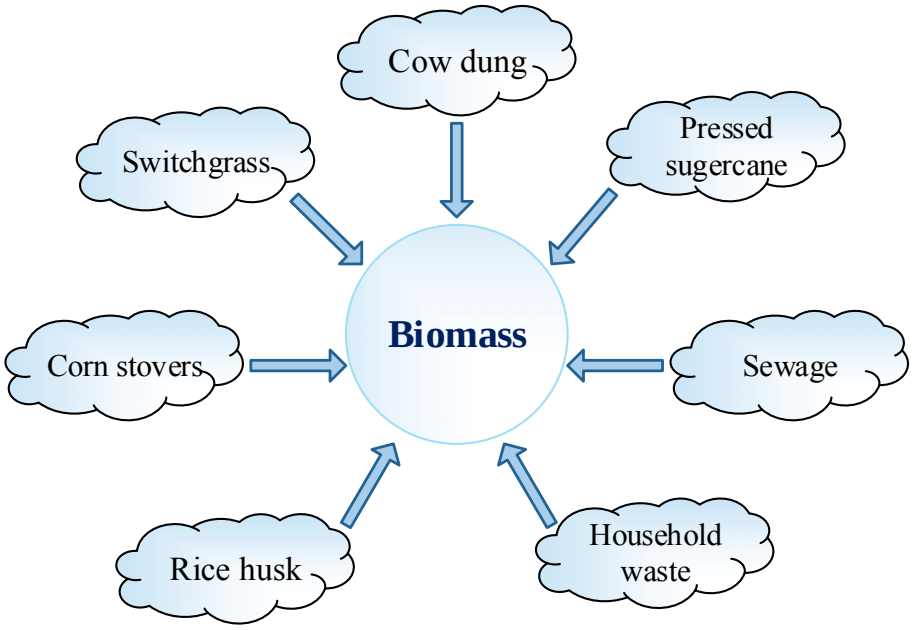

Figure 2.3: Biomass distributed energy resources

2.2.1.8. Geothermal - The heat energy is stored inside the Earth which can be used as a geothermal power. This technology is used in the countries across the world. The geothermal power plant is environment-friendly, and cost of the generating station is less as compared to other station [44]. However, availability of geothermal hot spots is very less in all over the world.

2.2.1.9. Solar Thermal - The solar thermal technology converts the solar energy power into thermal energy. In this technology, high temperature is generated to produce the steam which can drive the electric turbine generators and to the production of hydrogen in the chemical process [45]. According to temperature generation, this technology is classified into three parts which are low-, medium-, or high-temperature collectors. Further, the low- and medium-temperature collectors are used the flat plates to warm the water to the residential and commercial purpose. Moreover, high-temperature collectors have used the mirrors to concentrate sunlight. Therefore last collector technology is mostly used to generate the electrical power.

Further, the applications of the DER technology depend on demerit and merit which is shown in Table 2.2.

Table 2.2: DERs technology and their specialty with drawback [46]

S. No.	DERs Technologies	Operating Range	Specialty	Drawback
1.	Reciprocating engines	1 to 250 kW	• Less starting time • Less capital cost • Effective efficiency	• High emission • High maintenance cost
2.	Gas turbine	27 kW – 250 MW	• Low emission • High efficiency • High reliability	• High capital cost • Low efficiency at lower level
3.	Electrochemical device	1 kW- 5 MW	• Eco-friendly • High efficiency • Wide option regarding the fuel	• High capital cost • Less life • Requirement of fuel Processing
4.	Photovoltaic	1 MW – 80 MW	• Fuel less technology • Environment friendly • Less maintenance cost	• Uncertain nature • High capital cost
5.	Wind energy conversion system	200 W – 3 MW	• Low operating cost • Fuel less technology	• Uncertain nature • Noise pollution • Bird hazard
6.	Biomass	100 kW – 20 MW	• Renewable Source • Reduce GHG emission • Stop desertification	• Air pollution • maintenance is more • Soil erosion
7.	Small hydropower generation	5 kW – 100 MW	• Eco-friendly • Zero operating cost • Renewable Source	• Affected in flood time • High capital cost • Less efficiency
8.	Geothermal	5 MW – 100 MW	• Economical • Fuel-free • Constant price with time	• Water pollution • Gases spread out into atmosphere • Noise pollution
9.	Solar thermal	10 MW - 377 MW	• Fuel Free • Eco-friendly	• High capital cost • Large solar collector

2.2.2 Shunt Capacitors

The SCs are mostly used to supply the required reactive power in the system. It is connected near the load in the distribution system to maximize the effectiveness [47]. The capacitor is supported to enhance the voltage profile and indirectly help to increase the power loss reduction in the system because the unity power factor operated DG is the requirement to increase the penetration level of DGs to fill the gap of demand. Further, the voltage rise problem is introduced in the system. Therefore, simultaneous allocation of DERs is the best approach to maximize the energy loss reduction and limit the total harmonics distortion along with enhanced voltage profile of the distribution system.

2.3 Approaches of DERs Allocation

The allocation of the DERs has various approaches to accommodation in the radial distribution system. In the literature, authors have chosen the various types of DERs in prescribed approach. The approaches of the DERs allocation are bifurcated in four sections which are followed as:

2.3.1 Planning Objective

In the literature [2]-[158], the DERs are accommodated according to various objectives which are exhibited in Figure 2.4. The DERs allocation was carried out for minimizing power loss in the distribution system [13], [48]-[68].

Naresh *et al*. [48] has suggested the precise loss formulation to minimize the power losses by optimal allocation of the DER. Further, Hung *et al*. [13] suggested an analytical method to the optimal allocation of the DER unit which minimizes power loss. Lee and Park [49] used an algorithm to find out the optimal allocation of multiple DERs by considering power loss approach. In [50]-[51], authors proposed a conventional method to minimize the power losses by the optimal location in the rural system. Atwa and Saadany [52] suggested a mixed integer non-linear programming based placement of the DERs under constant peak load profile. Kumar *et al.* [53] used a heuristic algorithm which determined the optimal design variable to reduce the technical losses. Mostafa *et al.* [54], considered the economic as well as environmental aspects which are solved by non-dominated sorting genetic algorithm. Prenc *et al.* [55] also applied the GA method to determined size and site of the DERs

in time varying load profile of the radial distribution system. In [56]-[57], the GA method is applied to place the three different types of DERs to reduce the cumulative average daily active power losses. Prenc *et al.* [58] suggested an index to accommodate the DERs for various load models.

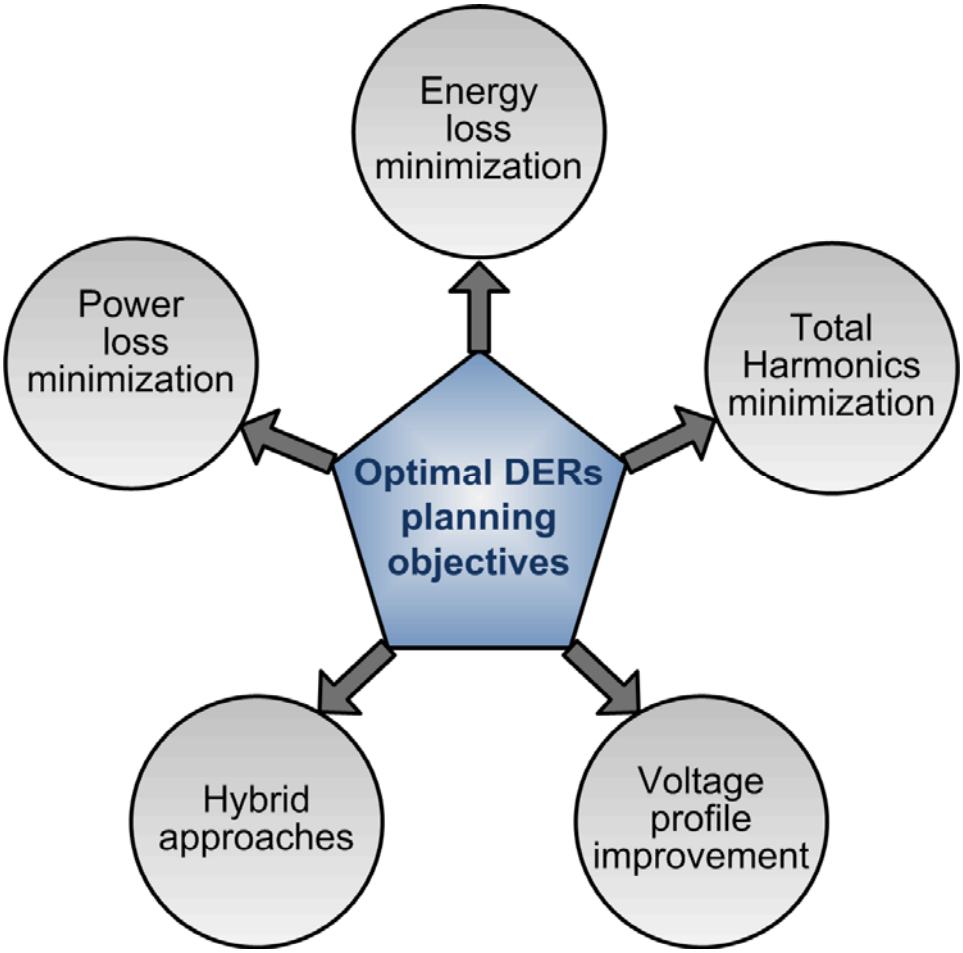

Figure 2.4: Tree diagram of selected DERs planning objectives

Muttaqi *et al.* [59] have suggested the optimal size and allocation of the DER unit with the help of PSO to minimize the power losses in respect of overall investment and operational cost of the power distribution network. Mahdi and Ahmad [60] have proposed an algorithm to minimize the power losses by the allocation of the DERs with perfect penetration. Sajjadi *et al.* [61], optimally accommodated the DERs in the radial distribution network by using a hybrid algorithm to reduce the power loss along with enhancement in the voltage profile. Elazim *et al.* [62] proposed a flower pollination optimization algorithm to solve the DGs allocation problem in the balanced radial distribution networks. Nayeripourn *et al.* [63] used the combination of the shuffled frog-leaping and PSO for the optimal allocation of multiple micro-

turbines to improve the power loss reduction while maintaining the transient stability index and voltage profile. Moradia *et al.* [64] applied a hybrid algorithm to reduce the power losses by optimizing the location and size of the DERs while maintaining the voltage profile. Moradini and Abedini [65] proposed a combined operation of PSO and GA to optimize the allocation of the DER in the radial distribution networks. Rueda-Medina *et al.* [66] applied a mixed-integer linear programming approach to obtain the optimal type, size and site of the DERs in radial distribution systems. Abu-Mouti *et al.* [67] used the heuristic curve-fitted technique to minimize the power loss. A. Saif *et al.* [68] applied a hybrid PSO algorithm to determine the optimal location of the DERs in different voltage-dependent load model scenarios. Most of the studies are planned with the real power loss minimization as an objective to enhance the performance of the distribution system by integration of the DERs.

The planning of the hybrid DERs under uncertainties of load growth has been presented in [69]-[73]. Kim *et al.* [74] proposed the restoration methods for the planning of the renewable DERs considering the energy not supplied and the energy loss from the perspective of the independent system operator. In [75]-[81], proposed method has been used to optimize the energy losses for various allocations of multiple DERs among the candidate buses. In [82]-[84], the energy loss was criteria to place fixed and variable size of capacitors with variable power injection under different load level for the distributed system. Singh and Goswami [85] applied the meta-heuristic approach to place the unity and non-unity DERs in typical Indian distribution systems and obtain the best trade-off benefit of the utility. Therefore, maximization of the energy loss reduction is a most prominent object for the planning of the DERs in the radial distribution system.

In [41], [61], [86]-[95], authors mainly addressed on the improvement of voltage profile or voltage stability. Atwa *et al*. [86] proposed an algorithm for allocation of DERs based on power stability index in the distribution systems. Esmaili [87] maximized the potential benefits by the optimal placement of DERs in the distribution system. In. [88]-[89], authors placed the DERs to improve the voltage stability margin with consideration of three voltage stability index in the presence of load growth of the distribution system. In [90]-[93], optimally integrated the DERs is improved the voltage stability analysis as a security measure. Dahal *et al.* invested the impact on voltage stability with increment of DER penetration in the radial distribution system. Othman *et al.* [95] investigated the margin of steady state voltage by the allocation of

different type of DERs in the distribution system. However, most of the authors considered the power loss reduction along with the voltage profile enhancement.

In [16], [20], [22], [28], [40], [96]-[103], harmonics distortion objective have been used for the allocation of the DERs in the harmonics distorted radial distribution system. Mohammadi *et al.* [18] placed the capacitor and DG to minimize the power quality distortion and fill the gap of energy demand in the distribution system within the presence of a heavy nonlinear load. In [16], [20], [28], authors have used the heuristic optimization techniques to accommodate the DERs with consideration of real power loss, voltage deviation, and harmonics distortion in the radial distribution system. Vichakorn *et al.* [40] proposed an approach for optimal penetration of photovoltaic distributed generator to reduce the power losses along with harmonic distortion.

In the present scenario, inverter based DER have increased which are responsible to raise the harmonics in the system [96]. Therefore, planning of simultaneous DERs is necessary to limit the harmonics in IEEE 519 standard. Imran and Kowsalya [97] used a bacterial foraging optimization algorithm to determine the size and location to minimize the harmonic distortion. In [98]-[99], an optimization algorithm is used to optimize the penetration level of the DERs while limiting the distortions in various load profile. Therefore, most research is planned to accommodate the DERs with a variety of design variable to enhance the efficiency and power quality level in the radial distribution system. The standard of power quality should be satisfied according to IEEE 519-1992 standard because some technical issue is introduced in the presence of harmonics like as life of insulation, more heating loss, reducing power factor and affecting the power plant efficiency [100]-[103]. In addition, switchgear protection of the power system is also affected by the presence of harmonics as protection device is designed for the normal operating condition. However, harmonics distortion for multi-load has not been considered in the literature.

2.3.2 Constraints

The DERs are integrated with the distribution system then necessary operating condition of the network should not exceed from its permissible region. Therefore, planning of the DERs allocation is necessary to create the healthy condition in the distribution system. Further, the most common power system constraints in the radial distribution network are node voltage profile, power balance, the power factor of

DERs and feeder ampacity. Moreover, the utility constraints are the number, size, type, and penetration level of the DERs, and capacity of the entire system. If any constraint crosses the specified boundaries then the solution is not acceptable for the planning consideration.

2.3.3 Design Variables

The several DERs accommodation approaches are used in the literature. However, the approaches are classified according to nature of the distribution system demand, design variable and characteristic of the Radial Distribution System (RDS). The classification of DERs approaches with design variable are shown in Figure 2.5. In the literature, some researchers have planned the allocation problem with consideration of single load profiles [41], [49], [53], [65], [67], [71], [78]-[79], [81], [85]-[87], [93], [114], [123], [129]-[130], [135], [143], [147], [156]. However, the load demand of the distribution system is not a constant. It is varying throughout the day. Although the distribution system planners pointed out the various important issues to the allocation of the DERs, energy loss based placement considering time-varying (practical system loads) load profile introduces the realistic planning as the constant demand will not stay for a whole day load profile. However, the planning of the DERs according to constant demand may lead higher energy loss. Therefore, it causes an important need for DERs planning considering energy loss criterion for variable loading conditions [15], [52], [58], [68], [75], [86], [92], [125]-[126], [128], [136].

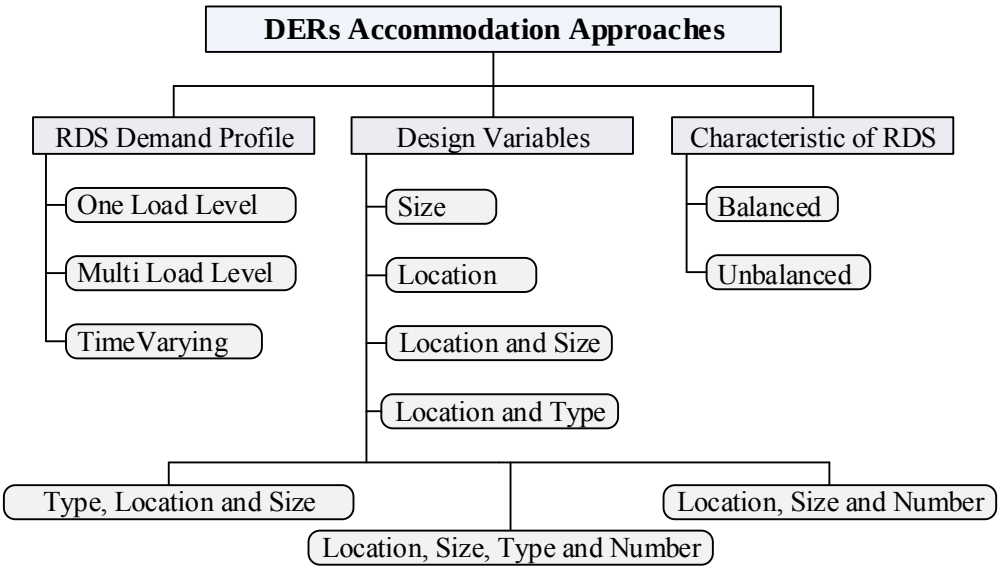

Figure 2.5: Approaches to the DERs allocation

Moreover, most of authors accommodated the DERs according to three level demand of the distribution system [23], [28], [47], [54]-[57], [60], [64], [66], [74], [76], [82]-[83], [89], [90], [102], [117], [124], [127], [146], [153]-[154], [157]. The growth of the electrical distribution system demand is split into three level as light, nominal and peak demand. Therefore, the planning of DERs should be considered to supply electrical power according to the load demand; otherwise, the network losses may increase at another load level.

The number of DERs is also computed in the planning which depends on the availability of the DERs rating. Most of the planner have installed the multiple DERs (two and more than two) [41]-[70], [76]-[90], [93]-[101], [103]-[107], whereas few placed only single DER [39]-[41], [71]-[75], [91]-[92], [102] in distribution network. Further, seven combinations of four design variables (size, location, number, type) are used for DERs planning. Most of the planning have optimized the size and location of DERs [39], [44]-[58], [62]-[63], [69]-[71], [79]-[84], [87]-[89], [94]-[102]. However, some renewable technology has location constraints which are located according to the availability of fuel in the specified geographical region. Therefore, optimal penetration of the DERs is prominent design variable to achieve the economical and technical benefit of the distribution system [60]-[61], [64], [85], [91]. Moreover, few DERs technology has supplied the discrete power generation. Further, these types of generation have filled the gap of required power demand by increasing the number of unit of power generation.

In [13]-[93], optimization methods have been employed to accommodate the DERs in the balance radial distribution system. Further, the optimal DERs allocation has maximized the efficiency of the system. However, line of the distribution system is un-transposed. Moreover, loads of the distribution system is unequally distributed in the whole power system. Therefore, DERs planning according to the balanced distribution network is not a practical approach. However, few articles have incorporated the realistic nature of radial distribution system. In addition, Eajal *et al.* [99] used the PSO method to minimize the annual energy losses by proper integration of the DER in the unbalanced distribution systems. Othman *et al.* [95] applied the supervised firefly algorithm to find the optimal location and capacity of dispatchable DERs in unbalanced distribution feeders for power loss minimization without violating the system constraints. Samir *et al.* [94] also used the PSO algorithm for optimal allocation of the DERs in the unbalanced distribution system.

2.4 DERs Planning Algorithms

The Optimal allocation of the DERs in the radial distribution network is a sophisticated and combinatorial problem. A lot of methods have been applied to solve this complex optimization problem by the researchers. Therefore, the invented theory based algorithms can be applied for the DERs accommodation problem and compare their performance to get a better solution. The categorization of optimization algorithms is illustrated to understand the behavior of algorithms via a graphical presentation in Figure 2.6.

Each algorithm is applied to achieve better solution regarding the DERs accommodation optimization problem. The algorithms are categorized into two major sections. The first section describes traditional search methods which cover both calculus and numerical methods. Further, another category is artificial intelligence based algorithms which can include the sub-categories as nature-inspired, physics based algorithms. The analysis of these all category and their subcategory is described as follows:

2.4.1 Calculus-Based Algorithms

Calculus is the base of modern mathematics formulation. The calculus is a gateway from basics to more advanced techniques in mathematics devoted to the study of functions and limits. It creates an availability of way to build up the quantitative methods and their consequence. The calculus-based algorithms depend on the objective to finding minimum and maximum values of the problem definition and their solution. The calculus-based optimization algorithms are as follows:

2.4.1.1. Conventional Techniques: The conventional optimization methods are the combination of the mathematical approaches, derivation, their assumption techniques, theorems behind any procedure, and differential equality models. These methods formulate the mathematical expression and equations. Some of the convention techniques are as follows:

***(i) Eigen Values (Egn)*:** Egn based optimization applied in symmetric and non-symmetric problems like as semi definite constraint, linear constraints, non-linear constraint [104]. Although the dual theory of Eigen values fails in case of non-linearity.

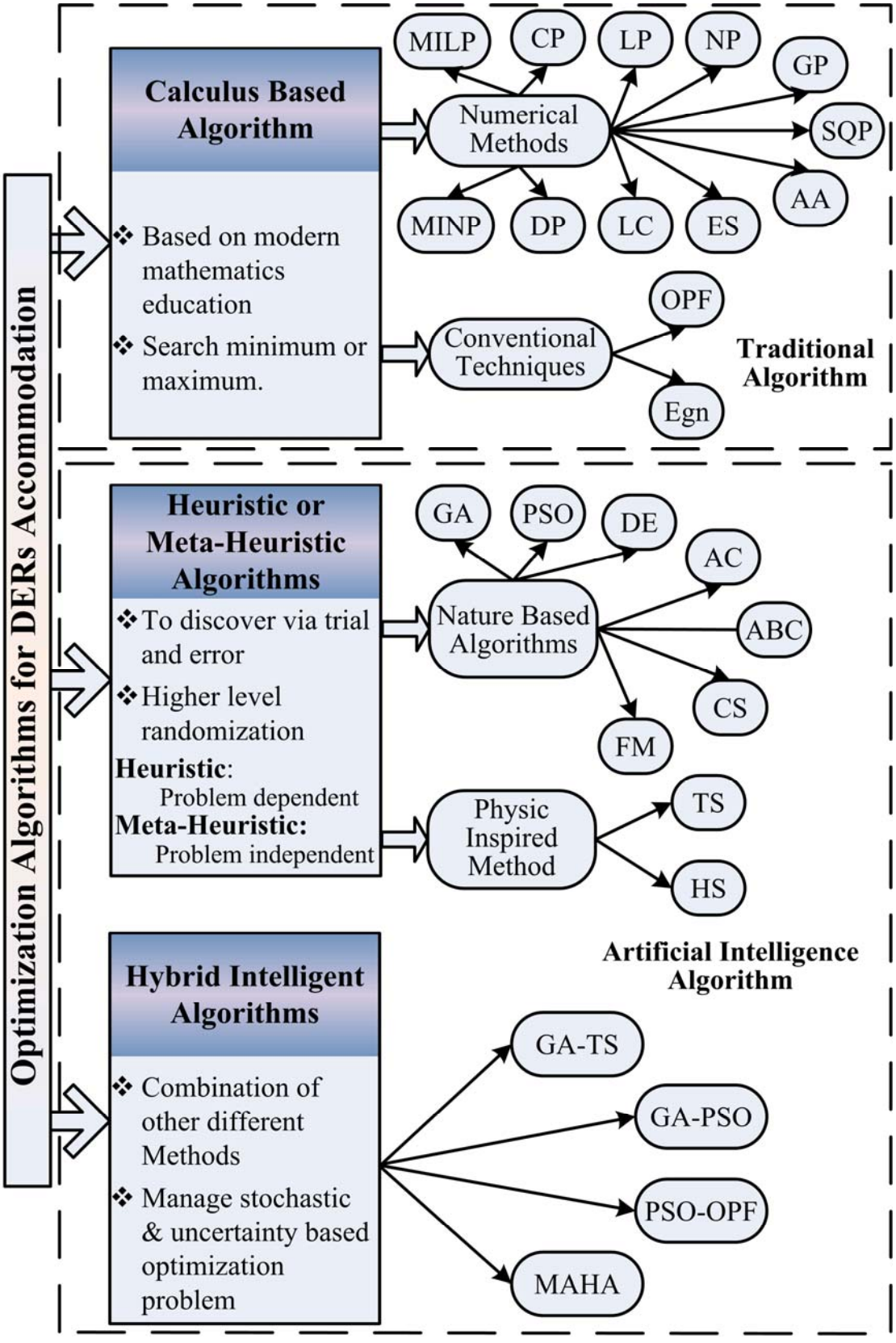

Figure 2.6: Categorization of optimization algorithms

(ii) Optimum Power Flow (OPF): OPF is a conventional method that is used to solve the complex planning problems of distribution system [105]-[106]. The OPF

can avail the highest precision value for optimization within the efficient time. The limitations of the OPF are rigid problem formulation, and few variants can be included in the calculations [107]-[109].

***2.4.1.2. Numerical Methods*:** The numerical methods are mostly based on the mathematical solution of the problem. In this review, some of those algorithms are described under the following subsection:

***(i) Analytical Algorithm (AA)*:** This algorithm provides a solution of algebraic expression after analyzing the functioning of the system. Further, analytical approaches reached near optimum solution with the accuracy which depends on the versatility of the developed prototype [78]. However, it is often observed that proposed modal may disqualify to provide an accurate solution to complex problems. The analytical approach mostly depends upon their substitute prototypes means rules about rules which is also evolved from the experimental results or numerical simulations of the system [82], [110], [111]. The analytical approach is mostly applied for the single DER allocation optimization. The analytical algorithm is refined and reproduced to locate the DER in the distributed network system by appending an extra feature as loss formula [48], [112], [113].

***(ii) Goal Programming (GP)*:** GP can handle normally conflicting objective measures with the multiple objectives. Every measure has the own target value to complete their task with the achievement of objective functions. The major benefits of goal programming are simple to implement aims at a tradeoff solution and ease of use. A large number of goal programming applications are introduced in many and diverse fields [90], [114]. This algorithm is, required very high computation, practically time-consuming method, ability to produce solutions is not efficient.

***(iii) Exhaustive Search (ES)*:** ES is single variable optimization algorithm [45]. This algorithm is simple to encode and apply on objectives. The ES method failed whenever applied to large or complex distribution systems [115]-[116].

***(iv) Cone Programming (CP)*:** CP is a class of nonlinear convex optimization problems which is a natural hiding of semi-definite programming [117]. These conic optimization problems can be coded as the linear programming with their objective and constraints which specifies that variables are formed by decision variables within constrained and closed convex cone. This approach does not converge for the realistic complex problem.

***(v) Sequential Quadratic Programming (SQP)*:** SQP is a group of algorithms which is most effective method for solving the non-linear optimization problem [118]. SQP detects a way away from the present situation by using the minimization and linearization of the constrained. When the problem contains only equality constraints, SQP apply the method with first-order optimality conditions. The convergence graph on the basic SQP algorithm can be improved by using a line search. The SQP approach could not be satisfied the constraints in minimum number of iterations [119]. Therefore, SQP is an iterative method with perfectness to solving non-linear formulation with the constraints of the objective function.

***(vi) Linear Programming (LP)*:** LP is an approach to get best results in mathematical procedure which needs the linear relationships and used to optimize the linear objective functions with linear equality or inequality constraints. The LP method has an important role in real-life problems. The real-life problems may remain hundreds of variables or more, while using LP with algebra it will be work as simple and easy. The procedure of LP determines the coordinates of the intersection point in feasibility region's corners and detect their coordinate's points with finding the highest or lowest value [120].

***(vii) Mixed Integer Linear Programming (MILP)*:** MILP is a used to solve the optimization problems which have the properties of linearization and integral values with linear constraints but does not contain the non-linear properties of constraints [49], [66], [121]. The MILP approach is a conventional algorithm which could optimize the design parameters of any non-linear problem.

***(viii) Non-Linear Programming (NLP)*:** NLP is different from linear programming with only one point which is the main condition of the objective function should be non-linear with non-linear constraints in equalities or inequalities condition. NLP is more difficult to implement than LP [87].

***(ix) Mixed Integer Non-Linear Programming (MINP)*:** MINP is used to solve the optimization problems which have the properties of non-linearization and integral values with non-linear constraints [86], [96], [122]-[123]. However, it does not contain the linear properties of constraints.

***(x) Dynamic Programming (DP)*:** DP is a class of method for solving a complex problem by dividing it down into a collection of simpler sub-problems. Further, the DP solves each of those sub-problems just once and storing their solutions in memory [124]. Further, it saves the computation time with indexing of each sub-problem

solution. The DP approach converts the complex problems into simpler problems by splitting it.

2.4.2 Heuristic/Meta-Heuristic Algorithms

In optimization algorithms, heuristic and meta-heuristic methods are developed to create strategies for the optimal solution. The heuristic approaches are usually problem-dependent whereas meta-heuristic is a problem independent technique that can be applied to real problems. A meta-heuristic can be applied without knowing anything about the problem. Consequently, the meta-heuristic is problem specific implementation of a fundamental heuristic algorithm according to the guidelines structured in such a framework. Following algorithms are considered in this category of optimization:

2.4.2.1. Nature/Biology based Algorithm:

***(i) Differential Evolution (DE)*:** DE is a type of evolutionary programming which is developed by Rainer Storn and Kenneth Price in 1997 for optimization of non-linear problems. The evolutionary-based algorithm has not required differentiating the objective function and constraints. This artificial intelligence algorithm is inspired by the concept of evolution. Therefore, this algorithm is based on populations and fitness value to achieve the global optimal solution. In [93], [125], authors have applied the evolutionary programming approach to optimal allocate the renewable energy resources in the radial distribution network for reducing the active energy loss. The pareto-frontier DE method solved a multi-objective problem in [80].These algorithms use the robustness and efficient way to detect the nearest optimal solution of the overall procedure while in some cases it may produce the worst factors as premature convergence, local optima, low precision.

***(ii) Genetic Algorithm (GA)*:** GA is a type of adaptive heuristic search algorithm and depends on the concept of natural selection and genetics. The basic concept of the GA approach is an analogy with the genetic structure and behavior of chromosomes within a population of individuals. Shaaban *et al.* [126] applied the GA for optimal allocation of the DER to reduce the interruption cost [126]. In [56]-[57], the GA is used to obtain the contract pricing and location of dispatchable DER unit in radial distribution network. In [114], [127], this algorithm has been utilized for the optimal penetration of the DERs to minimize the network loss and cost, and improve the

reliability of the supply to the utility. Simultaneously, DERs and remote controllable switches are placed in the distribution system with the help of this algorithm [83]. The multi-objective formulation has been solved by this approach to determine the most satisfactory non-inferior solution [85], [128] and, loadability and profit to distribution utility [129]-[130].

The optimal allocation of the DERs for the daily average power production and consumption curves has been achieved by the modification in the GA approach [55]. The Non-dominated sorting GA (NSGA) is upgraded version which is applied in the uncertainty of load to obtain the perfect integration of the DERs in the system [54]. Further, modification in NSGA is presented in [131], and this algorithm is to solve the multi-objective optimization problems of the distribution system. This approach does not get trap in the local optima because of initial solution doesn't affect the future solution. However, the computational time is more in complex problems. It can take several hours, may be waiting for days to the solution.

***(iii) Partial Swarm Optimization (PSO)*:** The first research article published in 1995 on the PSO algorithm, since then there has been a lot of research using the PSO in power system itself [132]-[133]. The PSO algorithm is an efficient algorithm to determine the global and local solution. It is capable to explore widely with very few parameters. This method is a derivative-free algorithm that means it is a more stable algorithm. The PSO algorithm follows the concurrency and parallelizing process for searching a global solution. Therefore, this method can be scaled in multi-design variables [134].

The PSO algorithm is applied to determine size and site of the DER units in the distribution system and enhance the voltage profile with loadability [15], [81]. The PSO method has been used to obtain the optimal DERs accommodations that are connected through an inverter or directly (synchronous-based) [102], [135]. Different types of DERs are optimally allocated by using the algorithm to minimize the real power loss by active and reactive power compensation [47], [79]. The multi-objective PSO method determined the optimal penetration level of the DERs for several locations to maximize the benefit of the Distribution Company and utility, simultaneously [136]-[138]. However, the global optimal solution of the PSO algorithm depends on initial local optima. Therefore, it shows the tendency to converse at the local best of the problem which reduces its convergence speed.

***(iv) Ant Colony Optimization (ACO)*:** AC based optimization is one of the most successful examples of algorithms based on the biological concepts. Ant system is introduced by Marco Dorigo in 1992 and Ant Colony was introduced in 1997 by Gambardella Dorigo [139]. This nature-oriented technique is inspired by the behavior of real ant colonies through their collective trail-laying to solve the discrete optimization problems. This artificial intelligent and heuristic based method with soft computing technique has solved the hard discrete optimization problems and a very general class of computational problems through the more efficient procedure. In [140], the ant colony optimization technique reconstructed which is optimizing the DERs site and size to increase the reliability of the system. This optimization is simple to simulate and requires less computation time. Moreover, this approach can be applied in dynamic or run time generation applications [141]. However, the setting of the parameter of this algorithm is difficult to achieve the target value because the probability of the distribution is varying at each iteration.

***(v) Artificial Bee Colony (ABC)*:** ABC algorithm is introduced by Dervis Karaboga in 2005 [142]. It is inspired by the intelligent behavior of survival of honeybees. This algorithm uses the quality and ability of artificial bees of flying surrounding the multidimensional search region. This algorithm was initially proposed for numerical optimization. The artificial bee colony determined the optimal DERs allocation with a perfect number to reduce power loss of the distribution network at non-unity power factor [143]. The ABC is refined and restructured by including many extra features or properties with their procedure to the optimization of distributed network system [144]. Moreover, the new ABC applied to compute the optimal DERs in the system by concentrating the losses and consumption. This algorithm has robustness, flexibility, and ability to explore local solutions into a global solution. Moreover, it has only a few controlled parameters [145]. However, it consumes the maximum number of trials to improve the solution. Therefore, this algorithm takes more evaluation for sequential processing and consequently, the cost for computation is automatically increased with increasing iterations or consumed memory.

***(vi) Cuckoo Search (CS)*:** CS is a swarm intelligence based algorithm which has been proposed by Yang and Deb in 2009. This meta-heuristic algorithm is inspired by the natural behavior and reproduction ways of the cuckoos and influenced by the parasitic egg laying of cuckoo species. The CS method is a simple to implement or

understand and better or effective global optimization algorithm. This method has been applied to solve various types of the real-world optimization problem. In [146], authors introduced the new generation part to avoid being trapped in local extremism and get better performance of the system. In [147]-[148], the CS algorithm is applied to optimize DERs allocation to increase the percentage power loss reduction of the distribution system. This algorithm does not generate the diversity in the population which shows the low accuracy of the process.

***(vii) Firefly Method (FM)*:** FM is a globally accepted meta-heuristic algorithm for optimization, which is inspired by the ideal model of the fireflies flashing behavior. This algorithm was proposed by Xin-She Yang in 2008. In mathematical optimization, the primary purpose of a firefly's flash is to act as a signal to attract other fireflies. In [149], the FM is updated with the extra features appended for the allocation of the DERs to fulfill various conditions as minimize both active and reactive power losses and improve the voltage profile using different load model. FM is capable to efficiently solve the highly non-linear, multi-modal optimization problems [150]. The convergence of solution is very fast in probability to solving the objective problems. FM is a flexible algorithm in comparison to other optimization techniques. However, this algorithm is trapping into several local optima and has large differences in the scale of parameters.

2.4.2.2. Physic Inspired Method:

(i) *Tabu Search (TS)*: TS is created by Glover and McMillan in 1986 [151]. This meta-heuristic optimization technique is invented on the theory of the performance of human memory. Further, this algorithm is applied in planning and management problems. Through TS as planning algorithm, various factors of the objective function are identified such as the setting of network, objective value size, their location, step size of regulators. Nara and Hayashi [69] have applied the technique of coordinate or decompose with the tabu search optimization algorithm for optimal distributed generators allocation on optimal location in the distributed network. This approach depends upon the constraints of minimum power losses and improves the voltage profile of the system. Further, this approach has fast convergence properties that can get local optimal solutions with the easy tuning of the controller parameters in an efficient way of low computation time. However, many parameters are present in this algorithm, which make the process of global solution complex. Moreover, it depends upon the initial solution which is the most near to the final solution.

(ii) ***Harmony Search (HS)*:** The basic harmony search algorithm was proposed by Zong Woo Geem in 2001 [152]. The harmony search is a mimicking meta-heuristic algorithm which is society inspired algorithm by music harmony as a group of sounds considered. This meta-heuristic is based on the concept of decision variable (musician) generates (plays) a value (note) for searching a best global optimum (harmony). This algorithm is effectively directed through so many parameters as harmony memory considering rate, pitch adjusting rate, size of harmony, amount of maximum change in pitch adjustments and amount between two neighboring values.

The harmony search algorithm was proposed to simultaneously reconfigure the distribution system by DG placement, to minimize power system losses in a distribution network [153]. Further, an improved multi-objective harmony search (IMOHS) used to determine the impact of DG placement in the distribution system. In [154], Nekooei and Farsangi *et al.* modified and extended the algorithm to obtain the global solution in multiple-objective planning framework. The method has developed a strategy known as IMOHS which is based on the novel global harmony search. However, the performance of the algorithm depends on the parameter setting which is not dynamically generated. The static parameter values are not conducive to balancing intensification and diversification. Therefore, the number of iterations increases to find an optimal solution.

2.4.3 Hybrid Intelligent Algorithms

The hybrid intelligent algorithms are developed to refine the limitations of the single AI techniques by hybridization which is an efficient way to detect optimum solution. These hybrid approaches are capable of managing the complex optimization problems. However, implementation of these type approaches is comparatively hard as compared to a single method. The hybrid intelligent algorithm is a combination of features of multiple heuristic algorithms which are run simultaneously. The hybrid intelligent algorithms are used to obtain the optimal penetration of the DERs in the radial distribution system in the following subsection.

***2.4.3.1 Genetic-Tabu Search Optimization*:** The hybrid algorithm is a combination of GA and TS algorithm (GA-TS). It was developed for optimal DERs accommodation in the distribution system to reduce the power losses while maintaining the harmonics distortion limit. This combination achieves more accuracy and convergence speed over the individual GA and TA algorithm [60], [155]. A

hybridization of GA-TB based is extending the search region via using the property of GA as a population of individuals. Moreover, the search space became compact by using the feature of TS method.

***2.4.3.2 Genetic-Particle Swarm Optimization*:** The hybridization of GA and PSO (GA-PSO) has been introduced for optimal allocation of DERs by aiming at minimization of power losses and improvement of voltages profile [65]. These methods are implemented within the defined or required constraints of the radial distribution network. The strategy for achieving the global solution is divided into two parts. First is optimal positioning which is solved by the approach of the GA. Further, second is optimal sizing of DERs that is evaluated by the technique of the PSO. The binary nature is beneficial for positioning, and swarm-based nature of the PSO is proficient in sizing.

***2.4.3.3 Particle Swarm Optimization-Optimal Power Flow*:** The combination of the PSO features and OPF techniques (PSO-OPF) has been implemented for the optimal accommodation of DERs to minimize the power losses of the distribution network to optimized the size and site and identified the number of DERs [156]. In this creation, the objective function has been illustrated as simultaneous minimization of losses and maximization of DG capacity. The discrete particles of PSO have been initialized as DG installation locations, and the OPF procedure identified the optimal size for DER units considering the imposed constraints for the distribution network.

***2.4.3.4 Miscellaneous Hybrid Heuristic Algorithms (MHHA)*:** The PSO and the shuffled frog-leaping based approach identified the pareto optimal solutions to enhance the index of the transient stability by the DERs allocation in the distribution system [63]. A formulation of multi-objective DERs allocation has been solved by a combination of improved PSO algorithm and Monte Carlo simulation [68], [157]. In [64], an imperialist competitive algorithm and GA is used to find out the optimal accommodation of DERs and capacitor, simultaneously. The GA and Monte Carlo simulation-based methodology are applied to minimize the energy losses in variable load profile of the distribution system [70]. The GA and mixed-integer programming tools are proposed to obtain the optimal location and size of the DERs [145]. As another example of the combination of methods, the GA and probabilistic power flow are employed to determine the optimal allocation of the DER in uncertain nature of the distribution system [52].

The heuristic optimization algorithms have become a popular choice in searching the global or near to global solution for the optimal allocation of multi-type DERs in large-scale distribution networks. Moreover, the GA and PSO algorithm are widely used algorithms for the DERs planning considering various constraints in the radial distribution network. In addition, hybrid heuristic methods are used to get rid of shortcomings of other algorithms. However, hybrid algorithms increase the computational time with efficiency. Further, single evolutionary method is suitable to obtain the optimal solution for DERs planning.

2.5 Critical Review

The optimal DERs accommodations in deregulated electrical system introduce the several challenges for the planner in the modern distribution system. Further, the performance of the distribution system can be measured by three vital parameters as energy losses, total harmonics distortion and voltage profile of the system. However, system performance can be improved by planning and regulating the number, size, location, and penetration of the DERs in the distribution system.

The planning of the DERs allocation in existing distribution networks has not considered the realistic conditions. Further, DERs to be installed into the radial network might be influenced by the practical situations. The allocation problem with consideration of different nature of load profile can become crucial planning. However, inappropriate modeling of load provides the improper solution. Moreover, threaten might be introduced that give a false gain in the desired purpose of the planning. In actual distribution systems, there exists load diversity among the different class of customers which varies each hour of a day. The modeling of load profile should take into account these diversities.

In the distribution network, many power electronics based switches and converters are present that introduce the harmonics in supply. Therefore, extensive research can incorporate the simultaneous allocation of the DGs and capacitors to reduce the energy losses with the permissible distortion of supply in the distribution system. However, future distribution systems require integrated and coordinated solutions for the allocation of distributed energy resources which reflect coexistence of these technologies to obtain more efficient accommodation strategy. Some most commonly used residential and commercial nonlinear loads have been simulated and validated

experimentally in the literature to verify their characteristics whether they behave like a harmonic source. The shortcoming of usual DER planning is that it disregards non-linearity in the distribution network under different load conditions.

The artificial intelligence-based heuristic algorithms always search the target to near the global solution. However, some algorithm-specific control parameters are required to be tuned for the optimal solution. Therefore, this process becomes complicated and increases the computational time of convergence.

Most of the research works have been performed on balanced distribution networks. However, an overhead line of the distribution system is untransposed, unlike the transmission system. The loads of each phase are unequally distributed in the radial distribution network. Moreover, loads of the distribution systems are also unequally distributed in the whole power system. Therefore, DERs planning according to the balanced distribution network is not a realistic approach. The DERs allocation problems become so tedious complex combinatorial exercise that even these powerful heuristics suffer from poor convergence, accuracy, and efficiency, particularly in the unbalanced distribution system.

2.6 Research Objectives

On the basis of above critical review, the following research objectives have been identified.

- To develop modified/improved optimization techniques to solve the optimal DERs allocation problem of the radial distribution system with the adequate accuracy.
- To develop an approach for the optimal planning of the DERs in the radial distribution networks to minimize annual energy loss and to enhance node voltage profiles under the different time varying load profile.
- To develop an efficient harmonics power flow to analyze the harmonic distortion in radial distribution network.
- To develop a mathematical model for simultaneous allocation of the DERs to maintain the total harmonics distortion in the harmonics distorted distribution networks under piecewise multi-level load profile.

- To develop a suitable mathematical model of the practical unbalanced distribution system which can be considered under the impact of actual three-phase distribution system in the planning of the DERs allocation.
- To formulate a co-simulation framework to obtain the practical DERs planning in the unbalanced radial distribution system.

In this chapter, the literature survey of different methods and approaches for DERs allocation is presented in an effective way. The critical analysis of the literature survey related to these aspects has been carried out, and the research objectives have been formulated. In the next chapter, the optimal accommodation of the DERs units is analyzed along with the performance of the proposed scheme under different scenarios.

Chapter – 3

DISTRIBUTED ENERGY RESOURCES PLANNING IN VARIABLE LOAD PROFILE

3.1 Introduction

The electrical power system has many reforms in last few years. In the present scenario, deregulation has brought many changes in the power system. The key benefit of the deregulation has enhanced the efficiency of the power system. Therefore, several countries, Chile, USA, etc., have already adopted restructuring of their power systems. Moreover, many of the existing transmission and distribution networks are about to complete their operating life. They can be replaced either by the new assets or to be re-designed incorporating the DERs facilities as an alternate solution to defer of not only distribution network expansion but also transmission network expansions [5].

In previous chapter, several studies are conducted considering various techniques for locating the DERs in the distribution networks. The optimal allocation of embedded generation fulfills the consumer demands that can reduce the power losses. The power loss minimization has always been one of the principal concerns of the distribution system [13], [23] [78]. The DER planners pointed out the various important issues and proposed a different method for the allocation of the DERs, energy loss based placement considering time-varying load profile has hardly been addressed, as the DERs size and location were obtained at peak load condition of the distribution system. In a practical scenario, the peak demand will stay for a small period of a whole day load profile. However, it may lead higher energy loss. Therefore, it causes an important need for the DERs planning considering energy loss criterion for variable loading conditions. The energy loss is an important criterion, especially, when the load has significant variation over the whole day. The peak load demand supply is a typical case of the distribution system and advanced infrastructure of digital technology to admonish and manage to transmit electricity from all generators to satisfy the departing load demands in the smart grid connected distribution feeder. It is desirable that all planning for the DER must address time-varying characteristic of the load for the whole day. Further, an artificial intelligence

based heuristic is required to optimize the size and site of the DERs in variable load profile of the radial distribution system. Therefore, the PSO based proposed algorithm is used to the optimal allocation of the unity and non-unity power factor operated DERs.

This chapter has depicted the compression of time characteristic and peak load based planning of the DERs. To show the effectiveness, the proposed approach for allocation of the DERs is tested on 16-bus (practical system), standard 33-bus, and standard 69-bus radial distribution networks. Further, the results of the DER placement by the proposed method are compared with published result in [13], [23], and [78].

3.2 Distribution System Load Flow

Forward/Backward load flow technique is an essential tool to analyze the characteristic of the distribution networks because specific characteristics of distribution systems are different from transmission systems such as high resistance to reactance ratio and radial structure of the networks [159]. Therefore, the conventional power flow methods as Newton-Raphson, Gauss–Seidel and fast decoupled approach based load-flow have not converged in the radial distribution system. Further, the Bus Injection to Branch-Current (BIBC) matrix and Branch Current to Bus-Voltage (BCBV) matrix are used to enhance the conversion speed of the load. These matrices have been directly applied to obtain the load flow solution.

The BIBC matrix is applied to find out the variations of the branch currents in co-occurrence to the changes of bus current injections.

$$[B] = [BIBC][I] \tag{3.1}$$

where, B is branch current and I is current injection through load of the system. The node voltages are calculated by using the forward sweep approach. The expression of this approach is

$$V_{\beta} = V_{\alpha} - Z_{\alpha\beta}.B_{\alpha\beta} \qquad \alpha \in n_n, \beta \in n_b \tag{3.2}$$

where, V_{α} is node voltage at α^{th} node and Z is line impedance of branch between α^{th} to β^{th} node of the system. n_n is count of nodes index and n_b is count of branch index.

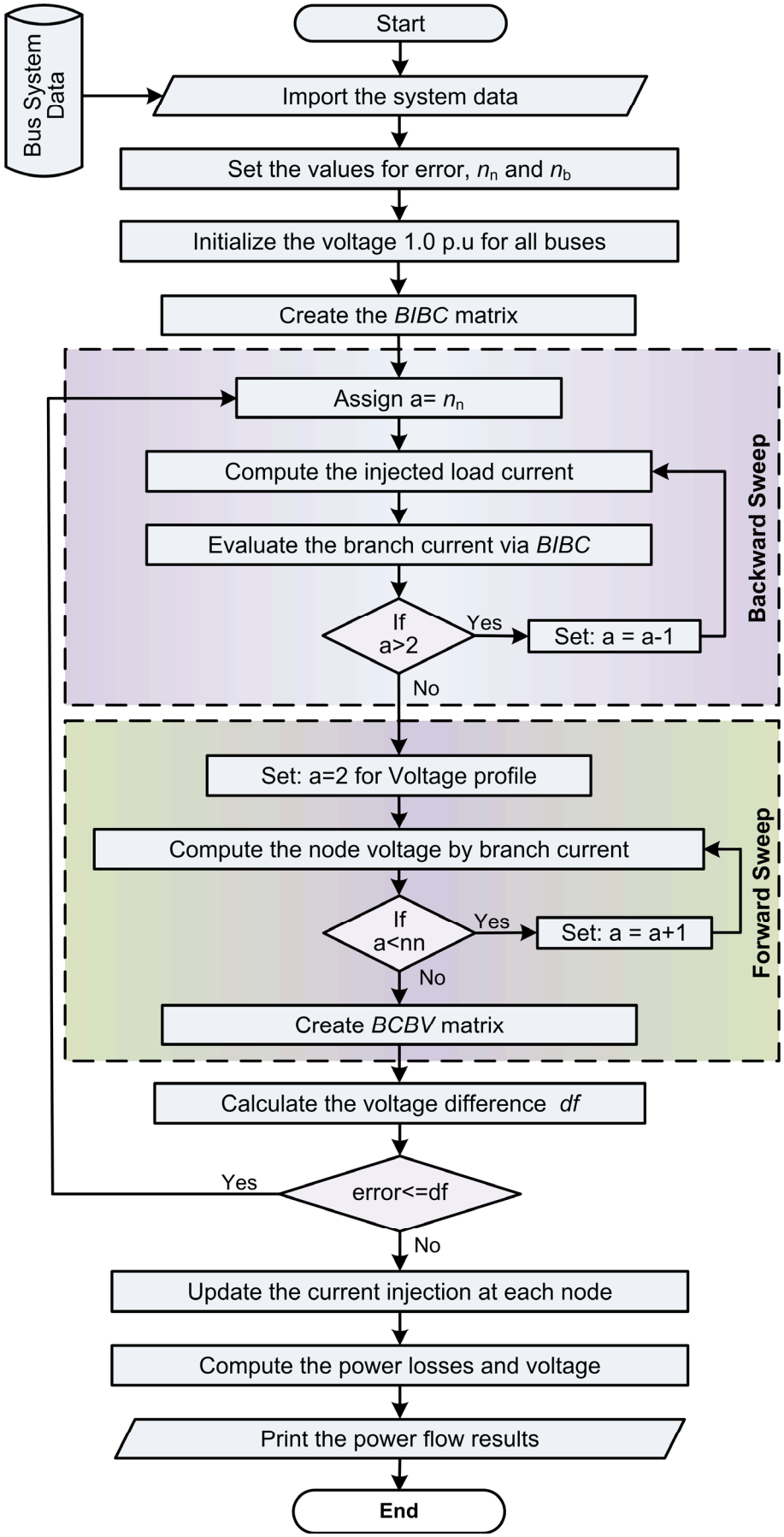

Figure 3.1: Flowchart of Forward/Backward sweep load flow technique

Moreover, the BCBV matrix is applied to estimate the variations of node voltages in relation to the deviations of branch current.

$$[\Delta V] = [BCBV][B] \tag{3.3}$$

The BIBC matrix has been applied to find the variations of branch currents in conjunction to the changes of load current injections. Moreover, the BCBV matrix is employed to compute the variations of bus voltages in relation to the changes of branch currents. The process of the load flow is repeated until the specified error is not satisfied which is demonstrated in Figure 3.1.

3.3 Problem Description

The DER planning is influenced by several factors such as power output, load variation, and technology of the DER (based on biomass, wind, solar photovoltaic, and diesel). The DER planning can be either deterministic or probabilistic based on the type of the DER. The deterministic approach is usually suitable where the load profile is with less variation and generation can also be considered constant. The probabilistic approach is desirable when the load profile has wide load deviation, and generation is also intermittent in the output.

The problem of this work is to minimize the energy losses using multiple DERs. The planning of the DERs is to be carried out considering whole day load profile for the distribution load. A new approach is to be proposed to solve the equation (3.4) using heuristic method,

$$F = \min\left[\sum_{t=1}^{T}\sum_{\alpha=1}^{n_n} \mathrm{Re}(B_\alpha{}^2 \times Z_\alpha) + a_\alpha \rho_\alpha\right] \tag{3.4}$$

where,

F is function of energy loss,

a is decision coefficient of penalty (either 0 or 1),

G is penalty factor for constraints limit violation,

T is total hours in a day (i.e. 24 hours).

The penalty factor helps to separating the solutions into the feasible and non-feasible solutions. The solutions that decline the system limits using decision penalty

variable are called non-feasible solutions. In this chapter, any locational constraint is not considered on the DER. However, any locational constraint of the DER can be easily included by the proposed PSO based method. In such cases, the applied algorithm searches only the identified nodes of the system for the best solution.

$a_i = 1,$ if any costraint declines the permissible limit.

$a_i = 0,$ if all costraints satisfy all conditions.

The following equality and inequality constraints are satisfied in all distribution systems to find out the optimal DERs placement and size.

3.3.1 Equality Constraints

Two equality constraints have been considered for this work.

3.3.1.1. Power Balanced: In the network, total generation of power from the grid and distributed energy resources must be equal to the summation of load demand and power losses of the system.

$$S_{Grid} + \sum_{\alpha=1}^{n_n} S_{DER} - \sum_{\alpha=1}^{n_n} \sum_{\beta=\alpha+1}^{n_b} B_{\beta}^{2} \cdot Z_{\alpha\beta} = \sum_{\alpha=2}^{n_n} S_D \tag{3.5}$$

where, S_{Grid} is total power supplied by grid substation. S_{DER} is generation of power from distributed generation and S_D is load demand of the system.

3.3.1.2. Power Factor of DER: The optimal power factor of non-unity DER should be equal to combined load power factor [13].

$$\frac{P_D}{\sqrt{P_D^2 + Q_D^2}} = PF_D = PF_{DER} \tag{3.6}$$

where, P_D and Q_D are the active and reactive demand of the system. PF_D and PF_{DER} are power factor of the system load demand and DER.

3.3.2 Inequality Constraints

3.3.2.1. Voltage Limits at Slack Bus and Load Buses: Bus voltage must operate within the prescribed limits.

$$0.95 p.u. \le V_m \le 1.05 p.u. \tag{3.7}$$

The slack bus voltage magnitude and angle must be one and zero throughout the planning period, respectively.

3.3.2.2. DER Generator Constraint: The DER unit size is considered only in permissible operating region.

$$S_{DER}^{\min} < S_{DER,\alpha} \leq S_{DER}^{\max} \tag{3.8}$$

where, $S_{DER}^{\min}$ and $S_{DER}^{\min}$ are lower and an upper limit of the DER's power, whereas S_{DERs} value should not exceed to the comparable all three references either initialization or updating process of the optimization.

3.3.2.3. Distribution Thermal Constraints: The thermal capacity of the distribution feeder of the network transcends their permissible value.

$$\left|S_{\alpha\beta}\right| \leq \left|S_{line}^{\max}\right| \tag{3.9}$$

where, S^{max} is a maximum permissible limit of the distribution line, and $S_{\alpha\beta}$ is power flow capacity of the branch between node α^{th} and node β^{th}.

3.4 Proposed Methodology for DERs Planning

It is an illustrious fact that the conventional computing methods face difficulty to handle the practical problems such as non-convex, discontinuous and non-linear characteristic. The PSO algorithm is a heuristic method which can overcome the drawback of the conventional methods [160]. The origin of the PSO algorithm is carried out from "swarm's strategy of moving together in crowd" by Eberhart and Kennedy in 1995 [133]. The concept behind the PSO approach is based on the behavior of the swarm means the characteristics, properties and strategies of the all flying insects. Further, the PSO method can be said as the swarm based optimization technique. The idea is fetched from the theory or analysis about the flocking behavior of birds, analyzed by a biologist Craig Reynolds [161].

The behavior of swarm can be related with the optimization algorithm using the following terms are described as:

***(i). Particles*:** The birds or flying insects are defined in this algorithm as particles of a swarm. The particles have some own properties, such as their fitness function,

solution, and velocity, to search their objectives. Initially, the particles are randomly generated to find the fitness value. Further, the particles will update by the velocity of particles and other vectors of the swarm.

***(ii). Optimization Function*:** The strategy or way of finding food by birds or insects can be related with the objective function of problem definition.

***(iii). Velocity* (*v*):** The speed of movement towards the decided or fixed direction is known as a velocity. The swarms move towards the food according to updated velocity. Each particle has own individual velocity variable.

(iv). Personal Best (P_{best}): The 'P_{best}' indicates which value is the best solution individually for a particular particle. Every particle has a solution that is evaluated in all iterations. The P_{best} is the best solution of that particle in the whole iteration which is evaluated.

(v). Global Best (G_{best}): This term denotes the best value decided globally and best fitness of a particle among all particles in whole iterations is called as G_{best}. The decision of selecting G_{best} is taken with the satisfaction of all given condition by the particle swarm optimizer.

***(vi). Local Best* (L_{best}):** The best solution of particle in each iteration is known as local best (L_{best}) which has to compare with P_{best} till previous iteration.

***(vii). Stopping Criteria*:** Each optimization problem has some stopping conditions. A few conditions regarding the swarm are like: food is not there, food is detected and food is not sufficient.

***(viii). Destination Value*:** The optimization algorithm is applied to move the particles from initial value to the destination value. The aimed value is always constant. In this algorithm, destination value for swarm is food.

***(ix). Population*:** The swarm is known as population. The swarm can be described as the group of the particles or birds which indicates the society of the birds. They move together to find out their food. This term is used in the process as population.

***(x). Vision*:** The vision of the swarm is known as search space of the optimization function which can hold the minimum and maximum value in search criteria.

The parameters in the PSO algorithm are used as following:

- Total size of population is N_{p},
- The position of the particles is X_{u},
- The velocity of the particles is v_{u},

- The solution of the particles is *fitness*,
- The personal best of particles is P_{best},
- The global best is G_{best},
- Inertia factor is χ (weight),
- Total number of iteration permitted is K^{max},
- Constriction factor = c
- Two random numbers are defines as $r_1, r_2 \in \{0,1\}$
- The velocity criteria $\{-v_{max}, v_{max}\}$ for instance, the range of particle velocity is {-20 20} then the velocity length is 40.
- Two acceleration coefficients are c_1 and c_2, where c_1 and c_2 is the self confidence value of particles-influence and swarm-influence, respectively. The value of constant factors should be varied between 0 and 4. They are also known as learning factors. Moreover, addition of acceleration coefficient should be greater than four.

This algorithm chooses the best particle among all particles in multi-dimensional search space, which computes and improves the velocity and position according to equations (3.10)-(3.12).

$$v_u^{itr+1} = \chi\left(v_u^{itr+1} + \underbrace{c_1 * r_1\left(P_{best}^{itr} - X_u^{itr}\right)}_{Partial\ Influence} + \underbrace{c_2 * r_2\left(G_{best}^{itr} - X_u^{itr}\right)}_{Swarm\ Influence} \right) \tag{3.10}$$

where, v_u are the velocity of uth particle. *itr* is iteration number or number of generation, and X_u^K is the position of the uth particle for *itr*th iteration.

whereas, inertia weight value has been computing by the following equation as

$$\chi = \frac{2}{\left|2 - c - \sqrt{c^2 - 4c}\right|} \tag{3.11}$$

and updated position of the particle from previous position is depended on the updated velocity as

$$X_u^{itr+1} = X_u^{itr} + V_u^{itr+1} \tag{3.12}$$

The proposed DER planning can be carried out in stages for the DERs as shown in Figure 3.2. The initial randomly generated sizes of the DERs are placed at different nodes of the system and applied the backward forward load flow algorithm. Further, analysis the parameter of the distribution system and check the constraints limit on basis of parameter of distribution system. If the constraints are violate the limit of the system then discard the solution by applied the penalty factor.

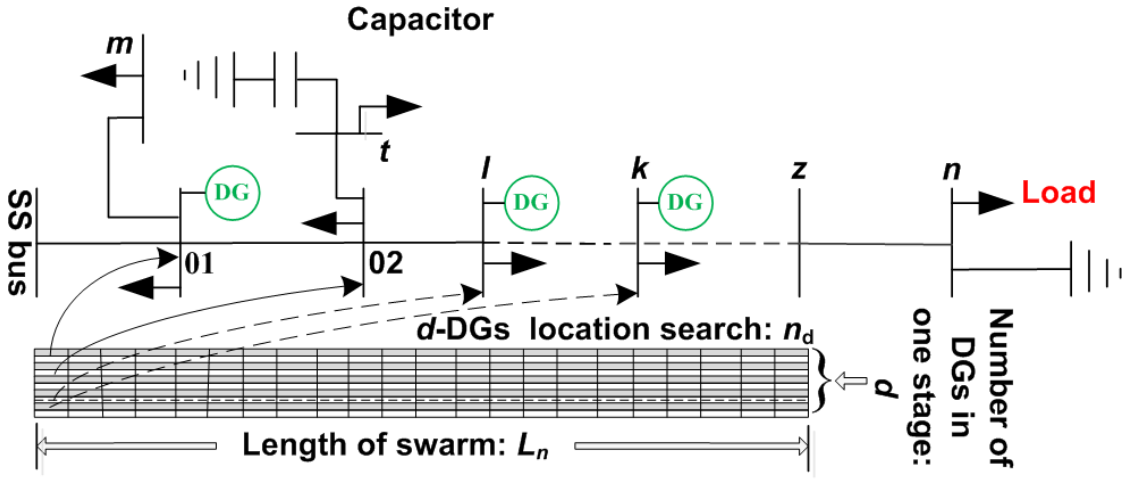

Figure 3.2: Optimal DER planning using optimization approach

This process is repeated for each node of the every system except the slack bus of the network. The size, number, location and type are the design variables in the DER which value is updated in next iteration according to the updated velocity of each individual decision variable. The updating population process is simultaneously proceeding for each variable. Further, updated value of design variable is accepted whenever energy losses of the system in year are minimum from pervious iteration. This process repeated for each node in each iteration by the optimization algorithm.

The procedure of the PSO is illustrated through the Figure 3.3. It clearly shows that each particle of population should have the own value and update that value by computing the velocity. The solutions of every particle are generated and select the best value for that particle called as P_{best} of the particle. Further, the only single particle is selected as the G_{best} which is nearest to the targeted value from all other particles' solutions. This process will continue until the stopping conditions does not meet, like the all permitted iteration evaluated and any error. The graphical presentation of iterative process of the PSO method is presents in Figure 3.4.

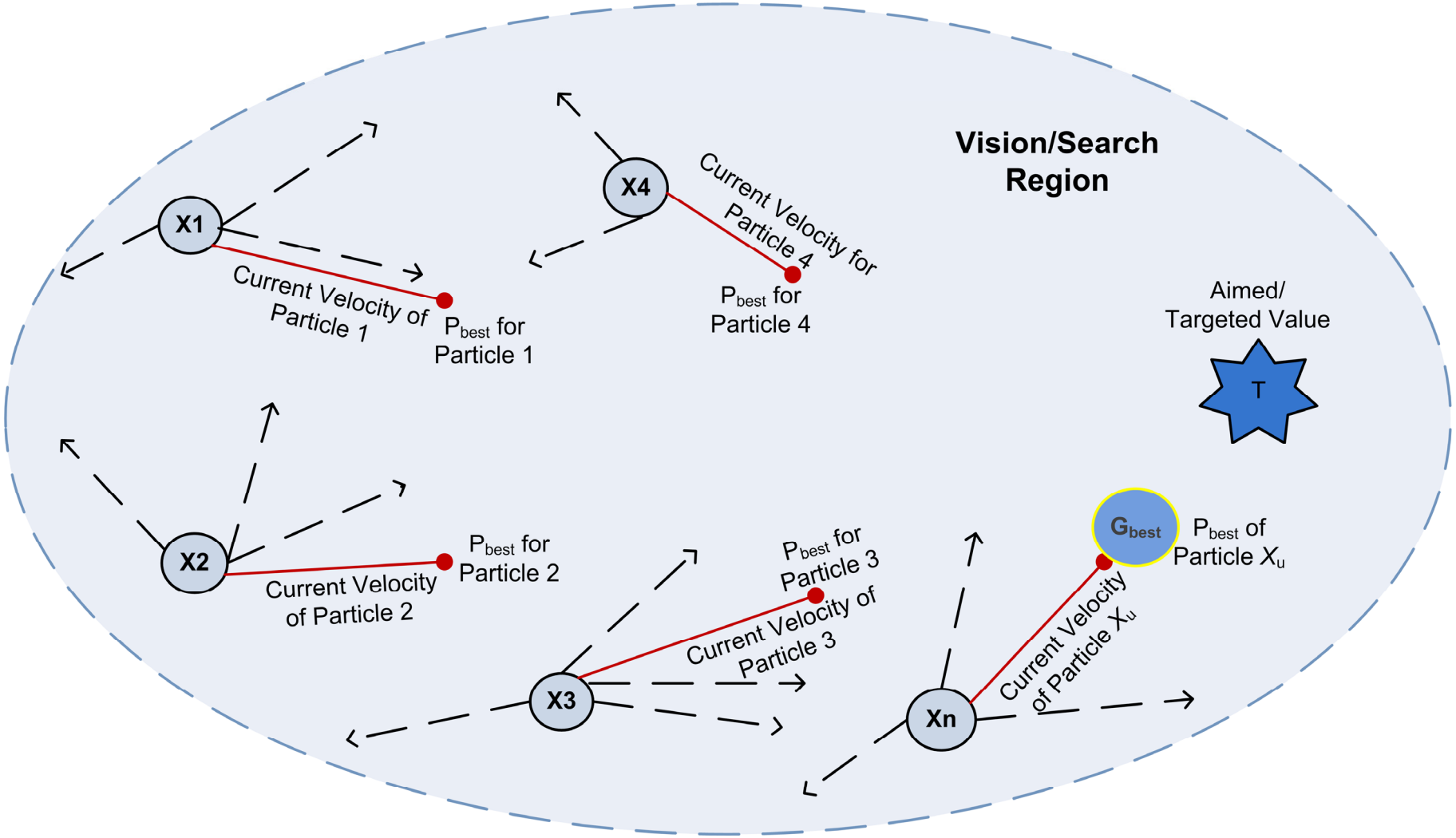

Figure 3.3: Selection procedure of the personal and global best particle

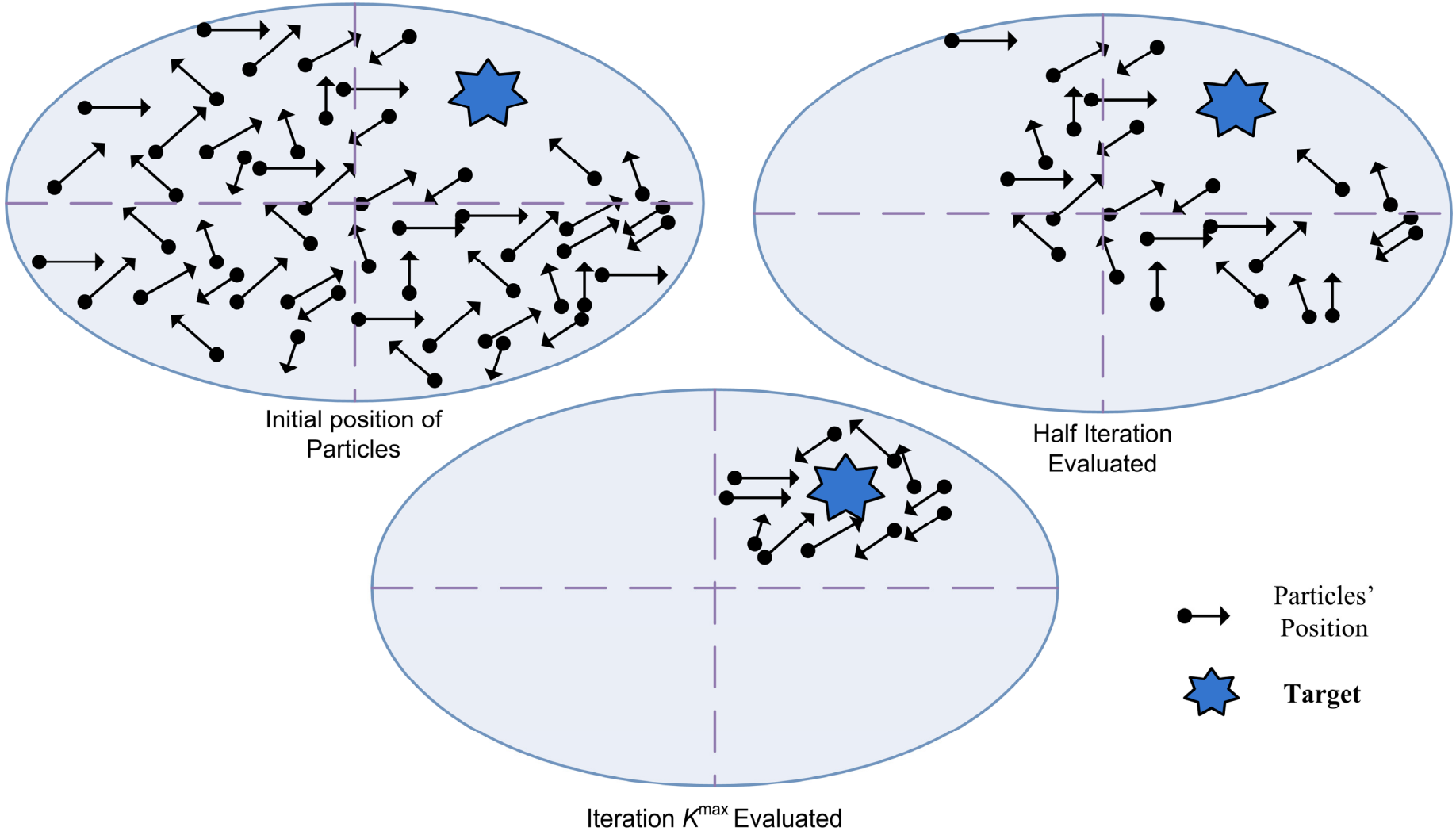

Figure 3.4: Iterative representation of the particle position

Figure 3.4 depicts the understanding behavior of iteration role with the PSO in optimization. The first ellipse shows the initial state of the PSO where all particles are spread in whole the search region. Afterward, the second ellipse describes that after the 50 percent iteration evaluated, the particles has gone in the half area of search region which nearest to targeted value. The final ellipse which elaborate that all the allowed iteration generated, therefore, the particles has reached the nearest to the targeted value.

The step by step procedure of the fundamental PSO works as following:

Step 1. Define the objective function as given problem formulation.

Step 2. Initialize the parameters to the constant value as

Set: N_p, N_d, χ, c_1, c_2, v_{max} parameters with the effective value according to given problem.

Step 3. Initialize the particles with their positions and values as randomly.

Step 4. Compile the objective function to compute the initial values of the PSO Parameters and evaluate the inertia weight value by equation (3.11).

Step 5. Update the velocity of the particle using equation (3.10).

Step 6. Calculate the constriction factor or particles for next movement towards the destination as given equation (3.12)

Step 7. Further, improve the swarm by updating their values.

Step 8. Afterward, evaluate the objective function and find out the fitness.

Step 9. Whether, the new fitness is better than the P_{best}, update the P_{best} with new one, otherwise, reject the new swarm.

Step 10. The above steps from 4 to 9 will be repeated for all dimension and particles.

Step 11. Locate the global best and check if newly located global best is better than the previous G_{best} then update the particles with their fitness value, otherwise, reject the current solution.

Step 12. Apply the constraints handling mechanism, whether single one constraint is not satisfied then apply the penalty and regenerate new swarm.

Step 13. Check the condition of stopping criteria, if it satisfied then stop and display the optimal solution of the defined problem. Else repeat from step 4.

Step 14. Output and terminate the procedure.

The PSO based proposed algorithm is applied to minimize the energy loss of the distribution system to determine optimal allocation of multiple DERs. The procedure

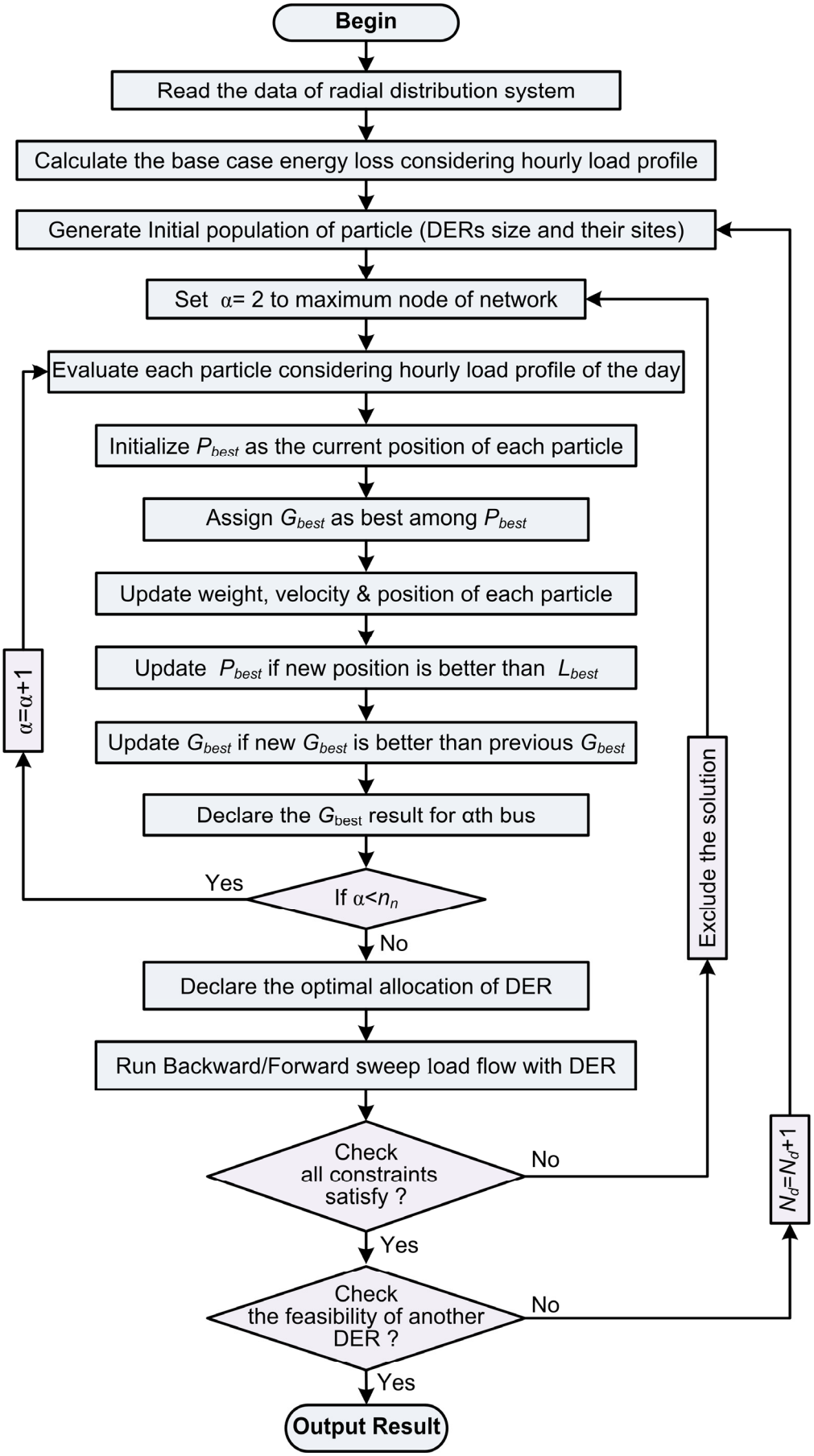

Figure 3.5: Flowchart of the PSO based proposed algorithm approach

of proposed algorithm considering hourly load variation in the problem of optimal allocation of DERs is shown in Figure 3.5 which is the symbolic representation of the flow to understanding the PSO based algorithm handling with the load variations of per hour/day/month or year. The following outline of procedure summarizes the coding structure of program's flow.

Pseudo Code:

Begin

Set: all parameters of the PSO method as K^{max}= maximum iterations
Initialize particles randomly
Evaluate objective function
Set: initial values of the PSO parameters as: itr=1, u=1, P_{best}, $G_{best.}$
While itr < K^{max}
For u=1 to each particle X_u
Calculate the velocity
Update the particles
Evaluate the objective function
If new fitness is better than P_{best}
Then
Update P_{best} with new one
Else
Reject newly fitness
End If
End For
Compute the new G_{best} and update with previous G_{best}
If stopping criteria is true or Error=true
Then
Terminate and display results
End If
Increase itr=itr+1
End while
Show the optimal result

End

The pseudo code for the PSO based proposed algorithm is given to implement the algorithm easily into the program.

3.5 Application Study and Simulation Results

In section 3.3, the proposed algorithm for the optimal DERs allocation and size has been presented. The PSO based proposed method is tested on three radial distribution

test systems, 16-bus, 33-bus and 69-bus systems having the hourly variable load profile and compared with the results of [13], [23], [78].

A 23 kV, 16 buses radial distribution system is used to validate the proposed algorithm as shown in Figure 3.6. In this system, three feeders are individually connected to system. Therefore, three slack buses are present in this system. It is a realistic condition of the actual radial distribution system. This system is a small section of the practical radial distribution system of the Taiwan power company. The active demand of the system is 28.7 MW [160]. Moreover, 11.4 MVAr of reactive demand is supplied by capacitors (base case), and remaining 5.9 MVAr is supplied either by the DERs or Grid Sub Station (GSS). The peak demand losses of base case system are 511.43 kW. Further, minimum node voltage is 0.9692 p.u. at the 13th bus.

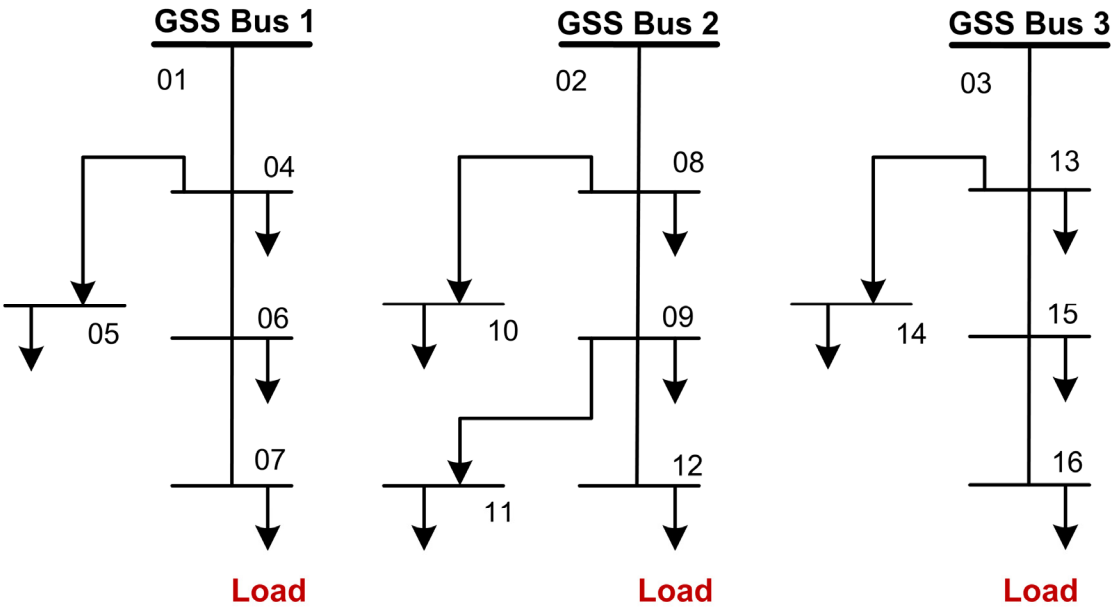

Figure 3.6: 16-bus radial distribution system

The standard 33 bus system is second test system which has the total load demand active and reactive power of 3.7 MW and 2.3MVar, respectively. The load of the system is present at every node that is spread out in three limbs from the main branch of the system. This system is operated at 12.66 kV [48]. In this system, peak demand losses are 211.20 kW and minimum node voltage is 0.9037 p.u. at the 18th bus. The designing of the system is more important because load of the system at 18th bus is so far from substation. Further, the voltage level is low from the predefined value of the distribution system regulation. Therefore, the DERs integration is required to supply the desirer voltage level. This system is shown in Figure 3.7.

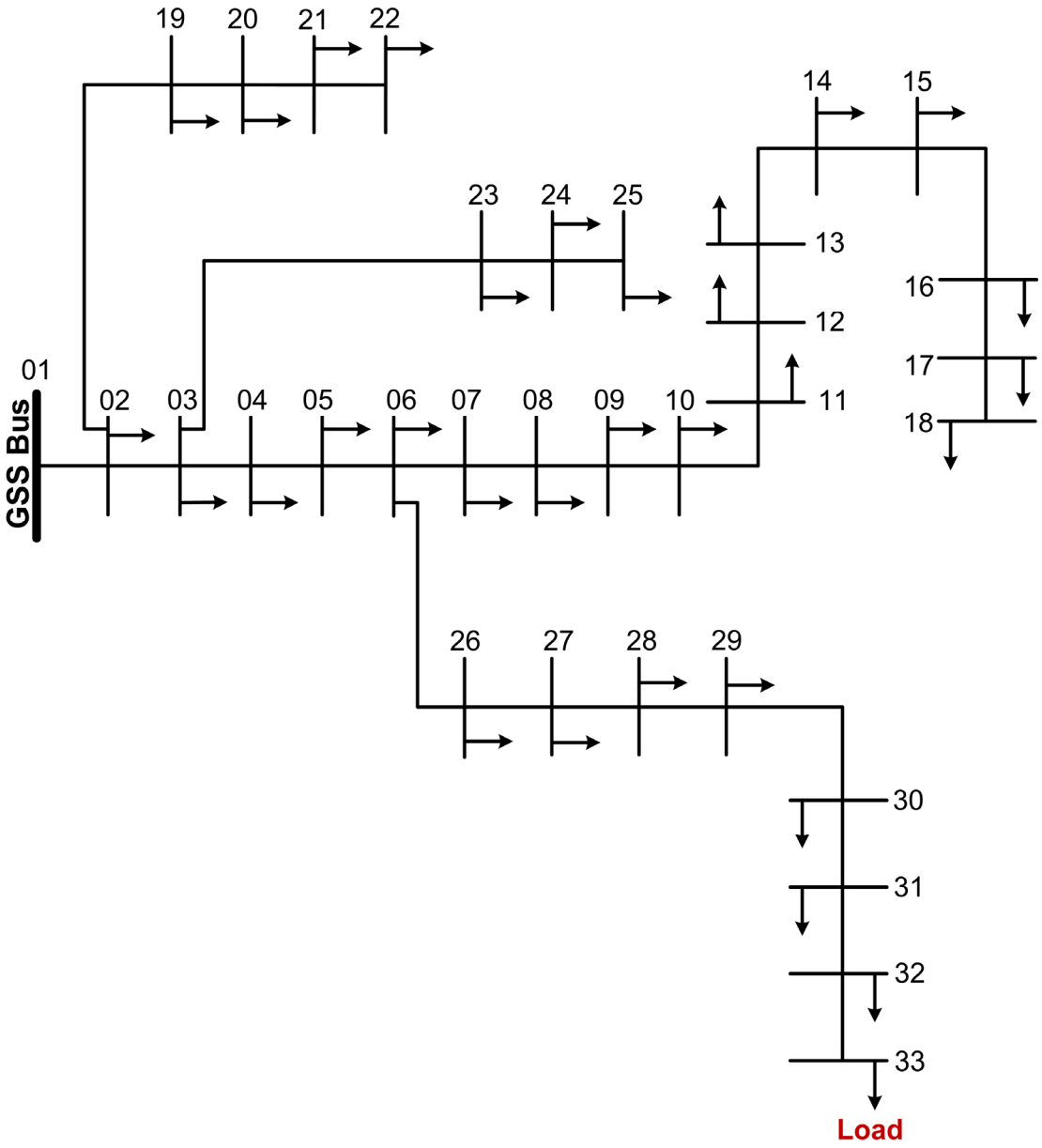

Figure 3.7: 33-bus radial distribution system

Further, proposed method is tested on a 12.66 kV, 69-node radial distribution system [48]. Figure 3.8 exhibits the line diagram of the system. This system has highest number of nodes as compare to other systems. However, the demand of the system is less from 16-bus and approximates equal to 33-bus system. The active and reactive demand of the system is 3.8 MW and 2.69 MVAr, respectively. Peak demand has been supplied by a grid with 219.28 kW losses. Minimum system voltage is 0.9102 p.u. at 65^{th} node. In this system, node 65^{th} is far away to the grid substation and this branch is highly loaded. Therefore, voltage level at this node does not follow the regulation of the distribution system.

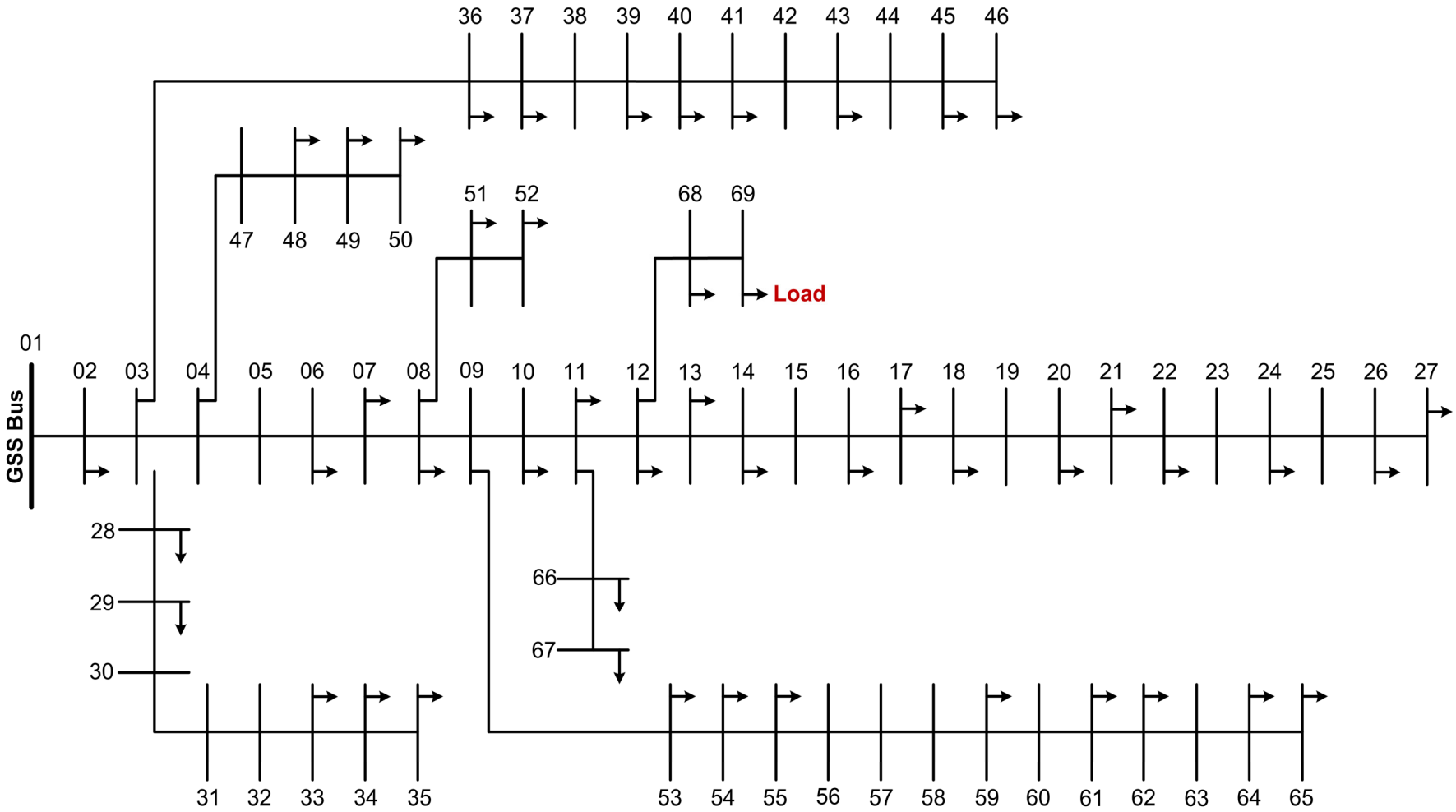

Figure 3.8: 69-bus radial distribution system

The daily load profile shape is referred to [23] and assumed to be the constant whole year. The following assumptions are made for simplicity in this chapter:

(a) Load demand of the system equals to feeder capacity.

(b) Slack bus voltage to be constant during the DER planning.

(c) The hourly variation is assumed to be constant in load variation curve, and its Load Scaling Factor (LSF) is shown in Figure 3.9.

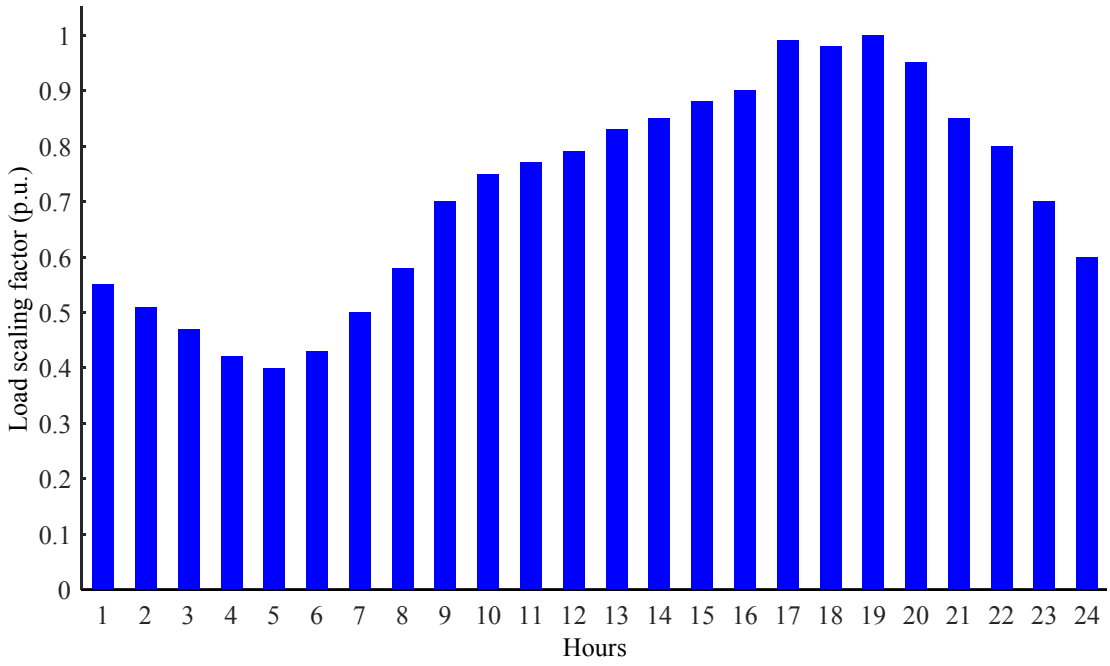

Figure 3.9: Load scaling factor of a time variant distribution load

The proposed algorithm has been executed in the MATLAB software operating on a personal computer with Intel processor i5, 3.2 GHz, and 4 GB RAM. Constructive coefficients are same for each distribution system. The population size and numbers of generation are 25 for 16-bus system and 50 for 33-bus distribution system. Further, population size and a number of generations are 75 and 100 for 69-bus distribution system, respectively. The population size and number of generation are decided by the repetition of fitness function value.

The PSO based proposed method is compared with three established and well-accepted algorithms as Loss Sensitivity Factor Approach (LSFA) [78], Improved Analytical Method (IAM) [13], and Constriction Coefficient PSO Approach (CCPSOA) [23] in each radial distribution system as discussed above in this chapter. In [13], [23] and [78], the DER planning was carried out at peak load profile for

power loss minimization, whereas in the proposed DER planning, the planning is carried out for hourly variable load profile for energy loss minimization.

The proposed method (PM) suggests planning solutions to the DERs, which can supply only active power, or both real and reactive power (lagging or leading) to the distribution system. The results are classified according to the power delivering capability of the DER at unity power factor and non-unity power factor. The DERs are operating at unity power factor (UPF) which is considered in the first subsection, whereas non-unity power factor (Non-UPF) DERs are used for the second subsection.

3.5.1 Planning of the DERs at Unity Power Factor

This section presents results of the DERs, which can supply only real power to the distribution networks. The result of the DER planning for realistic time-varying load profile approach is presented in Table 3.1.

The observation for 16-bus system is given as under:

(a) DERs are placed at bus-6 (1.2167 MW), bus-12 (3.5883 MW) and bus-16 (1.9024 MW).

(b) Minimum bus voltages (1.0 pu) are at buses 1, 2, 3 as shown in Figure 3.10 because bus number 1, 2 and 3 are slack bus of the system. Further, it is improving due to local power generation. In this system, seven capacitors are already fixed. Therefore, voltage profile of this system is already in effectual situation. Further, DERs integration can be introduced the problem of over voltage. However, the voltage profile is near to unity with help of the proposed algorithm.

(c) Energy loss increases using LSFA [78], IAM [13] and CCPSOA [23] algorithms, even, with respect to the base case, whereas, the proposed method suggests the DER solution for the reduction of energy loss.

It is interesting to note that the energy loss is increased in [13], [23] and [78] with time varying load due to reverse power flow during lightly loaded cases with the inclusion of the DER, as the DER planning was carried for peak load conditions in [13], [23] and [78]. Since, the DERs at a non-optimal location with non-optimal size, losses can be even higher than without any DER (may be more than five times in extreme cases) [162]. The voltage profile of the system by using the PSO based proposed is near to 1 p.u. as compare to each algorithm.

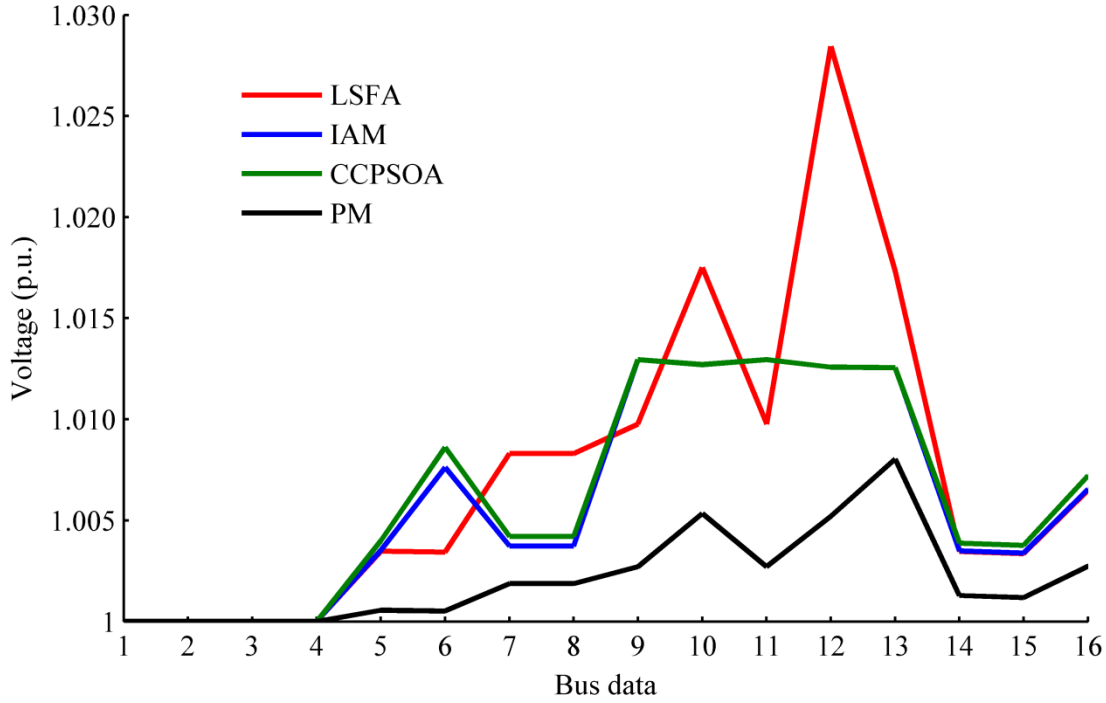

Figure 3.10: Voltage profile in the 16-bus system with three UPF DERs

The results of 33-bus system are discussed follows:

(a) Minimum bus voltage is 0.9839 at bus number 33, and overall voltage profile is shown in Figure 3.11.

(b) The size of DERs at bus-6 is 1.8434 MW; bus-15 is 0.3427 MW, and bus-25 is 0.4566 MW.

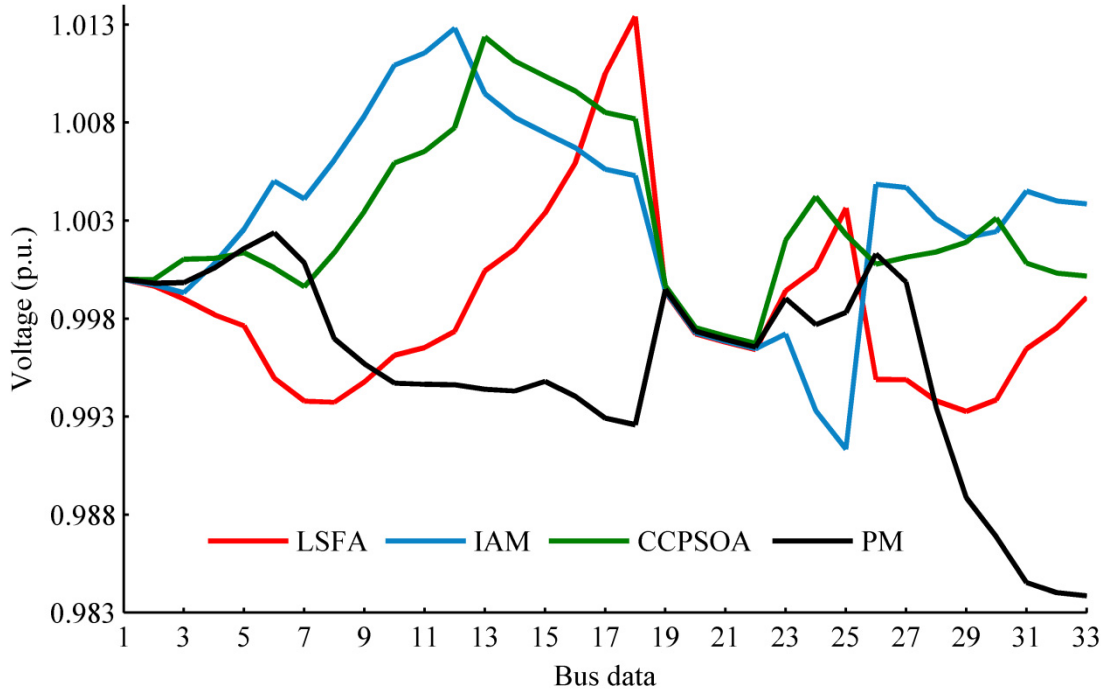

Figure 3.11: Voltage profile in the 33-bus system with three UPF DERs

(c) The proposed algorithm achieves highest loss reduction as compared to [13], [23] and [78]. It reduces more energy losses with the placement of more number of DERs.

The result in 69-bus system is given as under:

(a) Minimum bus voltage is 0.998 at bus number 56 which is approximate to 1 p.u. The voltage profile is inversely proportional to the distance as shown in Figure 3.12. In this system, nodes 27 and 65 are far away from the substation. The proposed algorithm has enhanced the voltage profile of each node of the system. However, other algorithms have not improved the voltage profile whenever increase the distance of load.

(b) The size of DERs at bus-61 is 1.349, and DERs at bus-17 is 0.37 MW, and bus-50 is 0.515 MW.

(c) Table 3.1 shows that PSO based proposed method reduces more energy loss as compared to LSFA [78], IAM [13] and CCPSOA [23].

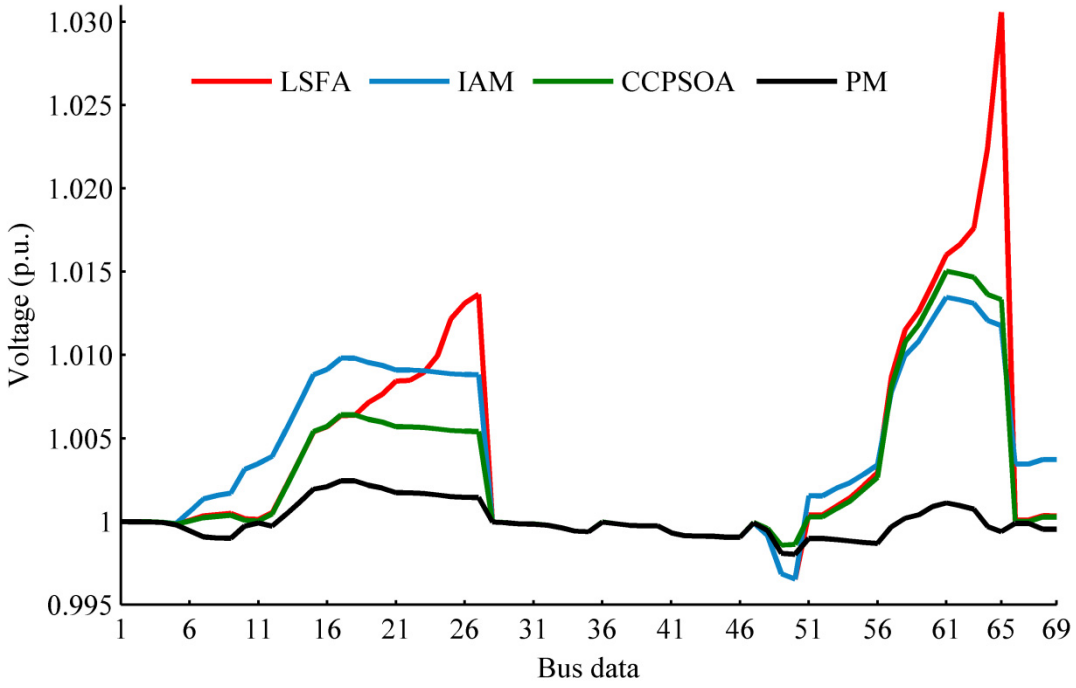

Figure 3.12: Voltage profile in the 69-bus system with three UPF DERs

The effectiveness of the proposed method is examined with 16-, 33-, and 69- bus distribution system which is tabulated in Table 3.1. Since, the optimal allocation is the only goal of this work, the results with proposed method for the DERs placement are compared with results obtained by [13], [23], and [78]. For effective comparison, the test system is simulated with DERs operating at unity power factors.

Table 3.1: Total yearly energy loss (with UPF-DERs) for the hourly varying load

Number of DERs	**Base Case (MWh)**	**Energy loss (MWh) with DERs**			
		LSFA [78]	IAM [13]	CCPSOA [23]	PM
16-bus distribution system					
Single DER	567.93	1852.23	1193.10	1171.18	261.60
Double DERs		2055.48	1390.50	1439.91	187.46
Three DERs		2041.98	1378.83	1479.05	165.98
Total Energy Saving (%)with three DERs		-	-	-	70.77
33-bus distribution system					
Single DER	987.42	716.18	625.22	623.46	557.68
Two DERs		564.54	549.77	516.15	491.13
Three DERs		509.31	522.84	484.15	457.75
Total Energy Saving (%)with three DERs		48.42	47.05	50.97	53.64
69-bus distribution system					
Single DER	1049.57	658.57	526.56	499.21	437.51
Two DERs		625.62	448.96	479.39	387.78
Three DERs		679.93	466.55	473.75	380.99
Total Energy Saving (%)with three DERs		34.67	55.54	54.86	63.70

The distribution energy losses depend on the size and location of the DERs, and system's load value in the presence of distributed generators. Moreover, losses may increase with DERs, if planned with non-optimal size at non-optimal locations for the 16-bus system. Since, the DER planning was carried out for peak demand of the system; however, if the DER was considered at other than peak load gives more system losses. Therefore, planning of the DER at peak load is not beneficial for time varying load profile in 16-bus system with DERs [13], [23], [78]. However, it is observed that the performance of the proposed method provides better results as compared to the results of [13], [23], [78] for energy loss reduction with the hourly varying load. In the each bus system, the proposed algorithm has minimized the energy losses with increment the number of the DERs. However, this pattern has not followed by each compared algorithm which validates of planning for the DER allocation. Moreover, the PSO based proposed algorithm is achieved the highest energy loss reduction with the UPF-DERs in every distribution test system.

3.5.2 Planning of the DERs at Non-Unity Power Factor

This sub-section deals with the DERs which can inject both real and reactive power to a distribution network. This type of the DERs are planned for three radial test systems as 16-, 33- and 69-bus distribution systems considering the need to assess the impact of both real and reactive power (together) locally.

The PSO based proposed algorithm has been applied to obtain the optimal location (s), size (s) and power factor to reduce energy losses in the 16 bus distribution system as shown in Table 3.2. The energy loss has been reduced by 19.70 %, 65.31 %, and 68.61 % with the presence of single- double- and triple-DERs, respectively. However, CCPSOA and IAM do not have beneficial outcome considering daily load profile as they have more losses with respect to the base case energy loss. This is crucial outcome for the DER planning in the radial distribution system. Therefore, the optimal allocation of the DERs is essential for the planning of the distribution system.

Table 3.3 depicts that design variable of the proposed algorithm which is used to achieve the highest percentage reduction in energy losses as compared to CCPSOA and IAM in the 33-bus distribution system. Moreover, reduction of the losses is increased with increment the number of the DERs. The highest percentage reduction of the losses is 74.56. However, the CCPSOA is not suitable to place three Non-UPF DERs in the 33-bus distribution system.

Table 3.2: DERs (Non-UPF) allocation in the 16-bus distribution system

Cases	**Techniques**	**DER Size (MVA) (Optimum Location)**			**Energy Loss (MWh)**	**Energy Loss Reduction (%)**
One DER	IAM [13]	13.12 (9) PF=0.99	---	---	1278	No Benefits
	CCPSOA [23]	13.122 (9) PF=0.9905	---	---	1275.3	
	PM	3.5883 (12) PF=0.99	---	---	456.07	19.70
Two DERs	IAM [13]	13.13 (9) PF=0.99	5.91 (6)	---	1571.9	No Benefits
	CCPSOA [23]	13.1156 (9) PF=0.99	5.9022 (6) PF=0.9902	---	1569.9	
	PM	3.5883 (12) PF=0.99	1.9024 (16)	---	197.0	65.31
Three DERs	IAM [13]	13.13 (9)	5.91 (6)	3.94 (15) PF=0.99	1587.5	No Benefits
	CCPSOA [23]	13.0473 (9) PF=0.99	5.8986 (6) PF=0.9898	3.9526 (15) PF=0.9906	1572.6	
	PM	1.12167 (6)	3.5883 (12)	1.9024 (16) PF=0.99	178.25	68.61

Table 3.3: DERs (Non-UPF) allocation in the 33-bus distribution system

Cases	Techniques	DER Size (MVA) (Optimum Location)			Energy Loss (MWh)	Energy Loss Reduction (%)
One DER	IAM [13]	3.107 (6) PF=0.82	---	---	642.24	34.25
	CCPSOA [23]	3.097 (6) PF=0.8259	---	---	629.40	36.26
	PM	1.8434 (6) PF=0.85	---	---	368.64	62.67
Two DERs	IAM [13]	2.195 (6)	1.098 (30) PF=0.82	---	663.03	32.85
	CCPSOA [23]	0.9951 (12) PF=0.8221	2.0756 (29) PF=0.8190	---	848.56	14.06
	PM	1.8434 (6)	0.3427 (15) PF=0.85	---	290.72	70.56
Three DERs	IAM [13]	1.098 (6)	1.098 (30)	0.768 (14) PF=0.82	492.60	50.11
	CCPSOA [23]	0.9343 (13) PF=0.8193	1.2325 (24) PF=0.8671	3.9526 (30) PF=0.8269	3702.3	No Benefits
	PM	1.8434 (6)	0.3427 (15)	0.4566 (25) PF=0.85	251.15	74.56

The power factor of the DERs is same for each number of the DERs. Moreover, it is equal to the system load power factor to determine the maximum benefit in the system. It is depicted from Figure 3.13 that the voltage profile of the PSO based proposed method accomplished the highest enhancement as compared to other algorithms.

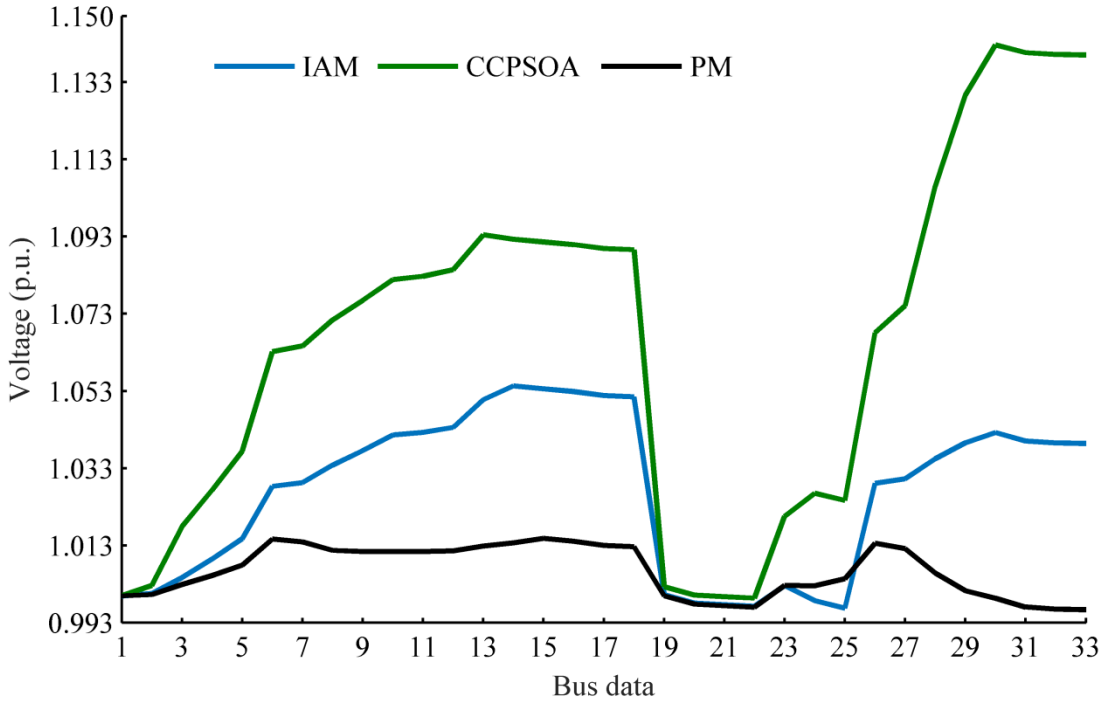

Figure 3.13: Voltage profile in the 33-bus system with three (Non-UPF) DERs

Table 3.4 shows that the Non-UPF three DERs are optimal accommodated by the PSO based proposed algorithm in the 69 bus distribution system. The energy loss reduction is 84.21% for one DER by proposed algorithm. It is large as compare to IAM and CCPSOA algorithms. Further, the optimal allocation of the two and three number of DERs has achieved the 90% above energy losses reduction in a year. because the percentage reduction of energy losses is 91.14. Moreover, IAM and CCPSOA algorithms did not obtain the energy loss reduction above the 63%. There are large loss reduction differences between proposed and compared algorithm. The compared algorithm optimized the power factor for each number of the DERs. However, the proposed approach has not optimized the power factor value. It takes according to the load of the system. Figures 3.14 show that the voltage profile is at acceptable level of the peak load demand with suggested penetration of three DERs in 69-bus networks.

Table 3.4: DERs (Non-UPF) allocation in the 69-bus distribution system

Cases	**Techniques**	**DER Size (MVA) (Optimum Location)**			**Energy Loss (MWh)**	**Energy Loss Reduction (%)**
One DER	IAM [13]	2.243 (61) PF=0.82	---	---	500.94	52.27
	CCPSOA [23]	2.207 (61) PF=0.8241	---	---	470.09	55.21
	PM	1.349 (61) PF=0.821	---	---	165.63	84.21
Two DERs	IAM [13]	2.195 (61) PF=0.82	0.659 (17)	---	520.74	50.39
	CCPSOA [23]	2.1075 (61) PF=0.8272	0.6416 (17) PF=0.8161	---	438.81	58.19
	PM	1.349 (61) PF=0.821	0.370 (17)	---	96.88	90.76
Three DERs	IAM [13]	2.073 (61) PF=0.82	0.622 (17)	0.829 (50)	414.33	60.52
	CCPSOA [23]	2.086 (61) PF=0.8318	0.6134 (18) PF=0.8279	0.8454 (50) PF=0.8276	392.12	62.64
	PM	1.349 (61) PF=0.821	0.370 (17)	0.515 (50)	86.58	91.75

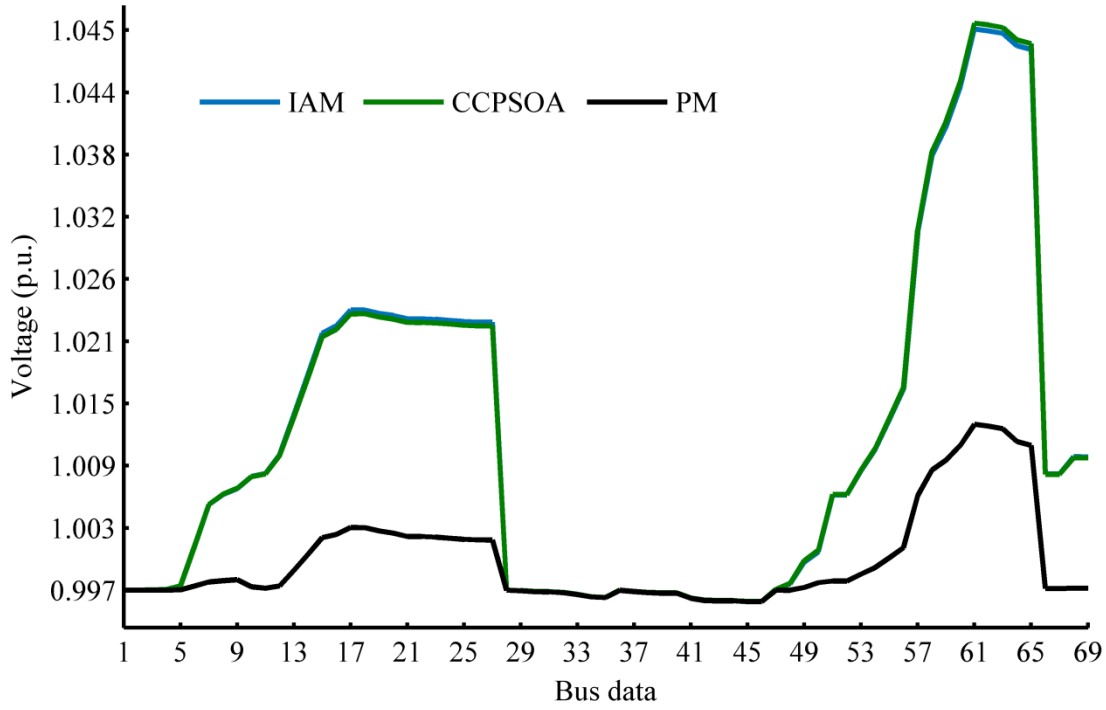

Figure 3.14: Voltage profile in the 69-bus system with three (Non-UPF) DERs

The results clearly show that the implementation of proposed method has reduced the energy losses and acceptably improved the voltage profile in three test systems. It is noticed that the Non-UPF DERs give a better reduction of energy losses as compared to UPF DERs by using to proposed algorithm. However, it is not applicable for other algorithm.

3.6 Conclusion

This chapter has proposed an approach for the multiple DERs planning considering the system energy loss minimization and voltage profile improvement as an objective which is solved by the PSO based algorithm. The results of the proposed method for allocation of unity and non unity power factor operated DER are compared with loss sensitivity factor, improved analytical method and constriction coefficient PSO approach in three different charactorestic test systems to check the validity of the proposed method. The proposed algorithm has compensated the drawback of conventional algorithms and achieves the best performance in time varying load profile of each radial distribution systems to provide more practical solution. The energy losses are reduced with increment the number of DERs in prescribed penetration by the proposed algorithm. However, other compared algorithms have not

followed the pattern. Therefore, the plannning of DERs accommdation is essential for amplification the system performance. It is found that the proposed method gives better results in terms of energy loss reduction. The positive impacts of optimally DERs allocate are also reflected regarding the improvement in voltage profile.

Chapter – 4

DISTRIBUTED ENERGY RESOURCES PLANNING IN MULTI-LOAD LEVEL

4.1. Introduction

Increasing energy demand is a major challenge in the future electrical power system as it is a precious key factor for the development of the economy. It is estimated that the power generation in upcoming decade will require the double capacity from current production [1]. The increasing load growth can be supplied by expanding the existing substation. Moreover, regulatory environment and technological innovations under forthcoming economy have resulted in a renewed interest in the DERs especially in the smart grid paradigm. Therefore, planners have filled the gap between supply and demand by renewable and non-renewable DERs. Integration of renewable source has reduced the dependency on fossil fuel; moreover, reduces the pollutant contents in the environment [163]. The conventional power system has turned into active distribution system after the interconnection of the DERs. Thus, the DER planning is important to minimize the future reconfiguration of the distribution service [27].

In the literature, most of the planning of the distribution systems is based on the peak load profile. However, multi-load levels construct the firm planning of the distribution system to minimize the energy losses [24]. Therefore, it is necessary to supply electrical power according to the load demand; otherwise, the network losses may increase in another load level. Therefore, it is an essential requirement to rigid planning in point of the demand side of the radial medium voltage distribution system.

The DFs and SCs can separately act and dominant to the power flow in the distribution system. However, the optimal accommodation of these modules is not individualistic. Moreover, the existence of one may influence the optimal allocation of the other and vice-versa. Simultaneous allocation strategy of DGs and SCs is to be investigated with the different constraints of distribution system. The optimal DGs and SCs allocation can improve the performance of the system in terms of reduction the power losses and improving node voltage of the system. However, non-optimal

accomodation may increase the system losses and impermissible voltage which is already validated in pervious chapter. Moreover, the private investor of DERs and power distribution utility are coordinated to find the optimal allocation of the DERs and gain technical and economical advantages [7]. Several optimization algorithms [2]-[158] have been used to determine the optimal allocation of DERs in the radial distribution system which is discribed in the chapter-2. The artificial intelligence based heuristic algorithms have greater diversity and exploration in a single as well as in multi-dimensional population(s). Further, momentum effect of the particles helps to achieve the faster convergence. However, some algorithm-specific control parameters are required to be tuned for the optimal solution. Therefore, this process becomes complicated and increases the computational time of convergence. Though, Teaching–Learning-Based Optimization (TLBO) algorithm is parameter-less optimization approach, which requires only number of maximum iteration and population size [164].

This chapter addresses the important issues of the distribution system with the DERs planning. Further, a new MG-TLBO algorithm is proposed with some alterations in basic TLBO for simultaneous optimal allocation of the DERs with SCs to minimize the energy loss while maintaining node voltage. The proposed algorithm is tested on the two standard 33-bus and 69-bus radial distribution systems and one practical 83-bus radial distribution system. To show the effectiveness of the proposed algorithm, the simulation results are compared with well-established algorithms such as ITLBO [24], PSO [82], ABC [143], KH [165], BFO [97], and BSO [166].

The salient contributions of the chapter are given below:

(i). The energy demand of the distribution system is addressed by optimal allocation of the DERs for multi-level load pattern.

(ii). The Modified Group-experience TLBO viz. MG-TLBO approach is proposed and used in this chapter. It is simple, generic and parameter-less algorithm. This algorithm incorporates some modifications in basic TLBO to achieve exemplary outcomes.

4.2. Problem Description

The power flow in presence of the DERs with optimal penetration at appropriate locations alters the radial distribution system which is the main reason to minimize the

energy loss while preserving better bus voltage profile. The benefits associated with the DERs mainly depend upon how optimally they are allocated in the radial distribution system.

The objective of the chapter is to minimizing the annual energy losses of the system in presence of the DERs for three load level pattern which is formulated as:

$$F = \max\left[\rho\left(\sum_{\tau=1}^{n_{lv}} P_{loss^b}^{\tau} * t_{\tau} - \sum_{\tau=1}^{n_{lv}} P_{loss^a}^{\tau} * t_{\tau}\right)\right] \tag{4.1}$$

where, $P_{loss^b}^{\tau}$ and $P_{loss^b}^{\tau}$ are the power losses of the load level with and without penetration of DERs, respectively. t_τ is time duration of each load level. n_{lv} is number of load level. ρ is the bus voltage deviation penalty factor, given by equation (4.2)

$$\rho = {}^{1}\Big/\left(1 + Max\left(\nabla V_{\beta}^{\tau}\right)\right) \qquad \forall \beta \in n_b,\ \forall \tau \in n_{\text{lv}} \tag{4.2}$$

Where,

$$\nabla V_{\beta}^{\tau} = \begin{Bmatrix} 0 & V_{\min} \le V_{\beta}^{\tau} \le V_{\max} \\ \text{large value multiplier} & \text{else} \end{Bmatrix} \tag{4.3}$$

The penalty factor helps to classify the solution into the feasible and non-feasible groups. The solutions that decline the system limits using decision penalty variable are called non-feasible solutions.

Total real power losses of the system can be compute by the following equation,

$$P_{loss} = \left(\sum_{\alpha=1}^{n_n} \sum_{\beta=\beta+1}^{n_b} \text{Re}\left(\frac{P_{\alpha}^2 + Q_{\alpha}^2}{V_{\alpha}^2} \times Z_{\alpha\beta}\right)\right) \tag{4.4}$$

where, I_α is current injection at α^{th} node. $Z_{\alpha\beta}$ is branch impedance between α^{th} and β^{th} node of the system.

4.2.1 Power Flow Constraint

The total power supplied by the grid utility and generation of distributed energy resource should be balanced with power losses and demand of the distribution system.

$$P_{\alpha+1} = P_{\alpha} - R_{\alpha\beta}\frac{P_{\alpha}^2 + Q_{\alpha}^2}{V_{\alpha}^2} - P_{Grid,\alpha}^{\tau} \qquad \forall \alpha \in n_n, \forall \beta \in n_b, \forall \tau \in n_l$$

$$
\begin{aligned}
&Q_{\alpha+1} = Q_{\alpha} - X_{\alpha\beta}\frac{P_{\alpha}^{2}+Q_{\alpha}^{2}}{V_{\alpha}^{2}} - Q_{Grid,\alpha}^{\tau} \qquad \forall \alpha \in n_n, \forall \beta \in n_b, \forall \tau \in n_l \\
&P_{Grid,\alpha}^{\tau} = \sum_{\beta=1}^{n_b} P_{loss}^{\tau} - \sum_{\alpha=2}^{n_n} P_{DGs}^{\tau} \qquad \forall \alpha \in n_n, \forall \beta \in n_b, \forall \tau \in n_l \\
&Q_{Grid,\alpha}^{\tau} = \sum_{\beta=1}^{n_b} Q_{loss}^{\tau} - \sum_{\alpha=2}^{n_n} Q_{SCs}^{\tau} \qquad \forall \alpha \in n_n, \forall \beta \in n_b, \forall \tau \in n_l
\end{aligned} \tag{4.5}
$$

where, P_{Grid} and Q_{Grid} is total active and reactive supplied by the grid substation. The generation of active and reactive power from distributed energy resources is denoted by P_{DGs} and Q_{SCs}, respectively. P_D and Q_D is active and reactive load demand of the system for each load level.

4.2.2 Distribution Line Thermal Limit

The thermal capacity of the distribution feeder of the network transcends their permissible value.

$$\left|S_{\alpha\beta}\right| \le \left|S_{line}^{\max}\right| \tag{4.6}$$

where, $S_{line}^{\max}$ is a maximum allowable limit of the distribution line, and $S_{\alpha\beta}$ is power flow capacity of the branch between bus α^{th} and bus β^{th}.

4.2.3 Node Voltage Constraint

Node voltage must operate within the maximum and minimum permissible region according to the regulations of the distribution system which is usually five percentages from the rated value.

$$V_{\min} \le V_{m} \le V_{\max} \tag{4.7}$$

4.2.4 Bus Compensation Limit

The DGs and SCs unit size is considered only in the permissible operating region as per equation (4.8).

$$
\begin{aligned}
&P^{\min} < P_{DGs} \le P^{\max} \\
&Q^{\min} < Q_{SCs} \le Q^{\max}
\end{aligned} \tag{4.8}
$$

where, $P^{\min}$ and $P^{\max}$ are lower and upper limit of the DGs size. Similarly, $Q^{\min}$

and Q^{max} are also lower and upper bound for injected reactive power by shunt capacitor, whereas P_{DGs} and Q_{SCs} value should not exceed to the comparable reference either during the initialization or updating process of optimization.

4.2.5 Network Compensation Limit

Total active (P_{DGs}) and reactive power injection (Q_{SCs}) by the DGs and SCs must be less than the active (P_D) and reactive demand (Q_D) of the network, respectively.

$$\begin{aligned} &\sum_{\alpha=2}^{n_n} P_{DGs,\alpha} \le P_D \\ &\sum_{\alpha=2}^{n_n} Q_{SCs,\alpha} \le Q_D \end{aligned} \tag{4.9}$$

The candidate site (*loc*) of each the DGs and SCs should not repeat in every iteration which is defined as

$$\begin{aligned} &loc_{\alpha}^{DERs} = loc_{\alpha+1}^{DERs} \quad \alpha \in n_n, \alpha \neq 1 \\ &loc_{\alpha}^{SCs} = loc_{\alpha+1}^{SCs} \quad \alpha \in n_n, \alpha \neq 1 \end{aligned} \tag{4.10}$$

In this chapter, the MG-TLBO algorithm has been proposed to optimize the size, site and number of the DERs in described formulation to minimize the energy losses for three load level with satisfying the all constraints of power system.

4.3. Proposed Modified Group-experience of Teaching Learning Based Optimization Approach

The MG-TLBO is proposed and sequentially explained with basic methodology of TLBO in the following section.

4.3.1 Basic Teaching Learning Based Optimization

The basic TLBO is introduced by Rao in [164]. This population-based algorithm is proposed to obtain the optimum and global solutions for continuous non-linear functions with high consistency and less computational efforts. The process of this algorithm is inspired by the Teaching-Learning process. It is based on the impact of a teacher on the results of learners in the classroom. This prime characteristic of TLBO is dissimilar from other optimization techniques. This algorithm does not require any

specific parameter and it needs only population size and maximum number of iterations. Therefore, TLBO can be said as an algorithm-specific parameter-less algorithm. In this heuristic algorithm, a group of tentative solutions as learners is considered as population and different subjects offered to the learners are considered as different design variables of the optimization problem. Further, learners first acquire knowledge from the teacher and thereafter it interacts with other learners. It uses the mean value of population to update the solution. Moreover, this algorithm has a temptation to accept the best solution through the iterative process. Therefore, the best learner is considered as the final solution. The process of TLBO is divided into two parts, 'Teacher phase' and 'Learner phase'. The process of both these phases is summarized below.

4.3.1.1. Teacher Phase: In the teacher phase, the mean result of the population is used to achieve the optimal solution. A teacher tries to obtain the best mean result from the existing mean result of a class in every subject. Improvement in results depend upon his/her capability of teaching. Therefore, the quality of teacher affects the grades of learners.

It is assumed that the teacher has the highest knowledge in a class. Therefore, he imparts the knowledge to all learners. The best scoring learner for each design variable among all learners is nominated as a 'Teacher'. The performance of the learners is assessed by computing the difference between the score of the $Teacher_{ik}$ and average score ($Mean_{ik}$) of all learners in each subject as stated in equation (4.11).

$$Difference_{ik} = rand * (\mathrm{Teacher}_{ik} - \mathrm{T}_F * \mathrm{Mean}_{ik}) \quad \forall i \in N_p, \forall k \in N_d \tag{4.11}$$

where, *rand* generates a random number between 0 and 1. T_F is not a parameter of the TLBO algorithm. The value of T_F is not given as an input to the algorithm and its value in TLBO method is evaluated by the equation (4.12) by rounding off the value.

$$T_{F_i} = round(1 + rand) \tag{4.12}$$

Now, the teacher enhances the performance of each learner by updating its Pop_{old} using equation (4.13).

$$Pop_{new_{ik}} = Pop_{old_{ik}} + Difference_{ik} \tag{4.13}$$

Further, the performance of the learner is re-evaluated. The learners showing improvement in the score are allowed to retain newer population; otherwise it is reversed to keep older population.

4.3.1.2. Learner Phase: In the learner phase, learners acquire more knowledge through interaction with other randomly selected learners in the class. The exchange of knowledge among the learners enhances their results. The learning phenomenon of learner phase is explained as follows:

In each iteration, every learner Pop_i is compared with a randomly selected learner Pop_{r}. Whenever, Pop_{r} has more knowledge and new things from Pop_i, then their difference will be added in the learner's achievements as expressed in (4.13).

$$Pop_{new_{ik}} = Pop_i + (Pop_i - Pop_r) \tag{4.14}$$

However, Pop_i has more knowledge and new things from $Pop_{r,}$ then the difference will be added in selected learner as given in equation (4.15).

$$Pop_{new_{ik}} = Pop_i + (Pop_r - Pop_i) \tag{4.15}$$

The above process and evaluation are used to minimize the objective function. Further, Pop_{new} gives better function value to previous function value then accept randomly selected learner otherwise retain the previous learner.

4.3.2 Modified Group-experience of TLBO

Modified Group experience of Teaching Learning Based Optimization (MG-TLBO) is an improved variant of basic TLBO. However, TLBO is an efficient and popular optimization algorithm [24], [164]. Though, it has few drawbacks such as slow convergence speed and weak learning ability. Moreover, a robust optimization algorithm establishes a balance between exploration and exploitation. Further, exploration affects the search regions of the optimal solution and exploitation refers the converging speed. However, the premature convergence may occur due to the presence of multiple local optimal solutions for solving the complex problems. Therefore, MG-TLBO is proposed with some modifications to improve the ability and performance of the algorithm for global search, and avoid premature convergence. The modifications in generalized TLBO are described as:

4.3.2.1. Grouping Mechanism to Enhance the Diversity: In the MG-TLBO, learners are divided into small sized groups as shown in Figure 4.1. The learners share their knowledge in the groups. In the basic TLBO, only two learners share their knowledge at a time. Therefore, limited knowledge is circulated in a class during prescribed time. Further, the proposed MG-TLBO creates more interaction among learners in each group. However, all groups should have at least two learners. The quantity of group members can increase the learning level and gain more knowledge. A number of students study with the discussion in a group. As a consequence, performance can be enhanced and achieve a good mean score of the class. In each group, every student learns by each other and shares their knowledge. Two mechanisms are mostly used to implement learners in the groups as explained below:

- In the first mechanism, randomly choose 'm' learners from the class and group them.
- The second process is based on Euclidean distance. In this technique, population is sorted in descending order of grades and the distance between the first student and other students is computed. Further, initial 'm' learners are kept in a group and next 'm' learners in another group and so forth.

4.3.2.2. Teacher Phase of MG-TLBO: The mechanism of basic TLBO slows the speed of convergence. Therefore, modification has been incorporated in teaching phase of TLBO as given below

(i) Teaching factor (T_F): T_F is evaluated by equation (4.16). It helps to find the better solution in minimum time. It creates an area which has an optimal solution and MG-TLBO searches the solution in this area so it consumes minimum time than basic TLBO.

$$T_{F_i} = F_{\mathrm{Re}sult_i} \Big/ F_{\mathrm{Re}sult_t} \qquad \forall i \in N_p \tag{4.16}$$

***(ii) Learner modification*:** In basic TLBO, students update their knowledge from the teacher and compute the difference from the mean of the class. Therefore, premature convergence may occur. In the proposed method, difference mean has been calculated by mean of the group instead of class mean to rid from that situation. Further, it enhances the search region and explorative nature which improves the diversity of population in MG-TLBO.

$$Pop_{new_{ik}} = Pop_{old_{ik}} + rand * (\text{Teacher}_{ik} - \text{T}_F * GrpMean_{ik}) \quad (4.17)$$

***(iii) Learning Experience*:** Two learners are randomly selected (Pop_i and Pop_k) from groups and modified according to a perfectionist. Whenever Pop_j is better than Pop_i then Pop_i is modified with equation (4.18) otherwise modified as per equation (4.19).

$$Pop_{new_{ik}} = Pop_{old_i} + rand * (\text{Teacher}_{ik} - Pop_{old_k}) \quad (4.18)$$

$$Pop_{new_{ik}} = Pop_{old_i} + rand * (\text{Teacher}_{ik} - Pop_{old_i}) \quad (4.19)$$

4.3.2.3. Learner Phase of MG-TLBO: The learning phase of basic TLBO has got some modifications which are incorporated in the MG-TLBO. The subsequent modifications in the learning phase of MG-TLBO are highly impacted by better performance for optimal planning of DERs.

***(i) Learning Factor*:** In the learning phase of TLBO, two learners are randomly selected and gain knowledge from each other. However, MG-TLBO uses learning factor for the better performance of entire class that reduces the time consumption and gain more knowledge. L_F can be evaluated by following equation

$$L_F = Pop_r.result / Pop_i.result \quad (4.20)$$

***(ii) Learner modification*:** Each learner can grasp more knowledge from the best knowledgeable learner (Pop_g^{best}) in a group. It also creates a new search region which is closest and achieves the optimal solution with less computation effort.

Suppose a group of 5 learners is *GP*, a learner Pop_g is selected from this group *GP*, the group of members is randomly selected. Further, the selected learner has more knowledge and experience than other members of *GP*. Therefore, the selected learner is the best learner or the teacher of the group. Except for Pop_g learner, all member of *GP* learn and follow the direction of the best learner. It means learning ability of that learner is accepted by others and improved the grades. This process is done for all groups simultaneously.

$$Pop_{new_g} = Pop_g + rand * (Pop_g^{best} - L_F * Pop_g) \quad (4.21)$$

where, Pop_g^{best} is the best learner of group/high-level learner of group Pop_g and a new set of improved learners are obtained. Learning process is based on the best learner of each group. Therefore, convergence speed is improved.

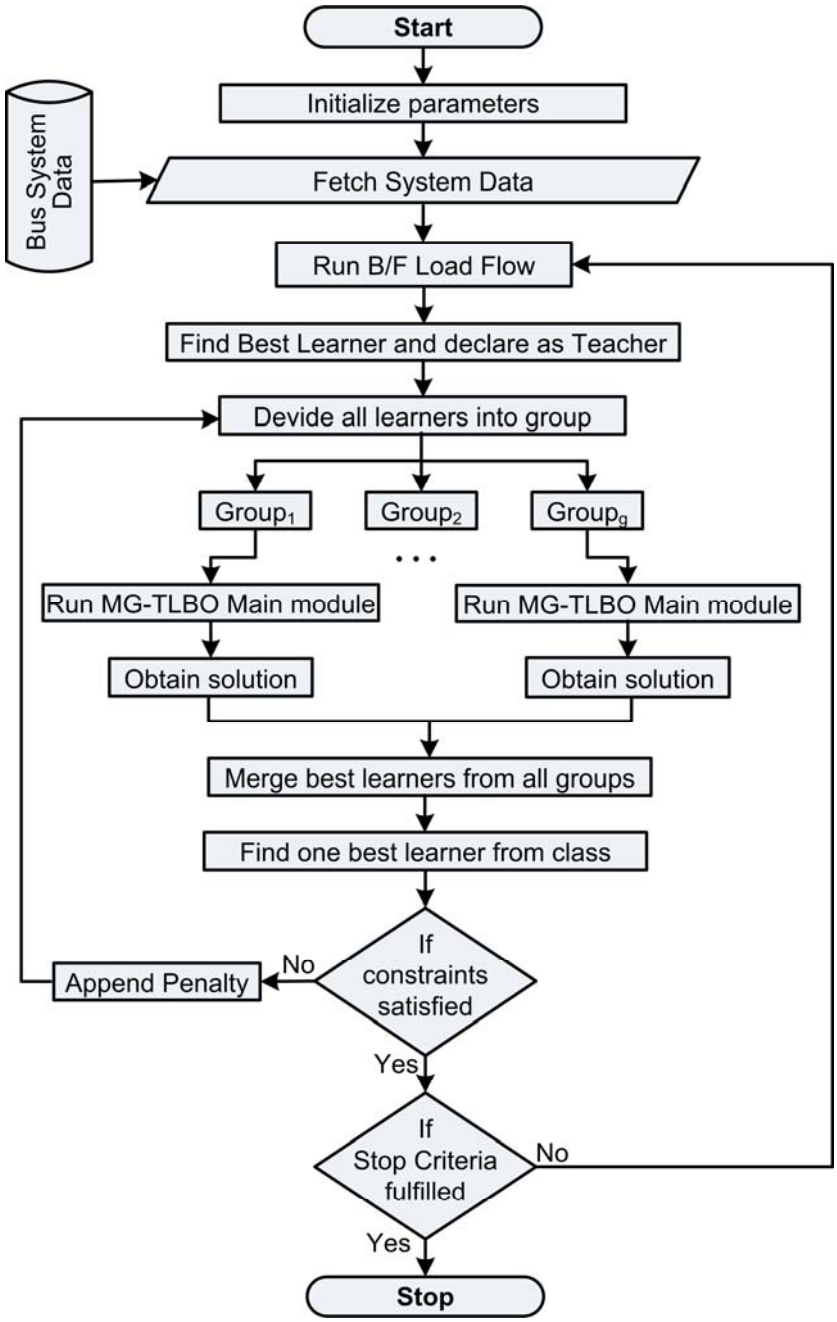

Figure 4.1: Flowchart of the proposed algorithm for allocation of DERs

***(iii) Mutation and Crossover for Diversity*:** The proposed algorithm uses the mutation operations which is similar to differential evolution as shown in Figure 4.2. It is a strategy to diversify the learners for improving the ability of searching the global solution. In this process, three students are randomly selected from the updated population by learner phase.

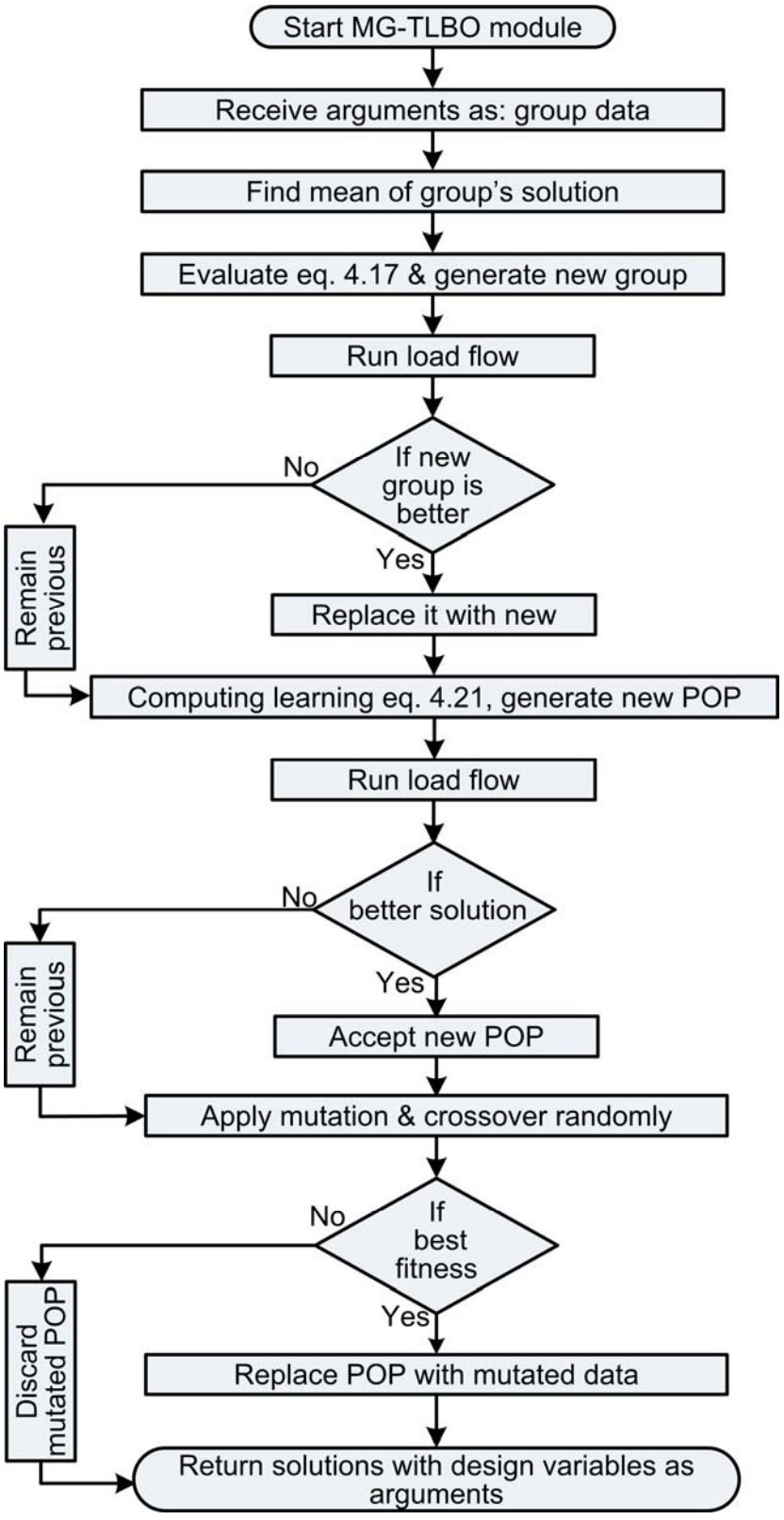

Figure 4.2: Flowchart of the proposed MG-TLBO algorithm

Further, mutation is done as

$$Pop_{mut} = Pop_{r1} + rand * (Pop_{r2} - Pop_{r3}) \tag{4.22}$$

Crossover is the next process of mutation. This process turned the adjustability in mutation phase. The implementation of Pop_{new} is done as per the expression given in equation (4.23).

$$Pop_{new} = \begin{pmatrix} Pop_{mut} & if\ rand_1 <= rand_2 \\ Pop_i & else \end{pmatrix} \tag{4.23}$$

where, $rand_1$ and $rand_2$ are random numbers which decide the value of Pop_{new}. Further, Pop_{new} is accepted if it gives a better solution than Pop_{old}.

4.3.3 Implementation of MG-TLBO for DERs Accommodation

In this paper, MG-TLBO is applied to find the optimal size as well as location of DERs to minimize the annual energy losses while maintaining the bus voltage, generation constraints, power balance and power flow capacity within the prescribed limits of a given power system. The performance of the distribution system is calculated after placing the DERs (which have the optimal size) at the optimal position as a reduction of the real power loss and enhancement of voltage profile.

The step-by-step process of MG-TLBO implementation for solving the problem of optimal DERs allocation is expressed as following:

Step 1. Initialize the MG-TLBO variables/common control parameters and define the objective problem as:

- Number of learners/populations N_{p} = 10 (case study 1 and 2) / 20 (case study 3)
- Decision Parameters: S_{z}, S_{t} (S_{z} :DER Size, S_{t} : DER Site)
- Number of design variables/ Subjects of learners (DERs) N_{d} = 3 (case study 1 and 2) / 5 (only linear load case study 3) / 9 (altered case study 3)
- Iteration (number of generations) K^{max} = 300
- Limits of subjects' grades: $L_{\text{L}} \leq S_{\text{z}}$, $S_{\text{t}} \geq U_{\text{L}}$; U_{L}-Upper limit, L_{L}- Lower Limit.

U_{L} and L_{L} for S_{z} will be initialized according to the calculated demand value. Further, U_{L} and L_{L} for S_{t} depend upon the number of buses in the system.

The objective function as defined in equation (4.24) will be maximized by this algorithm.

$$Maximize\ f(X) = \left(\sum_{\tau=1}^{n_{lv}} E_b^{\tau} - \sum_{\tau=1}^{n_{lv}} E_a^{\tau} \right) \tag{4.24}$$

f(X) is the objective function to compute the annual energy loss reduction in the distribution system with and without harmonics.

Step 2. Generate the different size and site of DERs as Pop_{ik} randomly which satisfies the constraints of decision variable. It is expressed as:

$$Pop_i = DERs(S_z, S_t) \qquad \forall i \in N_p \tag{4.25}$$

$$Pop_i.\mathrm{Sz}_k = \{DERs\ size : \Omega \to k\} \qquad \forall k \in N_d, \quad \forall i \in N_p \tag{4.26}$$

$$Pop_i.\mathrm{St}_k = \{DERs\ location : \Omega \to k\} \qquad \forall k \in N_d, \quad \forall i \in N_p \tag{4.27}$$

The population for every decision variable is represented as:

For S_z Decision parameter For S_t Decision Parameter

$$Pop.S_z = \begin{pmatrix} x_{1,1} & x_{1,2}..... & x_{1,\mathrm{N}_d} \\ x_{2,1} & x_{2,2}..... & x_{2,\mathrm{N}_d} \\ x_{N_p,1} & x_{3,2}..... & x_{N_p,\mathrm{N}_d} \end{pmatrix} \qquad Pop.S_t = \begin{pmatrix} x_{1,1} & x_{1,2}..... & x_{1,\mathrm{N}_d} \\ x_{2,1} & x_{2,2}..... & x_{2,\mathrm{N}_d} \\ x_{N_p,1} & x_{3,2}..... & x_{N_p,\mathrm{N}_d} \end{pmatrix} \tag{4.28}$$

Step 3. Evaluate the objective function $f(X)$, which computes the annual energy losses of the system, for all population Pop_i. This Paper has used the backward-forward load flow to determine the network parameter of the original system and applied harmonic load flow to compute the harmonic distortion in the radial distribution system.

$$F_{Result_i} = f(X) \tag{4.29}$$

$$St.\ to \quad V_{\mathrm{m}}, THD_v, S_{\mathrm{line}}, I_{\mathrm{limit}} \tag{4.30}$$

Step 4. In teaching phase, select a learner who gives the best solution from Pop_i according to the solutions F_{Result_i} of all learners and assign it as the Teacherik of the class. Further, apply the grouping mechanism as described in section 4.3.1 and divide all learners into groups. Moreover, instead of computing the mean of class, determine the group mean ($Mean_{ik}^{Grp}$) for all design variables of the learners' group.

$$Mean.S_{z_k}^{Grp} = \ mean(\mathrm{Sz}_k^g) \quad \forall k \in N_d \tag{4.31}$$

$$Mean.S_{t_k}^{Grp} = \ mean(\mathrm{St}_k^g) \quad \forall k \in N_d \tag{4.32}$$

$$Teacher.S_z = Size\ of\ best\ Solution\ (F_{Result_i}) \tag{4.33}$$

$$Teacher.S_t = Site\ of\ best\ Solution\ (F_{Result_i}) \tag{4.34}$$

Step 5. Evaluate the difference between existing mean ($MeanSz_k^{Grp}$, $MeanSt_k^{Grp}$) and intelligent student of class ($Teacher.Sz_k$, $Teacher.St_k$) for the each design variable as following

$$Diff_k^{Sz} = rand * (\mathrm{Teacher.Sz}_k - \mathrm{T}_F * Mean.Sz_k^{Grp}) \tag{4.35}$$

$$Diff_k^{St} = rand * (\mathrm{Teacher.St}_k - \mathrm{T}_F * Mean.St_k^{Grp}) \tag{4.36}$$

$T_{\mathrm{F},}$ is evaluated through

$$T_{F_i} = F_{Result_i} \big/ F_{Result_t} \tag{4.37}$$

$$F_{Result_i} \to \forall i \in N_p \;\; F_{Result_t} \to t \in Teacher \tag{4.38}$$

Step 6. Modify subjects' grades (for all decision parameters of DERs) of every learner using the concept of teacher phase which is expressed as

$$Pop_{New} \cdot Sz_k = Pop_{Old} \cdot Sz_k + Diff_k^{Sz} \tag{4.39}$$

$$Pop_{New} \cdot Sz_k = Pop_{Old} . Sz_k + Diff_k^{Sz} \tag{4.40}$$

Now, compute the optimization function *f(X)* for new updated values of learners ($Pop_{New} \cdot Sz_k$ and $Pop_{New} \cdot St_k$). Further, newly generated values of learners will be accepted, whenever it gives the better solution to $Pop_{old_{ik}}$.

Step 7. In this step, Pop_i and Pop_k are randomly selected from newly generated population via step 6. Whenever, Pop_k is better from Pop_i , then Pop_i is modified with equation (4.18) otherwise equation (4.19). The updated population will be accepted when updated solution is better than the previous solution.

Step 8. In learner phase, again apply the grouping mechanism. Improve the grades of each learner using the process of learning phase as discussed in section 4.2 as learners increase their knowledge through mutual interaction to each other. Further, select two learners randomly and compare to each other in a group. In all group, more

intelligent learner share the knowledge to all learner in that group. Equation (4.20) and (4.21) are used to compute $Pop_{New_{ik}}$. The qualified population in learner phase will be updated when the student achieves the good score than previous grades.

Step 9. In the mutation and crossover phase, three learners are randomly selected from a qualified population which is produced by mutual iteration of the students in step 8. Further, mutated population (Pop_{mut}) is determined in equation (4.22). Thereafter, crossover process is performed on the mutated population by equation (4.23). Moreover, enumerate the fitness value for Pop_{new} and replace the Pop_{old} when it obtains the better solution.

Step 10. Subsequently, apply the constraint handling mechanism to check the limits of the updated decision parameters, whenever it is not satisfied, then again randomly generate S_z and S_t of the learner. Moreover, assure the modified DERs have not repeated location. If it is repeated then remove their duplicity through generating a new S_t randomly.

Step 11. Terminate/Stop, if the maximum number of generation 'K^{max}' is achieved and print the optimal result. Otherwise, repeat from the step number 4 and run the whole process until stopping criterion is not satisfied.

4.4. Investigation of MG-TLBO on Standard Mathematical Benchmark Functions

In order to verify the effectiveness of the MG-TLBO algorithm, a few different experiments have been conducted on 15 unconstrained benchmark functions and 5 constrained benchmark functions of CEC 2006 [167]. The proposed algorithm is performed on each benchmark function and results compared with previously published experimental results.

4.4.1 Unconstrained Benchmark Function

The best obtained solution of the proposed algorithm is compared with heuristic algorithms as ABC [168], PSO [169], and DE [169] to evaluate the performance. The number of design variables and search region are different for each benchmark function. The comparison and details of this algorithm are shown in Table 4.1. Each unconstrained benchmark functions have two types of characteristics which are uni-modality or multimodality and separable or non-separable.

Table 4.1: Comparative study of the proposed algorithm on benchmark functions

S. No.	Function	*Chr /Dim*	Index	PSO	DE	ABC	MG-TLBO
1.	Sphere	US/30	Mean	0	0	0	0
			SD	0.00E+00	0.00E+00	0.00E+00	0.00E+00
2.	Ackley	MN/30	Mean	0.1646	0	0	0
			SD	0.4938	0.00E+00	0.00E+00	0.00E+00
3.	Sum Squares	US/30	Mean	0	0	0	0
			SD	0.00E+00	0.00E+00	0.00E+00	0.00E+00
4.	Beale	UN/5	Mean	0	0	0	0
			SD	0.00E+00	0.00E+00	0.00E+00	0.00E+00
5.	Easom	UN/2	Mean	-1	-1	-1	-1
			SD	0.00E+00	0.00E+00	0.00E+00	0.00E+00
6.	Matyas	UN/2	Mean	0	0	0	0
			SD	0.00E+00	0.00E+00	0.00E+00	0.00E+00
7.	Colville	UN/4	Mean	0	0.04091	0.0929674	0
			SD	0.00E+00	0.0820	0.066277	0.00E+00
8.	Rosen-brock	UN/30	Mean	15.08862	18.2039	0.08877	1.62E-05
			SD	24.17020	5.03619	0.07739	3.34E-05
9.	Schwefel 2.22	MS/2	Mean	0	0	0	0
			SD	0.00E+00	0.00E+00	0.00E+00	0.00E+00
10.	Branin	MS/2	Mean	0.397887	0.39789	0.3978874	0.3978873
			SD	0.00E+00	0.00E+00	0.00E+00	0.00E+00
11.	Booth	MS/2	Mean	0	0	0	0
			SD	0.00E+00	0.00E+00	0.00E+00	0.00E+00
12.	Gold Stein-Price	MN/2	Mean	3	3	3	3
			SD	0.00E+00	0.00E+00	0.00E+00	0.00E+00
13.	Griewank	MN/5	Mean	0.017391	0.00148	5.82E-06	0
			SD	0.020808	0.00296	3.13E-05	0.00E+00
14.	Rastrigin	MS/5	Mean	43.97714	11.7168	0	0
			SD	11.728676	2.53817	0.00E+00	0.00E+00
15.	Schwefel	MS/5	Mean	-6909.136	-10266	-12569.48	-12569.5
			SD	457.9578	521.849	0.00E+00	0.00E+00

The proposed algorithm is required less functional evaluations as comparison with DE, GA, PSO, and ABC. The number of functional evaluation of 50000 is evaluated for this experiment.

4.4.2 Constrained Benchmark Function

The five constrained benchmark function are considered and compare the performance with heuristic algorithms as ABC [168], PSO [169], DE [169], and GA [169]. In this computation process, population size and number of generation are 50 and 100 for proposed algorithm, respectively. However, each compared algorithm is obtained the final solution with greater than or equal to proposed algorithm's number of generation and population size. The features and results of benchmark functions are described individually as:

***(i). Benchmark Function-1 (BF-1)*:** it is minimized with thirteen design variables, nine linear inequality constraints and six active constraints. The Proposed algorithms find the better result and mean solution than other considered algorithm which is described in Table 4.2 . The optimum solution for this BF-1 is

$f(x) = -15$

$x_i = (1\ 1\ 1\ 1\ 1\ 1\ 1\ 1\ 1\ 3\ 3\ 3\ 1)$, where $i = 1 \ldots N_d$.

***(ii). Benchmark Function-2 (BF-2)*:** it is minimization problem which have five design variable, six inequality constraints and two active constraints. The optimum solution for the function is

$f(x) = -30665.538$

$x_i = (78, 33, 29.9953, 45, 36.7758)$

***(iii). Benchmark Function-3 (BF-3)*:** it is also minimize with two design variable, two linear inequality constraints, and two active constraints. The proposed algorithm is achieved the function value is

$f(x) = -6961.8138$

$x_i = (14.095, 0.84296)$

***(iv). Benchmark Function-4 (BF-4)*:** it is determined the best optimal solution with two design variable and two linear inequality constraints by the proposed algorithm. The optimum solution is

$f(x) = -0.0958250$

x_i = (1.228, 4.2454)

***(v). Benchmark Function-5 (BF-5)*:** it is obtained the global solution by the proposed algorithm with two design and linear inequality constraints. The optimum solution for this function is

f(x) = -5.50801327

x_i = (2.329520197, 3.178493074)

The proposed algorithm is applied on each function and obtained the best fitness value as compare to GA, ABC and PSO algorithm. The comparison of algorithm for each constrained function is shown in Table 4.2.

Table 4.2: Comparative results of constrained benchmark functions

Function	Algorithms	Optimum	Best	Mean	SD
BF-1	GA	-15	14.44	14.236	NA
	ABC		-15	-15	NA
	PSO		-15	-14.71	NA
	MG-TLBO		-15	-15	0.00E+00
BF-2	DE	-30665.54	-30665.539	-30665.536	5.07E-03
	ABC		-30665.539	-30665.54	0.00E+00
	PSO		-30663.86	-30570.93	8.10E+01
	MG-TLBO		-30665.54	-30665.54	1.38E-11
BF-3	DE	-6961.814	-6961.814	-6961.814	NA
	ABC		-6961.814	-6961.813	2.00E-03
	PSO		-6961.814	-6961.814	6.50E-06
	MG-TLBO		-6961.814	-6961.814	1.469E-11
BF-4	GA	-0.092825	-0.095825	-0.095825	2.70E-09
	ABC		-0.095825	-0.095825	0.00E+00
	PSO		-0.095825	-0.094525	9.40E-03
	MG-TLBO		-0.095825	-0.095825	1.288E-17
BF-5	DE	-5.508013	-5.508013	-5.508013	NA
	ABC		-5.508013	-5.508013	NA
	PSO		-5.508013	-5.508013	NA
	MG-TLBO		-5.508013	-5.508013	0.00E+00

The basis of above results obtained, it can be concluded that the MG-TLBO method has been working efficiently and effectively on these test functions.

4.5. Simulation Results and Discussion

In this section, proposed methodology has been tested on the benchmark 33-bus [48], 69-bus [48], and 83-bus practical radial distribution system of Taiwan Power Company [141]. The each system line and bus data with line diagram is described in Appendix-A. The results of PSO and ITLBO [24] are compared with proposed algorithm in each distribution system. The yearly load profile is assumed to be piecewise segmented in three different load level, i.e., light (L), nominal (N), and peak (P) which is 50, 100 and 160 percentage of the nominal system load, respectively. The hourly duration of the corresponding load level is chosen as 2000, 5260, and 1500 hours in a year, respectively. The backward/forward power flow method is used for load flow of the radial distribution networks.

The proposed algorithm has been tested on each system and compared the results with well-established PSO and ITLBO based algorithm which are described in case I and case II for all the test systems. The comparison of the proposed algorithm result is divided into two cases as case-III and case-IV. In the first circumstance, location is same with as ITLBO algorithms' result. Moreover, size is optimized by proposed algorithm that is shown in case-III. In the second experimental condition, applied algorithms will optimize the size and location of the DERs as present in case-IV. Further, comparisons of all four cases are distinguished in each test system. However, the site of DERs are same for each load level in all three test systems and it is a realistic approach to DER planning in the radial distribution system.

4.5.1 *33-Bus Distribution System*

The standard 33-bus distribution system has been used to validate the proposed method. This system originates from a substation and spreads to different types of consumer loads. Total peak demand of system is 4.37 MVA, and the average power factor is 0.8502. In this system, all data have been used in per unit whereas the base value of power and voltage is 100 MVA and 12.66 kV, respectively.

The DERs have obtained the best size for each load level in case-III with the same location of the case-II after 100 autonomous trails. Further, the proposed method achieves the largest annual energy loss reduction. Moreover, the proposed method has been applied to optimize the both site and size of the DERs in the fourth case and achieve the more reduction of annual energy losses as compared to the others cases.

The decision parameters of all the cases and the corresponding performance for this case study are presented in Table 4.3. These parameters are enhanced the system performance as shown in Table 4.4.

Table 4.3: Optimal performance parameters for the 33-bus test system

Cases	Load Level	Optimal dispatches of DGs (kW) / SCs (kVAr)
I	Light	33(511), 14(314), 24(589) / 30(300), 17(100), 28(300)
	Nominal	33(819), 14(784), 24(1111) / 30(500), 17(400), 28(600)
	Peak	33(1167), 14(1011), 24(727) /30(700), 17(600), 28(400)
II	Light	14(374), 24(540), 30(517) / 15(200), 24(300), 30(500)
	Nominal	14(747), 24(1074), 30(1054) / 15(300), 24(500), 30(1000)
	Peak	14(823), 24(1074), 30(1067) / 15(300), 24(600), 30(1200)
III	Light	14(374), 24(540), 30(517) / 15(200), 24(300), 30(500)
	Nominal	14(747), 24(1074), 30(1054) / 15(300), 24(500), 30(1000)
	Peak	14(1142), 24(558), 30(1175) /15(500), 24(400), 30(1300)
IV	Light	13(388), 30(516), 24(534) / 30(500), 25(200), 14(200)
	Nominal	13(780), 30(1030), 24(1064) / 30(1000), 25(400), 14(300)
	Peak	13(1175), 30(1295), 24(501) / 30(1300), 25(300), 14(500)

Table 4.4: Comparison of the system performance for the 33-bus test system

Cases	Load Level	P_{loss} (kW)	V_{min} (p.u.)	Annual E_{loss} (MWh)	Annual E_{loss} Reduction (%)
I	Light	5.16	0.9935	254.20	87.43
	Nominal	20.17	0.9901		
	Peak	92.17	0.9620		
II	Light	3.02	0.9963	191.83	90.52
	Nominal	11.94	0.9911		
	Peak	81.99	0.9500		
III	Light	3.02	0.9963	174.21	91.38
	Nominal	11.94	0.9911		
	Peak	70.25	0.9625		
IV	Light	2.97	0.9964	170.67	91.57
	Nominal	12.09	0.9912		
	Peak	67.43	0.9665		

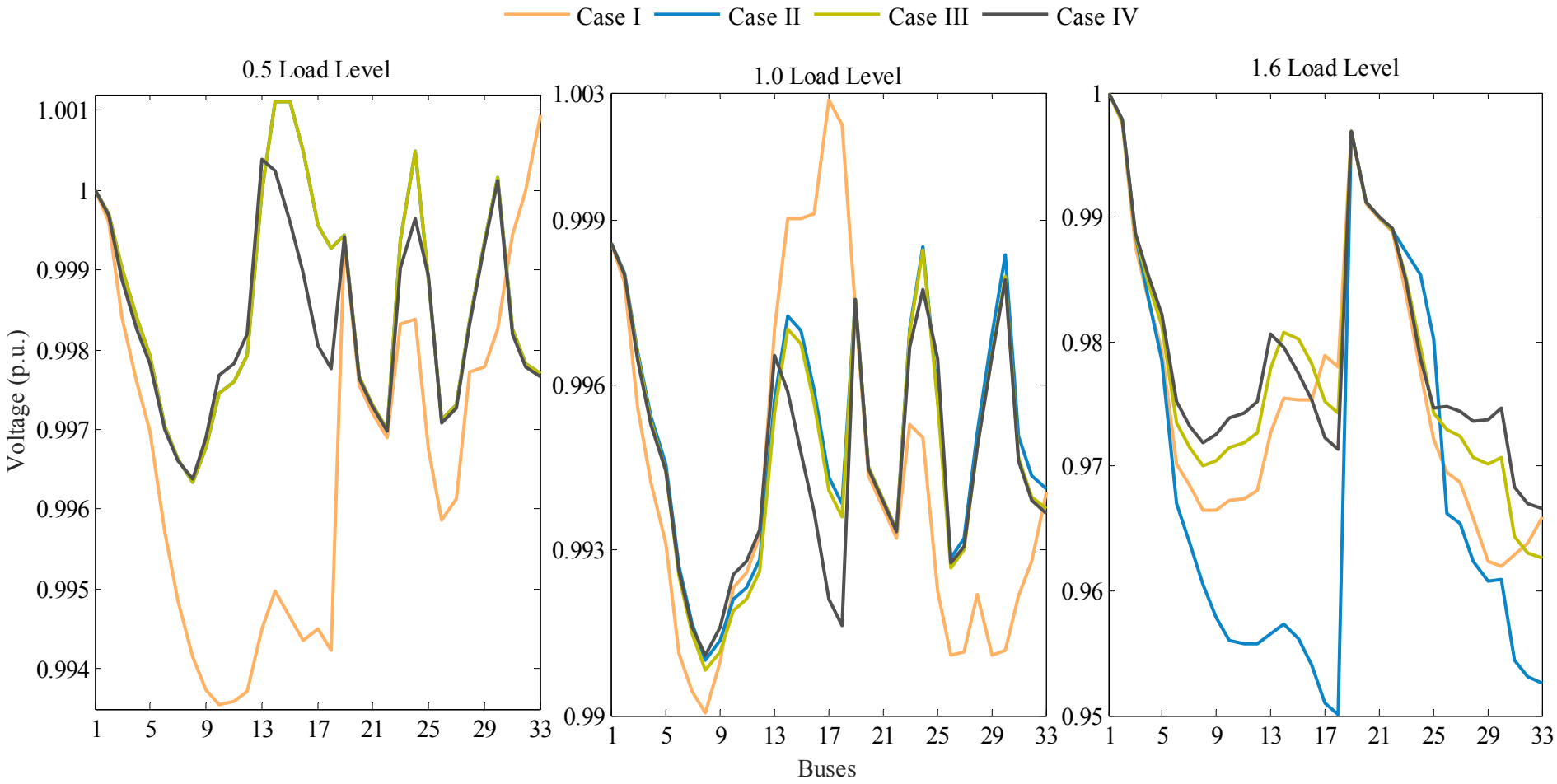

Figure 4.3: Bus voltage profile of the IEEE 33-bus system for each load level

In the fourth case, losses are increased as compared to case-II and case-III for nominal load level. However, other two load level losses are lower as compared to the second and third cases and it shows the most optimistic value of the DERs in this test system. The PSO algorithm obtained the worst parameter which achieved the highest losses in each load level as compared to all cases.

Figure 4.3 depicts the comparison the bus voltage profile for each load level and all cases of this test system. In case-II, voltage profile in peak load level has laid on the boundary of voltage regulation limit which is not optimistic planning. However, proposed method has been achieved the significant improvement in the bus voltage profile in each load level.

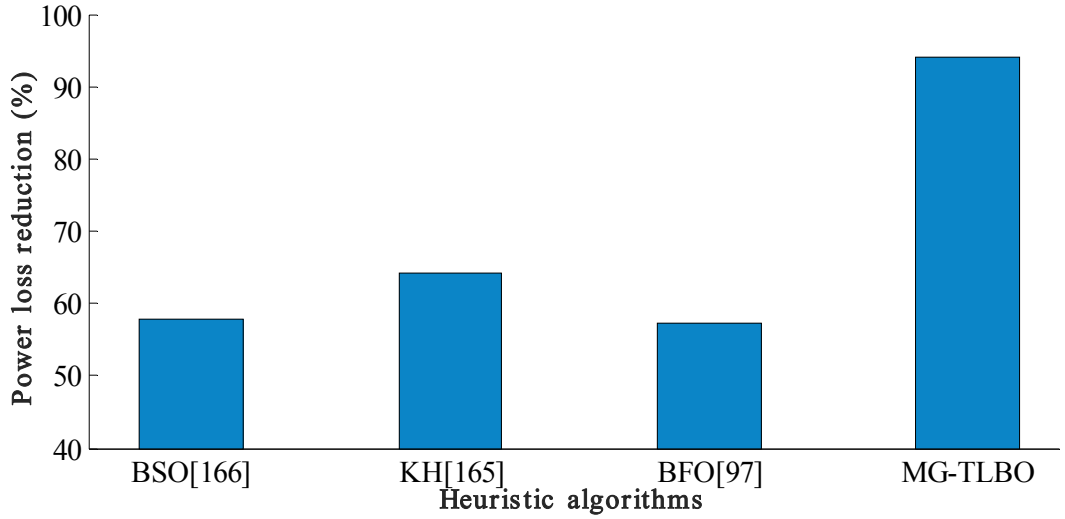

(a) Loss Reduction

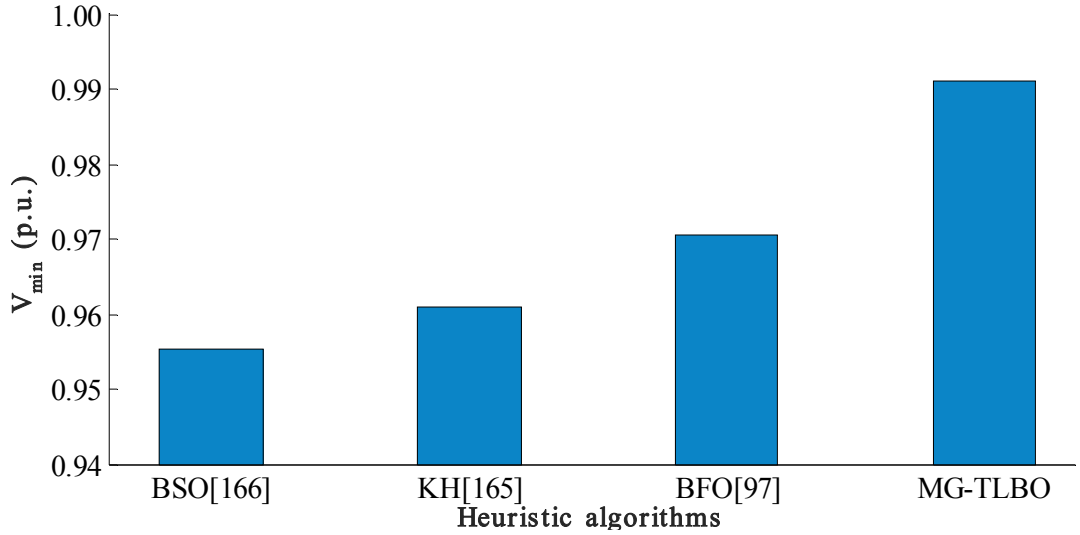

(b) Minimum Node Voltage

Figure 4.4: Comparison of the performance of heuristic algorithms on 33-bus system

Figure 4.4 show that the proposed algorithm is also compared with the other available established methods in the literature survey. The MG-TLBO algorithm achieves the maximum power loss reduction. Further, minimum voltage level is highest from other heuristics methods.

4.5.2 *69-Bus Distribution System*

The standard 69-bus distribution system is studied as the second test case. The proposed method is applied on this system to determine the optimal site and size of the DERs subject to minimize the energy losses. Total peak demand of the system is 4.66 MVA, and the average power factor is 0.8158 (lagging). In this system, all data have been used in per unit. The base value of power and voltage is 100 MVA and 12.66 kV, respectively.

The decision parameters for optimal allocation of the DERs are obtained to optimally allocate for each load level by the proposed method as given in Table 4.5. In case-III, the proposed method is used to optimize the penetration of the DERs while keeping the same location of both as considered in case-II. Further, the proposed method achieved more reduction of losses in case-III as compared to case-I

Table 4.5: Optimal performance parameters for the 69-bus test system

Cases	Load Level	Optimal dispatches of DGs (kW) / SCs (kVAr)
I	Light	62(709), 43(203), 59(220) / 64(500), 26(100), 52(100)
	Nominal	62(1589), 43(358), 59(356) / 64(1100), 26(200), 52(200)
	Peak	62(1741), 43(302), 59(622) / 64(1200), 26(200), 52(400)
II	Light	11(236), 18(192), 61(839) / 11(200),18(100), 61(600)
	Nominal	11(485), 18(382), 61(1675) / 11(300),18(300), 61(1200)
	Peak	11(485), 18(382), 61(1822) / 11(300),18(300), 61(1200)
III	Light	11(253), 18(178), 61(841) / 11(200),18(100), 61(600)
	Nominal	11(495), 18(379), 61(1674) / 11(300),18(300), 61(1200)
	Peak	11(466), 18(446), 61(1821) / 11(300),18(400), 61(1200)
IV	Light	17(288), 64(116), 61(743) / 61(500),21(200), 64(100)
	Nominal	17(522), 64(289), 61(1444) / 61(1000),21(300), 64(200)
	Peak	17(424), 64(518), 61(1794) / 61(1200),21(300), 64(400)

and case-II after 100 successive trials. Moreover, the MG-TLBO method has been applied to optimize both site and size of the DERs in case-IV and achieves the large reduction of annual energy losses as compared to other cases. The power loss reduction in nominal case is more as compared to the PSO and ITLBO algorithm. However, the overall percentage energy loss reduction is more. The proposed algorithm has been reduced the energy losses till 95.48 % in a year as shown in Table 4.6.

Table 4.6: Comparison of the system performance for the 69-bus test system

Cases	**Load Level**	**P_{loss} (kW)**	**V_{min} (p.u.)**	**Annual E_{loss} (MWh)**	**Annual E_{loss} Reduction (%)**
I	Light	6.18	0.9882	281.87	87.56
	Nominal	24.76	0.9769		
	Peak	92.81	0.9542		
II	Light	1.082	0.9971	134.16	94.08
	Nominal	4.331	0.9943		
	Peak	72.81	0.9500		
III	Light	1.081	0.9972	128.46	94.33
	Nominal	4.330	0.9943		
	Peak	69.02	0.9506		
IV	Light	1.745	0.9971	102.52	95.48
	Nominal	6.714	0.9938		
	Peak	42.48	0.9730		

A comparison of voltage profile for each load level of all cases of this test system is demonstrated in Figure 4.5. The ITLBO algorithm attained the low energy losses as compare to the PSO. However, voltage profile in peak condition produces the critical condition which can introduce the hazards in the system. However, there is a significant improvement in bus voltage profile in each load level for the fourth case as determined by the proposed method. The total active and reactive power injection by the DGs and SCs should not exceed the total active and reactive demand of the system, respectively. The DERs are available with different characteristics which are depended on the source. A comparison of the population based heuristic technique with MG-TLBO algorithm is presented in Figure 4.6.

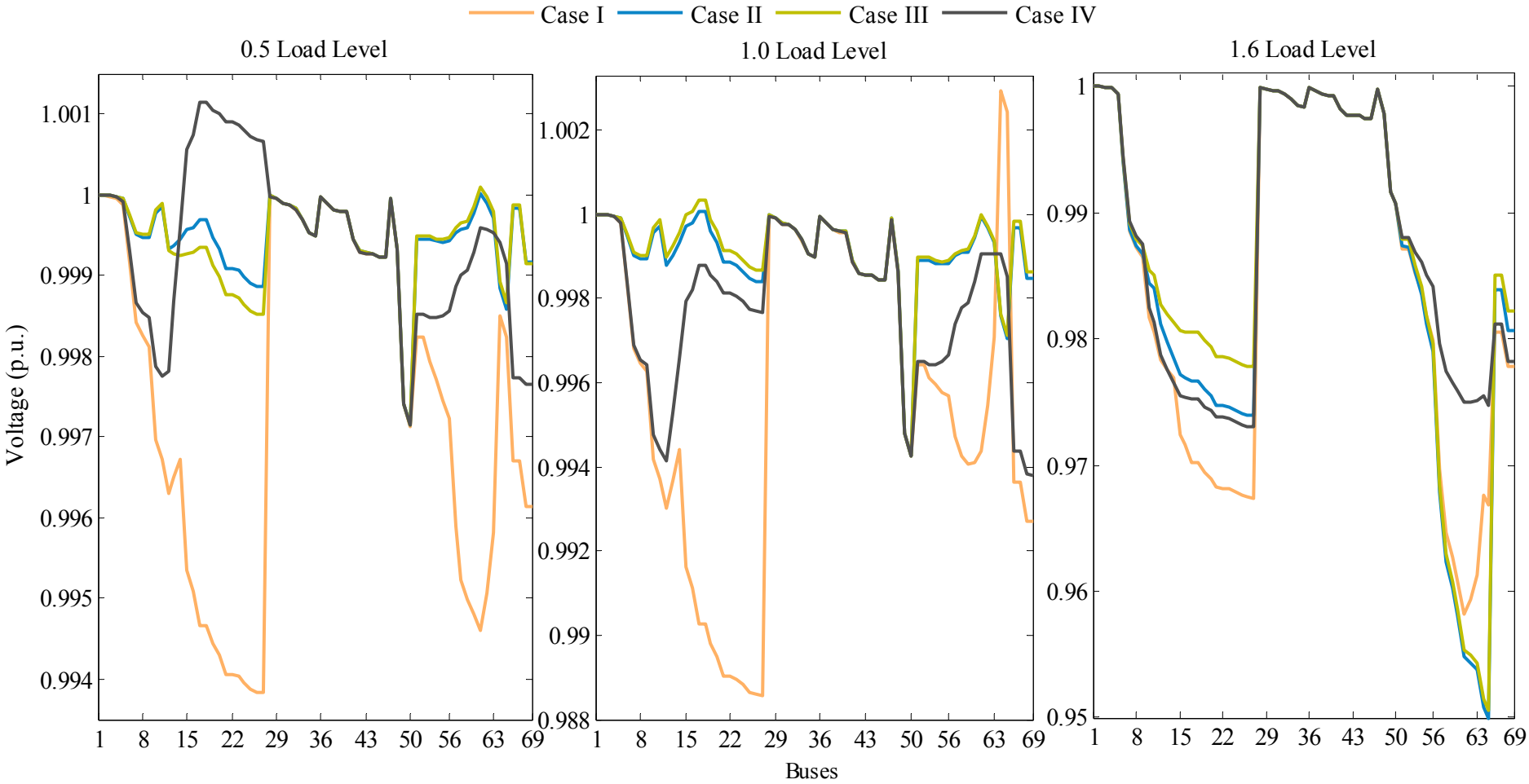

Figure 4.5: Bus voltage profile of the IEEE 69-bus system for each load level

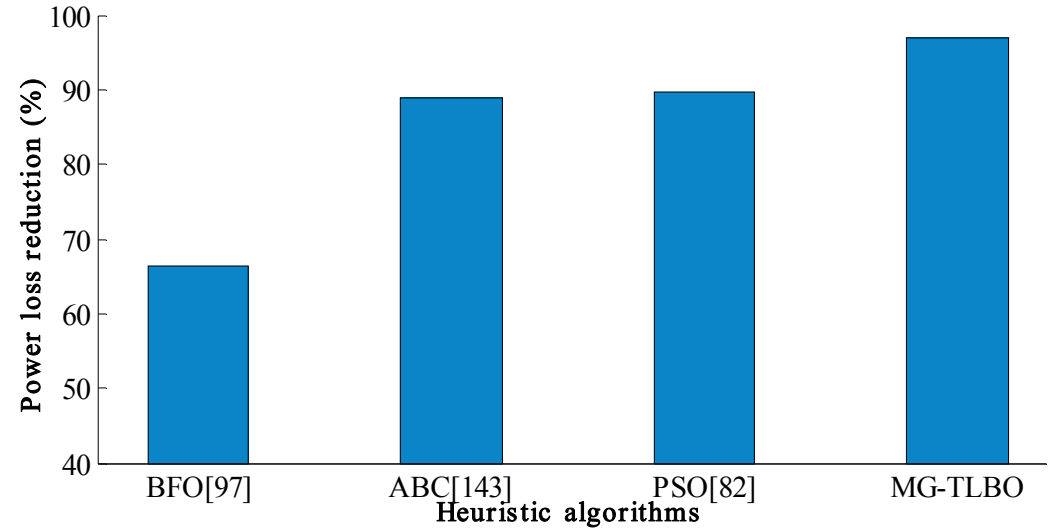

(a) Loss Reduction

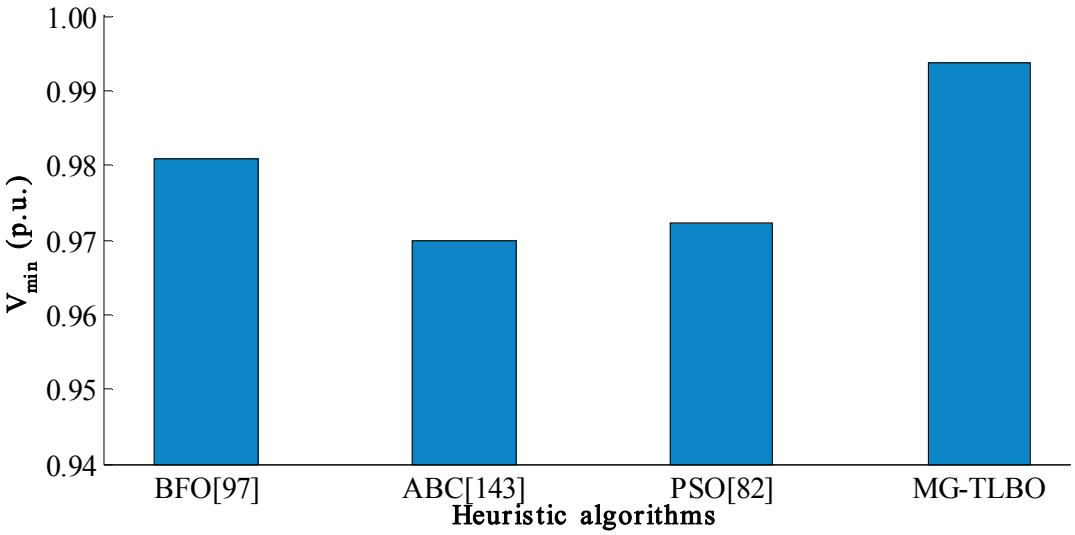

(b) Minimum Node Voltage

Figure 4.6: Comparison of the performance of heuristic algorithms on 69-bus system

The proposed algorithm is compared with well known heuristic algorithms. The proposed method is capable to reduce the maximum power loss reduction with better voltage profile for this distribution system.

4.5.3 *83-Bus Practical System of Taiwan Power Company*

An actual 11.4 kV practical radial distribution network belonging to the Taiwan Power Company is employed as a third test case. The system contains 11 feeders with 35.10 MVA (total peak demand) and 0.8076 average power factor (lagging).

Table 4.7 demonstrates that one more decision parameter is also optimized by the proposed algorithm to achieve the optimal accommodation of the DERs. The proposed method has been applied to enhance the system performance in the third and fourth cases after 100 trails. Further, annual energy loss reduction is very low in case-I and case-II as compared to case-III. It shows that the proposed method can also be applied to a practical distribution system.

Table 4.7: Optimal performance parameters for the 83-bus test system

Cases	**Load Level**	**Optimal Dispatches of DERs**
I	Light (DG/SC)	10(1465), 74 (255), 73(1310), 51(1501), 27(896)
		78(1000), 2(100), 13(900), 8(1000), 82(600)
	Nominal (DG/SC)	10(2714), 74(1439), 73(2134), 51(2839), 27(1892)
		78(1900), 2(1000), 13(1500), 8(2000), 82(1300)
	Peak (DG/SC)	10(3641), 74 (2200), 73(3271), 51(3963), 27(1656)
		78(2600), 2(1600), 13(2300), 8(2800), 82(1200)
II	Light (DG/SC)	79(1776), 19 (1502), 71(1251), 6(1599), 52(1201)
		62(400), 6(1100), 79(1300), 31(1400), 71(1000)
	Nominal (DG/SC)	79(3500), 19 (3099), 71(2449), 6(2984), 52(2668)
		62(800), 6(2200), 79(2200), 31(3000), 71(1900)
	Peak (DG/SC)	79(3500), 19 (3200), 71(2500), 6(3000), 52(2700)
		62(1100), 6(2200), 79(2200), 31(3300), 71(2200)
III	Light (DG/SC)	79(1600), 19(1535), 71(1329), 6(1539), 52(1327)
		62(400), 6(1100), 79(1200), 31(1100), 71(700)
	Nominal (DG/SC)	79(3472), 19 (3150), 71(2563), 6(3170), 52(2736)
		62(900), 6(2100), 79(2600), 31(2800), 71(1900)
	Peak (DG/SC)	79(5000), 19 (4999), 71(4088), 6(5000), 52(4314)
		62(1300), 6(3400), 79(4200), 31(4700), 71(3000)
IV	Light (DG/SC)	8(1492), 54(1202), 20(1317), 72(1106), 81(1515)
		35(700), 9(900), 58(500), 79(1300), 72(700)
	Nominal (DG/SC)	8(3067), 54(2512), 20(2993), 72(2524), 81(3023)
		35(1500), 9(2000), 58(700), 79(2100), 72(1700)
	Peak (DG/SC)	8(4879), 54(3884), 20(4943), 72(4028), 81(4829)
		35(3200), 9(3100), 58(1700), 79(3200), 72(2600)

Table 4.8 depicted that the MG-TLBO is applied to optimize the both decision parameter of DERs for each load level in the last case and acquire the large power reduction in each load level. In the fourth case, the MG-TLBO achieves the maximum reduction of annual energy losses. In this system, the proposed algorithm is achieved the maximum 64.21% energy loss reduction that is very low as compare to other test system. In an actual system, fifty percentages above energy loss reduction has a significant improvement for the validation planning.

Table 4.8: Comparison of the system performance for the 83-bus test system

Cases	**Load Level**	**P_{loss} (kW)**	**V_{min} (p.u.)**	**Annual E_{loss} (MWh)**	**Annual E_{loss} Reduction (%)**
I	Light	75.06	0.9804	2982.51	42.89
	Nominal	304.46	0.9601		
	Peak	934.62	0.9346		
II	Light	49.73	0.9847	2152.90	58.78
	Nominal	203.15	0.9696		
	Peak	656.58	0.9455		
III	Light	50.41	0.9838	1964.70	62.37
	Nominal	202.40	0.9690		
	Peak	532.83	0.9501		
IV	Light	47.95	0.9872	1869.71	64.21
	Nominal	193.64	0.9752		
	Peak	503.51	0.9603		

It can be remarked from Figure 4.7 that voltage profile for the fourth case has been enhanced significantly over all load levels by proposed method. The PSO and ITLBO are failed to optimize the parameter for peak load level which is shown in Case-I and Case-II, respectively. Therefore, these comparisons show that load level should be considered for rigid DERs planning in the radial distribution system.

In this chapter, the DER and SCs penetration should be equal or less than from case II for all case studies. The PSO, ITLBO, and the proposed method search the optimal solution within the specified penetration of DERs. However, the PSO and ITLBO have not obtained the significant loss reduction in the practical distribution system. Moreover, the proposed method achieves the best solution in each load level of the standard as well as practical distribution system.

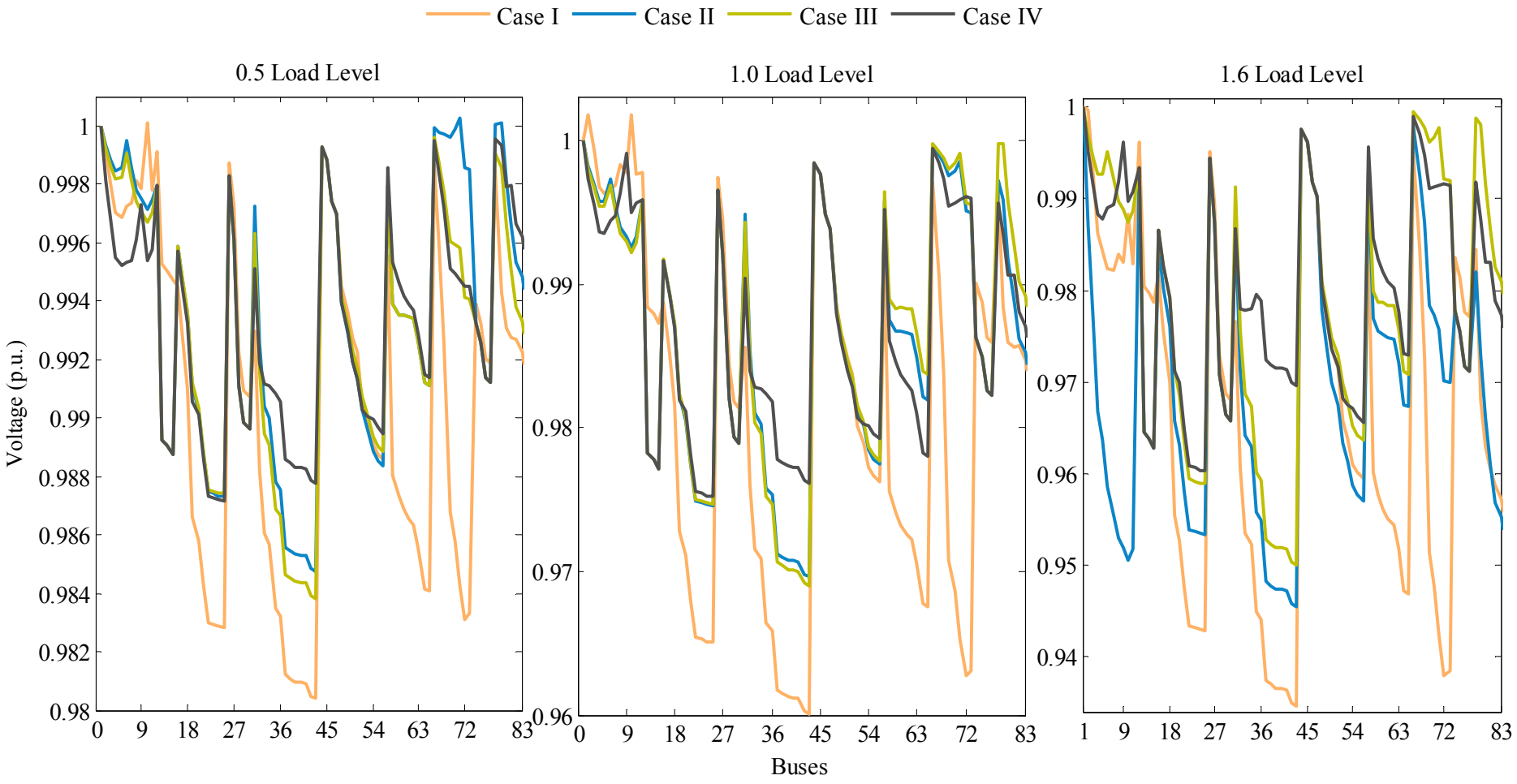

Figure 4.7: Bus voltage profile of the practical 83-bus system for each load level

4.6. Conclusion

Integrating DERs in the distribution systems is attaining worldwide popularity due to the more positive impacts. The MG-TLBO is proposed to optimize the simultaneous active and reactive power injection of the DERs at particular places in the medium voltage radial distribution networks for three load levels. The proposed method incorporated some modification such as grouping mechanism, modified teaching, learning factor, mutation, and crossover for diversity to furnish the drawbacks of basic TLBO. The application results show better performance of the proposed method using MG-TLBO as compared to ITLBO and PSO in every case study. Further, the proposed algorithm has achieved the best result in each load level of the distribution system. The result shows that consideration of load level produced the rigid planning.

The PSO and ITLBO have not satisfied the each constraint at peak load level of the realistic Taiwan distribution system. In the practical system, the PSO algorithm has not achieved the truthful reduction of energy losses which is less than the fifty percentage. Moreover, the proposed algorithm has achieved loss reduction in less time as compared to other system. Although, the energy loss reduction is above the fifty and maximum by proposed method as compare to both algorithms. The PSO and ITLBO have performed with in specify boundaries of constraints in standards distribution system. Therefore, the realistic system has been required to evaluate a perfect DER planning. Moreover, proposed algorithm has been compared for performance with some other published result which has used the heuristic algorithms. The MG-TLBO method is well tested for various simulated cases including the practical system for its robustness and reliability.

Chapter – 5

PERFORMANCE ANALYSIS OF DISTRIBUTED ENERGY RESOURCES IN HARMONICS POLLUTED DISTRIBUTION SYSTEMS

5.1 Introduction

The smarter distribution system is expected to drive the good quality of power to the distribution system. However, it is a complicated task to maintain according to present load scenario. Nowadays, non-linear load and power switching apparatus are increasing rapidly due to the high efficiency as well as ease of operation and control. Further, application of power electronics devices are dominating, which introduces the harmonic distortion in the electrical distribution system [103]. It is a well-known fact that harmonic distortion originates some problem in a system like decreasing the life of insulation, more heating loss, reducing power factor and affecting the power plant efficiency [18]. In addition, switchgear protection of the power system is also affected by the presence of harmonics as protection device is designed for normal operating condition (sinusoidal waveform of voltage and current). Therefore, it is necessary to reduce this harmonic distortion of a distribution system according to IEEE 519-1992 standard [21]. Two processes are presented in [22] to solve this problem, first is transient-state analyze such as the wavelet and time domain analyze and the second process is steady state analyze. A steady state based algorithm is better over transient-state based algorithms due to the computational efficiency. Therefore, it can be used for large scale power system analyze. Many conventional harmonic load flow methods are presented like admittance matrix, impedance matrix and Newton-Raphson. However, these methods can't be used in the radial distribution system due to its very high resistance to reactance ratio. Therefore, backward/forward sweep-based harmonic load flow method has been used to obtain harmonic penetration in the distribution networks [170]. Further, harmonic distortion becomes the most complex problem with the presence of harmonic resonance, which is introduced by various components of electronics [19]. Therefore, planning is necessary to maintain the system harmonics in specified limit otherwise there will be poor quality of power with

more energy loss, which is not a desirable situation under competitive energy market scenario. According to pervious chapter, multi-load levels construct the firm planning of distribution system to minimize the energy losses and harmonics distortion [24]. Therefore, it is necessary to supply electrical power according to the load demand; otherwise, the network losses and total harmonics distortion may increase in another load level. The optimal DER allocation (site and size) can improve the performance of the system in terms of reduction of harmonic distortion for improving node voltage and reducing the energy losses of the system. Further, non-optimal placement may increase the system losses, impermissible voltage and harmonics.

In this chapter, the MG-TLBO algorithm is applied to optimized penetration level at best locations in harmonics distorted distribution system to minimize the energy loss while maintaining permissible harmonic distortion and node voltage. To find out the robustness of the proposed algorithm is also tested on two modified 33-bus and 69-bus radial distribution systems and one practical 83-bus radial distribution system in presence of non-linear loads. Further, the simulation results are compared with well-established algorithms such as ITLBO [24] and PSO [82].

The salient contributions of the chapter are given below:

(i). The energy demand and power quality illness of the distribution system are addressed by optimal allocation of the DERs for multi-level load pattern.

(ii). The Modified Group-experience TLBO viz. MG-TLBO approach is applied in harmonics distorted distribution system.

5.2 Distribution System Harmonics Load Flow

The proposed work is applied the backward/forward sweep (BFS) approach for harmonics analysis in the radial distribution system considering linear and non-linear loads. The backward/forward sweep is an effective method to analysis the radial distribution system in presence of non-linear loads [170]. However, it has been not directly applied for harmonic analysis. A lot of capacitors are installed in the distribution system. Further, sequentially same numbers of resonant frequency exist. Therefore, load flow might be diverging even at the lowest frequency. First of all, compute the harmonics current absorbed by the shunt capacitors. Moreover, the BFS approach can be applied to find out the branch current and node voltage of each harmonics directly. The system data must be prepared in a perfect manner to apply the

algorithm by using some set of formulation. For simplification, harmonic current is bifurcated. First is Ih^h, which is contributed by linear load impedance and non-linear load, and second is Is^h that is absorbed by shunt capacitor.

$$\left[I^{\mathrm{h}}\right]=\begin{bmatrix} Ih^{\mathrm{h}} \\ \ldots \\ Is^{\mathrm{h}} \end{bmatrix} \tag{5.1}$$

where, [Ih] is h^{th} order system harmonics current vector. In the distribution system, n number of harmonics source, linear load impedance and m number of shunt capacitor are present. The size of vector [Ih^h] is n x 1, vector [Is^{h}] size is m x 1 vector and vector I^h size is (n+m) x 1.

Further, coefficient vector (A^h) is depicted the presence of harmonics current flow through a branch. The backward sweep has been used to build the coefficient vector by for a branch of the system as shown in equation (5.2).

$$\left[A^h_{\alpha\beta}\right]=\begin{bmatrix} Ah^h_{\alpha\beta} \\ \ldots \\ As^h_{\alpha\beta} \end{bmatrix} \tag{5.2}$$

where, $A^h_{\alpha\beta}$ is coefficient vector of the branch between buses α^{th} to β^{th}. $Ah^h_{\alpha\beta}$ is coefficient vector of harmonics contribute to the presence of a linear and non-linear load and $As^h_{\alpha\beta}$ is a coefficient vector of harmonics absorbed by shunt capacitor for the branch. The coefficient vector made of '0' or '1'. If either shunt capacitor or load present at bus then puts '1' at a place which is specified to a particular bus, otherwise, '0' will be placed that location. The branch current vector can be calculated between all buses with the use of coefficient vector and harmonics current vector.

$$\left[B^h_{\alpha\beta}\right]=\left[A^h_{\alpha\beta}\right]^T\left[I^h\right] \tag{5.3}$$

The branch voltage drop vector compute from branch current vector and line impedance data $Z^h_{\alpha\beta}$ can be express as

$$\left[\nabla V^h_{\alpha\beta}\right]=Z^h_{\alpha\beta}\left[A^h_{\alpha\beta}\right]\left[I^h\right] \tag{5.4}$$

The forward sweep approach has been applied to build the bus voltage variations on the system harmonics vector as shown in following equations,

$$\left[V_1^h\right]-\left[V_n^h\right]=\left[\sum_{\alpha=1}^{n_b}\sum_{\beta=1}^{n_n} Z_{\alpha\beta}^h\left[A_{\alpha\beta}^h\right]^T\right]\left[I^h\right] \tag{5.5}$$

$$\left[V^h\right]=\left[HA\right]\left[I^h\right] \tag{5.6}$$

The relationship between bus voltage vector V^h and system harmonics current vector I^h are shown in relationship matrix [*HA*]. Further, voltage matrix of each node that places the capacitors is connected to the system.

$$\left[V_s^h\right]=\left[HA_s\right]\left[I^h\right] \tag{5.7}$$

The matrix [*HA*] has been divided into two part according to harmonics load current HA_h and HA_{sh} capacitor current. Further, equation (5.7) can be rewritten as

$$-\left[Z_s I_s\right]=\left[HA_h \vdots HA_{sh}\right]\begin{bmatrix} Ih^h \\ \cdots \\ Is^h \end{bmatrix} \tag{5.8}$$

where, Z_s is shunt capacitor load impedance. Equation (5.8) can write as follows

$$\left(\left[HA_{sh}\right]+\begin{bmatrix} Z_s^h & & & \\ & \ddots & & \\ & & Z_{s_{n_n-1}}^h & \\ & & & Z_{s_{n_n}}^h \end{bmatrix}\right)\left[Is^h\right]=-\left[HA_h\right]\left[Ih^h\right] \tag{5.9}$$

$$\left[HLF\right]\left[Is^h\right]=-\left[HA_h\right]\left[Ih^h\right] \tag{5.10}$$

where,

$$\left[HLF\right]=\left[HA_{sh}\right]\left[Z_s^h\right] \tag{5.11}$$

If *m* capacitors are connected in the distribution system, the size of [*HLF*] matrix size is *m* x *m*. Equation (5.8) gives the value of shunt capacitor after putting the

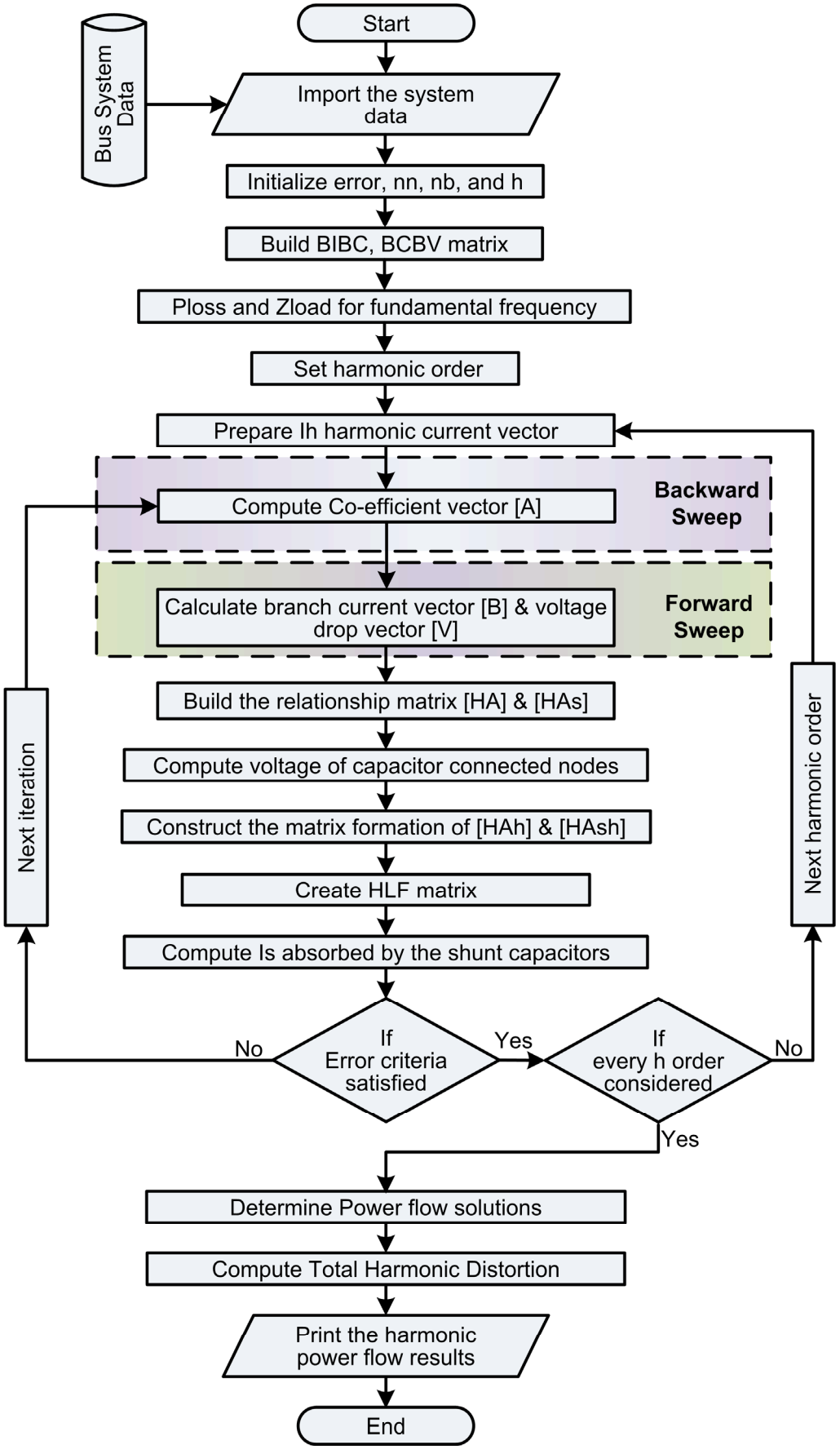

Figure 5.1: Flowchart of harmonics backward/forward sweep approach

harmonics load current. Further, branch current can be obtained with the help of equation (5.3), branch voltage drop and bus voltage obtained from equations (5.4) and (5.6), respectively. This process for h^{th} order of harmonics repeated as shown in Figure 5.1. Further, it fulfills the termination criteria. This process iterated for each order of harmonics. In addition, real power loss calculated for h^{th} harmonics by

$$P_{loss}^{h} = \left[R^{h} \right] \cdot \left| \left[A^{h} \right] \left[I^{h} \right] \right|^{2} \tag{5.12}$$

Root mean square value of bus voltage is calculated by each harmonics frequency's bus voltage,

$$V_{rms_{\alpha}} = \sqrt{\left| V_{\alpha}^{(1)} \right|^{2} + \sum_{h=h_{\min}}^{h_{\max}} \left| V_{\alpha}^{h} \right|^{2}} \qquad \forall \alpha \in n_{n} \tag{5.13}$$

where, $V_{\alpha}^{(1)}$ is fundamental magnitude component of the bus voltage. Total harmonics distortion level at particular node is computed as,

$$THD_{\alpha}(\%) = \frac{\sqrt{\sum_{h=h_{\min}}^{h_{\max}} \left| V_{\alpha}^{h} \right|^{2}}}{\left| V_{\alpha}^{(1)} \right|^{2}} \qquad \forall \alpha \in n_{n} \tag{5.14}$$

The load flow outputs are required to be used in optimizing the DERs planning.

5.3 Modeling of Harmonics Distorted Distribution System

There is some modification in line impedance, load impedance, and capacitor reactance at different harmonics frequency. These are detailed as follows:

5.3.1 Line Parameter's Modeling

Line impedance of system depends on frequency. Therefore, it changes with frequency and given at h^{th} harmonic.

$$Z_{\alpha\beta}^{h} = R_{\alpha\beta}^{h} + j\,\mathrm{X}_{\alpha\beta}^{h} * h \tag{5.15}$$

where, $R_{\alpha\beta}^{h}$ and $X_{\alpha\beta}^{h}$ is resistance and reactance of the line between the α^{th} and β^{th} bus.

5.3.2 Shunt Capacitor Modeling

The shunt capacitor is a constant impedance load at a given frequency. However, it will be changed with frequency.

$$X_{capacitor,\alpha} = \frac{V_\alpha^2}{Q_\alpha} \tag{5.16}$$

$$Y^h_{capacitor,\alpha} = \frac{1}{X^h_{capacitor,\alpha}} \tag{5.17}$$

$$Y^h_{capacitor,\alpha} = h * Y^h_{capacitor,\alpha} \tag{5.18}$$

where, Q_α is reactive power supplied by the capacitor at α^{th} bus. $Y^h_{capacitor,\alpha}$ and $X^h_{capacitor,\alpha}$ are admittance and reactance of the capacitor at h^{th} harmonic, respectively.

5.3.3 Linear and Non-linear Load Modeling

Linear loads are treated as constant impedance for each harmonic frequency. However, the non-linear loads are usually treated as constant current source. Both types of the load vary with different harmonic frequency.

$$Z^h_\alpha = R_\alpha + j\,\mathrm{X}_\alpha * h \tag{5.19}$$

$$I_{l_\alpha} = \frac{V_\alpha}{Z^h_\alpha} \tag{5.20}$$

$$\left[Ih^h_{nl} \right] = \left[Ih^h_1 \quad Ih^h_2 \quad \ldots \quad Ih^h_\alpha \right] \tag{5.21}$$

where, Z^h_α is the h^{th} harmonic equivalent impedance of the linear load at bus. R_α and X_α are equivalent resistance and reactance of the linear load of α^{th} bus. I_{l_α} and I^h_{nl} are the currents contributed by linear and non-linear loads, respectively.

This formulation considers different types of harmonics spectrums, which have different values of the non-linear current sources [148]. Further, linear load impedances are also changed with a particular harmonic same as line impedance.

5.4 Problem Description

The optimal accommodation of DERs for perfect injection of power is formulated with the objective to maximize the annual energy loss reduction while preserving better bus voltage profile and permissible limit of total harmonic distortion of voltage (THD_V). The erroneous allocation may lead to over THD_V, undesirable voltage profile and increase the network power losses. Therefore, THD_V and node voltage should be preserved in proper boundary to maintain the safe and reliable operation along with the quality of supply.

The goal of this work is to maximize the annual energy loss reduction with and without DERs allocations. Also, maintaining the THD_V and bus voltage profile within the limits under multi-level load pattern which is formulated as

$$F = \max\left[\rho\left(\sum_{\tau=1}^{n_{lv}}\left(E_{loss,b\tau}\left(V_{node},THD_v\right)\right) - \sum_{\tau=1}^{n_{lv}}\left(E_{loss,a\,\tau}\left(V_{node},THD_v\right)\right)\right)\right] \quad \forall\,\tau \in n_{lv} \tag{5.22}$$

where, $E_{\text{loss,b}\tau}$ and $E_{\text{loss,a}\tau}$ is the energy losses of each load level with and without penetration of DERs, respectively. t_τ is time duration of each load level. ρ is the bus voltage deviation penalty factor which is explained in pervious chapter by using the equations (4.2) and (4.3).

The objective function of the DER planning has considered only fundamental component in absence of non-linear load in the system. Otherwise, power losses are computed for each harmonic. In this formulation, any location constraint is not considered on the DERs. However, any location constraint of the DERs can be easily included by the proposed method. In such cases, the applied algorithm searches only the identified nodes of the system for the best solution.

5.4.1 Total Harmonic Distortion of Voltage (THD_v)

The THD_V at each bus of the system (THD_v^{bus}) should not exceed their maximum permissible value ($THD_v^{\max}$) according to IEEE 519-1992 standard as given in equation (5.23),

$$THD_v^{bus} \le THD_v^{\max} \tag{5.23}$$

The value of THD_v^{bus} is computed by following equation (15).

$$THD_v^{bus}(\%) = \sqrt{\sum_{h=h_{\min}}^{h_{\max}} \left|V_\alpha^h\right|^2} \Big/ \left|V_\alpha^{(1)}\right|^2 \tag{5.24}$$

Moreover, every order of harmonic voltage should be less than three percent at each node of the system.

$$V^h \le V_{\max}^h \tag{5.25}$$

5.4.2 Voltage Limits at Slack Bus and Load Buses

The slack bus voltage magnitude and angle must be one and zero throughout the planning period, respectively. This conventional hard system bus voltage constraints is shown in (5.26).

$$V_{\min} \le V_m \le V_{\max} \tag{5.26}$$

The lower voltage limit (V_{min}) and the upper voltage limit (V_{max}) is 0.95 p.u. is 1.05 p.u., respectively.

5.4.3 Bus Compensation Limit of DGs

The active power injection of the DGs must in the permissible operating region as per equation (5.27).

$$P^{\min} < P_{DGs} \le P^{\max} \tag{5.27}$$

The boundries of P_{DGs} is constant either during the initialization or updating process of optimization.

5.4.4 Bus Compensation Limit of SCs

The active power injection of the DERs must in the permissible operating region as per equation (5.28).

$$Q^{\min} < Q_{\mathrm{SCs}} \le Q^{\max} \tag{5.28}$$

The size of Q_{SCs} has been considered in step size in whole process of the computation.

5.4.5 Power Flow Constraints

The power flow equation must be satisfied for each node of the system. The active power injected by DERs and supplied by the grid should be equal to losses and active demand of the system. Further reactive power injection by SCs and reactive power of the system must also be balanced with demand and losses of reactive power in the system.

$$\begin{aligned} P_{\alpha+1} &= P_{\alpha} - R_{\alpha\beta}\frac{P_{\alpha}^2 + Q_{\alpha}^2}{V_{\alpha}^2} - P_{Grid,\alpha}^{\tau} \qquad \forall \alpha \in n_n, \forall \beta \in n_b, \forall \tau \in n_{lv} \\ Q_{\alpha+1} &= Q_{\alpha} - X_{\alpha\beta}\frac{P_{\alpha}^2 + Q_{\alpha}^2}{V_{\alpha}^2} - Q_{Grid,\alpha}^{\tau} \\ P_{Grid,\alpha}^{\tau} &= \sum_{\beta=1}^{n_b} P_{loss}^{\tau} - \sum_{\alpha=2}^{n_n} P_{DGs}^{\tau} \\ Q_{Grid,\alpha}^{\tau} &= \sum_{\beta=1}^{n_b} Q_{loss}^{\tau} - \sum_{\alpha=2}^{n_n} Q_{SCs}^{\tau} \end{aligned} \tag{5.29}$$

5.4.6 Line Flow Capacity

The line flow capacity must consider as constraints because line of the system should be capable of transmitting the power at given condition. The limitation of power flow depends on the thermal parameter of the line.

$$S_{\alpha\beta}^{\max} \geq S_{\alpha\beta} \tag{5.30}$$

$$S_{\beta\alpha}^{\max} \geq S_{\beta\alpha} \tag{5.31}$$

where, $S_{\alpha\beta}^{\max}$ is a maximum permissible limit of the distribution line. Further, $S_{\alpha\beta}$ is power flow capacity of the branch between bus α^{th} and bus β^{th} should not exceed from the permissible limit which is fix at a time of manufacturing.

5.4.7 DGs Penetration Limit

Total active power (P_{DG}) injection by the DERs must be less than the nominal active demand (P_D) of the system.

$$\sum_{\alpha=2}^{n_n} P_{DG,\alpha} \le P_D \tag{5.32}$$

5.4.8 SCs Penetration Limit

Total reactive injection (Q_{SCs}) by the SCs must be less than the nominal reactive demand (Q_D) of the system.

$$\sum_{\alpha=2}^{n_n} Q_{SCs,\alpha} \le S_D \tag{5.33}$$

5.4.9 System Site Constraints

The candidate site (*loc*) of each the DGs and SCs should not repeat in every iteration which is defined as

$$\begin{aligned} loc_{\alpha}^{DGs} &= loc_{\alpha+1}^{DGs} \quad \alpha \in n_n, \alpha \neq 1 \\ loc_{\alpha}^{SCs} &= loc_{\alpha+1}^{SCs} \quad \alpha \in n_n, \alpha \neq 1 \end{aligned} \tag{5.34}$$

In this chapter, the proposed algorithm in the previous chapter has been applied to optimize decision parameters of the DERs and SCs as the size, site, and number. Further, optimized parameters in the described formulation are to minimize the harmonics distortion and increase the percentage annual energy losses reduction for three load level of small and large distribution networks with satisfied all constraints.

5.5 Simulation Result and Discussion

In this section, proposed methodology is applied on the modified standard 33-bus [78], 69-bus [48], and 83-bus practical radial distribution system [141] which has non-linear loads with linear loads. The alterations in the original systems to analyze the power quality problem introduced in the radial distribution networks. Each load level results of every system are compared with the results of the PSO in the presence of non-linear load. The annual load profile is assumed to be piecewise segmented in three different load level as mentioned in pervious chapter. The harmonics backward/forward power flow method is used to analyze the harmonics distorted radial distribution networks.

The impact of harmonics on the optimal allocation of the DERs has been investigated by using the load flow for each frequency of harmonics and fundamental,

where some non-linear loads and linear loads are connected in the network. The harmonic spectrums of three different types of non-linear load such as fluorescent, PC work station and Adjustable Speed Drive (ASD), which is used to control the speed of the motor, are given in Table 5.1.

Table 5.1: Harmonic spectrums of the non-linear loads [171]

Harmonic order	Non-linear loads					
	PC workstation		ASD		Fluorescent	
	Mag. (%)	Phase (deg.)	Mag. (%)	Phase (deg.)	Mag. (%)	Phase (deg.)
1	100	0	100	0	100	-2
5	3.9	-150	82.8	-135	3.9	-150
7	1.4	-28	77.5	69	2.9	-73
11	0.9	-176	46.3	-62	1.4	6
13	0.5	-60	41.2	139	0.8	29
17	0.5	139	14.2	9	0.2	-17
19	0.3	-126	9.7	-155	0.5	-56
23	0.3	112	1.5	-158	0.2	-65
25	0.3	-155	2.5	98	0	0
29	0.4	38	0	0	0	0
31	0.4	134	0	0	0	0
35	0.4	-44	0	0	0.1	-42
37	0.2	78	0	0	0	0
41	0.4	-102	0	0	0	0
43	0.4	-39	0	0	0	0
47	0.2	163	0	0	0.1	-137
49	0.2	-127	0	0	0	0

The proposed algorithm has been tested on each system and compared the results with base case and well-established PSO. Moreover, MG-TLBO has optimized the DERs allocation and size in harmonics polluted radial distribution system with limit the value of the maximum harmonic at all node of the system according to IEEE 519-1992 standard. However, locations of the DERs are same for each load level in all three test systems and it is a practical approach to the DER planning in the distribution system.

5.5.1 Test System A: 33-Bus Distribution System

The modified 33-bus distribution system given in [78] has been used to validate the MG-TLBO in the harmonics distorted distribution system. In this system, all data have been used in per unit whereas the base value of power and voltage is 100 MVA and 12.66 kV, respectively.

The 33-bus distribution network has been modified in [171] and it is utilized in this study. Three different types of non-linear loads are considered to demonstrate the effect of harmonics. The modeling of non-linear loads is based on an original power component of the system. The location and percentage of non-linear loads are shown in Table. 5.2.

Table 5.2: Non-linear loads data for the 33-bus system

Bus No.	**Non-linear load type**	**Percentage**
14, 22, 24	Fluorescent	43
	Personal Computer (PC)	29
	Adjustable Speed Drive (ASD)	29
30	ASD	65

Table 5.3: Optimal solution for harmonics polluted test system-A

Energy Resources	**Bus Location**	**Load level**		
		Light	**Nominal**	**Peak**
		kW/kVAr	**kW/kVAr**	**kW/kVAr**
PSO				
DGs	4	462	794	711
	32	503	990	1187
	16	373	726	1011
SCs	14	200	400	400
	30	300	600	700
	33	200	400	600
MG-TLBO				
DGs	27	705	799	1464
	12	489	837	1184
	32	162	659	1046
SCs	30	400	700	1000
	13	100	300	500
	6	500	600	1100

Non-optimal allocation of the DER can increase the percentage of harmonic distortion and energy losses from the base case. Therefore, the PSO and proposed method have been applied to optimize the decision parameter in the presence of non-linear load in the same system. The optimal solution obtained for each level of harmonic polluted IEEE benchmark 33-bus system after 100 trials of proposed method is shown in Table 5.3.

The optimal value of decision parameter improves the system performance. Table 5.4 shows that the PSO and proposed method reduce *THD*v below five percentages with improvement in the voltage profile for each load level. However, the proposed method gives the maximum annual energy loss reduction as compared to the PSO in modified 33 distribution system.

Table 5.4: System performance of harmonics polluted test system-A

Cases	Load Level	THD_V (max.)	V_{min} (p.u.)	P_{loss} (kW)	Annual E_{loss} (MWh)
Base Case	Light	6.0883	0.9583	50.97	2198.9
	Nominal	13.3889	0.9131	219.98	
	Peak	24.4528	0.8528	626.58	
	Annual E_{loss} (%) Reduction				-
PSO	Light	1.4300	0.9914	8.22	350.48
	Nominal	2.659	0.9821	33.29	
	Peak	3.0681	0.9658	105.94	
	Annual E_{loss} (%) Reduction				**84.06**
MG-TLBO	Light	1.7334	0.9921	8.41	274.46
	Nominal	2.3229	0.9816	28.09	
	Peak	3.2841	0.9706	73.26	
	Annual E_{loss} (%) Reduction				**87.52**

The proposed method has reduced the harmonic distortion for each load level as described in Figure 5.2. The characteristic of harmonic distortion in the system is same for each load level. However, the load scaling factor is simultaneously increased with distortion level. Figure 5.3 shows that DERs enhance the voltage profile from the base voltage at all load level by using of proposed method. Moreover, the bus voltage does not violate the desired permissible boundaries for each load level.

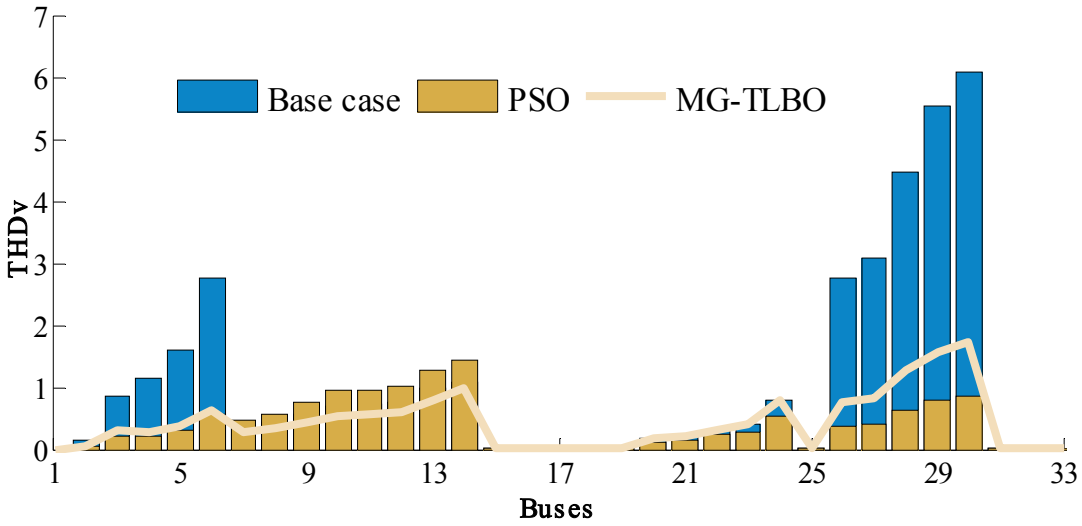

(a) Light Load

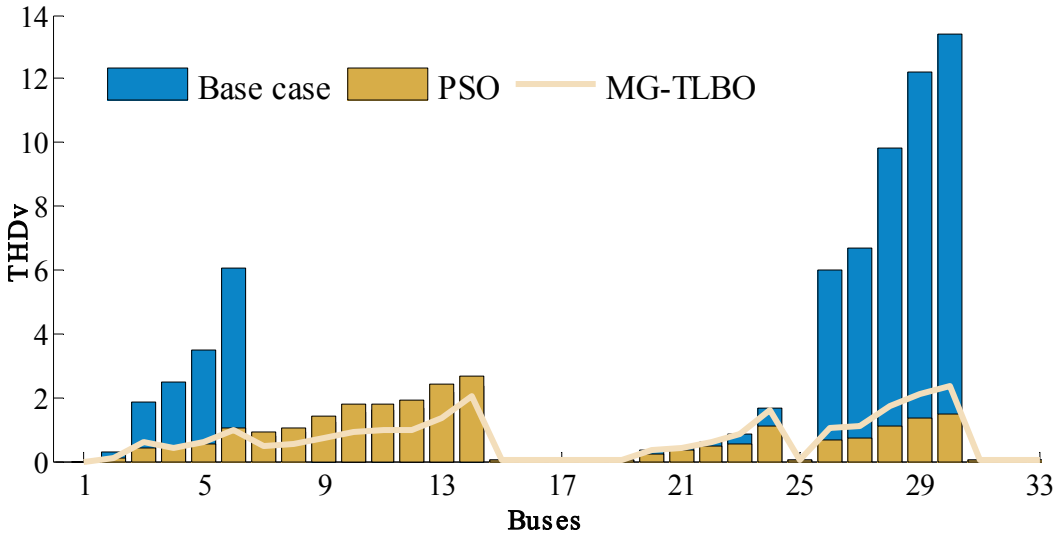

(b) Nominal Load

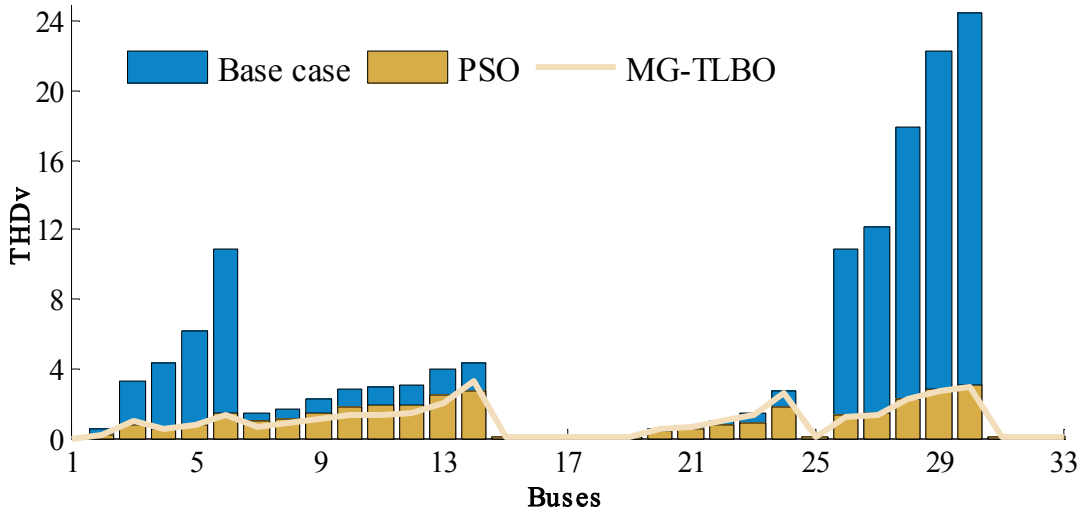

(c) Peak Load

Figure 5.2: Total harmonic distortion of 33-bus system for each load level

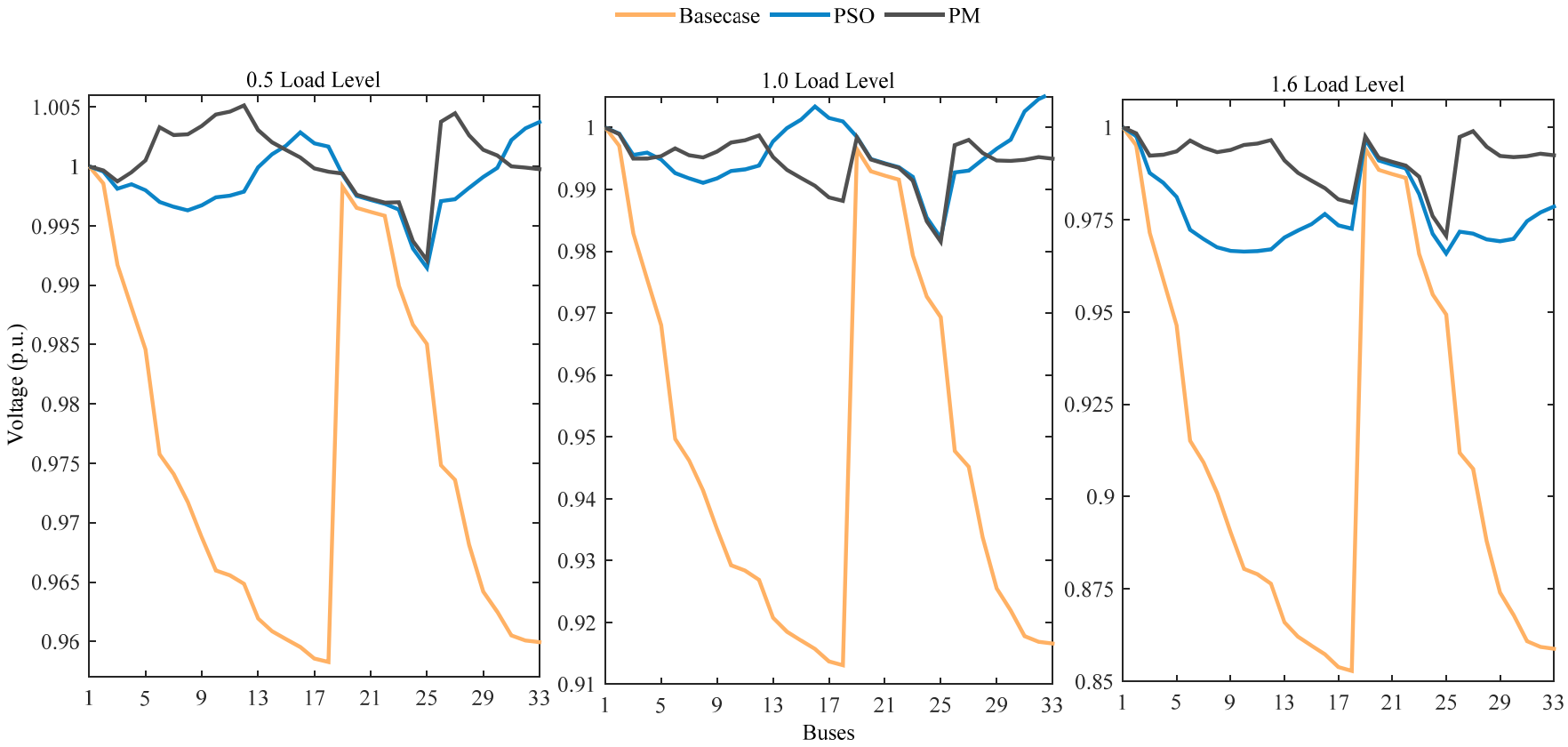

Figure 5.3: Voltage profile of the IEEE 33 bus system with non-linear load

5.5.2 Test Case B: 69-Bus Distribution System

The 69-bus distribution network has been investigated including non linear loads for power quality problem in the medium distribution system. Similar to the first case, three different types of non-linear loads are considered to analyze the effect of the harmonics. Non-linear loads are connected to different buses of system and percentage of non-linear loads is shown in Table 5.5.

Table 5.5: Non-linear loads data for the 69-bus system

Bus No.	**Non-linear load type**	**Percentage**
14, 18, 22, 24, 34, 37, 39, 43, 46, 51, 53, 55, 59, 62, 64, 67	Fluorescent	57
	Personal Computer (PC)	52
	Adjustable Speed Drive (ASD)	65
29	ASD	85

Table 5.6: Optimal solutions obtain for harmonics polluted test system-B

Energy Resources	**Bus Location**	**Load level**		
		Light	**Nominal**	**Peak**
		kW/kVAr	**kW/kVAr**	**kW/kVAr**
		PSO		
DERs	64	225	442	685
	13	251	413	259
	57	735	1560	1704
SCs	26	100	300	400
	29	100	200	100
	63	500	1100	1200
		MG-TLBO		
DERs	13	336	640	1077
	64	175	400	559
	61	688	1348	2196
SCs	8	200	500	700
	63	500	1100	1800
	16	200	300	500

The proposed method and PSO have been applied to optimize the decision parameter in the presence of non-linear load in the test system. Both algorithms achieve the optimal solution for all load levels of 69-bus system after 100 trials as shown in Table 5.6.

PSO approach provides constraints results with more energy losses as compared to the proposed algorithm as shown in Table 5.7. Moreover, PSO could not maintain the voltage profile in specified region for peak load level. Therefore, proposed algorithm is more capable to obtain better system performance parameter.

Table 5.7: System performance with harmonics polluted test system-B

Cases	Load Level	THD_V (max.)	V_{min} (p.u.)	P_{loss} (kW)	Annual E_{loss} (MWh)
Base Case	Light	3.23	0.9567	57.01	2504.52
	Nominal	7.08	0.9092	248.68	
	Peak	12.92	0.8445	721.63	
	Annual E_{loss} (%) Reduction				-
PSO	Light	1.5	0.9918	9.78	446.38
	Nominal	2.97	0.9861	39.05	
	Peak	4.93	0.9472	147.6	
	Annual E_{loss} (%) Reduction				**82.18**
MG-TLBO	Light	1.1	0.9965	4.36	162.01
	Nominal	2.53	0.9920	16.95	
	Peak	3.4	0.9881	42.76	
	Annual E_{loss} (%) Reduction				**93.53**

In the light load level, harmonic distortion is already in the permissible region. However, nominal and peak load level has the large value of THDv than amount specified by IEEE standard of harmonics. Therefore, actual planning of DERs in distribution system should consider non-linear nature of loads. Further, decision parameters with non-linear loads are much varied as compared to the planning with linear load only. Total Harmonic distortion at each node of the system is shown in Figure 5.4. The improvement of voltage profile without and with the presence of DERs for all level of load is shown in Figure 5.5. It is observed from the figure that incorporation of the DERs substantially improve the voltage profile with respect to the base case of the system at each level.

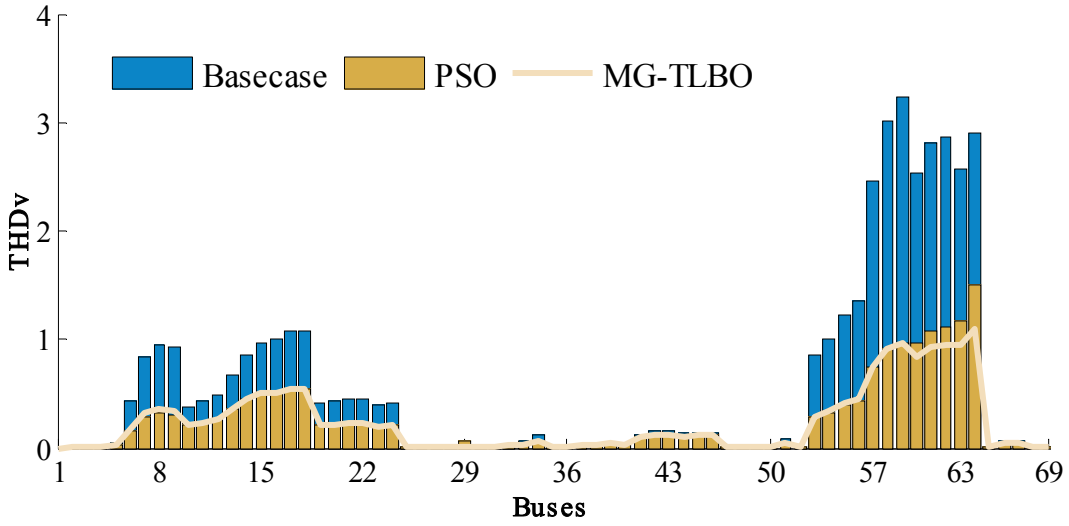

(a) Light Load

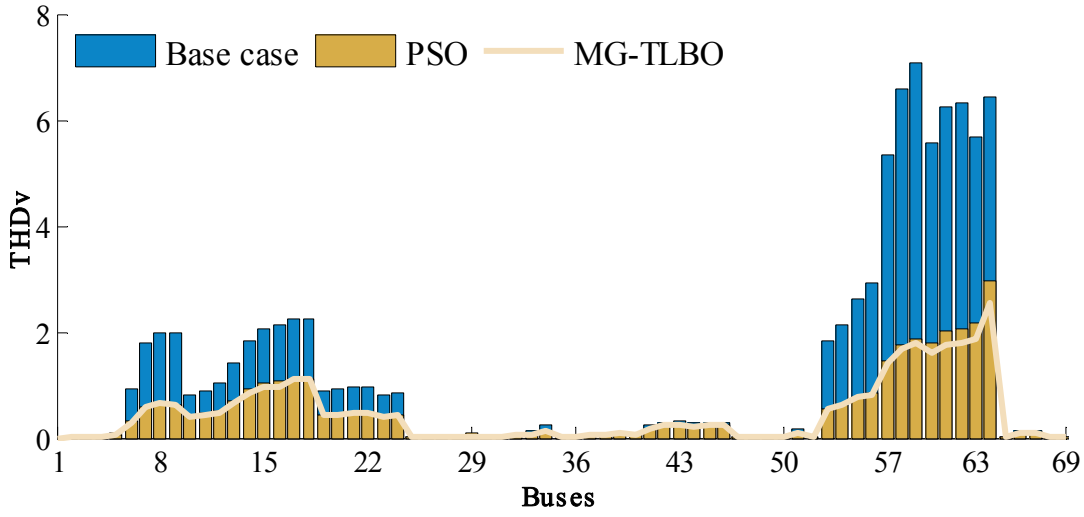

(b) Nominal Load

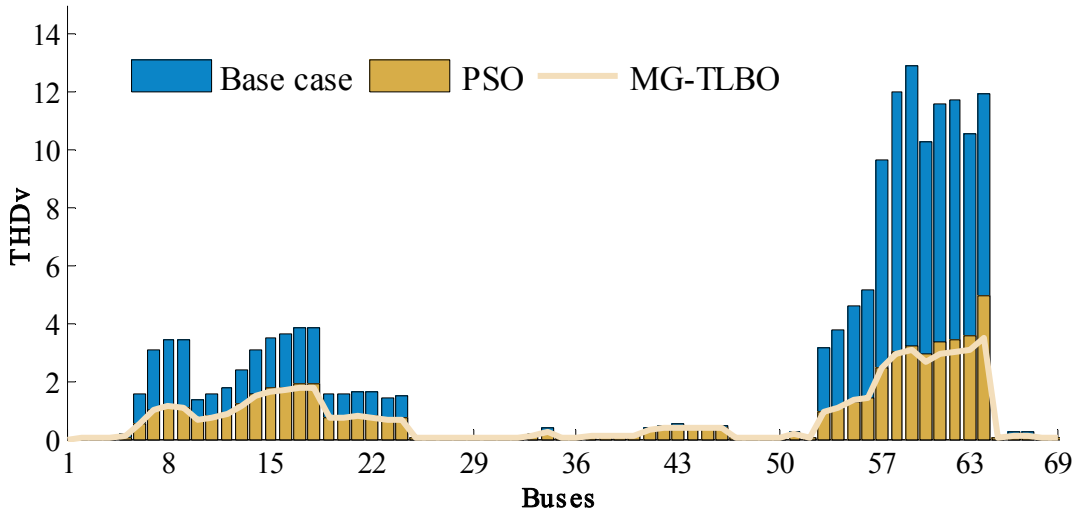

(c) Peak Load

Figure 5.4: Total harmonic distortion of 69-bus system for each load level

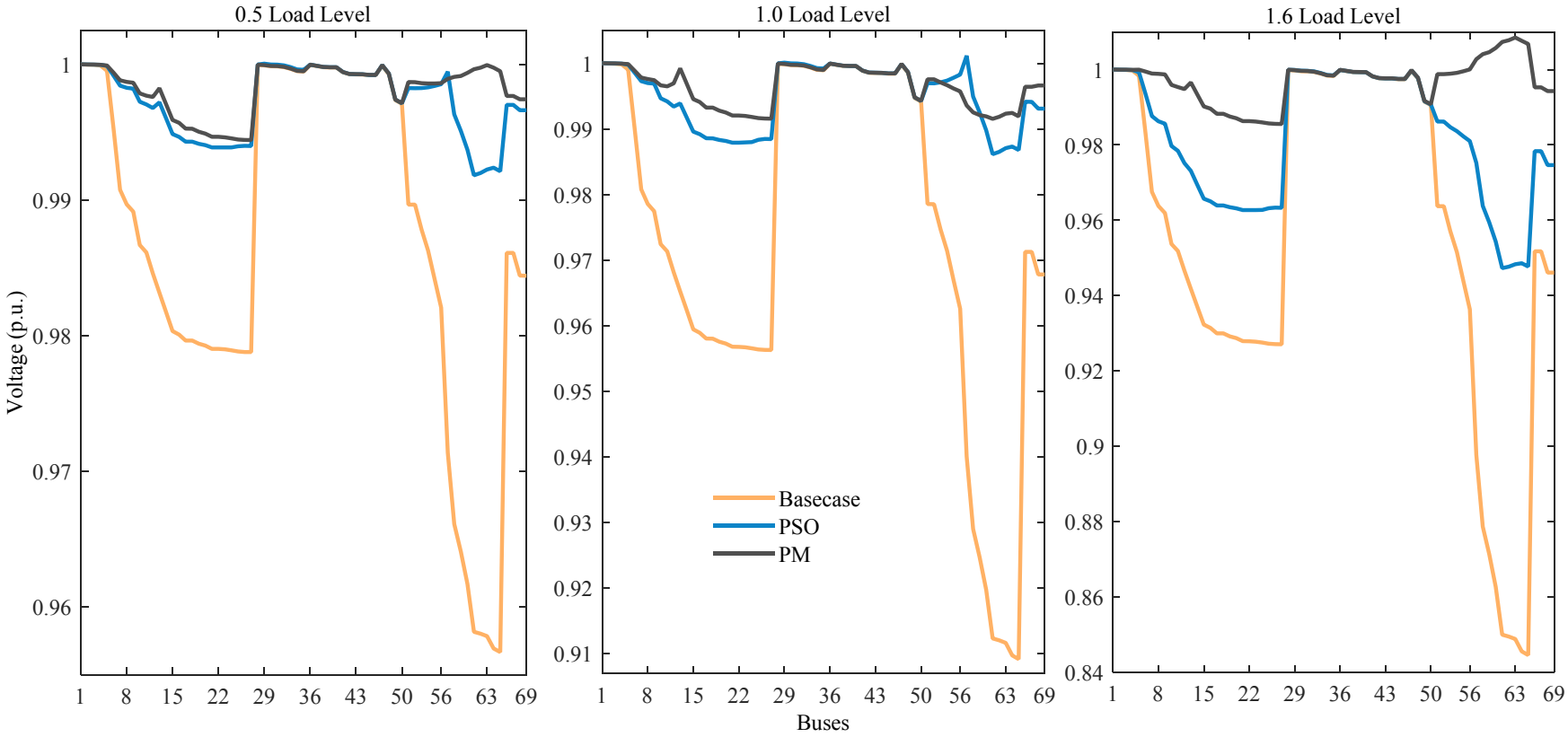

Figure 5.5: Voltage profile of the IEEE 69-bus system with non-linear loads

5.5.3 Test system C: 83-Bus Distribution System

An actual 11.4 kV practical radial distribution network belonging to the Taiwan Power Company is employed as a third test case. In addition, this system has incorporated some alterations considering practical planning of a radial distribution system with power quality issue. There are no changes in the spectrum of all three types of non-linear loads for each case study. In this system, non-linear loads are present at six buses and percentage of non-linear loads is shown in Table 5.8.

Table 5.8: Non-linear loads data for the 83-bus system

Bus No.	**Non-linear load type**	**Percentage**
34, 41, 45	Fluorescent	15
	Persomal Computer (PC)	10
	Adjustable Speed Drive (ASD)	15
6, 76, 81	ASD	30

Table 5.9: Optimal solution by using the PSO for harmonics polluted test system-C

Energy Resources	**Bus Location**	**Load level**		
		Light	**Nominal**	**Peak**
		kW/kVAr	**kW/kVAr**	**kW/kVAr**
DERs	56	472	1081	905
	27	588	1499	1332
	9	1304	2733	4596
	80	1622	3680	5316
	77	650	1285	1938
	71	1080	2699	3638
	34	1340	2762	4023
	20	1522	3059	4720
	52	774	1531	2684
SCs	80	500	1300	1700
	42	100	800	1800
	9	100	100	800
	64	300	900	200
	79	100	600	1400
	2	300	100	1300
	82	500	1100	300
	73	400	800	1400
	55	600	100	2700

The PSO algorithm is determined the optimal decision parameter that is shown in Table 5.9. The optimal planning of DERs requires one additional decision parameter in harmonic distorted third test system. It determines that nine buses is optimal number for this network. Moreover, optimal sizes of DERs are obtained adjoining their location.

The amelioration of the system performance after placing the optimal search value of decision parameter is shown in Table 5.10. The system performance is described in terms of reduction of THDV, enhancement of voltage profile and reduction of power losses for each load level. The proposed method achieves highest annual energy reduction as compared to the PSO approach in the 83-bus distribution systems.

Table 5.10: Optimal solution by using the MG-TLBO for harmonics polluted test system-C

Energy Resources	**Bus Location**	**Load level**		
		Light	**Nominal**	**Peak**
		kW/kVAr	**kW/kVAr**	**kW/kVAr**
DERs	55	988	2122	2850
	28	1117	2234	2470
	8	1609	3054	4332
	80	1518	3592	3138
	72	1360	2621	3293
	77	885	1496	2986
	20	761	2671	4504
	35	1021	2437	3994
	52	272	233	2032
SCs	42	300	800	1900
	80	200	800	600
	10	600	1500	1900
	64	300	600	1500
	84	300	300	900
	79	400	700	1200
	2	400	500	2900
	82	300	600	1000
	73	800	1500	2600

The MG-TLBO is applied to optimize the both decision parameter of DERs for each load level in the last case and acquires the large power reduction in each load level. In the fourth case, MG-TLBO achieves the maximum reduction of annual energy losses as shown in Table 5.11.

Table 5.11: System performance with harmonics polluted test system-C

Cases	Load Level	THD_V (max.)	V_{min} (p.u.)	P_{loss} (kW)	Annual E_{loss} (MWh)
Base Case	Light	7.1	0.9657	148.3	6036.89
	Nominal	14.2	0.9285	616.7	
	Peak	23.1	0.8787	1664.3	
	Annual E_{loss} (%) Reduction				-
PSO	Light	3.11	0.9791	56.36	2249.59
	Nominal	5.58	0.9560	233.5	
	Peak	7.54	0.9334	605.5	
	Annual E_{loss} (%) Reduction				62.73
MG-TLBO	Light	2.2	0.9854	45.36	1719.83
	Nominal	3.9	0.9742	169.5	
	Peak	4.9	0.9589	493.1	
	Annual E_{loss} (%) Reduction				71.51

In this case, the DER penetration should be equal or less than from case II for all case studies. The PSO and the proposed method search the optimal solution within the specified penetration of the DERs. However, the PSO has not obtained the significant loss reduction in the practical distribution system. Moreover, the proposed method achieves the best solution in each load level of the IEEE standard as well as practical distribution system.

The proposed algorithm is validated with comparison of the PSO algorithm in the actual distribution system. This system characteristic is different from standard distribution system so planning of the DERs allocation in this system obtained the realistic situation and solution to reduce the harmonics distortion. The comparison of bus voltage profile for each load level for all four cases is demonstrated in Figure 5.6. It can be remarked that voltage profile for the fourth case has been enhanced significantly over all load levels by proposed method. The voltage profile of the system is improved by using proposed method in each load level. This demonstrates

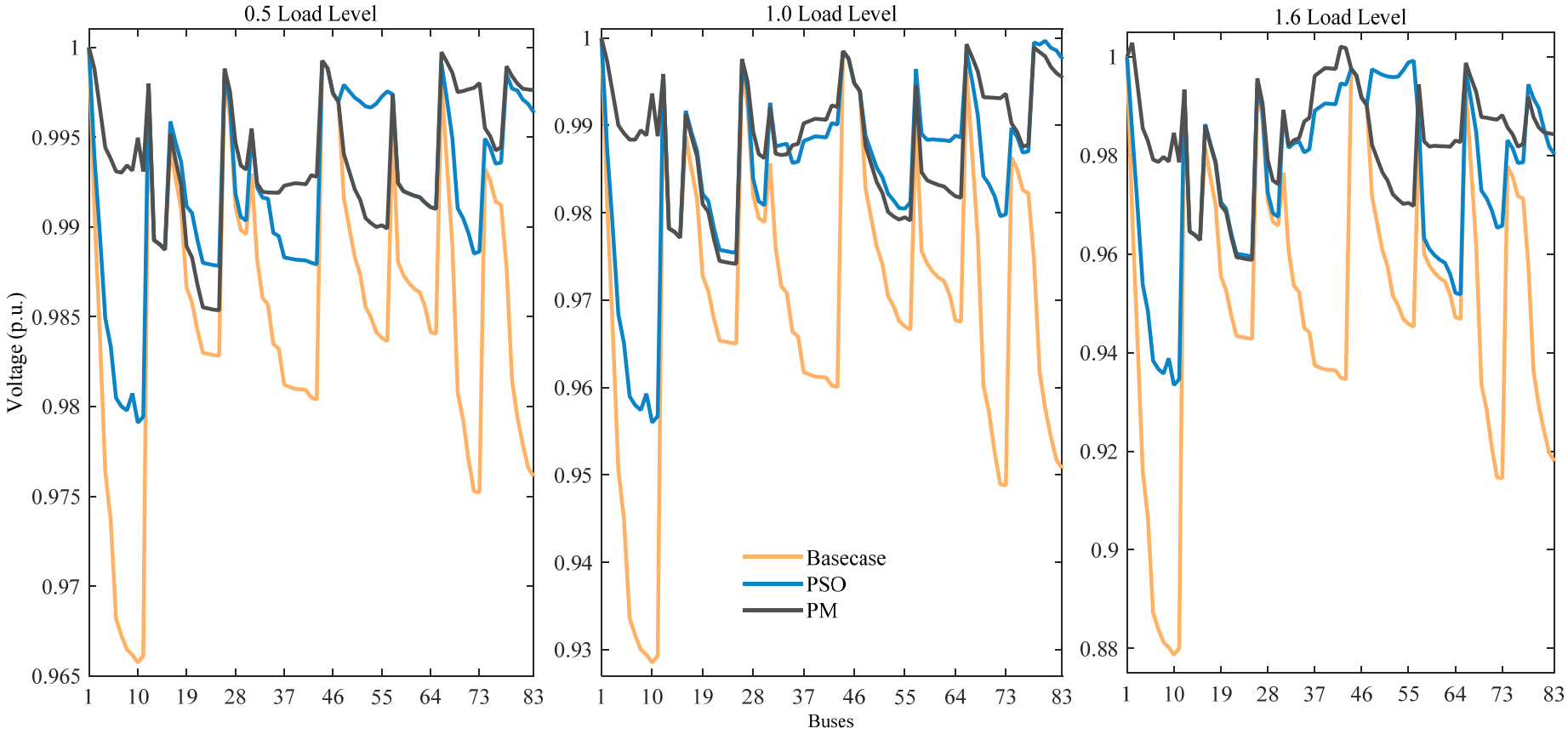

Figure 5.6: Voltage profile of the practical 83-bus system in presence of non-linear loads

the effectiveness of the proposed method in enhancing the voltage profile by a large margin.

5.6 Conclusion

The proposed work addresses the shortcomings of usual DER planning, which ignores non-linearity in the distribution system under different load conditions. The MG-TLBO is applied to optimize the power injection of the DERs at particular places in the medium voltage distribution system considering non-linear loads. The optimal penetration of the DERs at a proper location is compensated the harmonics distortion level acceding to IEEE 519 standard. The application results in better performance of the proposed method using MG-TLBO as compared to PSO algorithm in every case study. The PSO algorithm has not satisfied the each constraint in peak load level of the realistic Taiwan distribution system. Moreover, the proposed algorithm are achieved the best result in each load level of the distribution system. The MG-TLBO method is well tested for various simulated cases including the practical system with linear as well non-linear loads for its robustness and reliability.

Chapter – 6

PERFORMANCE ANALYSIS OF DISTRIBUTED ENERGY RESOURCES IN THREE-PHASE UNBALANCED DISTRIBUTION SYSTEMS

6.1 Introduction

Moreover, a lot of research work [2]-[171] with several approaches and optimization methods has been applied for the allocation of the DERs in the balance distribution system. However, distribution line of the system is untransposed. The end user loads of the distribution system are unequal distributed in the whole power system. Therefore, the DERs planning according to the assumption of the balanced distribution network is not a realistic approach. In the actual feeder, overhead line, underground cables, three type of loads (constant current, constant impedance, and constant power), and different type of transformer connection has been considered to introduce the realistic nature of the distribution system. Therefore, all practical consideration create the realistic planning of the DERs accommodation in the three-phase distribution system.

The OpenDSS simulator is used to analyze the characteristic of the unbalanced radial distribution system. Moreover, a parameterless optimization algorithm is required to optimize the DERs allocation optimization problem in the network. In the literature [157]-[160], artificial intelligence based heuristic algorithms have been widely practiced for the planning of distributed energy resources with any power system constraints. However, some algorithm-specific control parameters are used in all heuristic based methods, which need tuning for achieving the global solution. Moreover, the computational effort can be increased by improper tuning of algorithm-specific control parameters. Therefore, a Sharp Jaya algorithm is proposed for the planning of the DERs on an environmental structure of MATLAB® simulation by using the OpenDSS through the component object model. The Sharp Jaya algorithm is simple, single-phase and specific parameter-less, which is used to achieve admirable outcomes.

A co-simulation framework is utilized to provide a platform for interfacing between the structures of MATLAB® simulation and OpenDSS simulator. The co-

simulation environment with OpenDSS program is optimized the decision parameter for unity power factor and non-unity power factor operator DERs. The proposed algorithm sharpens the Standard Jaya algorithm using the shrinkage mechanism of the search area and parent-child model. The optimal placement and sizing of DERs are maximized the energy loss reduction while maintaining the desirable node voltage. The MG-TLBO and PSO algorithms are applied to compare with the S-Jaya approach in the simulation results which can show the strength of the proposed algorithm. Moreover, three IEEE radial distribution test systems (IEEE 13-bus, IEEE 37-bus, and IEEE 123-bus) have been used to validate the planning of the DER's allocation by the proposed algorithm.

6.2 Modeling of Distribution System Components

In radial distribution networks, distribution load flow is characterized by having only one path to flow the power from the feeder to each load of the system. A typical distribution network consists of one or more grid substations and each substation have one or more feeders. One or more following components are present in each feeder

6.2.1 Load Modeling

The consumer demand on distribution networks is typically specified by the consumed complex power. The assigned load is the maximum diversified demand of the system. The demand can be assigned as kW and kVAR, kW and power factor, or kVA and power factor. The feeder loads are modeled either delta connected or wye-connected. Further, the line-to-neutral voltage has been used to compute the current across the wye connected loads and the line-to-line voltage across the delta connected loads. Each calculation is done in per unit. Moreover, the loads can be single-phase, two-phase, or three-phase with any degree of unbalance which can be modeled as:

6.2.1.1. Constant power loads: The line current for constant power load (*PQ* loads) are computed by line-to-neutral voltages for wye-connected loads. Moreover, line-to-line voltages are used to calculate the current for delta connected loads.

$$I_r^{cp} = S_r^{cp} \Big/ V_r = \frac{\left|S_r^{cp}\right|}{\left|V_r\right|} \underline{\left|\zeta_r - \psi_r\right.}$$

$$I_y^{cp} = S_y^{cp} \Big/ V_y = \frac{\left|S_y^{cp}\right|}{\left|V_y\right|} \underline{\left|\zeta_y - \psi_y\right.} \qquad (6.1)$$

$$I_b^{cp} = S_b^{cp} \Big/ V_b = \frac{\left|S_b^{cp}\right|}{\left|V_b\right|} \underline{\left|\zeta_b - \psi_b\right.}$$

6.2.1.2. Constant impedance loads: In this type of loads, constant impedance of the loads has been determined by magnitude of line-to-neutral voltages for wye-connected loads and line-to-line voltages for delta connected loads.

$$Z_r = \left|V_r\right|^2 \Big/ S_r^* = \frac{\left|V\right|^2}{\left|S_r\right|} \underline{\left|\psi_r\right.}$$

$$Z_y = \left|V_y\right|^2 \Big/ S_y^* = \frac{\left|V\right|^2}{\left|S_y\right|} \underline{\left|\psi_Y\right.} \qquad (6.2)$$

$$Z_b = \left|V_b\right|^2 \Big/ S_b^* = \frac{\left|V\right|^2}{\left|S_b\right|} \underline{\left|\psi_b\right.}$$

The load current is calculated by using of equation (6.3).

$$I_r^{imp} = V_r \Big/ Z_r = \frac{\left|V_r\right|}{\left|Z_r\right|} \underline{\left|\zeta_r - \psi_r\right.}$$

$$I_r^{imp} = V_r \Big/ Z_r = \frac{\left|V_r\right|}{\left|Z_r\right|} \underline{\left|\zeta_r - \psi_r\right.} \qquad (6.3)$$

$$I_b^{imp} = V_b \Big/ Z_b = \frac{\left|V_b\right|}{\left|Z_b\right|} \underline{\left|\zeta_b - \psi_b\right.}$$

The voltage of each type of connection at consumer load might vary in each iteration. However, impedance of the load should be always constant during the iteration process of load flow.

6.2.1.3. Constant current loads: The magnitude of constant current load is fixed in each step of iteration and determines according the equation (6.1). The voltage angle across the load is changed in each iteration. Further, the angle of current also modify according the below equation (6.4). Therefore, the power factor of the load is always constant in whole process.

$$I_r^{cp} = \frac{\left|S_r^{cp}\right|}{\left|V_r\right|}\underline{\left|\zeta_r - \psi_r\right.}$$
$$I_y^{cp} = \frac{\left|S_y^{cp}\right|}{\left|V_y\right|}\underline{\left|\zeta_y - \psi_y\right.} \quad (6.4)$$
$$I_b^{cp} = \frac{\left|S_b^{cp}\right|}{\left|V_b\right|}\underline{\left|\zeta_b - \psi_b\right.}$$

6.2.1.4. Shunt Capacitors: Shunt capacitor bank is used to supply the reactive power support and improve the voltage regulation. Two types of capacitor connections are available, same as the load configuration, which are wye- and delta-connection,

$$I_r^{cap} = j\xi_r.\mathrm{V}$$
$$I_y^{cap} = j\xi_y.\mathrm{V} \quad (6.5)$$
$$I_b^{cap} = j\xi_b.\mathrm{V}$$

where, ξ is susceptance of capacitor which is computed by

$$\xi = \frac{\mathrm{var}\ specified\ rating\ of\ capacitor\ in\ per\ phase}{voltage\ rating\ across\ capacitor\ in\ per\ phase} \quad (6.6)$$

In the actual distribution system, all shunt capacitor are prototypes as three-phase bank whenever any phase does not exist then set the zero current value at phase.

6.2.2 Three-Phase Transformer Modeling:

In the distribution system, delta-ground wye type of transformer is present at four-wire wye feeder, and delta-delta type transformer is used to transform the voltage into three wire delta feeder. Further, five type of three-phase transformer is used in radial distribution system which are

- Delta–Delta
- Delta–Grounded Wye
- Ungrounded Wye-Delta
- Grounded Wye–Grounded Wye
- Open Wye–Open Delta

In this thesis work, first two types of transformer connection have been used in the three-phase distribution system. Generalized three-phase transformer connection is shown in Figure 6.1. The loads of the distribution system are connected to low voltage side of step-down transformers and high voltage side connected to grid substation.

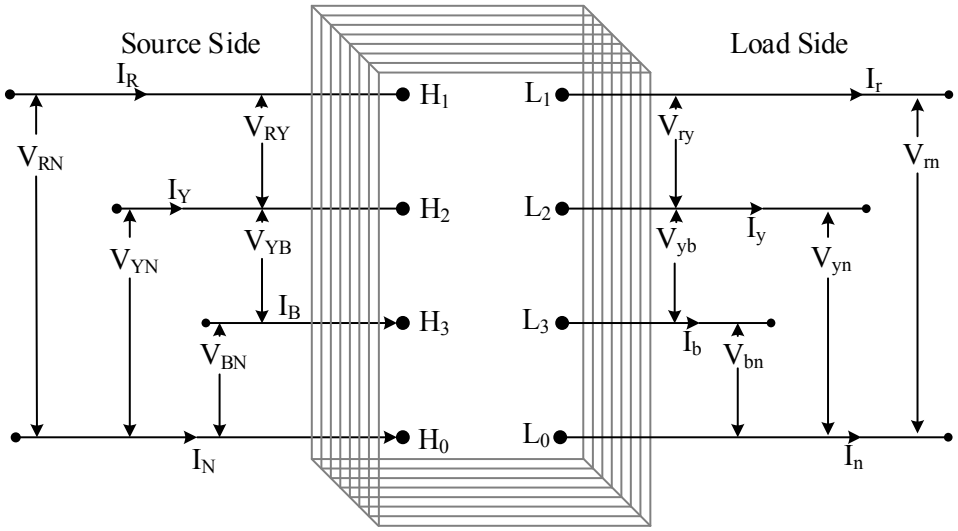

Figure 6.1: Generalized three phase transformer connection

***(i) Delta–Delta type connection of transformer winding*:** The delta-delta type connection is used at the primary stage of the distribution system. Further, this type of transformer can be supplied to three phase loads and three single phase delta-delta connected loads, which is depicted in Figure 6.2.

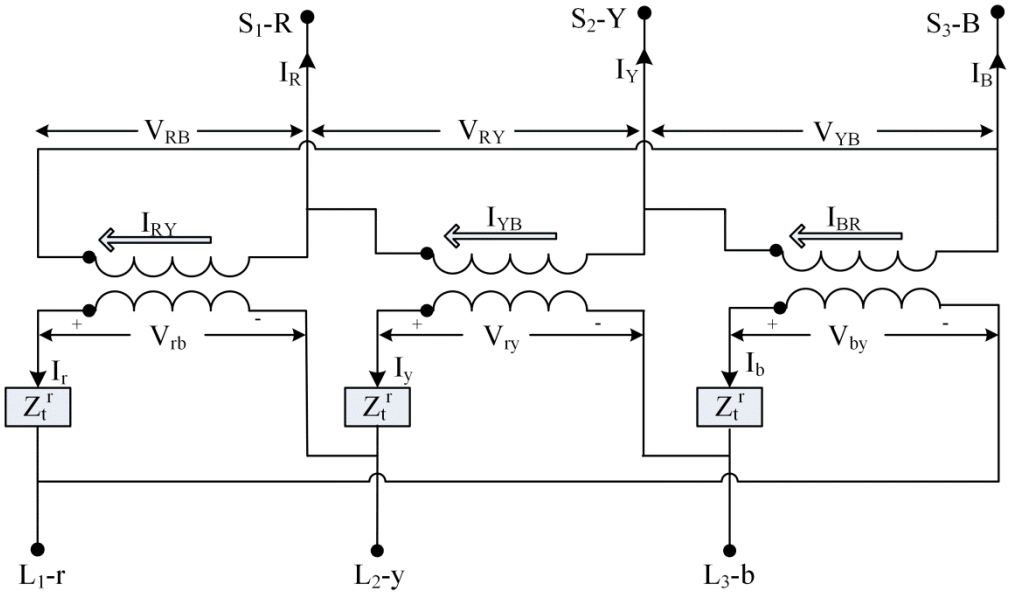

Figure 6.2: Delta–Delta type connection of transformer winding

The relation between source side line-line voltage (V_{LL}^{RYB}) and load side voltage (V_{tmr}^{ryb}) for this type of connection can be express by the following equation,

$$\begin{bmatrix} V_{LL}^{RY} \\ V_{LL}^{YB} \\ V_{LL}^{BR} \end{bmatrix} = \begin{bmatrix} n_t & 0 & 0 \\ 0 & n_t & 0 \\ 0 & 0 & n_t \end{bmatrix} \cdot \begin{bmatrix} V_{tmr}^{ry} \\ V_{tmr}^{yb} \\ V_{tmr}^{br} \end{bmatrix} \tag{6.7}$$

$$\left[V_{LL}^{RYB} \right] = \left[A_V^{dd} \right] \cdot \left[V_{tmr}^{ryb} \right] \tag{6.8}$$

Further, current across the load side (I_{ph}^{ryb}) of transformer as function of source current (I_{ph}^{RYB}) of the configuration

$$\begin{bmatrix} I_{ph}^{ry} \\ I_{ph}^{yb} \\ I_{ph}^{br} \end{bmatrix} = \begin{bmatrix} n_t & 0 & 0 \\ 0 & n_t & 0 \\ 0 & 0 & n_t \end{bmatrix} \begin{bmatrix} I_{ph}^{RY} \\ I_{ph}^{YB} \\ I_{ph}^{BR} \end{bmatrix} \tag{6.9}$$

$$\left[I_{ph}^{ryb} \right] = \left[A_I^{dd} \right] \cdot \left[I_{ph}^{RYB} \right] \tag{6.10}$$

where,

$$n_t = \frac{V_{LL}^h}{V_{LL}^l} \tag{6.11}$$

The source side line current as function of the phase currents that can be rewritten as

$$\left[I_L^{RYB} \right] = \left[D_I^{dd} \right] \cdot \left[I_{ph}^{RYB} \right] \tag{6.12}$$

$$\left[D_I^{dd} \right] = \begin{bmatrix} 1 & 0 & -1 \\ -1 & 1 & 0 \\ 0 & -1 & 1 \end{bmatrix} \tag{6.13}$$

The both side of line current in delta-delta connected transformer are in phase and only differ the magnitude by the transformer winding turn ratio. Further, the generalized equation of delta-delta transformer is determined with concerning the

line-neutral voltage.

$$\left[V_{tmr}^{ryb}\right]=\left[V_{LL}^{ryb}\right]+\left[Z_{tmr}^{ryb}\right].\left[I_{ph}^{ryb}\right] \tag{6.14}$$

where, Z_{tmr}^{ryb} is transformer winding impedance which may either same or different for each winding.

$$\left[Z_{tmr}^{ryb}\right]=\begin{bmatrix} Z_{tmr}^{ry} & 0 & 0 \\ 0 & Z_{tmr}^{yb} & 0 \\ 0 & 0 & Z_{tmr}^{br} \end{bmatrix} \tag{6.15}$$

Substitute the value of equation (6.14) into equation (6.8) then

$$\left[V_{LL}^{RYB}\right]=\left[A_{V}^{dd}\right]\cdot\left[V_{LL}^{ryb}\right]+\left[A_{V}^{dd}\right]\cdot\left[Z_{tmr}^{ryb}\right].\left[I_{ph}^{ryb}\right] \tag{6.16}$$

The load side line current is put at placed of phase current.

$$\left[V_{LL}^{RYB}\right]=\left[A_{V}^{dd}\right]\cdot\left[V_{LL}^{ryb}\right]+\left[A_{V}^{dd}\right]\cdot\left[Z_{tmr}^{ryb}\right].\left[G_{dd}\right]\cdot\left[I_{LL}^{ryb}\right] \tag{6.17}$$

where,

$$\left[G_{dd}\right]=\frac{1}{Z_{tmr}^{ry}+Z_{tmr}^{yb}+Z_{tmr}^{br}}\cdot\begin{bmatrix} Z_{tmr}^{br} & -Z_{tmr}^{yb} & 0 \\ Z_{tmr}^{ryb} & Z_{tmr}^{ry}+Z_{tmr}^{br} & 0 \\ -Z_{tmr}^{ry}-Z_{tmr}^{yb} & Z_{tmr}^{yb} & 0 \end{bmatrix} \tag{6.18}$$

Further, generalized matrices can be converted in line to neutral voltage.

$$\left[V_{LN}^{RYB}\right]=\left[W_{dd}\right]\cdot\left[V_{LL}^{RYB}\right] \tag{6.19}$$

$$\left[V_{LN}^{RYB}\right]=\left[W_{dd}\right]\cdot\left[A_{V}^{dd}\right]\cdot\left[D_{V}^{dd}\right]\left[V_{LN}^{ryb}\right]+\left[W_{dd}\right]\cdot\left[A_{V}^{dd}\right]\cdot\left[Z_{tmr}^{ryb}\right].\left[G_{dd}\right]\cdot\left[I_{LL}^{ryb}\right] \tag{6.20}$$

The generalized equation of current for delta connection are defined in term of line current

$$\left[I_{LL}^{RYB}\right]=\left[A_{I}^{dd}\right]^{-1}\cdot\left[I_{LL}^{ryb}\right] \tag{6.21}$$

The reverse generalized matrix is defined with use of equation (6.16).

$$\left[V_{LL}^{ryb}\right]=\left[A_{V}^{dd}\right]^{-1}\cdot\left[V_{LL}^{RYB}\right]-\left[Z_{tmr}^{ryb}\right].\left[I_{ph}^{ryb}\right] \tag{6.22}$$

$$\left[V_{LN}^{ryb}\right]=\left[W_{dd}\right]\left[A_{V}^{dd}\right]^{-1}\cdot\left[D_{V}^{dd}\right]\left[V_{LN}^{RYB}\right]-\left[W_{dd}\right]\left[Z_{tmr}^{ryb}\right].\left[G_{dd}\right]\left[I_{LL}^{ryb}\right] \tag{6.23}$$

The generalized matrices can be used in load flow analysis of the delta-delta connected distribution system.

***(ii) Delta–Grounded Wye type connection of transformer winding*:** This type of transformer can be supplied the service to balanced three single phase loads. In this connection, low voltage side current I_r and voltage V_{ry} leg by 30 degrees form high voltage side current I_R and voltage V_{RY}. The positive sequence phasor diagrams of various positive sequence voltage as shown in Figure 6.3.

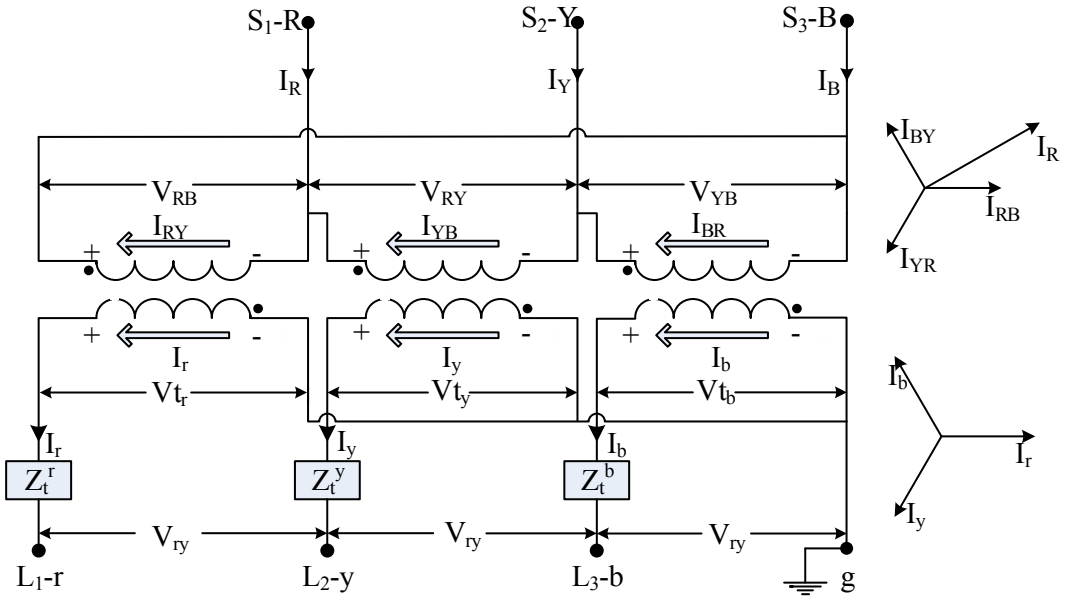

Figure 6.3: Delta–Grounded wye type connection of transformer winding

The change magnitude of voltage depends of turn ratio of transformer winding (n_t) or transformer ratio (a_t) which can be define as

$$n_t=\frac{V_{LL}^{h}}{V_{LN}^{l}} \tag{6.24}$$

$$a_t=\frac{n_t}{\sqrt{3}}=\frac{V_{LL}^{h}}{V_{LL}^{l}} \tag{6.25}$$

The source side of line to line voltage is related to load side of line to neutral voltage that is given by

$$\begin{bmatrix} V_{LL}^{RY} \\ V_{LL}^{YB} \\ V_{LL}^{BR} \end{bmatrix} = \begin{bmatrix} 0 & -n_t & 0 \\ 0 & 0 & -n_t \\ -n_t & 0 & 0 \end{bmatrix} \cdot \begin{bmatrix} V_{tmr}^{r} \\ V_{tmr}^{y} \\ V_{tmr}^{b} \end{bmatrix} \tag{6.26}$$

$$\left[V_{LL}^{RYB} \right] = \left[A_V \right] \cdot \left[V_{tmr}^{ryb} \right] \tag{6.27}$$

where

$$\left[A_V \right] = \begin{bmatrix} 0 & -n_t & 0 \\ 0 & 0 & -n_t \\ -n_t & 0 & 0 \end{bmatrix} \tag{6.28}$$

The line-neutral voltage can be find out as function of line-line voltage

$$\left[V_{LL}^{RYB} \right] = \left[D_V \right] \cdot \left[V_{LN}^{RYB} \right] \tag{6.29}$$

where

$$\left[D_V \right] = \begin{bmatrix} 1 & -1 & 0 \\ 0 & 1 & -1 \\ -1 & 0 & 1 \end{bmatrix} \tag{6.30}$$

The source side line to neutral voltage can be found by applying the Kirchhoff"s voltage law

$$\left[V_{LN}^{h} \right] = \left[a_t \right] \cdot \left[V_{LG}^{l} \right] + \left[b_t \right] \cdot \left[I_{ryb} \right] \tag{6.31}$$

where,

$$\left[b_t \right] = \left[a_t \right] \cdot \left[Z_t^{ryb} \right] \tag{6.32}$$

$$\left[Z_t^{ryb} \right] = \begin{bmatrix} Z_t^{r} & 0 & 0 \\ 0 & Z_t^{y} & 0 \\ 0 & 0 & Z_t^{b} \end{bmatrix} \tag{6.33}$$

The line current can be determine the delta connected source side of transformer as

$$\left[I_{ln}^{RYB}\right]=\left[D_V\right]\cdot\left[I_{dl}^{RYB}\right] \tag{6.34}$$

The source side line current are determine as function of the load side current which is given in equation (6.35)

$$\left[I_{dl}^{RYB}\right]=\frac{1}{n_t}\cdot\begin{bmatrix}1 & 0 & 0\\ 0 & 1 & 0\\ 0 & 0 & 1\end{bmatrix}\cdot\begin{bmatrix}I_r\\ I_y\\ I_b\end{bmatrix} \tag{6.35}$$

Further, above equation is used in equation (6.34) and found generalized equation of current

$$\left[I_{ln}^{RYB}\right]=\left[c_l\right].\left[V_{LG}^{ryb}\right]+\left[d_l\right]\cdot\left[I^{ryb}\right] \tag{6.36}$$

where,

$$\left[d_l\right]=\frac{1}{n_t}\cdot\begin{bmatrix}1 & -1 & 0\\ 0 & 1 & -1\\ -1 & 0 & 1\end{bmatrix} \tag{6.37}$$

$$\left[c_l\right]=\begin{bmatrix}0 & 0 & 0\\ 0 & 0 & 0\\ 0 & 0 & 0\end{bmatrix} \tag{6.38}$$

The load side line to ground voltage can be found by equation (6.39)

$$\left[V_{LG}^{ryb}\right]=\left[A_t\right]\cdot\left[V_{LN}^{RYB}\right]-\left[B_t\right]\cdot\left[I_{ryb}\right] \tag{6.39}$$

where

$$\left[A_t\right]=\left[A_V\right]^{-1}\cdot\left[D_V\right] \tag{6.40}$$

Equations (6.13) and (6.16) are the normalized equations for the step-down delta-grounded wye type of transformer.

6.2.3 Distribution System Line Modeling:

The series impedance of overhead and underground lines is not uniformly distributed in whole distribution system. Some end users require the only one-phase

while few two-phase (V-phase) and most of the distribution loads operate on three-phase supply

(i) Series impedance of overhead and underground lines: The surrounding atmosphere of the conductor of the distribution line consist the self and mutual components of impedance. The total circulating flux across the conductor is given by

$$\lambda = 2e^{-7} \cdot \left(I_1 \cdot \ln \frac{1}{D_{1\aleph}} + I_2 \cdot \ln \frac{1}{D_{2\aleph}} + \ldots + I_{\aleph} \cdot \ln \frac{1}{GMR_{\aleph}} \ldots + I_{\Re} \cdot \ln \frac{1}{D_{\Re\aleph}} \right) \tag{6.41}$$

where, $D_{\Re\aleph}$ is distance between $\Re^{th}$ and $\aleph^{th}$ conductor and $GMR_{\aleph}$ is geometric mean radius of $\aleph^{th}$ conductor. Moreover, self and mutual inductance of $\aleph^{th}$ conductor to $\Re^{th}$ conductor is elaborate in following equation

$$L_{\aleph\aleph} = \frac{\lambda_{\aleph\aleph}}{I_{\aleph}} = 2e^{-7} \cdot \ln \frac{1}{GMR_{\aleph}} \tag{6.42}$$

$$L_{\aleph\Re} = \frac{\lambda_{\aleph\Re}}{I_{\Re}} = 2e^{-7} \cdot \ln \frac{1}{D_{\aleph\Re}} \tag{6.43}$$

In this chapter, the conductor size, spacing between conductors, and transposition have been considered for accurate analysis. Further, Carson's technique is applied to calculate the self and mutual impedance for any arbitrary conductor of overhead line and underground cable.

$$Z_{\aleph\aleph} = \Gamma_{\aleph} + 4\omega \mathrm{P}_{\aleph\aleph} G + j\left(\chi_{\aleph} + 2\omega G . \ln \frac{D_{\aleph\aleph}^{img}}{\gamma_{\aleph}} + 4\omega \vartheta G \right) \tag{6.44}$$

$$Z_{\aleph\Re} = 4\omega \mathrm{P}_{\aleph\Re} G + j\left(2\omega G . \ln \frac{D_{\aleph\aleph}^{img}}{D_{\aleph\Re}} + 4\omega \vartheta G \right) \tag{6.45}$$

where,

$$\chi_{\aleph} = 2\omega G \cdot \ln \frac{\gamma}{GMR_{\aleph}} \tag{6.46}$$

$$P_{\aleph\Re} = \frac{\Pi}{8} - \frac{1}{3\sqrt{2}} \kappa_{\aleph\Re} \cos(\theta_{\aleph\Re}) + \frac{\kappa_{\aleph\Re}^2}{16} \cos(2\theta_{\aleph\Re}) . \left(0.6728 + \ln \frac{2}{\kappa_{\aleph\Re}} \right) \tag{6.47}$$

$$\vartheta_{\aleph\Re} = -0.0386 + \frac{1}{2}\cdot \ln\frac{2}{\kappa_{\aleph\Re}} + \frac{1}{3\sqrt{2}}\kappa_{\aleph\Re}\cos\left(\theta_{\aleph\Re}\right) \tag{6.48}$$

$$\kappa_{\aleph\Re} = 8.565e^{-4}.\mathrm{D}_{\aleph\Re}^{img}\cdot\sqrt{\frac{f}{\rho}} \tag{6.49}$$

where, $Z_{\aleph\aleph}$ and $Z_{\aleph\Re}$ are self and mutual impedance in Ω/mile. Γ is conductor resistance in Ω/mile. G is 0.1609344e^{-3} in Ω/mile. γ is radius of $\aleph^{th}$ conductor in feet. $D_{\aleph\aleph}^{img}$ is distance of $\aleph^{th}$ conductor and image of $\Re^{th}$ conductor in feet. P is resistivity of earth in Ω-meter. θ is angle between image of $\Re^{th}$ conductor line to own image line of $\aleph^{th}$ conductor. The resistance, GMR, and various distance are unknown parameter. Therefore, modified Carson's equations defined the missing parameters. The modified Carson's equations are shown in following equation

$$Z_{\aleph\aleph} = \Gamma_{\aleph} + 0.09530 + j0.12134\left(\ln\frac{1}{GMR_{\aleph}} + 7.93402\right) \tag{6.50}$$

$$Z_{\aleph\Re} = 0.09530 + j0.12134\left(\ln\frac{1}{D_{\aleph\Re}} + 7.93402\right) \tag{6.51}$$

These equations are used to compute the primitive mutual and self-impedance of underground and overhead distribution line of the electrical system. An overhead line consists of three phase four wire line segment which is shown in Figure 6.4. Further, primitive matrix becomes 4×4 matrix which has a neutral wire. However, three phase underground cable consisting three neutral then matrix size is 6×6.

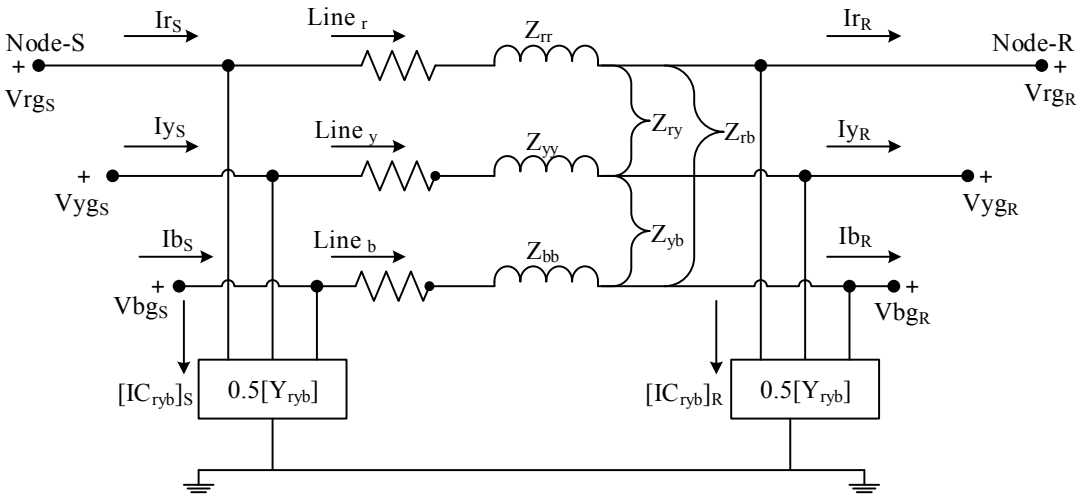

Figure 6.4: Line segment of distribution network

The Kron reduction method is applied to reduce the matrix in the size of 3×3 which is present in following equation (6.52). This equation is finalizing expression of phase impedance matrix.

$$\left[z_{ryb}\right]=\begin{bmatrix} z_{rr} & z_{ry} & z_{rb} \\ z_{yr} & z_{yy} & z_{yb} \\ z_{br} & z_{by} & z_{bb} \end{bmatrix} \tag{6.52}$$

The distribution system is not transpose. Therefore, the diagonal and off-diagonal are not equal to each other. If single phase and two-phase (V-phase) system are situated in the system then matrix become as

$$\left[z_{ryb}\right]=\begin{bmatrix} 0 & 0 & 0 \\ 0 & z_{yy} & 0 \\ 0 & 0 & 0 \end{bmatrix} \tag{6.53}$$

In equation (6.53) only phase y are present in the single phase. Moreover, phase ‘r’ and ‘b’ are present in equation (6.54).

$$\left[z_{ryb}\right]=\begin{bmatrix} z_{rr} & 0 & z_{rb} \\ 0 & 0 & 0 \\ z_{br} & 0 & z_{bb} \end{bmatrix} \tag{6.54}$$

The three phase delta system has not required the Kron reduction method which is determine only the application of Carson’s equation. Further, voltage equation in matrix form can be represent for each line segment of the radial distribution system as

$$\begin{bmatrix} V_{ry} \\ V_{yb} \\ V_{rb} \end{bmatrix}=\begin{bmatrix} V_r \\ V_y \\ V_b \end{bmatrix}+\begin{bmatrix} z_{rr} & z_{ry} & z_{rb} \\ z_{yr} & z_{yy} & z_{yb} \\ z_{br} & z_{by} & z_{bb} \end{bmatrix}\begin{bmatrix} I_r \\ I_y \\ I_b \end{bmatrix} \tag{6.55}$$

The generalized form of equation is present as

$$\left[V_{ryb}^{LG}\right]^{(1)}=\left[V_{ryb}^{LG}\right]^{(0)}+\left[Z_{abc}\right]\cdot\left[I_{abc}\right] \tag{6.56}$$

The actual value of phase impedance is support to the perfect calculation of voltage drop which is primary concern of the distribution system.

(ii) Shunt admittance of overhead and underground lines: The total value of admittance is due to the shunt capacitance because the value of conductance is very less as compared to shunt capacitance. An electrical field is produced in the presence of charged conductor which introduces the capacitance of the line due to the potential difference between the line conductors. Same as the previous point, Carson's equation is applied to develop the general voltage-drop equation for overhead lines in the presence of shunt capacitance.

$$\mathrm{P}_{\aleph\aleph} = 11.17689 \cdot \ln \frac{D_{\aleph\aleph}^{img}}{\gamma_{\aleph}} \tag{6.57}$$

$$\mathrm{P}_{\aleph\Re} = 11.17689 \cdot \ln \frac{D_{\aleph\aleph}^{img}}{D_{\Re\aleph}} \tag{6.58}$$

The matrix representation of primitive coefficient are shown as

$$\left[\mathrm{P}_{primitive}\right] = \begin{bmatrix} P_{\aleph\Re} & P_{\aleph \mathrm{N}_c} \\ P_{\mathrm{N}_c\Re} & P_{\mathrm{N}_c\mathrm{N}_c} \end{bmatrix} \tag{6.59}$$

The Kron reduction method is used to reduce the size of matrix in presence of neutral conductor. Then capacitance matrix computes as equation (6.60).

$$\left[C_{ryb}\right] = \left[P_{ryb}\right]^{-1} \tag{6.60}$$

$$\left[y_{ryb}\right] = j.\omega.\left[C_{ryb}\right] \tag{6.61}$$

Further, admittance matrix of a three phase line are determine as

$$\begin{bmatrix} I_r^{cap} \\ I_y^{cap} \\ I_b^{cap} \end{bmatrix} = \begin{bmatrix} y_{rr} & y_{ry} & y_{rb} \\ y_{yr} & y_{yy} & y_{yb} \\ y_{br} & y_{by} & y_{bb} \end{bmatrix} \begin{bmatrix} V_{rg} \\ V_{yg} \\ V_{bg} \end{bmatrix} \tag{6.62}$$

$$\left[I_{ryb}^{cap}\right] = \left[y_{ryb}\right] \cdot \left[V_{ryb}^{LG}\right] \tag{6.63}$$

The shunt admittance should include in light load condition. Moreover, the underground cable of distribution lines has high shunt admittance as compared to the

overhead line. The modeling of distribution line segment is an importance analysis with correct spacing between conductor and accurate phasing of the line. The line segment current and voltage of the distribution system is computed in equation (6.64) and (6.65) by using the Kirchhoff's current and voltage law.

$$\begin{bmatrix} I_r^{line} \\ I_y^{line} \\ I_b^{line} \end{bmatrix} = \begin{bmatrix} I_r \\ I_y \\ I_b \end{bmatrix} + \frac{1}{2} \cdot \begin{bmatrix} I_r^{cap} \\ I_y^{cap} \\ I_b^{cap} \end{bmatrix} \tag{6.64}$$

$$\begin{bmatrix} V_{rg} \\ V_{yg} \\ V_{rg} \end{bmatrix}^S = \begin{bmatrix} V_{rg} \\ V_{yg} \\ V_{rg} \end{bmatrix}^R + \begin{bmatrix} z_{rr} & z_{ry} & z_{rb} \\ z_{yr} & z_{yy} & z_{yb} \\ z_{br} & z_{by} & z_{bb} \end{bmatrix} \begin{bmatrix} I_r^{line} \\ I_y^{line} \\ I_b^{line} \end{bmatrix} \tag{6.65}$$

The value of line current substitute into equation (6.65) then voltage generalized equation is

$$\left[V_{ryb}^{LG}\right]^S = [ra].\left[V_{ryb}^{LG}\right]^R + [rb] \cdot \left[I_{ryb}\right]^R \tag{6.66}$$

where

$$\begin{aligned} [ra] &= [U] + \frac{1}{2} \cdot \left[Z_{ryb}\right] \cdot \left[Y_{ryb}\right] \\ [rb] &= \left[Z_{abc}\right] \end{aligned} \tag{6.67}$$

The source side current of the line segment is

$$\left[I_{ryb}\right]^S = \left[I_{ryb}^{Line}\right]^R + \frac{1}{2} \cdot \left[Y_{ryb}\right] \cdot \left[V_{ryb}^{LG}\right]^S \tag{6.68}$$

The value of line current substitute into equation (6.68) then current generalized equation is

$$\left[I_{ryb}\right]^S = [rc].\left[V_{ryb}^{LG}\right]^R + [rd] \cdot \left[I_{ryb}\right]^R \tag{6.69}$$

where

$$[rc] = \left[Y_{abc}\right] + \frac{1}{4} \cdot \left[Y_{ryb}\right] \cdot \left[Z_{ryb}\right] \cdot \left[Y_{ryb}\right]$$

$$[rd]=[U]+\frac{1}{2}\cdot[Z_{abc}]\cdot[Y_{abc}] \tag{6.70}$$

Further, equation (6.66) and (6.70) can be represent into partitioned matrix form in equation (6.71) as

$$\begin{bmatrix} V_{ryb}^{LG} \\ I_{ryb} \end{bmatrix}^{s} = \begin{bmatrix} ra & rb \\ rc & rd \end{bmatrix} \begin{bmatrix} V_{ryb}^{LG} \\ I_{ryb} \end{bmatrix}^{r} \tag{6.71}$$

This equation representation as the transmission line segment with ABCD parameter is shown in above equation. The generalized form can be used for distribution exact line segment modeling which has been used in the analysis the unbalanced distribution with the realistic condition of the system.

6.3 Problem Description

The optimal penetration of the DERs power for optimal allocation problem is formulated to minimizing the active power losses. The benefits associated with DERs mainly depend upon how optimally they are allocated in the radial distribution system while node voltage and all constraints of the power system should be preserved in the proper boundary. Further, the aim of this objective function is described as:

$$F=\max\left[\rho\left(P_{loss}^{b}-P_{loss}^{a}\right)\right] \tag{6.72}$$

where,

$$P_{loss}=\sum_{p=1}^{p_h}\sum_{\alpha=1}^{n_n}\sum_{\beta=1}^{n_b}\left(\begin{aligned}&\mathrm{R}_{CP}\cdot\frac{P_{CP_{p,\alpha,\beta}}^{2}+Q_{CP_{p,\alpha,\beta}}^{2}}{\left|V_{CP_{p,\alpha,\beta}}\right|^{2}}\\&+\mathrm{R}_{CI}\cdot\frac{P_{CI_{p,\alpha,\beta}}^{2}+Q_{CI_{p,\alpha,\beta}}^{2}}{\left|V_{CI_{p,\alpha,\beta}}\right|^{2}}\\&+\mathrm{R}_{CC}\cdot\frac{P_{CC_{p,\alpha,\beta}}^{2}+Q_{CC_{p,\alpha,\beta}}^{2}}{\left|V_{CC_{p,\alpha,\beta}}\right|^{2}}\end{aligned}\right) \tag{6.73}$$

The P_{loss}^{b} and P_{loss}^{a} are the power losses reduction in percentage before and after the allocation of the DERs which has been computed for each type of load characteristic

in each phase of the supply at every node of the system. Moreover, three type of load demand as constant power (CP), constant current (CC), constant impedance (CI) is present in the system. Therefore, power loss calculation is split according to the characteristic of loads. ρ is penalty factor for the situation of bus voltage deviation at each node of the system, given by equation (6.74).

$$\rho = \Big/\left(1 + Max\left(\nabla V_{p,\alpha,\beta}^{CP} + \nabla V_{p,\alpha,\beta}^{CI} + \nabla V_{p,\alpha,\beta}^{CC}\right)\right) \quad \forall \alpha \in n_n, p \in p_h, \beta \in n_b \qquad (6.74)$$

where,

$$\nabla V_{p,\alpha,\beta}^{CP,CI,CC} = \begin{Bmatrix} 0 & V_{\min} \le V_{p,\alpha,\beta} \le V_{\max} \\ \text{large value multiplier} & \text{else} \end{Bmatrix} \qquad (6.75)$$

The equation (6.75) exhibit the condition of penalty for each type of loads of the system. The penalty factor helps to classify the solution into the feasible and non-feasible groups. The solutions that decline the system limits using decision penalty variable are called non-feasible solutions.

6.3.1 Voltage Limits at Load Bus and Slack Bus

The each bus voltage should lie within the specified boundaries which is five percent from the rated value according to distribution feeder regulation. The voltage magnitudes and angle of the slack bus must be 1 and 0, respectively, throughout the duration of DERs planning.

$$V_{ryb}^{\min} \le V_{ryb,\alpha} \le V_{ryb}^{\max} \quad \forall \alpha \in n_n \qquad (6.76)$$

6.3.2 Power Balance

In the network, total power injection from the feeder of distribution substation and all DER power must be equal to the summation of the load demand and line losses of the distribution system.

$$S_{ryb}^{grid} + S_{ryb}^{DERs,\alpha} - B_{ryb,\alpha\beta}^{2} \cdot R_{ryb,\alpha\beta} = S_{ryb}^{load,\alpha} \quad \forall \alpha \in n_n \qquad (6.77)$$

6.3.3 Distribution Line Thermal Limit

The current carrying capacity of the distribution line must consider as the constraint because a line of the network should be capable of transmitting the power with the placement of the DERs in the distribution system. Otherwise, the excess power flows can melt the conductor.

$$I_{\alpha}^{\max} \geq I_{\alpha} \quad \forall \alpha \in n_n \tag{6.78}$$

6.3.4 DERs Power Flow Limit

The active and reactive power of DERs is considered only in the permissible operating region. The penetration of the DERs depends on optimal performance which has been decided by optimal scheduling in the different interval.

$$\begin{aligned} P_{\alpha}^{\min} < P_{DERs_{\alpha}} \leq P_{\alpha}^{\max} \quad \forall \alpha \in n_n \\ Q_{\alpha}^{\min} < Q_{DERs_{\alpha}} \leq Q_{\alpha}^{\max} \end{aligned} \tag{6.79}$$

The range of P_{DERs} and Q_{DERs} should not exceed the comparable literature either initialization or updating process of the optimization.

6.3.5 Active System Limits

The total power injection by the DERs in the radial three phase system must be less than from the total demand of the system.

$$\sum_{\chi=1}^{n_R} S_{\chi}^{DERs} \leq S_D \tag{6.80}$$

The DERs should not repeat the same location in the system which is filtered by following constraint.

$$loc_{\alpha_1}^{n_R} \neq loc_{\alpha_2}^{n_R} \tag{6.81}$$

The size of DERs present in discrete, so the number of DERs are increased to meet the incremental demand of the system within permissible limit.

$$S_{\alpha}^{DERs} \geq K_{\chi} S_d \quad \forall \alpha \in n_n, K_{\chi} \in n_g \tag{6.82}$$

The optimal numbers, size and siting of the DERs are used to determine the optimal solution.

6.4 Proposed Methodology

The proposed Sharp-Jaya algorithm (S-Jaya) uses an advanced effective algorithm named as 'Jaya' with some modifications in the underlying optimization strategy. The S-Jaya method has superior characteristics and capabilities. Therefore, the proposed algorithm is employed to solve optimal DERs allocation problem with minimization of power losses. The S-Jaya algorithm is interface with the co-simulation framework for three phase distribution system. The proposed algorithm not only optimizes the objective function but also helps and encourages for the convergence towards the global optimal solution. The S-Jaya is consecutively explained with the co-simulation framework and the basic strategy of the standard Jaya as follows:

6.4.1 Co-Simulation Framework

The interface between back-end system and front-end system is known as the co-simulation framework which is availed by the simulator. The back-end of the co-simulation framework is OpenDSS and front-end is any one coding sources. In this study, the MATLAB® simulator has been used for coding platform. Accordingly, the framework has been utilized to solve the DERs allocation problem in the unbalanced radial three-phase distribution network as shown in Figure 6.5.

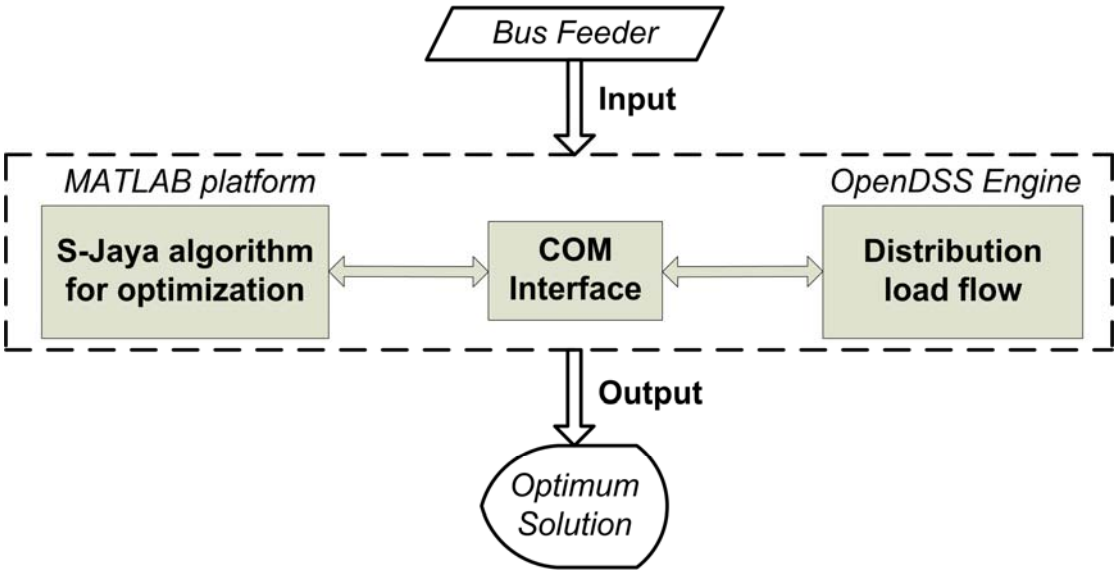

Figure 6.5: Procedure of the co-simulation framework

OpenDSS is an Open source electric power Distribution System Simulator (DSS) which analyzes the integration of the distributed resource and grid modernization. The functionality of the simulator is utilized through adding the looping advanced analysis

and visualization abilities of MATLAB®. The OpenDSS has been interfaced with MATLAB® through COM (Component Object Model) Server [172]. The commands to the simulator are executed from the environmental structure of MATLAB® and the results are displayed at front-end system.

6.4.2 Standard Jaya Algorithm

The Jaya algorithm is an advanced global search optimization algorithm which is firstly proposed by R. Venkata Rao and demonstrated to clarify the capability to solve both constrained and unconstrained problems of the optimization. This most effective Jaya algorithm has various virtues as: simpler to implement, easy to code, parameterless algorithm, robustness, better consistency and consumes less computation time or efforts. The S-Jaya is extended version of the Jaya, is motivated by the success of the Jaya in various applications.

The basic concept of the standard Jaya algorithm has been discussed before explaining the S-Jaya. The Jaya algorithm is a single phase method which is based on the best and worst solution of the objective function. The basic concept of robustness is based on two facts of the Jaya algorithm that try to reach near to best and away from the failure or worst solution. This approach has temptation to achieve the desired solution with consistency in a minimum time. The description of the Jaya method can be summarized as follows:

Let *f(x)* is an objective function which is being minimized or maximized. The objective function includes the parameters as design variables (N_d), population size (N_p), and maximum iteration (K^{max}).

At the iteration itr^{th}, J_Y is the data and solution for the p^{th} candidate. The Jaya equation is applied to modify the value of J_Y which helps to achieve optimal solution and avoid the worst solution.

$$J_Y^{'} = J_Y + r_1\left(J_Y^{best} - \left|J_Y\right|\right) - r_2\left(J_Y^{worst} - \left|J_Y\right|\right) \tag{6.83}$$

where, $J_Y^{'}$ is the new computed value of candidate, r_1 and r_2 are the random number between 0 and 1. The old value of the variable J_Y is replaced with the value of newly generated variable $J_Y^{'}$, if the solution of new candidate is better than pervious candidate. The flow of the proposed approach process is shown as Figure 6.6.

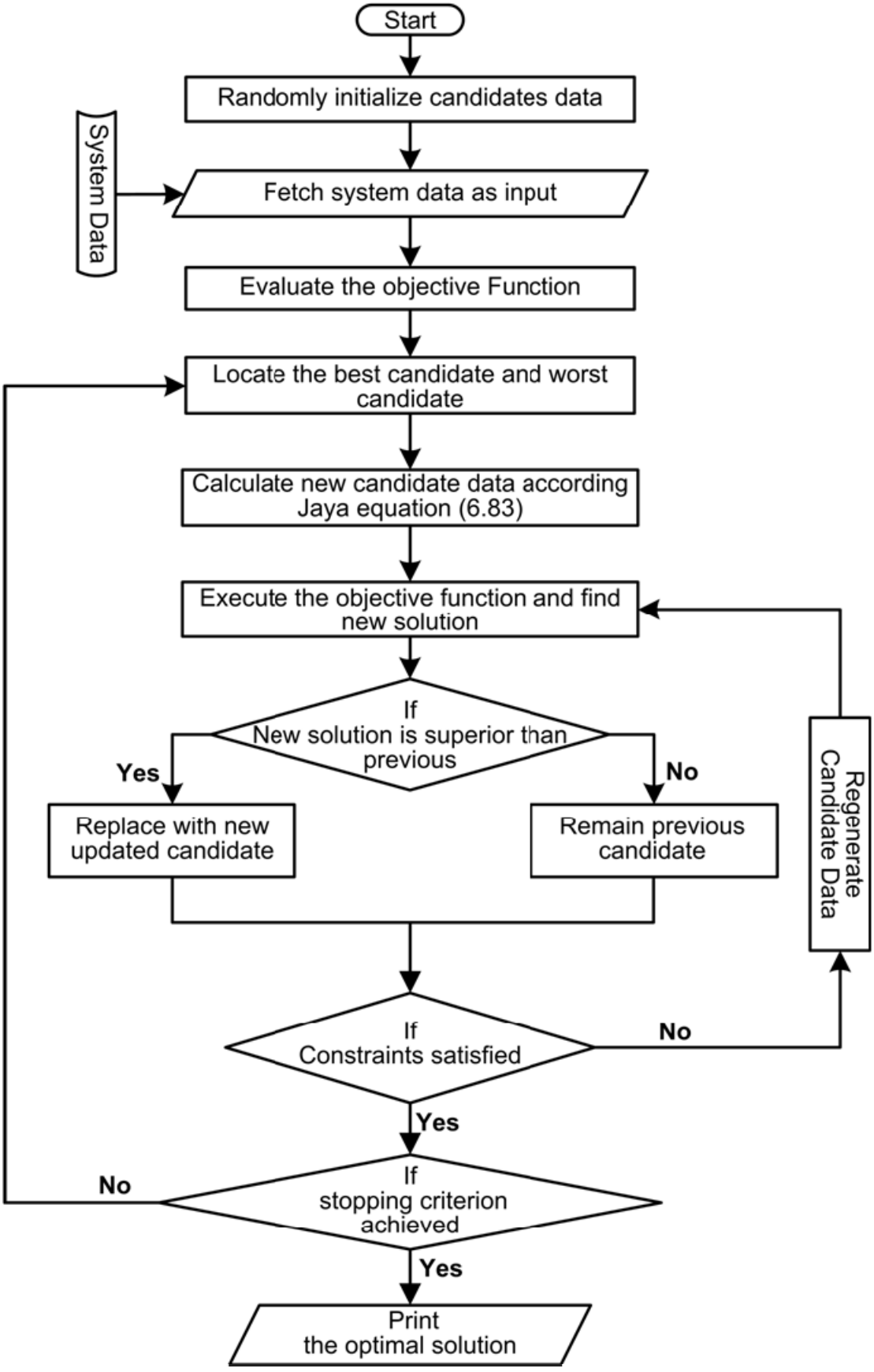

Figure: 6.6. Flowchart of the standard Jaya algorithm

The procedure of the standard Jaya algorithm is defined in the following steps:

Step 1. Define the objective function and initialize the common control parameters as: population size, number of design variables and maximum iterations.

Step 2. Compute the solution for the all candidates using the objective function with their constraints.

Step 3. Identify the best result among from all the candidates and worst solution in the population.

Step 4. Update the candidates' data using the Jaya equation (6.83) which depends on the computed best and worst solution.

Step 5. The newly generated candidate is accepted if the corresponding solution of new candidate is better than solution of Old candidate. Otherwise it remains as previously generated solution.

Step 6. Further, check that the termination criteria are fulfilled and maximum number of iteration are reached then display the optimal solution. Else repeat the steps from step 2.

Pseudo Code Standard JAYA Algorithm

```
Begin
    Initialize function and common control parameters as candidate
    Compute function
    For itr=1 to maximum iterations
        Find the best and worst candidate
        Generate new candidate using equation (6.83)
        If new candidate's solution is better
            Then
                Replace the candidate with new candidate values
            Else
                Remain same as previous
        End if
        If constraints are not satisfied          //check constraints
            Then
                Regenerate the candidate randomly
                Repeat
            Else
                If stopping criteria are not fulfilled
                    Then
                        Repeat for new generation
                    Else
                        Terminate the loop
                End If
        End If
    End For
    Print the optimal solution
End
```

6.4.3 Sharp-Jaya Algorithm

A new Sharp-Jaya algorithm (S-Jaya) is an extension of the Jaya algorithm, motivated by the success of the Jaya method in various applications. The S-Jaya algorithm is proposed for simultaneous optimal accommodation of the DERs to minimize the power losses in the practical radial distribution systems. The proposed algorithm sharpens the standard Jaya algorithm embedding the parent child model and shrinkage mechanism with existence of the basic concept of the Jaya algorithm. The proposed method strives to become victorious by sharpening their specific tools which are used to solving objective problems. These tools can easily puncture to all the barriers or obstacles like time consuming, local minima and most favorable slow convergence. Further, the proposed strategy could quickly and consistently achieve the desired solution. The sharpening technique of the S-Jaya helps to optimize the decision parameter in very least time with the accurate solution. The above mentioned mechanisms are appended to the basic Jaya algorithm which is described as the following subsections:

i. Shrinkage mechanism **-** The name of this mechanism implies its definition itself. The proposed method used the mechanism to shrink the search space of the candidates. This technique detaches the undesirable search area to reduce the conversion time. It keeps only the specific search region which have the global solution or near to global solution. Therefore, the proposed method is expected to produce global optimum solution in minimum efforts. The process of the shrinkage mechanism can be understand via an example- Let *f (x)* is the objective function to place the optimum DER at the optimal location in balanced or unbalanced radial distribution system. The most of the algorithms search the optimal location for the DER in the whole search area as shown in Figure 6.7 (a). Therefore, it can take several minutes and high efforts to achieve an optimal solution. The result is based on initial solution. While the situation will different in case of embedding shrinkage mechanism due to trimming the search region. The shrinkage mechanism trims all those area of search (unconscious) which does not satisfy the objective function's conditions i.e. contain the worst solution. Therefore, it saves the time to efforts doing in the wrong direction of the solution.

The shrinkage mechanism enables the algorithm to identify the part of search area which may have the worst solution and detach them from the search region of

problem formulation. The search criteria reduce their size according to the reduction rate which is a constant value in the percentage predefined by the user. The reduction rate is affected by the performance of the problem solution in dynamically. The structure of shrinkage mechanism theme can be described in Figure 6.7 (b).

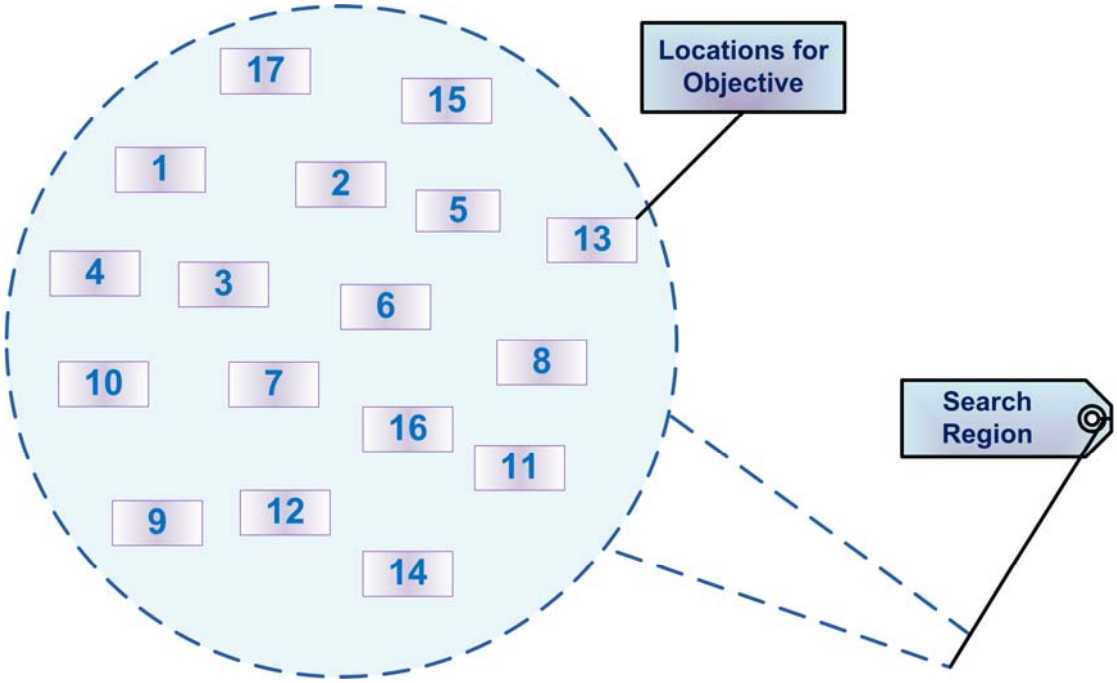

(a) Scenario of ordinary search mechanism

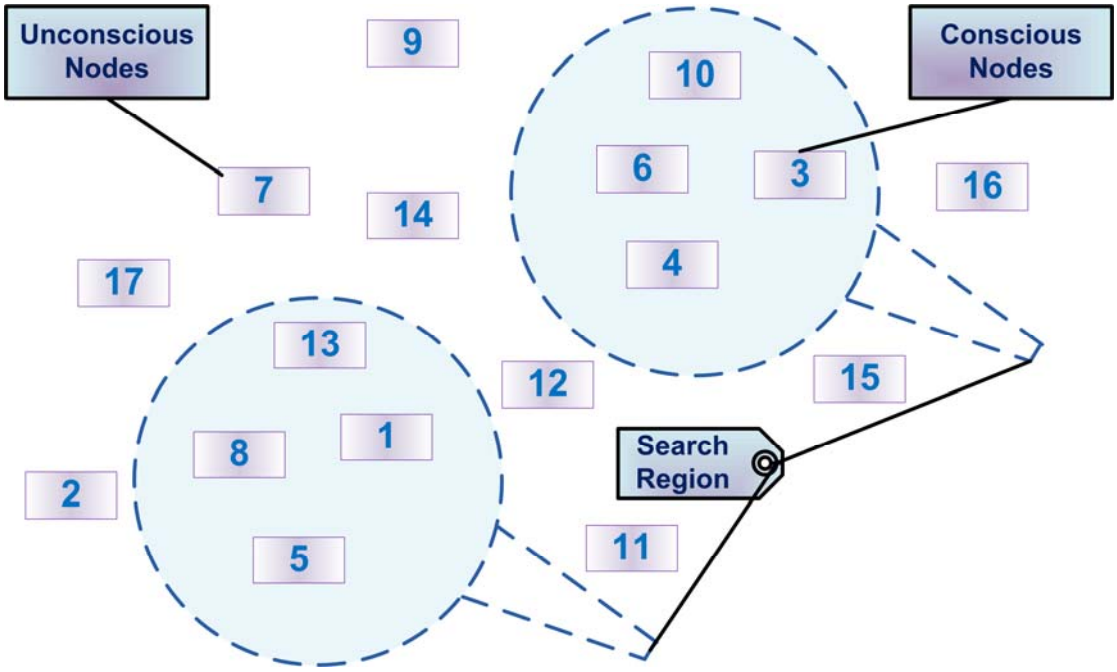

(b) Scenario of shrinkage search mechanism

Figure 6.7: Graphical representation of search mechanism

ii. Parent-child model - The parent-child model is a structure of the transactional analysis. In the proposed algorithm, the two states of the parent-child model are used as first is parent state and next stage is child state. Once the parent/child relationship is established then direction of control and teaching is always from the parent to the children. The parent state has the responsibility of making a precious decision and lessons to the child. Further, the child process follows the various predictions and assumptions, learning from parent's acts, and mimic of the parent spontaneity.

The proposed approach uses the parent child model. It formulates a scheme for grouping the population into sub groups which controls the exploitation and exploration of searching procedure. In the shrinkage process, the search space is reduced, but the parent child model is used to maintain the diversity of searching procedure. Further, it improves the intensifying the searching procedure.

The common control parameter 'Population' of the proposed algorithm is known as 'parent'. The proposed algorithm inherits the population into the sub groups of populations which can be denoted as 'child'. Therefore the sub groups of population are derived from the parent. The child has all the characteristics and properties of parent.

The parent state has the search region for the DERs which are minimized through the shrinkage mechanism and every child have own different search region. In view of, every child finds the solution in different search region, simultaneously. Therefore, the S-Jaya algorithm saves a lot of time in processing to solve the objective.

The one fact of parent-child model can be understood by daily experience example. A person has lost an item in a seminar hall then he tries to find it. However, many approaches may be applied to search that item. Four process to search the item are given as follows:

a. A person will search it in entire hall. It consumes a lot of times and efforts.
b. Many of people will search in entire hall one by one. It creates massy situation.
c. Many of people will search in entire hall simultaneously. It consumes a lot of time unnecessary.
d. Many people will decide their own search area and they all find out in their different search area simultaneously.

The fourth one is like the proposed approach behaves. In a little time, through little efforts and with highest accuracy problem can be solved using proposed approach.

The data structure of parent-child model is presented in graphical way in the Figure 6.8 (a). The attributes of the parent state and child state is similar but the values of their attributes are different. The first rectangle of model specifies the parent which is encapsulated with so many attributes and their properties. The other rectangles show the child states which hold all the attributes as S_r, S_t, S_z fragmented with their values by the parent state.

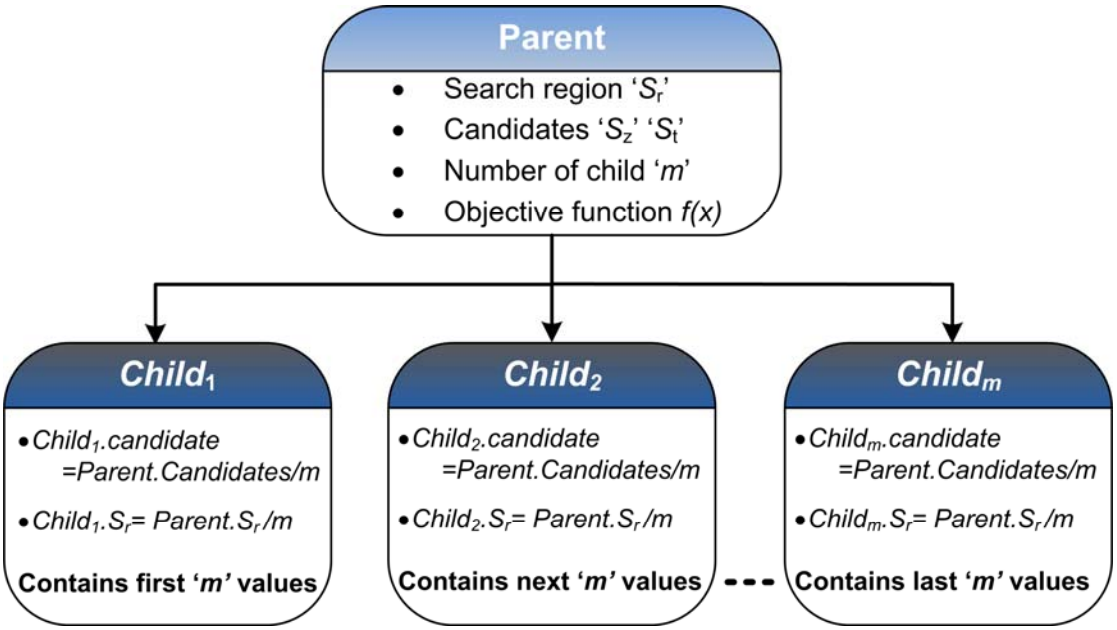

(a) Data structure of parent-child procedure

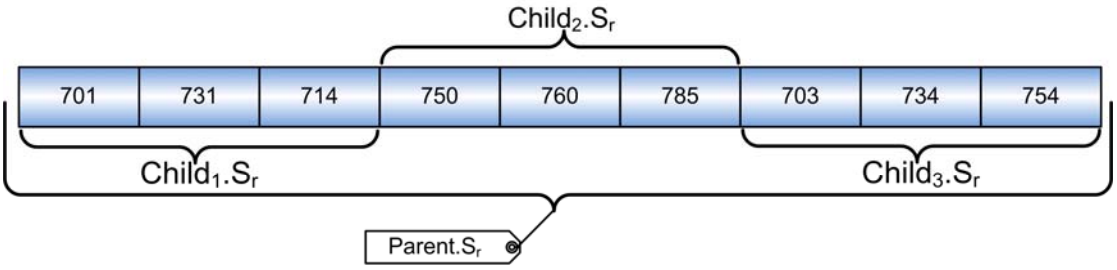

(b) Segmentation of search region

Figure 6.8: The parent-child model

The actual procedure for the segmentation of search region is illustrated in the Figure 6.8 (b) which shows the shrunk search region of parent. *Parent.*S_r is tagged in diagrammatically representation and held the nine search area. Further, parent state has three *child.*S_r and split the search region equally. Each child locates the solution in their own search region, simultaneously. Therefore the parent child model avail the convenient process for time and effort saving.

The proposed approach is easy to apply for maintaining the population diversity and reducing the search region. The characteristics held by the proposed algorithm are useful as following reasons:-

a. Maintain diversity of search process by applying parent-child model.
b. Reduce the consumed time for recognizing the best optimal solution.
c. Capable to search in various regions simultaneously.
d. The search procedure and its diversity are controlled by allocating the population into groups; further, all subgroups are situated in different region of search space.
e. The constraints handling mechanism are used which can retain the optimal solution of objective problem under all bounds. It escapes from going out of any bounds like: DERs size, duplicity, penetration, and voltage regulation.

The step-by-step process of the proposed approach is implemented to solve the optimal allocation of the DERs in unbalanced distribution system with co-simulation environment using the OpenDSS are following:

Step1. Initialize the variables/common control parameters and define the objective as:

- Number populations: $N_p = 10$, $\{p_s=1, 2 \dots N_p\}$
- Decision Parameters: S_z, S_t (S_z :DER Size, S_t : DER Site)
- Number of design variables: N_d, $\{d_s=1, 2 \dots N_d\}$
- Number of iterations: K^{max}, $\{itr=1, 2 \dots K^{max}\}$
- Limits of capacity: $L_L < S_z$, $S_t > U_L$; specify the search criteria with lower and upper limits by defined objective function.
- Reduction Rate: R_R
- Number of Groups/Child: c, $\{m=1, 2 \dots c\}$

Step2. Create OpenDSS circuit after running the OpenDSS server using COM interface. Run base case power flow and obtain the result from the OpenDSS.

Step3. Further, apply the shrinkage mechanism of the proposed method. Identify all nodes which produce high power losses and generate new search region (S_r) with the length of calculated value by R_R.

Step4. The search region is reduced, further, apply the parent child model. The population with their search region will divided into sub-groups called as a child. Number of child depends on the search region length.

Step5. Each child have own search region and run OpenDSS server which creates the circuit with the population as parent and get the solution.

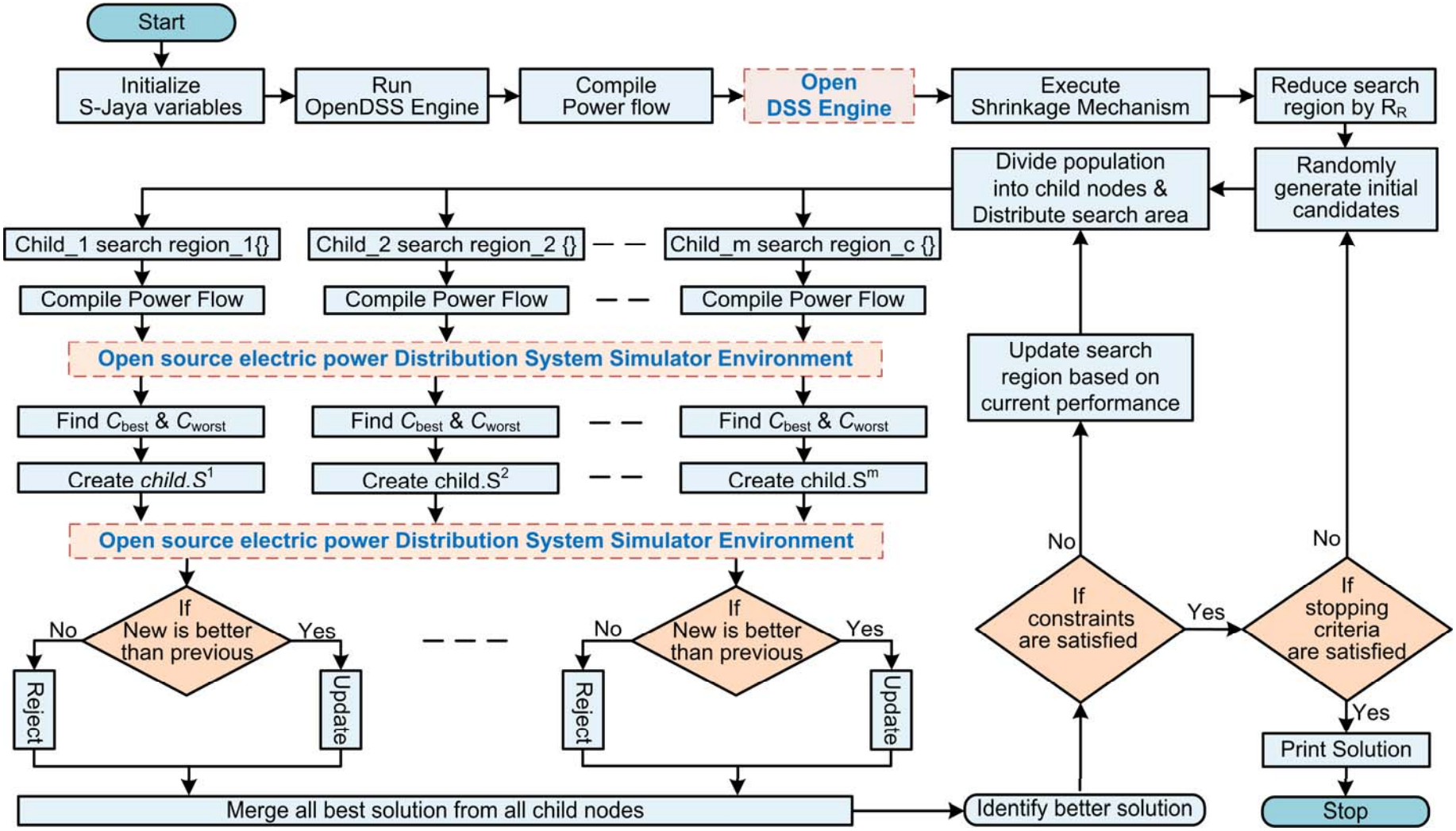

Figure 6.9: Flowchart of the S-Jaya algorithm

Step6. Select a candidate who obtained the best result and assigns it as C_{best} and detects the candidate who held the worst solution, assigns as C_{worst}. Further, apply the following equation on child's data:

$$Child.S^{\mathrm{m}'}_{itr,\mathrm{d}_s,\mathrm{p}_s} = Child.S^{\mathrm{m}}_{itr,\mathrm{d}_s,\mathrm{p}_s} + \underbrace{r_1(\mathrm{C}^{m}_{best,itr} - \left|Child.S^{\mathrm{m}}_{itr,\mathrm{d}_s,\mathrm{p}_s}\right|)}_{\text{Fascination term}} - \underbrace{r_2(\mathrm{C}^{m}_{worst,itr} - \left|Child.S^{\mathrm{m}}_{itr,\mathrm{d}_s,\mathrm{p}_s}\right|)}_{\text{Repulsion term}} \tag{6.84}$$

The first term fascinates the solution to reach at nearest optimal result. The second term repulses the solution to keeps away from the failure or worst result. Further, calculate the newly generated candidate for every child ($Child.S^{\mathrm{m}'}_{itr,\mathrm{d}_s,\mathrm{p}_s}$).

Step7. Afterword, again call the circuit and solve the power flow for newly generated population. If $Child.S^{\mathrm{m}'}_{itr,\mathrm{d}_s,\mathrm{p}_s}$ gives a better solution than $Child.S^{\mathrm{m}}_{itr,\mathrm{d}_s,\mathrm{p}_s}$. Further, accept the new generated child data otherwise remain as previously generated child's decision parameters.

Step8. Each child identifies the best optimal result in their search region. In this step, collect all optimal result from every child and merge them. Further, identify the better from the best solutions.

Step9. Moreover, use the constraint handling mechanism to check the limits of the updated decision parameters, whenever it is not satisfied, then regenerate the candidates. Further, ensure the duplicity is not present. Check all the constraints, if they are not fulfilled, add penalty value to the result.

Step10. Regenerate the S_r values depending upon the performance of the current generated data. Furthermore, all process will repeat for next generation using updated search region as shown in Figure 6.9.

Step11. Check the current generated solution. The newly generated values of the candidates will be accepted, whenever it gives the better solution than previously generated values. Otherwise remain same as previous.

Step12. Terminate, if the maximum number of iterations is reached and achieved the optimal result. Otherwise, the accepted solution of every generation is maintained and these values are used as inputs for the next generation. Further, run the whole process from step 4 until stopping criteria is not satisfied.

Pseudo Code S-Jaya algorithm

Begin

Initialize S-Jaya variables and common control parameters
Run OpenDSS Engine & activate circuit.
Execute commands from COM Interface
Evaluate distribution power flow
Obtain power flow results from OpenDSS Environment
Reduce the length of search region with R_R
S_r*: determined by shrinkage search mechanism*
Randomly generate candidates as parent
Simultaneously split candidates into 'c' child nodes & S_r
Compile power flow on OpenDSS
Identify C_{best} *and* C_{worst}
Update candidate with equation (6.84)
Compute power flow
If $Child.S^{m'}_{itr,d_s,p_s}$ *is better than* $Child.S^{m}_{itr,d_s,p_s}$
    Then
        Update previous data with New
    Otherwise
        Reject it
End If
Merge all local best fitness value from each child
Locate global best from local best
If Constraints not satisfied //Check Constraints
    Then
        Update S_r
    Else
        If Stopping Criteria not fulfilled
            Then
                Repeat process for next generation
        End If
End If
Print the Optimal Solution

End

The proposed algorithm is adopted the way of the pseudo code to obtain the optimal allocation of the DERs in the co-simulation framework.

6.5 Simulation Results

In this section, the S-Jaya algorithm is proposed to optimize the decision parameter to accommodate the DERs which is operated on Unity Power Factor (UPF) and Non-Unity Power Factor (Non-UPF). Moreover, proposed approach is tested on the IEEE 13-bus, IEEE 37-bus (California power company), and IEEE 123-bus radial unbalanced distribution system [173] and compared with the results of the PSO [27] and MG-TLBO [8] algorithm. The open source simulator OpenDSS has been used for the load flow analysis in the unbalanced radial distribution systems. The proposed

algorithm has been implemented in MATLAB® platform. Moreover, this approach is based on two-way data commutation between MATLAB® interface and OpenDSS simulator engine.

In practice, overhead lines, underground cables, reactive power compensation device, voltage control device and three types of load configurations with unbalanced loading are presented in the radial distribution network. Therefore, IEEE distribution test feeder working group sub-committee of distribution system analysis committee has been developed (13-bus and 123-bus distribution system) and formulate (37-bus actual feeder in California) distribution test network which provide the data to analysis the practical condition of the distribution system. Moreover, three type of load as constant current, constant impedance, and constant power present in the realistic condition of the system which makes a rigid condition for planning the distribution system.

6.5.1 IEEE 13-Bus Radial Distribution System

The IEEE 13-bus distribution system brief overview and complete data are provided in the Appendix-B which has been used to endorse the proposed approach. Three types of loads as constant current, constant power, and constant impedance are present with four type of phasing configuration of overhead line and two of underground cable. This system originates from a substation and spreads to three types of end users with unequal phasing. Total system peak demands of spot load in red, yellow and blue phase are 1.31 MVA, 1.16 MVA, and 1.36 MVA, respectively. Moreover, peak demand of the distributed load sequentially for each phase is 0.019 MVA, 0.076 MVA, and 0.135 MVA. In this system, all data have been used in per unit whereas the base value of power and voltage is 50 MVA and 4.16 kV, respectively.

6.5.1.1. Planning of the DERs at Unity Power Factor - The penetration of the UPF-DERs is changed from 10% of the maximum demand of the system which explores the optimal contribution in the system. The power loss is reducing with increment in the penetration of the DERs as shown in Table 6.1. Moreover, the power loss reduction by S-Jaya and MG-TLBO algorithms are large in each interval as compare to the PSO algorithm. The S-Jaya and MG-TLBO method has obtained the equal power loss reduction. However, the proposed method achieved the solution in less computation time as compared to the MG-TLBO algorithm. The optimal penetration interval chooses for the planning of the DERs in this system. Moreover, maximum power

injection is adjudicated according to optimal dispatch of each system. The comparison of the performance with selected penetration for each algorithm is presented in Table 6.2.

Table 6.1: Optimal dispatches of the UPF DER in the IEEE 13-bus test system

DER Power Interval (kW)	PSO		MG-TLBO		S-Jaya	
	DERs Location	$P_{reduction}^{loss}$ (%)	DERs Location	$P_{reduction}^{loss}$ (%)	DERs Location	$P_{reduction}^{loss}$ (%)
0- 250	675	12.84	675	12.84	675	12.84
251-500	675	24.23	675	24.24	675	24.24
501-750	675	24.24	675	34.20	675	34.20
751-1000	675	42.75	675	42.76	675	42.76
1001-1250	675	46.58	675	49.96	675	49.96
1250-1500	675	55.81	675	55.82	675	55.82
1501-1750	675	60.38	675	60.38	675	60.38
1751-2000	692	64.57	692	64.57	692	64.57
2001-2250	692	67.88	671	67.88	671	67.88
2251-2500	671	70.47	671	70.48	671	70.48

Table 6.2: Comparison of the performance for UPF DERs in the IEEE 13-bus test system

Method	DERs No.	Optimal Dispatches of DERs (kW)	V_{min} (p.u.)	Time (Sec.)	$P_{reduction}^{loss}$ (%)
PSO	Single	692 (2249.50)	0.9822	0.86	67.87
	Double	692 (1338.59), 675 (909.541)	0.9823	1.22	69.86
	Triple	680 (539.64), 675 (822.07), 692 (548.52)	0.9885	0.82	69.01
MGTLBO	Single	692 (2249.99)	0.9822	2.56	67.88
	Double	692 (1417.43), 675(830.27)	0.9823	2.19	69.91
	Triple	684(321.18), 671(1067.74), 675(815.69)	0.9885	1.85	70.63
S-Jaya	Single	671(2250.00)	0.9822	0.75	67.88
	Double	675(897.25), 692(1352.72)	0.9823	0.85	69.96
	Triple	675(767.76), 692(1283.47), 684(193.27)	0.9885	0.76	70.82

The Shrinkage mechanism of the proposed approach determined the initial solution near to the optimal as shown in Figure 6.10. The S-Jaya algorithm conversed in less time compared to both algorithms.

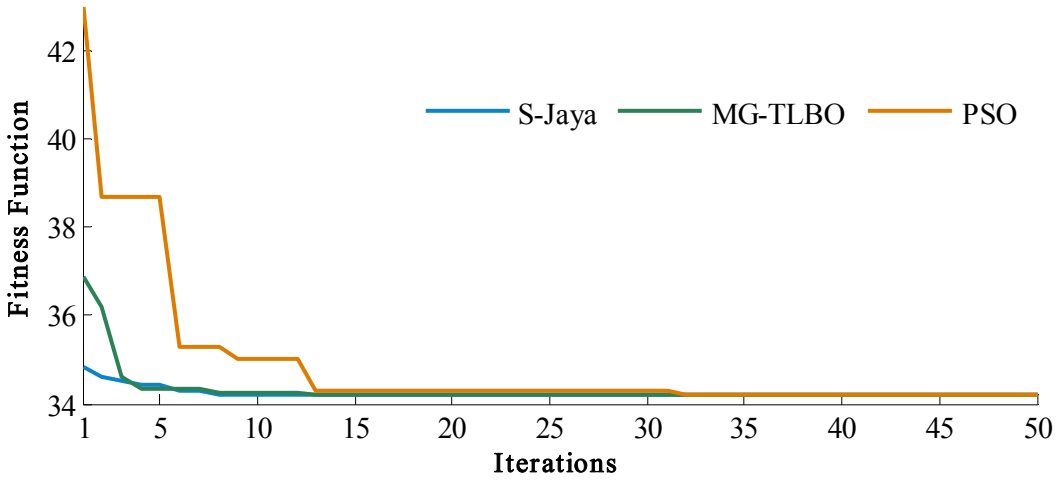

(a) One DER

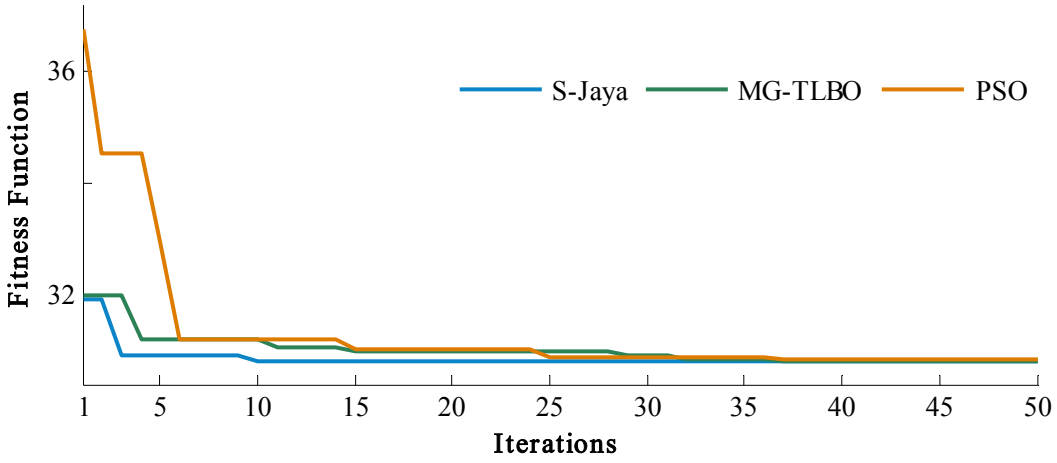

(b) Two DERs

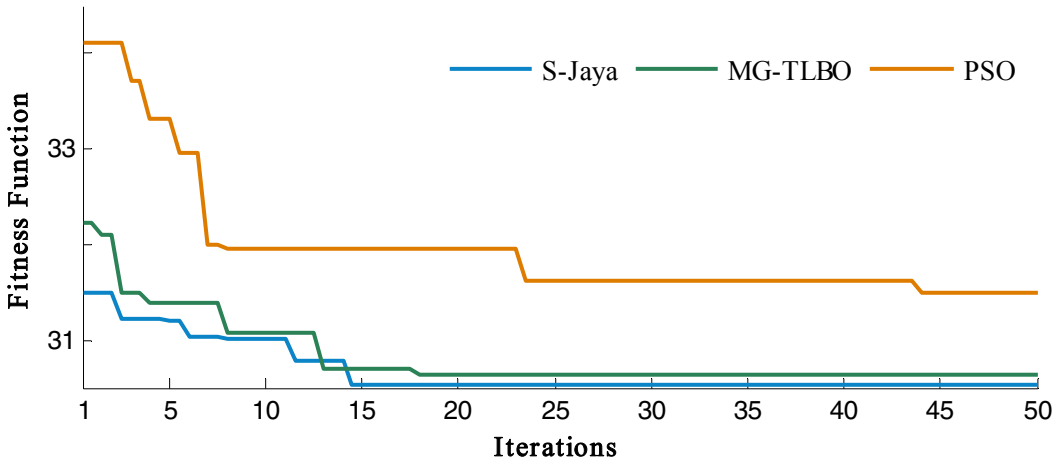

(c) Three DERs

Figure 6.10: Comparison of the algorithm performance for UPF DERs

The proposed algorithm is converse between ten to fifteen iterations to determine the optimum solution for each number of the DERs. Moreover, the S-Jaya method is retained the better voltage profile in all three phases as compare to both algorithms which is depicted in Figure 6.11.

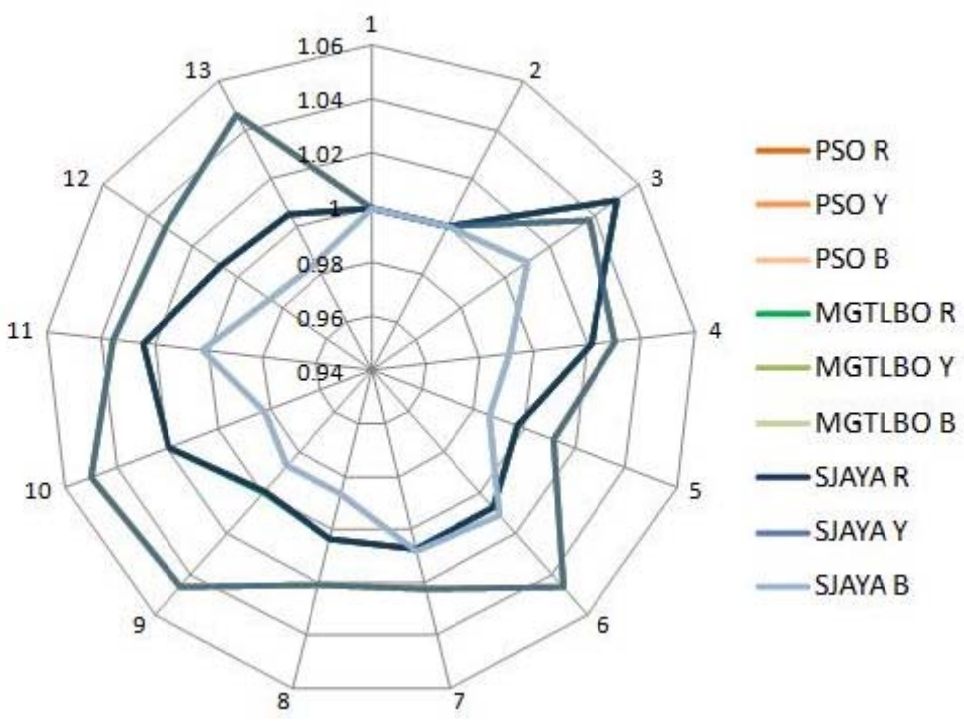

(a) Two DERs

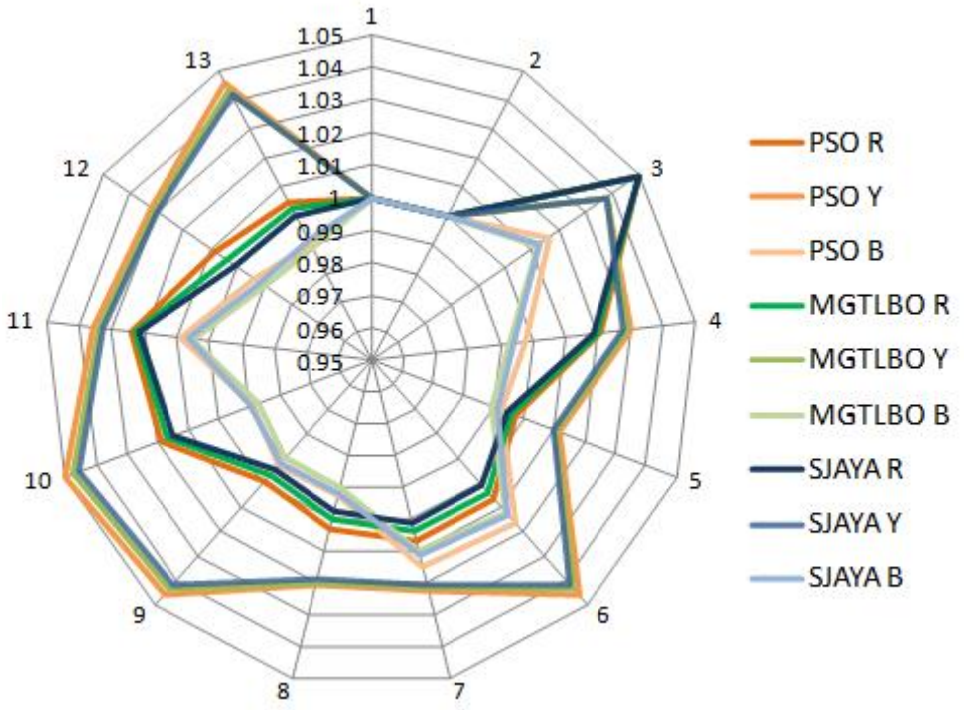

(b) Three DERs

Figure 6.11: Voltage profile of IEEE 13-bus radial distribution system for UPF DERs

6.5.1.2. Planning of the DERs at Non-Unity Power Factor: The power loss is minimized with increment the penetration of the non-unity DERs same as unity power factor operated DERs. However, reduction of the power loss in the same interval is more in non unity power factor operated DER. The optimal range of the non unity DERs is maximum permissible penetration of the system. The MG-TLBO has achieved the prominent power loss reduction as compared to the PSO method in every range of the Non-UPF DER dispatch as shown in Table 6.3. However, the computation time is more to the PSO. The MG-TLBO method is obtained same power losses as compare to proposed algorithm whenever simulation time of the proposed algorithm is less.

Table 6.3: Optimal dispatches of the Non-UPF DER in the IEEE 13-bus test system

DER Power Interval (kW)	**PSO**		**MG-TLBO**		**S-Jaya**	
	DERs Location	$P_{reduction}^{loss}$ (%)	**DERs Location**	$P_{reduction}^{loss}$ (%)	**DERs Location**	$P_{reduction}^{loss}$ (%)
0- 250	675	14.312	675	14.3261	675	14.3261
251-500	675	26.6637	675	26.7398	675	26.7398
501-750	675	37.3683	675	37.4218	675	37.4218
751-1000	675	47.0251	675	47.081	675	47.081
1001-1250	675	55.0376	675	55.0488	675	55.0488
1250-1500	692	62.2768	692	62.2815	692	62.2815
1501-1750	671	68.4893	671	68.5007	671	68.5007
1751-2000	671	73.3210	671	73.3255	671	73.3255
2001-2250	692	76.8007	692	76.8051	692	76.8051
2251-2500	692	78.9982	671	79.0015	671	79.0015

The non unity power factor operated DERs are obtained the optimal size and site by the proposed algorithm as shown in Table 6.4. The performance of the system after the integration of the DERs by using the proposed algorithm has been compared with the PSO and MG-TLBO algorithm. Each algorithm is applied to optimize the decision parameter and maximize the power loss reduction after 25 autonomous trials. Moreover, the proposed algorithm has been achieved the maximum power loss reduction in less computation time for every dispatch of the DERs. In this system, proposed algorithm has been achieved the eighty percentage above power loss

reduction with three number of the DERs which is not determined by the MG-TLBO and PSO algorithm.

Table 6.4: Comparison of the performance for Non-UPF DERs in the IEEE 13-bus test system

Method	**DERs No.**	**Optimal Dispatches of DERs (kW)**	**V_{min} (p.u.)**	**Time (Sec.)**	**$P^{loss}_{reduction}$ (%)**
PSO	Single	692 (2245.32)	0.9633	0.851	76.75
	Double	690 (1536.16), 675 (691.085)	0.9633	1.307	77.87
	Triple	692(764.48), 684 (777.03), 675(693)	0.9654	1.447	77.89
MGTLBO	Single	671 (2249.98)	0.9634	1.49	76.80
	Double	671(1619.018), 675(628.18)	0.9634	1.98	78.11
	Triple	671(936.00), 675(1089.00), 684(223.00)	0.9656	2.264	79.08
S-Jaya	Single	671(2250)	0.9635	0.805	76.81
	Double	692(1714.14), 684(534.45)	0.9662	1.06	79.34
	Triple	676(303.00), 684(579.01), 692(1368.00)	0.9671	1.087	80.27

Figure 6.12 show that the S-Jaya algorithm is conversed in minimum time to both compared algorithm. Figure 6.12 (b) concluded that the S-Jaya approach proceed more number of iterations to obtain the final solution with two number of DERs, however, it generate the optimal fitness value with less computation time because per iteration time is very less as compare to the MG-TLBO and PSO algorithm. Figure 6.13 demonstrate that voltage profile for each number of the DERs preserves the boundaries of the each phase in this system according to the regulation of the distribution system.

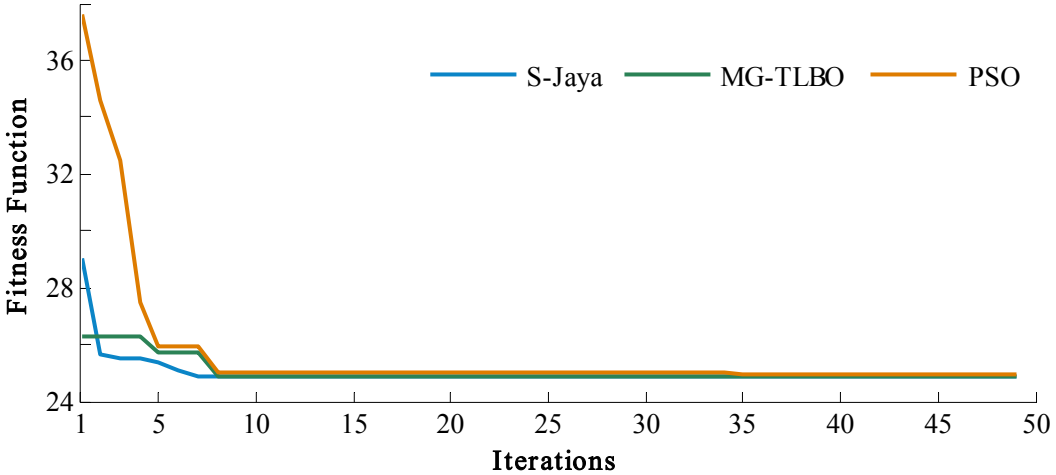

(a) One DERs

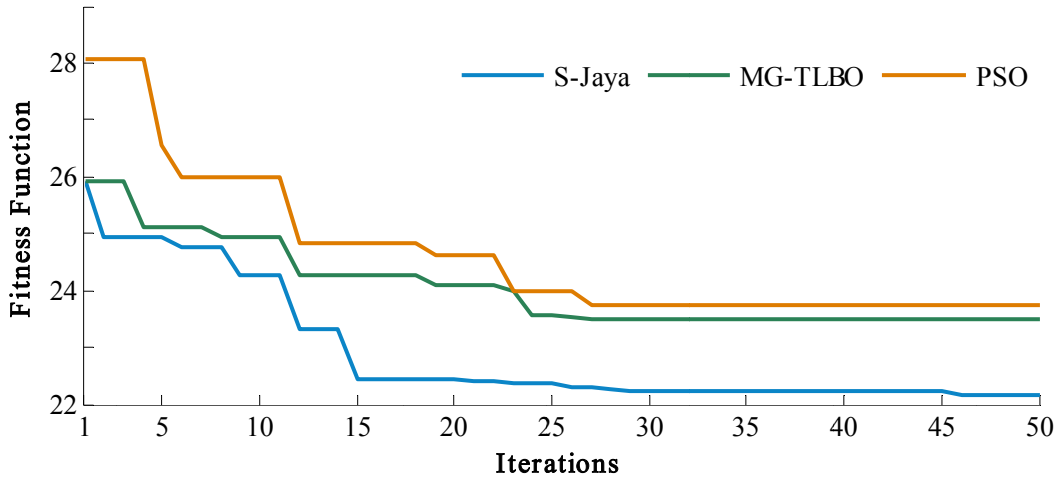

(b) Two DERs

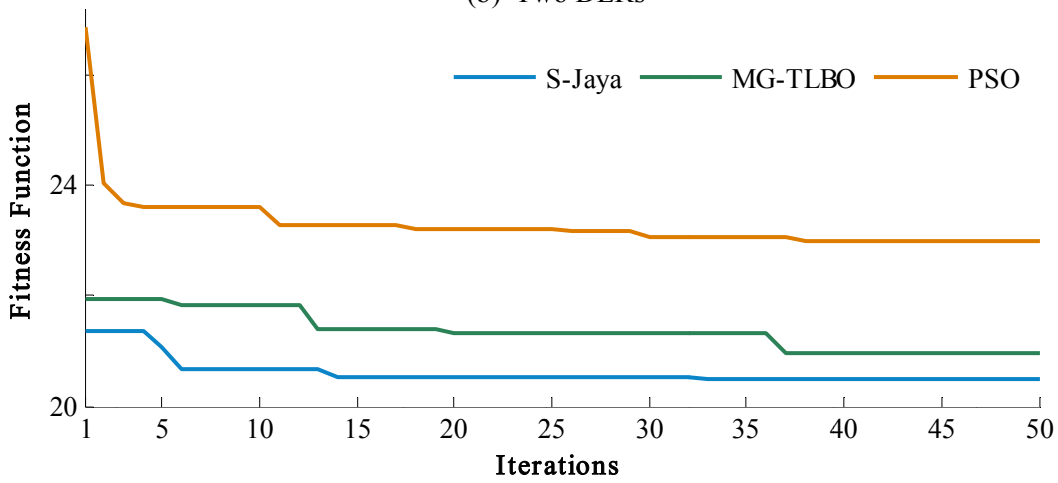

(c) Three DERs

Figure 6.12: Comparison of the algorithm performance for Non-UPF DERs

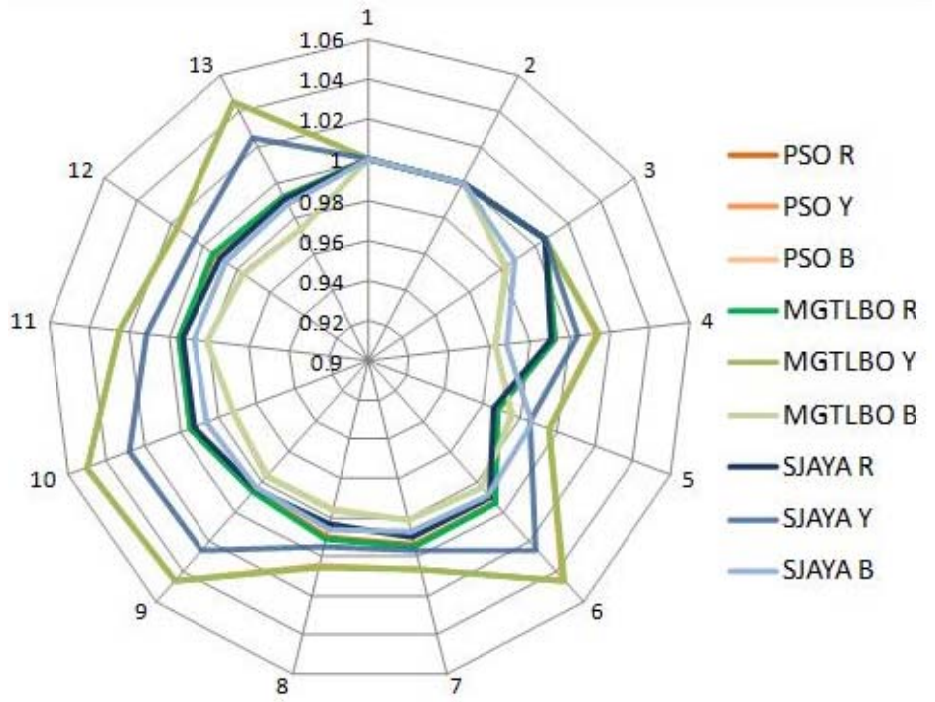

(a) Two DERs

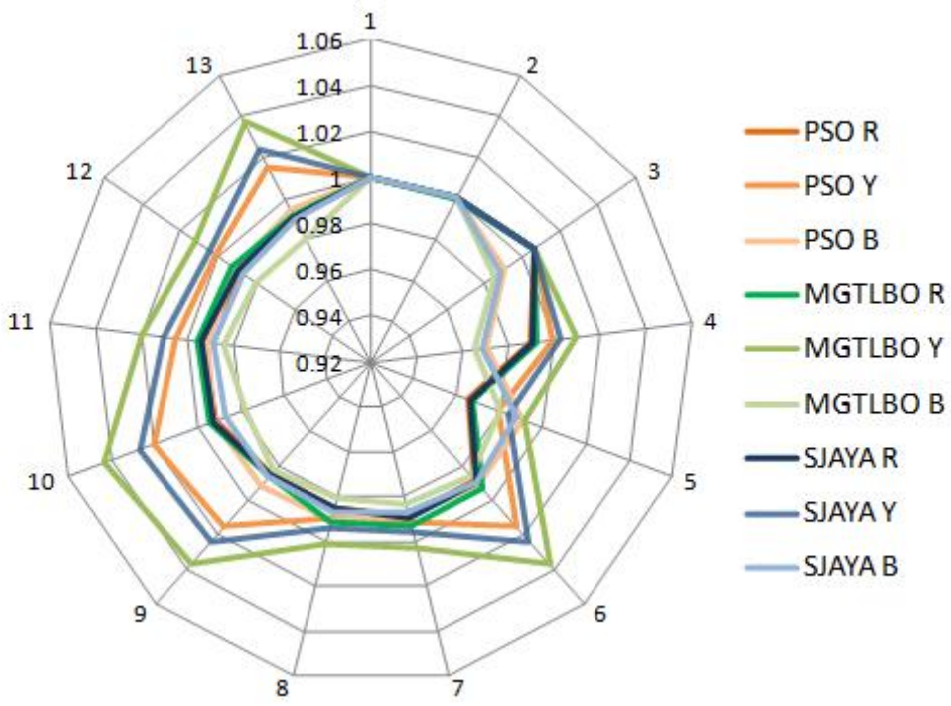

(b) Three DERs

Figure 6.13: Voltage profile of IEEE 13-bus radial distribution system for Non-UPF DERs

The S-Jaya achieves the most prominent reduction of the losses as compared to the PSO and the MG-TLBO. However, the losses are reduced whenever increase the number of the DER in all algorithms. Although the penetration level is equal to increased the number of the DERs. In addition, the proposed method gains the highest reduction in each number of the DERs while maintaining the voltage profile for each phase of the system. The power loss reduction by UPF DERs in each algorithm is less as compare to the Non-UPF DERs. Although the proposed method has achieved the highest loss reduction for each number of the unity and non-unity operated DREs in this test system.

6.5.2 IEEE 37-Bus Radial Distribution System

This feeder is a practical radial distribution network which is located in California. This test system has been used to authenticate the planning of the DERs in the realistic characteristics of the distribution system. The complete overview of this system is described in the Appendix-B. The unbalanced demands of the spot loads for each phase are 0.81 MVA, 0.71 MVA, and 1.21 MVA, respectively. Three types of spot loads as constant current, constant power, and constant impedance are present with the different configuration of the overhead line and underground cable. The regulator is not used to maximize the impact of the DERs. In this system, all data have

been used in per unit whereas the base value of power and voltage is 2.5 MVA and 4.8 kV, respectively.

6.5.2.1. Planning of the DERs at Unity Power Factor – The optimal dispatches of unity power factor operated DERs is varied from 10% to maximum demand of the system which explores the optimal contribution in each interval. The PSO algorithm achieved the maximum power loss reduction is 53.51 kW which is obtained in the interval of 1000-1250 kW. However, the MG-TLBO and S-Jaya have achieved the maximum power loss reduction as compared to the PSO in the power range of 1250-1500 kW, whenever, the proposed method is optimized the best decision parameter for that range of the power and compared to the MG-TLBO which is shown in Table 6.5.

Table 6.5: Optimal dispatches of the UPF DER in the IEEE 37-bus system

DER Power Interval (kW)	**PSO**		**MG-TLBO**		**S-Jaya**	
	DERs Location	$P_{reduction}^{loss}$ (%)	**DERs Location**	$P_{reduction}^{loss}$ (%)	**DERs Location**	$P_{reduction}^{loss}$ (%)
0- 250	738	22.86	738	22.89	738	22.89
251-500	738	34.44	737	38.50	737	38.50
501-750	737	38.50	734	48.03	734	48.03
751-1000	734	52.41	734	52.41	734	52.41
1001-1250	708	**53.51**	708	53.53	709	53.56
1250-1500	737	44.31	709	**53.77**	709	**53.77**
1501-1750	730	53.07	703	53.11	703	53.23
1751-2000	730	49.74	703	52.91	703	52.91
2001-2250	703	50.53	703	50.55	703	50.55
2251-2500	727	18.83	702	49.26	702	49.26

It is a fascinating observation that power loss reduction with optimal penetration level follows the V-curve by each algorithm in this system. Therefore, this actually situated feeder is formalized for the practical DERs planning in the three-phase unbalanced distribution system. The optimal performance of the UPF DERs has been achieved by the proposed algorithm as compared to the PSO and MG-TLBO that is demonstrated in Table 6.6.

The proposed algorithm is obtained the maximum power loss reduction with each number of the UPF DERs in minimum computation time in this realistic distribution

system. Moreover, the S-Jaya algorithm has achieved the highest power loss reduction with three number of the UPF DERs.

Table 6.6: Comparison of the performance for UPF DERs in the IEEE 37-bus system

Method	**DERs No.**	**Optimal Dispatches of DERs (kW)**	$\mathbf{V_{min}}$ **(p.u.)**	**Time (Sec.)**	$\boldsymbol{P_{reduction}^{loss}}$ **(%)**
PSO	Single	708(1240.85)	0.98	1.37	53.51
	Double	737(717.29), 720(526.49)	0.983	1.50	62.81
	Triple	733(475.19), 704(409.10), 707(359.64)	0.984	1.52	63.80
MGTLBO	Single	708(1329.66)	0.98	2.67	53.77
	Double	734(786.19), 720(462.39)	0.984	2.96	63.17
	Triple	738(386.06), 722(220.47), 730(638.33)	0.985	2.99	64.79
S-Jaya	Single	709(1329.66)	0.98	1.15	53.77
	Double	721(467.33), 734(785.66)	0.986	1.17	63.24
	Triple	722(330.30), 737(495.91), 730(425.14)	0.99	1.37	65.31

Figure 6.14 presents the conversion graph of the proposed algorithm with both compared algorithms. The PSO algorithm has not converse for the optimal fitness value in each number of the DERs. The proposed algorithm and MG-TLBO is converse in minimum iteration for one and two number of the DERs. However, S-Jaya method always converse in minimum time with best fitness value for each number. Figure 6.15 depicts that proposed method is optimized all decision parameter while maintaining the voltage profile for each number of the DERs in the system.

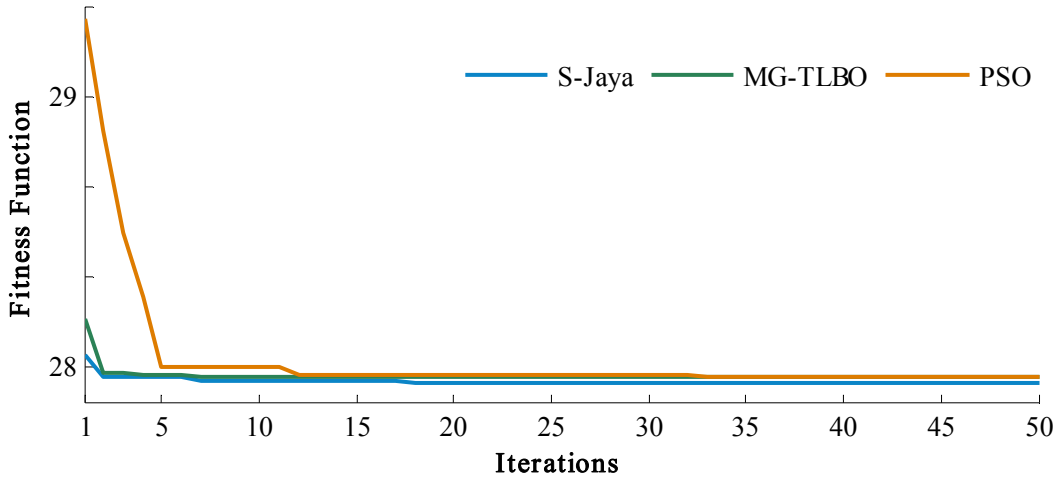

(a) One DERs

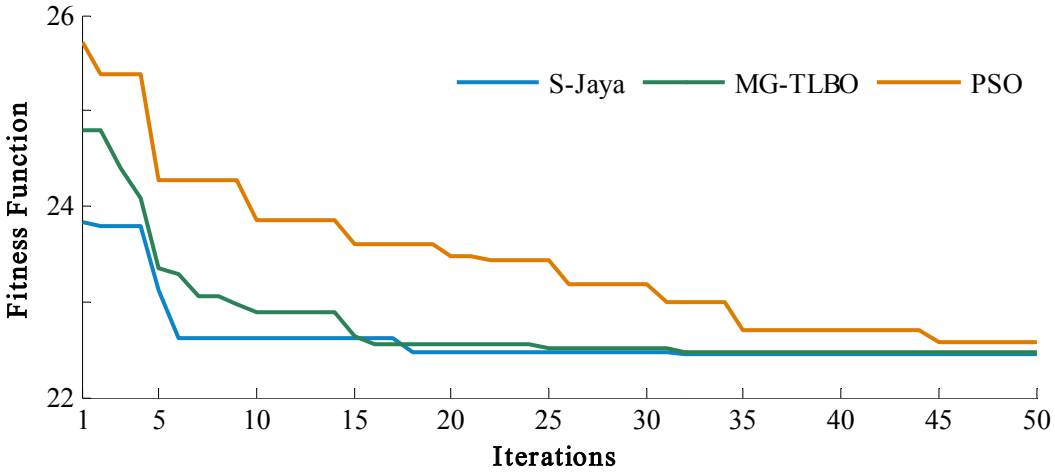

(b) Two DERs

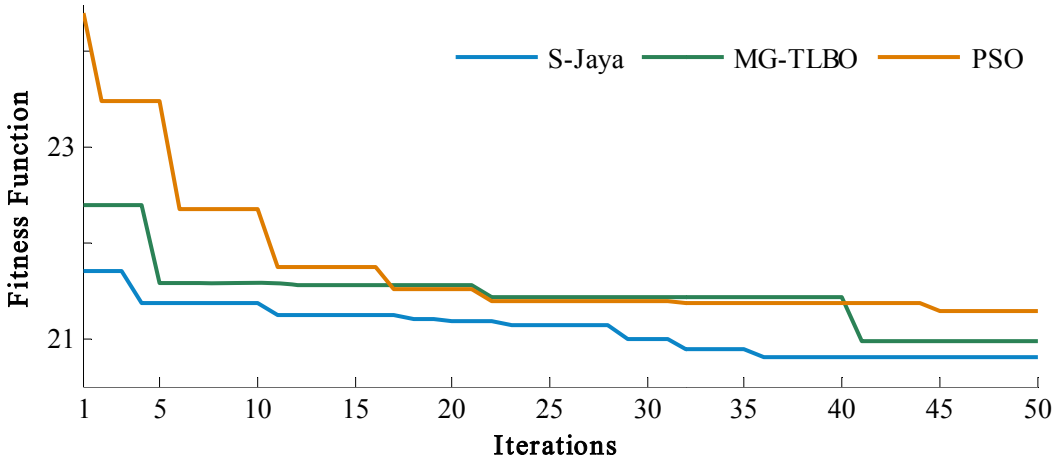

(c) Three DERs

Figure 6.14: Comparison of the algorithm performance for UPF DERs

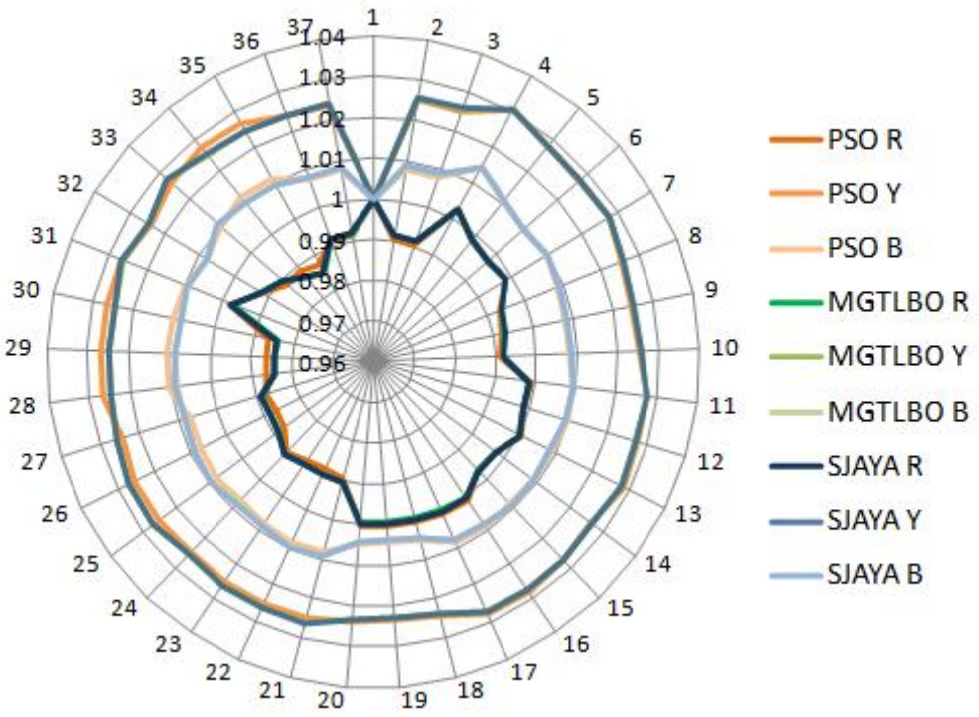

(a) Two DERs

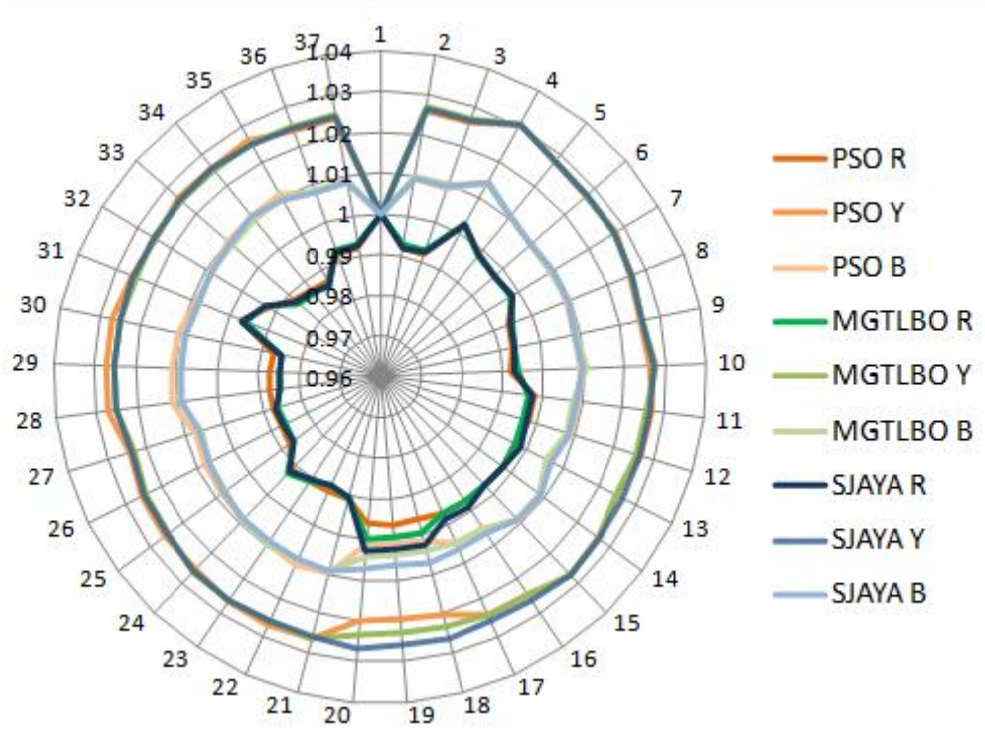

(b) Three DERs

Figure 6.15: Voltage profile of IEEE 37 bus radial distribution system for UPF DERs

6.5.2.2. Planning of the DERs at Non-Unity Power Factor – The optimal dispatch range of the non-unity DERs follows the V-curve as the unity power for this system. Although, Table 6.7 demonstrate that the improvement is accomplished in percentage

Table 6.7: Optimal dispatches of the Non-UPF DER in the IEEE 37-bus system

DER Power Interval (kW)	**PSO**		**MG-TLBO**		**S-Jaya**	
	DERs Location	$P_{reduction}^{loss}$ (%)	**DERs Location**	$P_{reduction}^{loss}$ (%)	**DERs Location**	$P_{reduction}^{loss}$ (%)
0- 250	711	30.50	738	30.72	738	30.72
251-500	737	50.18	738	50.23	737	50.23
501-750	734	49.42	734	60.29	734	60.29
751-1000	710	50.74	733	62.95	733	62.95
1001-1250	709	**65.58**	709	65.59	709	65.60
1251-1500	709	63.16	709	**65.61**	709	**65.62**
1501-1750	727	45.11	703	62.12	703	62.12
1751-2000	703	51.77	702	59.09	702	59.09
2001-2250	701	42.78	702	57.77	702	57.77
2251-2500	733	45.02	702	54.10	702	54.10

power loss by the proposed algorithm as well as the PSO and MG-TLBO. Further, the decision parameters of each number of the Non-UPF DERs the corresponding performance for every algorithm are shown in Table 6.8.

Table 6.8: Comparison of the performance for Non-UPF DERs in the IEEE 37-bus system

Method	**DERs No.**	**Optimal Dispatches of DERs (kW)**	$\mathbf{V_{min}}$ **(p.u.)**	**Time (Sec.)**	$\boldsymbol{P^{loss}_{reduction}}$ **(%)**
PSO	Single	(1243.93)	0.99	1.39	65.58
	Double	722(431.31), 737(813.28)	0.99	1.42	75.19
	Triple	720(418.90), 737(515.58), 744(308.51)	0.99	1.77	80.27
MGTLBO	Single	709(1253.00)	0.99	2.30	65.61
	Double	720(526.69), 734(717.67)	0.99	2.79	77.80
	Triple	722(192.57), 737(570.88), 703(487.89)	0.99	2.86	80.61
S-Jaya	Single	709(1253.00)	0.99	1.30	65.62
	Double	735(770.65), 720(482.33)	0.99	1.34	78.14
	Triple	728(379.09), 737(590.56), 707(283.54)	1.0	1.48	81.06

The three numbers of the Non-UPF DERs has obtained the highest power loss reduction as previous observations of this chapter. Moreover, the percentage power loss reduction has a large variation with increment the number of the non-unity DERs. Figure 6.16 shows that the proposed algorithm is achieved the minimum power loss within minimum iterations. Moreover, the S-Jaya method has not depended on the initial solution although initial fitness value is near to global solution or not, that shows the strength of the proposed algorithm.

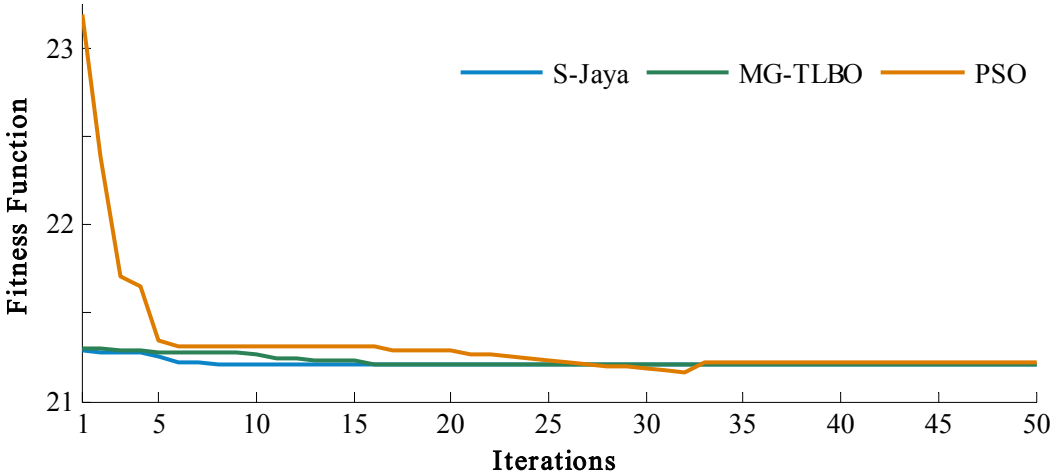

(a) One DERs

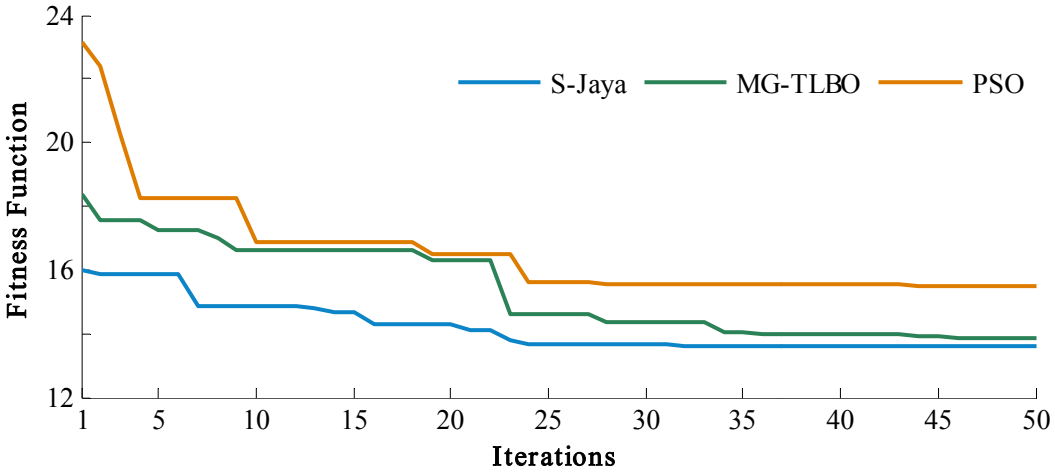

(b) Two DERs

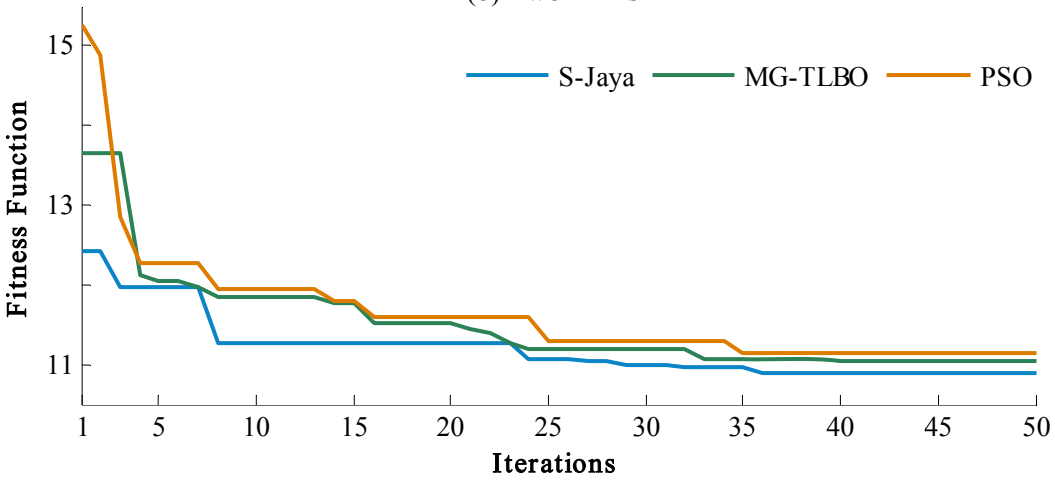

(c) Three DERs

Figure 6.16: Comparison of the algorithm performance for Non-UPF DERs

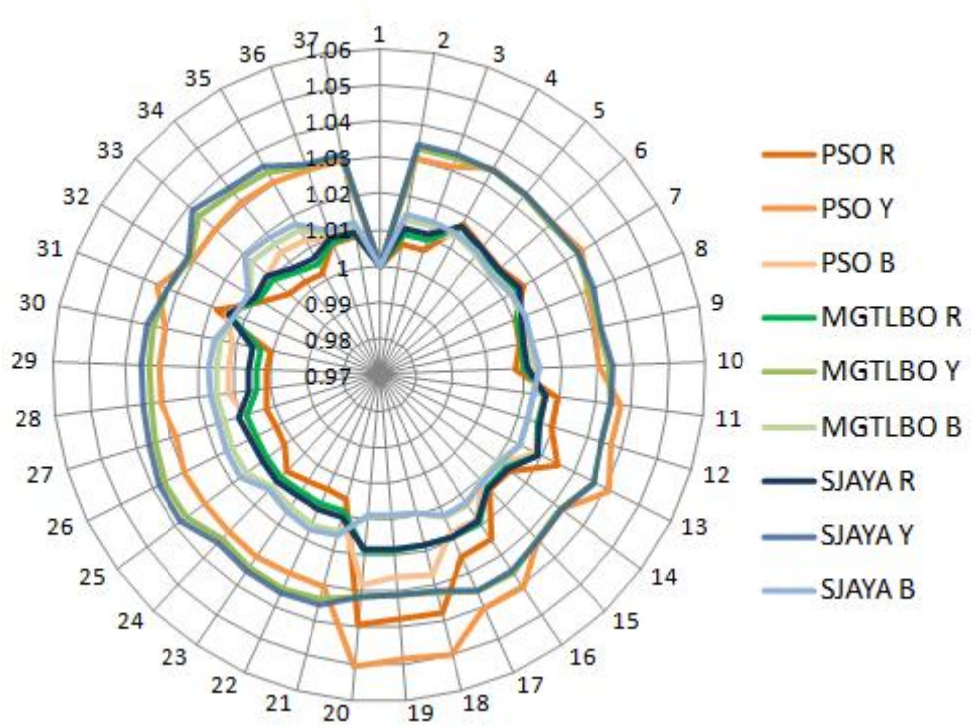

(a) Two DERs

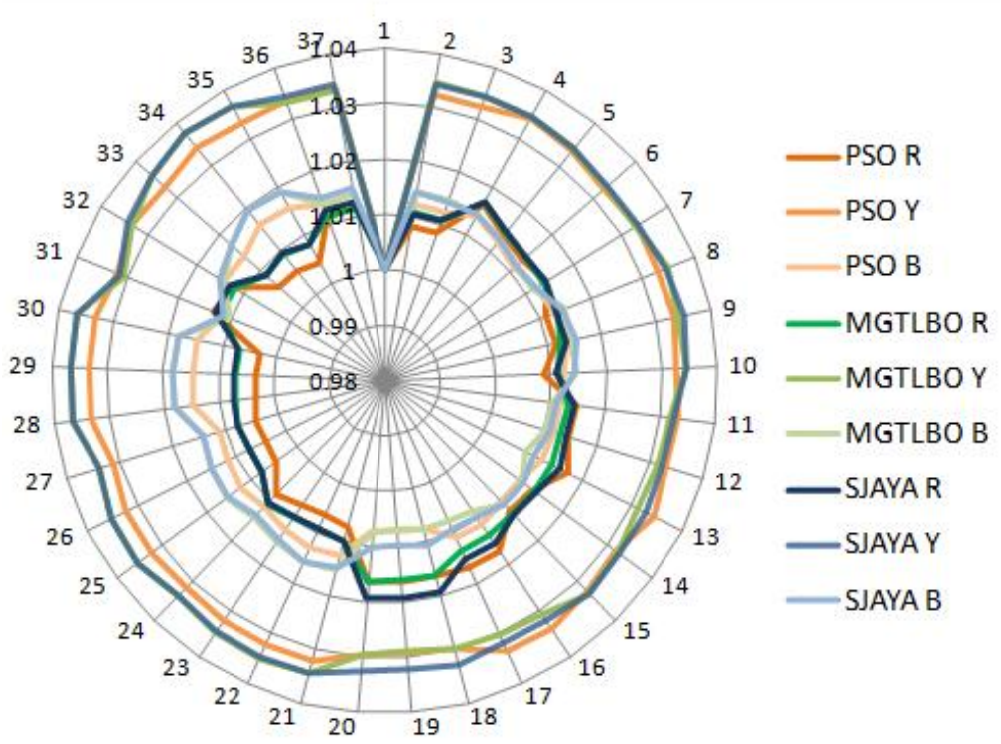

(b) Three DERs

Figure 6.17: Voltage profile of IEEE 37-bus radial distribution system for NON-UPF DERs

The proposed algorithm has endorsed to obtain the best performance maintaining the voltage profile in every condition. The voltage profile for non-unity DERs is the exhibit in Figure 6.17.

6.5.3 IEEE 123-Bus Radial Distribution System

The IEEE 123-bus test network is sizeable distribution system which has been used to validate the proposed algorithm for the allocation of the DERs. The Appendix-B has demonstrated the brief overview and complete data of this system. In this system, twelve type of overhead and underground line configuration is presented which describe the unbalancing of the system. All practical characteristic has been considered with a base value of power and voltage which is 5 MVA and 4.16 kV, respectively. The demand for spot-type loads of each phase is 1.62 MVA, 1.05 MVA, and 1.32 MVA, respectively.

6.5.3.1. Planning of the DERs at Unity Power Factor: The penetration of unity power factor DERs is varied in the several intervals of the system demand which is present in Table 6.9. The S-Jaya algorithm and both compared algorithm have obtained the optimal dispatch range is 2000-2270 kW. Afterward, the losses are increased with

Table 6.9: Optimal dispatches of the UPF DER in the IEEE 123-bus test system

DER Power Interval (kW)	PSO		MG-TLBO		S-Jaya	
	DERs Location	$P_{reduction}^{loss}$ (%)	DERs Location	$P_{reduction}^{loss}$ (%)	DERs Location	$P_{reduction}^{loss}$ (%)
0- 250	89	14.65	86	14.65	89	14.66
251-500	87	26.77	86	26.93	86	26.93
501-750	89	26.81	87	36.81	76	37.62
751-1000	197	45.26	76	46.52	76	46.52
1001-1250	76	51.60	197	52.39	76	53.62
1251-1500	78	56.16	76	58.97	72	58.99
1501-1750	96	58.95	67	62.96	67	62.96
1751-2000	101	61.35	67	65.77	67	65.77
2001-2270	197	**64.39**	67	**67.11**	67	**67.15**
2271-2500	160	55.30	67	67.01	67	67.11

rise in the power contribution of the DERs. Table 6.10 concludes that the S-Jaya algorithm has performed well as compared to MG-TLBO and PSO method for each number of the DERs in this system. The proposed algorithm takes a large number of iteration with three numbers of the DERs, however, reduction of power losses is elevated as compared to another number of the DERs as shown in Figure 6.18.

Table 6.10: Comparison of the performance for UPF DERs in the IEEE 123-bus test system

Method	DERs No.	Optimal Dispatches of DERs (kW)	V_{min} (p.u.)	Time (Sec.)	$P_{reduction}^{loss}$ (%)
PSO	Single	160(2267.27)	0.96	2.10	65.39
	Double	67(1674.78), 50(543.52)	0.96	2.12	72.42
	Triple	98(551.31), 44(831.21), 79(860.35)	0.96	2.41	72.22
MGTLBO	Single	67(2261.36)	0.96	4.05	67.11
	Double	47(725.24), 72(1541.46)	0.97	4.38	73.49
	Triple	101(315.01), 47(574.78), 67(1377.27)	0.97	4.72	73.56
S-Jaya	Single	67(2268)	0.97	1.89	67.15
	Double	48(654.60), 72(1612.06)	0.97	1.96	73.54
	Triple	73(1219.04), 101(382.98), 49(658.91)	0.97	2.13	73.99

The Figure 6.19 depicts that voltage profile of the system after the optimal allocation of the DERs by the proposed algorithm maintains the limits according to the regulation of distribution system.

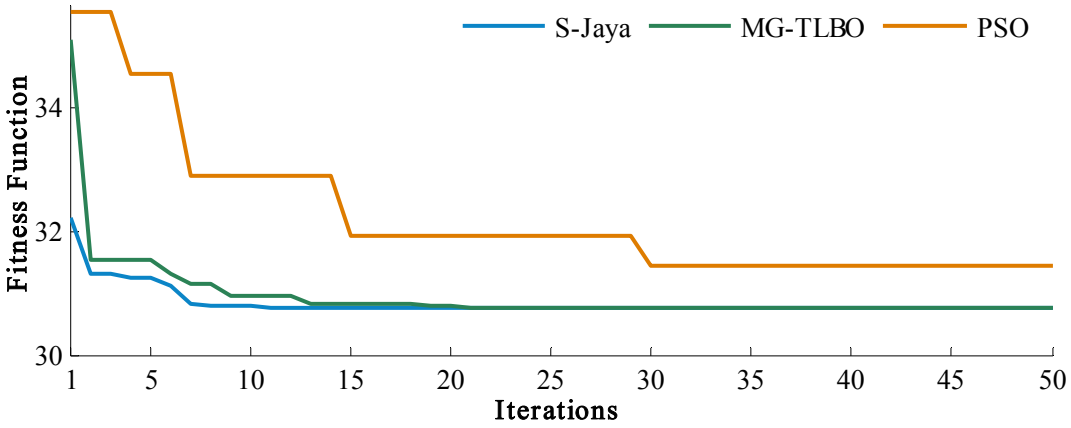

(a) One DERs

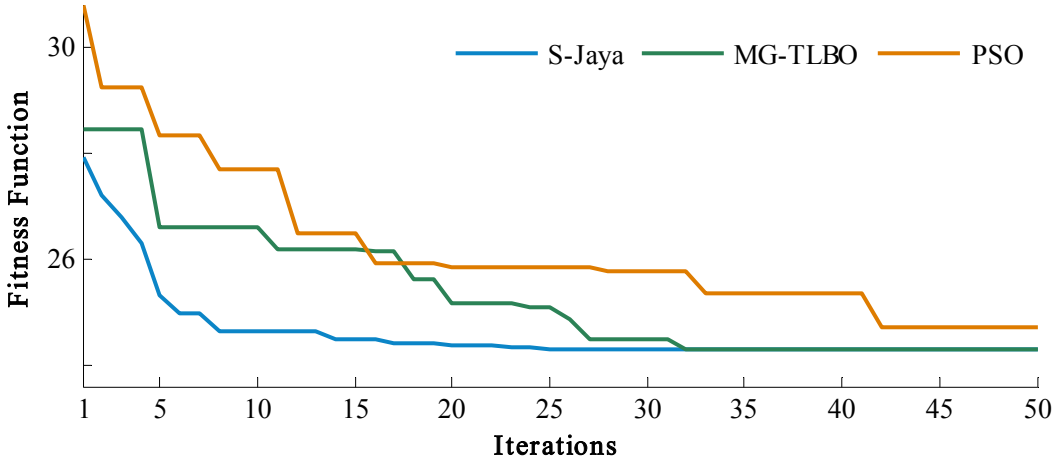

(b) Two DERs

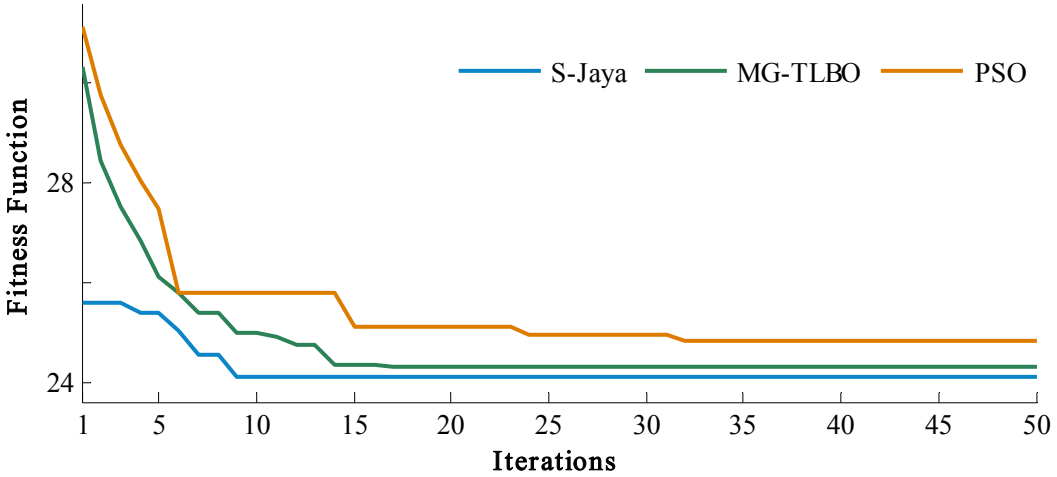

(c) Three DERs

Figure 6.18: Comparison of the algorithm performance for UPF DERs

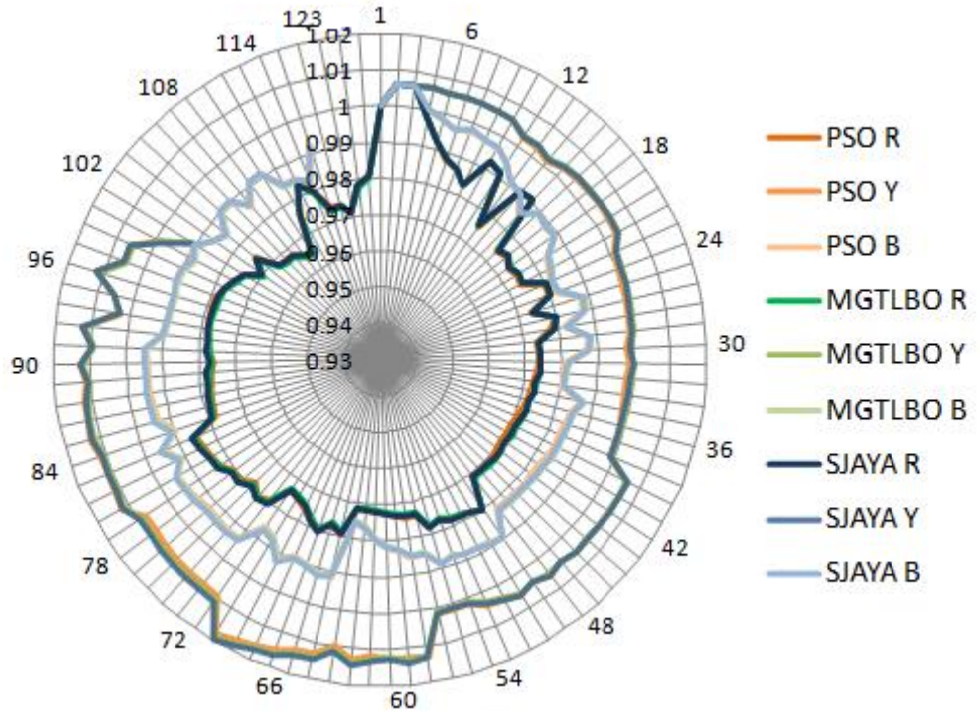

(a) Two DERs

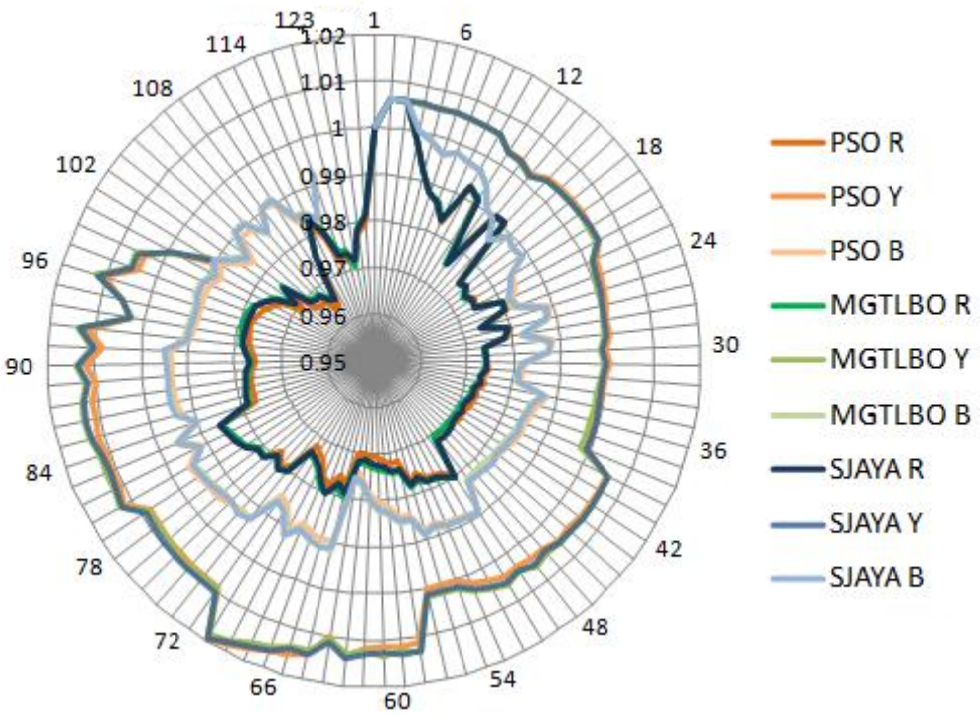

(b) Three DERs

Figure 6.19: Voltage profile of IEEE 123-bus radial distribution system for UPF DERs

6.5.3.2. Planning of the DERs at Non-Unity Power Factor: The optimal dispatch of the Non-UPF DERs also follows the same pattern as UPF DERs. However, the comparison of the power loss reduction between UPF- and Non-UPF DERs evidence

that the non-optimal allocation has increased the losses of the system. Moreover, higher penetration of the DERs could not improve the performance the system which is proved by Table 6.11. The optimal dispatch for Non-UPF DERs is 2000-2270 kW.

Table 6.11: Optimal dispatches of the Non-UPF DER in the IEEE 123-bus test system

DER Power Interval (kW)	**PSO**		**MG-TLBO**		**S-Jaya**	
	DERs Location	$P_{reduction}^{loss}$ (%)	**DERs Location**	$P_{reduction}^{loss}$ (%)	**DERs Location**	$P_{reduction}^{loss}$ (%)
0- 250	86	15.84	65	16.06	87	16.06
251-500	105	29.00	86	29.15	76	29.35
501-750	100	28.03	70	40.27	76	40.33
751-1000	101	48.19	70	49.07	72	49.07
1001-1250	160	54.05	67	55.95	67	55.95
1251-1500	67	60.89	67	60.95	67	60.95
1501-1750	97	62.38	67	64.05	67	64.05
1751-2000	86	54.12	67	65.31	67	65.31
2001-2270	67	**65.09**	67	**65.34**	67	**65.35**
2271-2500	67	64.79	60	65.01	60	65.01

Table 6.12: Comparison of the performance for Non-UPF DERs in IEEE 123-bus test system

Method	**DERs No.**	**Optimal Dispatches of DERs (kW)**	V_{min} **(p.u.)**	**Time (Sec.)**	$P_{reduction}^{loss}$ **(%)**
PSO	Single	67(2051.06)	0.97	2.21	65.10
	Double	160(1349.85), 48(908.27)	0.98	2.47	74.99
	Triple	47(854.29), 77(797.20), 63(615.04)	0.99	2.64	76.70
MGTLBO	Single	67(2051.30)	0.97	4.18	65.34
	Double	197(1370.53), 47(896.11)	0.99	4.20	76.40
	Triple	42(806.17), 65(479.25), 105(971.58)	0.99	4.36	77.66
S-Jaya	Single	67(2051.287)	0.97	1.97	65.35
	Double	68(1435.50), 47(832.09)	0.99	2.16	77.28
	Triple	68(1260.93), 48(775.04), 65(222.56)	0.99	2.43	78.63

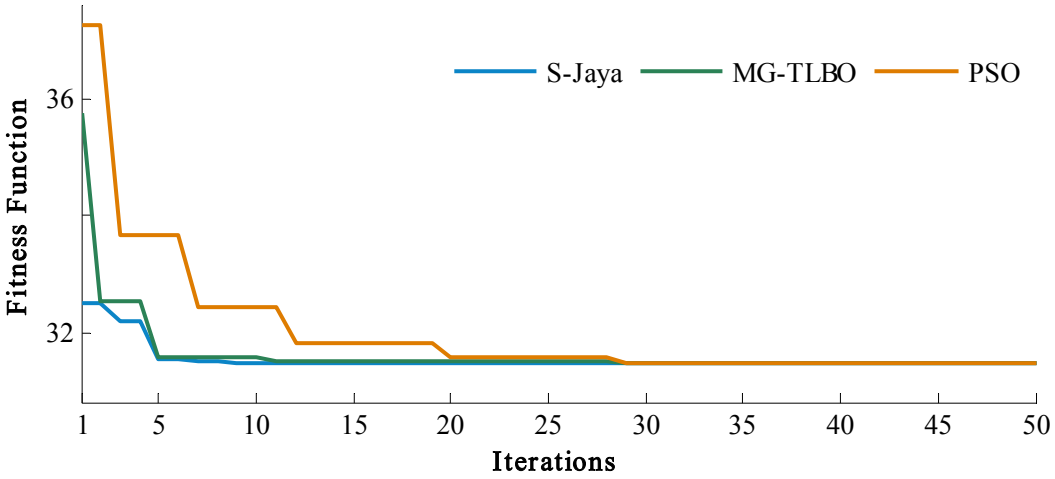

(a) One DERs

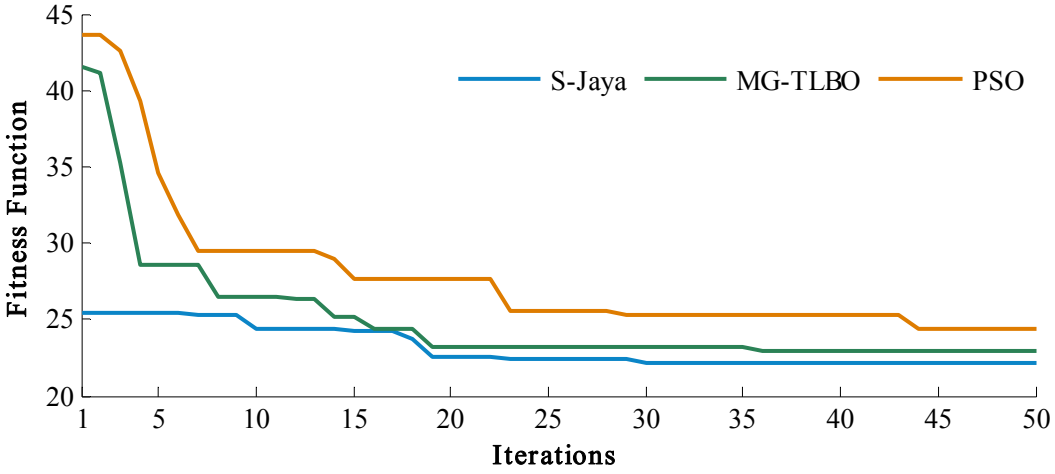

(b) Two DERs

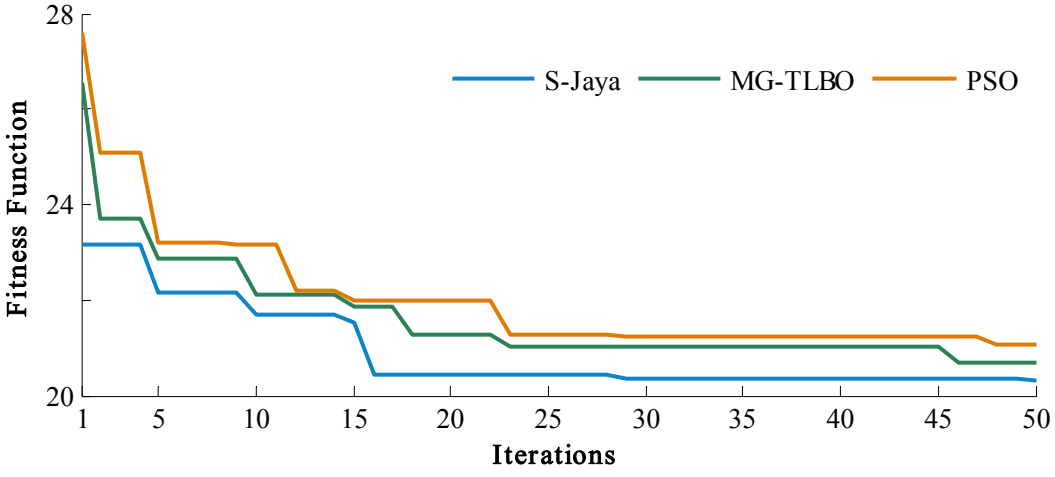

(c) Three DERs

Figure 6.20: Comparison of the algorithm performance for Non-UPF DERs

The power loss reduction value in the Non-UPF DER is less as compare to UPF DER because the fixed capacitors at a particular place are present in this system. Those fixed locations and sizes of the capacitors have introduced the

counterproductive consequences with the allocation of the Non-UPF DERs in the distribution system. The proposed algorithm has compared to The MG-TLBO and PSO algorithms for the Non-UPF DERs allocation in this system that is presented in Table 6.12.

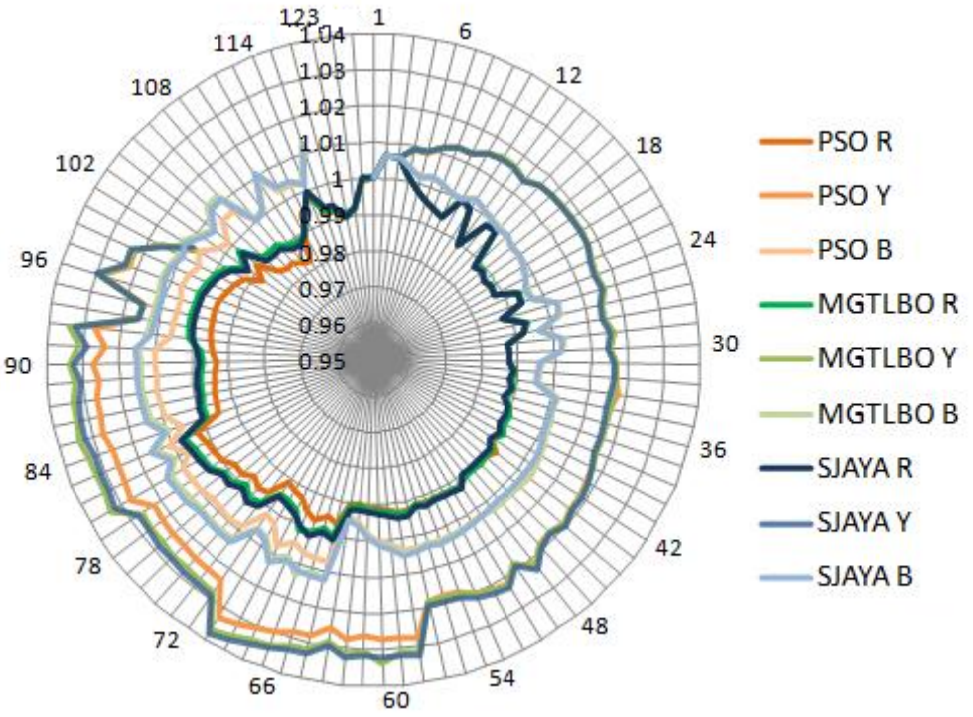

(a) Two DERs

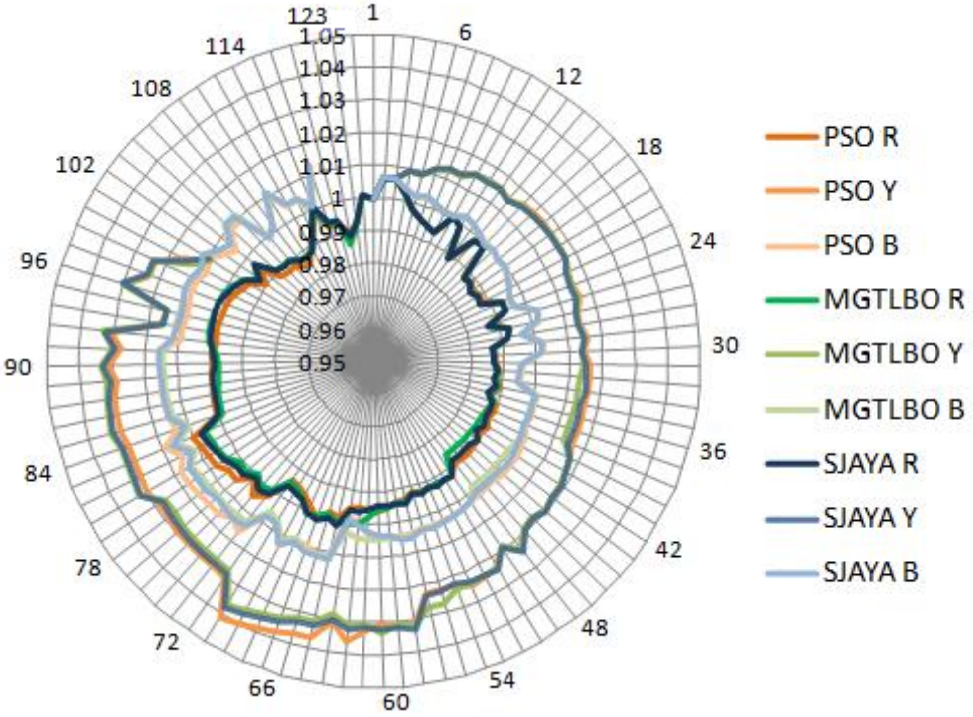

(b) Three DERs

Figure 6.21: Voltage profile of IEEE 123-bus radial distribution system for Non-UPF DERs

Figure 6.20 proved that the S-Jaya algorithm obtained the best performance in less computation time as compared to the MG-TLBO and PSO algorithms. Moreover, Figure 6.21 exhibits the voltage profile of system is situated in permissible region with best decision parameters for each number of the DERs which is optimized by the proposed algorithm.

6.6 Conclusion

Integrating distributed energy resources in the radial distribution system is striking the attention in the power system due to the more positive impacts. The modeling of the distribution system is described to explain the characteristic all component of the actual three-phase distribution system. In this chapter, IEEE 13, IEEE 37 and IEEE 123 are formulated to analysis the realistic feature of the distribution system for the practical planning of the DERs. Further, the S-Jaya algorithm is proposed to obtain the best decision parameter for the optimal accommodation in the unbalanced distribution system.

The S-Jaya algorithm has been incorporated some advanced feature in the basic Jaya method. The standard Jaya algorithm depends upon the initial solution, whether the initial solution is a worst then the performance of standard Jaya goes down and as well the consuming time increased to obtain the solution. However, the S-Jaya has reduced the most prominent weakness of standard Jaya via the shrinkage mechanism. This mechanism has filtered the non-sensitive search region and updated the search region. Therefore, the S-Jaya found the solutions in that region where the optimal solution could be converged. The proposed approach has consumed very minimum time because of the parent-child model which splits search area and distribute to 'childs' and received the solution simultaneously.

The S-Jaya algorithm has been executed in the structure of MATLAB® through the component object model. The OpenDSS simulator is interfaced with MATLAB® platform to acquire the power flow solution. Further, the co-simulation framework obtained the optimum penetration for the unity and non-unity power factor operated multiple DERs at the particular places in the unbalanced distribution system. The non-unity DERs are gained the maximum power loss reduction as compare to UPF DERs except the IEEE 123 bus system. This system has fixed capacitor at a pre-installed location which is affected the planning of the DERs allocation. The proposed method

is compared with the renowned PSO and MG-TLBO algorithm. Each algorithm has been applied to determine the best performance parameter for all three test systems. It is noticed that optimal penetration of the DERs created the V-curve in IEEE 37 and IEEE 123 distribution systems which follow the practical planning of the DERs.

The simulation result demonstrated that proposed algorithm achieve maximum reduction of power losses for each type and number of the DERs with the comparison to the MG-TLBO and PSO algorithm in unbalanced IEEE 13 bus, IEEE 37 bus and IEEE 123 bus radial three-phase distribution system. Moreover, the performance of the proposed method as compared to both algorithms is also better in respect of computation time. Also, the voltage profile is enhanced with the reduction of power losses for each type and number of the DER in the three-phase radial distribution network.

Chapter – 7

CONCLUSIONS AND FUTURE SCOPE

7.1 General

In the deregulated and competitive business environment, the distribution utilities are focused on enhancing the efficiency and power quality of the distribution system. Further, the incremental demand of the distribution system has affected the well-organized structure of power system which could not be able to the self-congratulatory for the end user utility. Therefore, DERs integration has created a new structure as a scintillating solution to the most prominent issue of energy crisis faced by the humankind.

The smarter distribution network is expected to drive the specified quality of power to the distribution system. Moreover, rapidly use of the power converter and switches are increased after the innovations in the power electronics technology. Further, these devices have introduced the nonlinearity in the supply due to device switching action. Therefore, quality of power supply by the utilities is becoming more difficult to maintain according to standards of the system.

In the practical distribution system, various components are present such as an overhead line, underground line, voltage regulator, different rating and configuration transformer, and unbalanced loading. Moreover, loading of end users is not equally distributed which introduced the unbalancing in the system. Further, analyze the characteristic of the unbalanced network through all components modeling has become a rigid interpretation. Moreover, efficiency of distribution system with integration of DERs in realistic three-phase unbalanced distribution system becomes a more complex problem.

This research attempts to developed the artificial intelligence based heuristic algorithms for optimal allocation of the DERs for each characteristic of the distribution system. The proposed algorithms are applied to optimized design variable to enhance the efficiency in time-varying load profile, multi-level load characteristic, presence of harmonics distortions and unbalanced distribution system. Further, developed approaches and algorithms have been illustrated through realistic case

studies. A summary of main findings of the research work carried out in this thesis and future scope in this area are presented in subsequent sections.

7.2 Summary of Significant Findings

The research work undertaken in this thesis is initiated by developing an approach for optimal allocation of the DERs in the radial distribution system. The particle swarm optimization based algorithm is applied to optimize the design parameters of the distribution networks. Further, the integration of the DERs has reduced the energy losses and improved the voltage profile of the system. In this consideration, time-varying load profile has been used to address the realistic consideration of the distribution system demand in a whole day. This chapter considered two types of the DERs in various scenarios for the planning purpose which builds the rigidness in the DERs planning.

Obtained results show that proposed approaches optioned the best optimized the decision parameter for the accommodation of the DERs in the radial distribution system. These parameters give better result in term of the annual energy loss reduction. The positive impacts of optimally distributed generator placement are also reflected regarding the improvement in voltage profile. The proposed method has achieved the best solution for both type of DERs (unity and non-unity power factor) which is authenticated by comparing with well-established algorithms as loss sensitivity factor, improved analytical method and construction coefficient PSO approach. Further, three standard distribution systems have been used to characterize the DERs planning in time-varying load profile from peak load condition of the distribution system.

This thesis also incorporates the increasing load demand of the distribution system. The multi-load level system represents the growing energy requirement in three load level of the demand as a light load, nominal load, and peak load. The backward/forward sweep based load flow method analyzes the characteristics of the radial distribution system which is applicable with high resistance value and radial structure of the distribution network. Further, algorithm-specific control parameters less method has been proposed to optimize the decision parameter for each load level. Moreover, the proposed Modified Group-experience Teaching Learning Based Optimization (MG-TLBO) method incorporated some modification such as grouping

mechanism, modified teaching, learning factor, mutation, and crossover for diversity to overcome the drawbacks of basic Teaching Learning Based Optimization (TLBO).

The proposed algorithm has simultaneous allocated the DGs and SCs to keep down the energy loss while maintaining the bus voltage at each level of the distribution demand. The simultaneous placement strategy of DGs and SCs is effective to regulate the active as well as the reactive power of the system whenever only unity power factor based DGs are available for accommodation. The proposed algorithm is validated by comparison with well-established algorithms such as ITLBO [12], PSO [17], ABC [24], KH [27], BFO [28], and BSO [29]. The MG-TLBO method is well tested on two standard 33-bus and 69-bus distribution systems and one practical radial 83-bus (Taiwan Power Company) distribution system for its robustness and reliability.

The thesis contributes by prominently address the shortcomings of usual DER planning, which ignores non-linearity in the distribution system under different load conditions. Therefore, the proposed MG-TLBO algorithm is applied to optimize the site and size of the DERs in presence of the non-linear loads. Further, optimal penetration of the DERs at the appropriate place in harmonics distorted system to maximize the energy loss reduction with the quality of power of end user. Moreover, backward/forward sweep-based harmonic load flow method is used to investigate the characteristic of harmonics distorted radial distribution network for fundamental and all harmonics frequency.

This thesis further contributed by enhancing the rigidness of the proposed MG-TLBO method to also validate in two modified 33-bus and 69-bus radial distribution systems and one actual feasible 83-bus radial distribution system with non-linearity of loads. The simultaneous DERs allocation strategy is formulated to maximize annual energy loss reduction with permissible harmonics distortion limit according to IEEE standard 519 while considering multi-level piece-wise load profile. The positive impacts of optimally accommodated DERs are also reflected regarding enhancement of voltage profile. Moreover, the simulation result of the proposed algorithm is compared with well-established PSO algorithms which establish the robustness and reliability of the proposed method.

Finally, this thesis considered the practical condition of the radial distribution system. In realistic condition, end-user demand and connection are unequal in the radial distribution network. Therefore, distribution line of the system is untransposed.

Further, overhead and underground cable, three type of load (constant current, constant impedance, and constant power), and different type of transformer connection have been considered to introduce the actual field connection of the distribution system. Therefore, all practical consideration is created the realistic planning of the DERs accommodation in the three-phase distribution system. Further, OpenDSS simulator is used to analyze the characteristic of unbalanced radial distribution. Moreover, an optimization algorithm is applied for the optimal allocation of the DERs in the system. A co-simulation framework is utilized to provide a platform for interfacing between the structures of MATLAB® simulation and OpenDSS simulator. Further, co-simulation environment with OpenDSS program is optimized the decision parameter for both types of DERs which operate at unity and non-unity power factor. However, this complex structure are required the single step based algorithm without the tuning of any algorithm-specific parameter. Therefore, a new Sharp-Jaya algorithm has been executed in the structure of MATLAB® by using the OpenDSS through the component object model. The proposed algorithm sharpens the Standard Jaya Algorithm using the shrinkage mechanism of the search area and the Parent-child Model.

The optimal placement and sizing of DERs have maximized the energy loss reduction while maintaining the desirable node voltage. To show the strength of the applied algorithm, simulation results are compared with the MG-TLBO and PSO algorithm. Moreover, simulation result demonstrated that proposed algorithm achieve maximum reduction of power with comparison of both algorithms in three unbalanced IEEE 13-bus, IEEE 37-bus and IEEE 123-bus radial distribution system.

7.3 Future Scope for Research

The innovation in research is the combination of already done work and hypothesis for new innovative thought which provides a path to future research work. Research is a process for continuous development in technology and society. Each step of research is exploring many directions for future action. Moreover, there is some issue which requires being the further improvement with urgent attention due to society point of view. The following points are delineating the future extension of thesis work:

1. The presented research could be further extended by considering the uncertain supply which may generate from renewable distributed energy resource in a discrete way using the switches and battery.
2. In the recent years, DERs integration leads to planning as well as operational challenges. An integrated planning method of the active distribution network can be proposed to achieve the best balance among the economic cost, clean energy utilization, and acceptability of DERs.
3. The integration of many micro producers of renewable energy into the system need to explore carefully considering the operational constraints of the network.
4. The maximum utilization of customers based renewable distributed generation system with the combination of the battery may extend in future with the renovation of technology and up-gradation in existence protection scheme. At present, the protection scheme is designed according to one-way power flow. However, there is scope to design according to two-way power flow.
5. The planning of the DERs accommodation in the uncertainty of power generation can also be extended to consider the contract pricing of the distributed generation which is the practical consideration in economical point of view.
6. The present work can be seen a solution for demand response of the distribution system and future growing market of electric vehicles by using a perfect approach to manage both of issue, simultaneously.
7. The work proposed in the thesis is focused on supply the power quality with maximum efficiency in balanced distribution networks. However, the DERs accommodation applicability in the radial practical three-phase distribution system can be proved with proposed algorithm.
8. The proposed methods and approaches may further applied in Indian real case studies. Further, these models can use to solve the present issue of Indian scenario which is the real contribution to society.
9. The work can be seen a solution for demand response and future growing market of electric vehicles. In future research work, the DR operation problem may be formulated to reflect market conditions such as distribution network pricing, demand response, congestion management, peak shaving, etc.
10. Design of efficient market model for the trading of electric power in the wind dominated electricity markets could be considered as an extension to work.

11. This work could be extended with consideration of various indices such as minimization of real power loss index, minimization of reactive power loss index, improvement of voltage profile index, short circuit current capacity index, system average interruption duration index and customers' average interruption duration index. These issues could be addressed either individually or multi-objective performance index for consideration of wide range of technical issue.

Apart from these issues for future research, large-scale wind power integration in competitive electricity markets poses several unique operation and planning challenges for power producers as well as for system operators. These challenges create ample opportunities for researchers in this area.

REFERENCES

[1]. A. Colmenar-Santos, C. Reino-Rio, D. Borge-Diez, and E. Collado-Fernández, “Distributed generation: A review of factors that can contribute most to achieve a scenario of DG units embedded in the new distribution networks,” *Renew. Sustain. Energy. Rev.*, vol. 59, pp. 1130-1148, 2016.

[2]. D. Q. Hung, N. Mithulananthan, and R. C Bansal, “An optimal investment planning framework for multiple distributed generation units in industrial distribution systems,” *Applied Energy*, vol. 124, no.1, pp. 62-72, July 2014.

[3]. V. Mohan, J. G. Singh, and W. Ongsakul, "Sortino ratio based portfolio optimization considering EVs and renewable energy in microgrid power market," *IEEE Trans Sustain. Energy*, vol. 8, no. 1, pp. 219-229, Jan. 2017.

[4]. N. M. Pindoriya, D. Dasgupta, D. Srinivasan, and M. Carvalho, “Infrastructure security for smart electric grids: A survey,” *Springer Berlin Heidelberg*, pp. 161-180, 2013.

[5]. A. Piccolo, and P. Siano, "Evaluating the impact of network investment deferral on distributed generation expansion," *IEEE Trans. Power Sys.*, vol. 24, no. 3, pp. 1559-1567, 2009.

[6]. N. R. Battu, A. R. Abhyankar and N. Senroy, “DG planning with amalgamation of operational and reliability considerations,” *Int. J. Emerging Elect. Power Syst.*, vol. 16, no. 2, pp. 1-11, 2016.

[7]. N. Jain, S. N. Singh and S. C. Srivastava, “Meta-Heuristic approach for distributed generation planning in electricity market paradigm,” *in Proc. of IEEE Int. Conf. Power and Energy Society General Meeting*, July 2012.

[8]. M. Kumawat, N. Gupta, N. Jain and R.C. Bansal, “Optimal planning of distributed energy resources in harmonics polluted distribution system,” *Swarm Evol. Comput.*, vol. 39, pp. 99-113, 2018.

[9]. P. Prakash, and D. K. Khatod, “Optimal sizing and siting techniques for distributed generation in distribution systems: A review,” *Renew. Sustain. Energy. Rev.*, vol. 57, pp. 111-130, 2016.

[10]. H. E. Farag, E. F. El-Saadany, R. El. Shatshat, A. Zidan, “A generalized power flow analysis for distribution systems with high penetration of distributed generation,” *Elect. Power Syst. Res.*, vol. 81, no. 7, pp. 1499-1506, 2011.

[11]. U. Sultana, A. B. Khairuddin, M. M. Aman, A.S. Mokhtar, and N. Zareen, “A review of optimum DG placement based on minimization of power losses and voltage stability enhancement of distribution system,” *Renew. Sustain. Energy. Rev.*, vol. 63, pp. 363-378, 2016.

[12]. P. K. Das, H. S. Behera and B. K. Panigrahi, “A hybridization of an improved particle swarm optimization and gravitational search algorithm for multi-robot path planning,” *Swarm Evol. Comput*., vol. 28, pp. 14-28, Jun. 2016.

[13]. D. Hung, N. Mithulananthan, and R. Bansal, "Analytical expressions for DG allocation in primary distribution networks," *IEEE Trans. Energy Convers*., vol. 25, no. 3, pp. 814-820, Sept. 2010.

[14]. A. R. Jordehi, “Allocation of distributed generation units in electric power systems: A review,” *Renew. Sustain. Energy. Rev.*, vol. 56, pp. 893–905, 2016.

[15]. K. D. Mistry and R. Roy, “Enhancement of loading capacity of distribution system through distributed generator placement considering techno-economic benefits with load growth,” *Int. J. Electr. Power Energy Syst*., vol. 54, no. 1, pp. 505-515, Jan. 2014.

[16]. S. Shukla, S. Mishra and B. Singh, “Power quality event classification under noisy conditions using EMD based de-noising techniques”, *IEEE Trans. Ind. Infor.*, vol. 10, no. 2, pp. 1044-1054, May 2014,.

[17]. S. Jain and S. Singh, "Harmonics estimation in emerging power system: key issues and challenges,” *Elect. Power Syst. Res.*, vol. 81, no. 9, pp. 1754-1766, 2011.

[18]. M. Mohammadi, “Bacterial foraging optimization and adaptive version for economically optimum sitting, sizing and harmonic tuning orders setting of LC harmonic passive power filters in radial distribution systems with linear and nonlinear loads,” *Appl. Soft Comput.*, vol. 29, pp. 345-356, 2015.

[19]. M. S. Munir, Y. W. Li and H. Tian, “Improved residential distribution system harmonic compensation scheme using power electronics interfaced DGs,” *IEEE Trans. Smart Grid*, vol. 7, no. 3, pp. 1191-1203, 2016.

[20]. M. Kumawat, N. Gupta and N. Jain, "Analyzing the impacts of optimally allocated distributed energy resources on harmonics in radial distribution networks," *in Proc. of IEEE Int. Conf. National Power Systems Conference, Bhubaneswar*, pp. 1-6, 2016.

[21]. IEEE Recommended Practices and Requirements for Harmonic Control in Electrical Power Systems, *IEEE Std.*, pp. 1-112, 1993.

[22]. G. T. Heydt and A. W. Galli, “Transient power quality problem analyzed using wavelet,” *IEEE Trans. Power Del.*, vol. 12, no. 2, pp. 908–915, 1997.

[23]. N. Jain, S. Singh and S. C. Srivastava, "A generalized approach for DG planning and viability analysis under market scenario," *IEEE Trans. Ind. Electron*., vol. 60, no. 11, pp. 5075-5085, Nov. 2013.

[24]. N. Kanwar, N. Gupta, K. R. Niazi and A. Swarnkar, “Simultaneous allocation of distributed resources using improved teaching learning based optimization,” *Energy Conver. Management*, vol. 103, pp. 387-400, Oct. 2015.

[25]. G. Pepermans, J. Driesen, D. Haeseldonckx, R. Belmans and W. D’haeseleer, “Distributed generation: definition, benefits and issues,” *Energy Policy*, vol. 33, no. 6, pp. 787-798, 2005.

[26]. N. Jain, S. Singh and S. C. Srivastava, "Distributed Generation in power system: An overview and key issue," *in Proc of 24th Indian Engineering Congress, Proceeding of IEC.*, pp. 1-8, 2009.

[27]. M. Kumawat, N. Gupta, N. Jain and R. C. Bansal, “Swarm-intelligence-based optimal planning of distributed generators in distribution network for minimizing energy loss,” *Elect. Power Comp. Sys.*, vol. 45, no. 6, pp. 589-600, Apr. 2017.

[28]. H. Hamedi and M. Gandomkar, “A straightforward approach to minimizing unsupplied energy and power loss through DG placement and evaluating power quality in relation to load variations over time,” *Int. J.*

Electr. Power Energy Syst., vol. 35, no. 1, pp. 93–96, Feb. 2012.

[29]. M. Kumawat, N. Gupta, N. Jain and D. Saxena, "Optimal distributed generation placement in power distributed networks: A review," *in Proc. of IEEE Int. Conf. Electrical, Electronics, Signals, Communication and Optimization*, Jan. 2015.

[30]. G. Pepermans, J. Driesen, D. Haeseldonckx, R. Belmans and W. D'haeseleer, "Distributed generation: definition benefits and issues," *Energy Policy*, vol. 33, no. 6, pp. 787-798, Apr. 2005.

[31]. T. Ackermann, G. Andersson, L. Söder, "Distributed generation: a definition," *Elect. Power Syst. Res.*, vol. 57, no. 3,pp. 195-204, 2001.

[32]. A. Keane and M. O'Malley, "Optimal allocation of embedded generation on distribution networks," *IEEE Trans. Power Syst.*, vol. 20, no. 3, pp. 1640-1646, Aug. 2005.

[33]. M. F. Akorede, H. Hizam, E. Pouresmaeil, "Distributed energy resources and benefits to the environment," *Renew. Sustain. Energy. Rev.*, vol. 14, no. 2, pp.724-734, 2010.

[34]. M. M. Aman, G. B. Jasmon, A. H. A. Bakar, H. Mokhlis and M. Karimi, "Optimum shunt capacitor placement in distribution system—A review and comparative study," *Renew. Sustain. Energy. Rev.*, vol. 30, pp. 429-439, 2014.

[35]. S. Haggmark, U. Axelsson, G. Karlsson, K. Kauhaniemi, M. Olsson and C. Liljegren, "Aspects of different distributed generation technologies," *CODGUNET WP 3 project report. VTT processes*, pp. 1-45, 2003.

[36]. L. M. Hajagos and G. R. Berube, "Utility experience with gas turbine testing and modeling," *in Proc. of IEEE power engineering society winter meeting*, pp. 671–677, 2001.

[37]. F. Jurado and J. R. Saenz, "Adaptive control of a fuel cell-microturbine hybrid power plant," *in Proc. of IEEE power engineering society summer*, pp. 76–81, 2002.

[38]. M. Boyce, "Gas turbine engineering handbook. Houston," *Gulf Publishing Company*, 1982.

[39]. X. Huang, Z. Zhang and J. Jiang, "Fuel cell technology for distributed

generation: an overview," *Quebec, Canada: IEEE ISIE Montreal*, 2006.

[40]. V. Hengsritawat, T. Tayjasanant and N. Nimpitiwan, "Optimal sizing of photovoltaic distributed generators in a distribution system with consideration of solar radiation and harmonic distortion," *Int. J. Electr. Power Energy Syst*., vol. 39, no. 1, pp. 36-47, Feb. 2012.

[41]. A. A. Tamimi, A. Pahwa and S. Starrett, "Effective wind farm sizing method for weak power systems using critical modes of voltage instability," *IEEE Trans. Power Syst.*, vol. 27, no. 3, pp. 1610-1617, Aug. 2012.

[42]. V. Kirubakaran et al., "A review on gasification of biomass," *Renew. Sustain. Energy. Rev.*, vol. 13, pp. 179-86, 2009.

[43]. CIGREWG37-23, "Impact of increasing contribution of dispersed generation on the power system," *Final Report. Electra,* Sep. 1998.

[44]. I. B. Fridleifsson, "Geothermal energy for the benefit of the people," *Renew. Sustain. Energy. Rev.*, vol. 5, pp. 299-312, 2001.

[45]. "Dispersed system impacts: survey and requirements study," *EPRI TR-103337, project*, pp. 3357-3401, 1994.

[46]. M. F. Akorede, H. Hizam and E. Pouresmaeil, "Distributed energy resources and benefits to the environment," *Renew. Sustain. Energy. Rev.*, vol. 14, no. 2, pp. 724-734, 2010.

[47]. S. G. Naik, D. K. Khatod and M. P. Sharma, "Optimal allocation of combined DG and capacitor for real power loss minimization in distribution networks," *Int. J. Electr. Power Energy Syst.*, vol. 53, no. 1, pp. 967-973, Dec. 2013.

[48]. N. Acharya, P. Mahat and N. Mithulananthan, "An analytical approach for DG allocation in primary distribution network," *Int. J. Elect. Power Energy Syst.*, vol. 28, no. 10, pp. 669-678, Dec. 2006.

[49]. S. H. Lee and J. W. Park, "Optimal placement and sizing of multiple DGs in a practical distribution system by considering power loss," *IEEE Trans. Power Syst.*, vol. 49, no. 5, pp. 683-695, Oct. 2013.

[50]. A. S. Mohammadi and M.T. Ameli, "Proper sizing and placement of distributed power generation aids the intentional islanding process,"

Elect. Power Syst. Res., vol. 106, no. 1, pp. 73-85, Jan. 2014.

[51]. G. J. S. Rosseti et. al, "Optimal allocation of distributed generation with reconfiguration in electric distribution systems," *Elect. Power Syst. Res.*, vol. 103, no. 1, pp. 178-183, Oct. 2013.

[52]. Y. M. Atwa and E. F. El-Saadany, "Probabilistic approach for optimal allocation of wind-based distributed generation in distribution systems," *IET Renew. Power Gener.*, vol. 5, no. 1, pp. 79-88, Jan. 2011.

[53]. D. Kumar, S. R. Samantaray, I. Kamwa and N.C.Sahoo, "Reliability-constrained based optimal placement and sizing of multiple distributed generators in power distribution network using cat swarm optimization," *Elect. Power Comp. Sys*., vol. 42, no. 2, pp. 149-164, Jan. 2014.

[54]. A. Zidan, M. F. Shaaban and E. F. El-Saadany, "Long -term multi-objective distribution network planning by DG allocation and feeders' reconfiguration," *Elect. Power Syst. Res.*, vol. 105, no. 1, pp. 95-104, Dec. 2013.

[55]. R. Prenc, D. Skrlec and V. Komen, "Distributed generation allocation based on average daily load and power production curves," *Int. J. Electr. Power Energy Syst.*, vol. 53, no. 1, pp. 612-622, Dec. 2013.

[56]. K. Singh, V. K. Yadav, N. P. Padhy and J. Sharma, "Congestion management considering optimal placement of distributed generator in deregulated power system networks," *Elect. Power Comp. Sys.*, vol. 42, no. 1, pp. 13-22, Dec. 2013.

[57]. J. M. Lezama, J. Contreras and A. P. Feltrin, "Location and contract pricing of distributed generation using a genetic algorithm," *Int. J. Electr. Power Energy Syst.*, vol. 36, no. 1, pp. 117-126, Mar. 2012.

[58]. R. Prenc, D. Åkrlec and V. Komen, "Distributed generation allocation based on average daily load and power production curves," *Int. J. Elect. Power Energy Syst.*, vol. 53, pp. 612-622, Dec. 2013.

[59]. K. M. Muttaqi, A. D. Le, J. Aghaei, E. Mahboubi-Moghaddam, M. Negnevitsky and G. Ledwich, "Optimizing distributed generation parameters through economic feasibility assessment, " *Applied Energy*, vol. 165, no. 1, pp. 893-903, Mar. 2016.

[60]. M. Mohammadi and Mehdi Nafar, "Optimal placement of multitypes DG as independent private sector under pool/hybrid power market using GA-based tabu search method," *Int. J. Electr. Power Energy Syst.,* vol. 51, no. 1, pp. 43-53, Mar. 2013.

[61]. S. M. Sajjadi, M. R. Haghifam and J. Salehi, "Simultaneous placement of distributed generation and capacitors in distribution networks considering voltage stability index," *Int. J. Electr. Power Energy Syst.*, vol. 46, no. 1, pp. 366-375, Mar. 2013.

[62]. A. Y. Abdelaziz, E. S. Ali and S. M. Elazim Abd, "Optimal sizing and locations of capacitors in radial distribution systems via flower pollination optimization algorithm and power loss index," *Eng. Sci. Technol. Int. J.*, vol. 19, no.1, pp. 610-618, Mar. 2016.

[63]. M. Nayeripourn, E. M. Moghaddam, J. Aghaei and A. A. Vahed, "Multi-objective placement and sizing of DGs in distribution networks ensuring transient stability using hybrid evolutionary algorithm," *Renew. Sustain. Energy. Rev.,* vol. 25, no. 1, pp. 759-767, Sep. 2013.

[64]. M. H. Moradia, A. Zeinalzadeh, Y. Mohammadi and M. Abedini, "An efficient hybrid method for solving the optimal sitting and sizing problem of DG and shunt capacitor banks simultaneously based on imperialist competitive algorithm and genetic algorithm," *Int. J. Electr. Power Energy Syst.*, vol. 54, no. 1, pp. 101-111, Jan. 2014.

[65]. M. H. Moradi and M. Abedini, "A combination of genetic algorithm and particle swarm optimization for optimal DG location and sizing in distribution systems," *Int. J. Electr. Power Energy Syst.,* vol. 34, no. 1, pp. 66-74, Jan. 2012.

[66]. A. C. Rueda-Medina, J. F. Franco, Marcos J. Rider, A. Padilha-Feltrin and Ruben Romero, "A mixed -integer linear programming approach for optimal type, size and allocation of distributed generation in radial distribution systems," *Elect. Power Syst. Res.*, vol. 97, no. 1, pp. 133-143, Apr. 2013.

[67]. F. S. Abu-Mouti and M. E. El-Hawary, "Heuristic curve-fitted technique for distributed generation optimisation in radial distribution feeder

systems," *IET Gener. Trans. Dist.*, vol. 5, no. 2, pp. 172-180, Feb. 2011.

[68]. A. Saif, V. R. Pandi, H. Zeineldin and S. Kenedy, "Optimal allocation of distributed energy resources through simulation-based optimization," *Elect. Power Syst. Res.*, vol. 104, no. 1, pp. 1-8, Nov. 2013.

[69]. C. Novoa and T. Jin, "Reliability centered planning for distributed generation considering wind power volatility," *Elect. Power Syst. Res.*, vol. 81, no. 8, pp. 1654-1661, Aug. 2011.

[70]. Z. Liu, F. Wen and G. Ledwich, "Optimal siting and sizing of distributed generators in distribution systems considering uncertainties," *IEEE Trans. Power Del*., vol. 26, no. 4, pp. 2541-2551, Oct. 2011.

[71]. A. Soroudi and M. Ehsan, "Efficient immune-GA method for DNOs in sizing and placement of distributed generation units," *Eur. Trans. Electr. Power*, vol. 21, no. 3, pp. 1361-1375, Apr. 2011.

[72]. V. A. Evangelopoulos and P. S. Georgilakis, "Optimal distributed generation placement under uncertainties based on point estimate method embedded genetic algorithm," *IET Gener. Trans. Dist.*, vol. 8, no. 3, pp. 389-400, Sep. 2013.

[73]. N. G. A. Hemdan and M. Kurrat, "Efficient integration of distributed generation for meeting the increased load demand," *Int. J. Electr. Power Energy Syst.*, vol. 33, no. 9, pp. 1572-1583, Nov. 2011.

[74]. S. Y. Kim, W. W. Kim and J. O. Kim, "Determining the optimal capacity of renewable distributed generation using restoration methods," *IEEE Trans. Power Syst.*, vol. 29, no. 5, pp. 2001-2013, sep. 2014.

[75]. F. Ugranli and E. Karatepe, "Long-term performance comparison of multiple DG allocations using a clustering-based method," *Elect. Power Comp. Sys.*, vol. 40, no. 2, pp.195-218, Dec. 2011.

[76]. S. K. Injeti and N. P. Kumar, "A novel approach to identify optimal access point and capacity of multiple DGs in a small, medium and large scale radial distribution systems," *Int. J. Electr. Power Energy Syst.*, vol. 45, no. 1, pp. 142-151, Feb. 2013.

[77]. S. H. Lee and J. W. Park, "Selection of optimal location and size of multiple distributed generations by using kalman filter algorithm," *IEEE*

Trans. Power Syst., vol. 24, no. 3, pp. 1393-1400, Aug. 2009.

[78]. D. Q. Hung and N. Mithulananthan, "Multiple distributed generators placement in primary distribution networks for loss reduction," *IEEE Trans. Ind. Electron.*, vol. 60, no. 4, pp. 1700-1708, Apr. 2013.

[79]. W. Prommee and W. Ongsakul, "Optimal multiple distributed generation placement in microgrid system by improved reinitialized social structures particle swarm optimization," *Euro. Trans. Electr. Power*, vol. 21, no. 1, pp. 489-504, Jan. 2011.

[80]. M. Moradi, S. Tousi and M. Abedini, "Multi-objective PFDE algorithm solving the optimal siting and sizing problem of multiple DG sources," *Int. J. Electr. Power Energy Syst.*, vol. 56, no. 1, pp. 117-126, Mar. 2014.

[81]. N. C. Hien, N. Mithulananthan and R. C. Bansal, "Optimal placement and sizing of multiple DGs in a distribution system by considering power loss," *IEEE Syst. J.*, vol. 7, no. 4, pp. 797-806, Dec. 2013.

[82]. S. Kansal, V. Kumar and B. Tyagi, "Optimal placement of different type of DG sources in distribution networks," *Int. J. Electr. Power Energy Syst.*, vol. 53, no. 1, pp. 752-760, Dec. 2013.

[83]. M. Raoofat, "Simultaneous allocation of DGs and remote controllable switches in distribution networks considering multilevel load model," *Int. J. Electr. Power Energy Syst.*, vol. 33, no. 8, pp. 1429-1436, Oct. 2011.

[84]. D. K. Singh, "Multiobjective optimization for dg planning with load models," *IEEE Trans. Power Syst.*, vol. 24, no. 1, pp. 427-436, Feb. 2009.

[85]. R. K. Singh and S. K. Goswami, "Multi-objective optimization of distributed generation planning using impact indices and trade-off technique," *Elect. Power Comp. Sys.*, vol. 39, no. 11, pp. 1175-1190, Aug. 2011.

[86]. R. S. Al Abri, E. F. El-Saadany and Y. M. Atwa, "Optimal placement and sizing method to improve the voltage stability margin in a distribution system using distributed generation," *IEEE Trans. Power Syst.*, vol. 28, no. 1, pp. 326-334, Feb. 2013.

[87]. M. Esmaili, "Placement of minimum distributed generation units observing power losses and voltage stability with network constraints," *IET Gener.*

Trans. Dist., vol. 7, no. 8, pp. 813-821, May. 2013.

[88]. A. A. Tamimi, A. Pahwa and S. Starrett, “Effective wind farm sizing method for weak power systems using critical modes of voltage instability,” *IEEE Trans. Power Syst.,* vol. 27, no. 3, pp. 1610-1617, Aug. 2012.

[89]. S. M. Sajjadi, M. R. Haghifam and J. Salehi, "Simultaneous placement of distributed generation and capacitors in distribution networks considering voltage stability index," *Int. J. Elect. Power Energy Syst.,* vol. 46, pp. 366-375, Mar. 2013.

[90]. V.V.S.N. Murthy and A. Kumar, “Comparison of optimal DG allocation methods in radial distribution systems based on sensitivity approaches,” *Int. J. Electr. Power Energy Syst*., vol. 53, no. 1, pp. 450-467, Dec. 2013.

[91]. M. M. Aman, G. B. Jasmon, H. Mokhlis and A. H. A. Bakar, “Optimal placement and sizing of a DG based on a new power stability index and line losses,” *Int. J. Elect. Power Energy Syst.,* vol. 43, no. 1, pp.1296-1304, Dec. 2012.

[92]. A. T. Davda, B. Azzopardi, B. R. Parekh and M. D. Desai, “Dispersed generation enable loss reduction and voltage profile improvement in distribution network-case study, Gujarat, India,” *IEEE Trans. Power Syst.,* vol. 29, no. 3, pp. 1242-1249, May 2014.

[93]. L. D. Arya, A. Koshti and S. C. Choube, “Distributed generation planning using differential evolution accounting voltage stability consideration,” *Int. J. Electr. Power Energy Syst.,* vol. 42, no. 1, pp. 196-207, Nov. 2012.

[94]. S. Dahal and H. Salehfar, “Impact of distributed generators in the power loss and voltage profile of three phase unbalanced distribution network,” *Int. J. Electr. Power Energy Syst.,* vol. 77, pp. 256-262, May 2016.

[95]. M. M. Othman, W. El-Khattam, Y. G. Hegazy and Y. A. Abdelaziz, “Optimal placement and sizing of voltage controlled distributed generators in unbalanced distribution networks using supervised firefly algorithm,” *Int. J. Electr. Power Energy Syst.,* vol. 82, pp. 105-113, Nov. 2016

[96]. A. A. Abdelsalam and E. F. El-saadany, "Probabilistic Approach for Optimal Planning of Distributed Generators with Controlling Harmonic

Distortions," *IET Gener. Trans. Dist.*, vol. 7, no. 10, pp. 1105-1115, Oct. 2013.

[97]. A. M. Imran and M. Kowsalya, "Optimal size and siting of multiple distributed generators in distribution system using bacterial foraging optimization," *Swarm. Evol. Comput*., vol. 15, pp. 58-65, Apr. 2014.

[98]. A. Ulinuha, M. A. S. Masoum and S. Islam, "Hybrid Genetic-Fuzzy algorithm for volt/var/total harmonic distortion control of distribution systems with high penetration of non-linear loads," *IET Gener. Trans. Dist.*, vol. 5, no. 4, pp. 425-439, Apr. 2011.

[99]. A. A. Eajal and M. E. El-Hawary, "Optimal capacitor placement and sizing in unbalanced distribution systems with harmonics consideration using particle swarm optimization," *IEEE Trans. Power Del.*, vol. 25, no. 3, pp. 1734-1741, July 2010.

[100]. W. Grady, "Understanding power system harmonics," *Dept of Electrical & Computer Engineering, Univ of Texas at Austin*, 2012.

[101]. C. B. Ibrahim and K. Engin, "Influence of phasor adjustment of harmonic sources on the allowable penetration level of distributed generation," *Int. J. Electr. Power Energy Syst.*, vol. 87, pp. 1-15, May 2017.

[102]. V. R. Pandi, H. H. Zeineldin and W. Xiao, "Determining optimal location and size of distributed generation resources considering harmonic and protection coordination limits," *IEEE Trans. Power Syst.*, vol. 28, no. 2, pp. 1245-1254, May. 2013.

[103]. P. Bagheri, W. Xu and T. Ding, "A distributed filtering scheme to mitigate harmonics in residential distribution systems," *IEEE Trans. Power Del.*, vol. 31, no. 2, pp. 648-656, Apr. 2016.

[104]. B. Singh, V. Mukherjee and P. Tiwari, "A survey on impact assessment of DG and FACTS controllers in power systems," *Renew. Sustain. Energy. Rev.*, vol. 42, no. C, pp. 846–928, 2015.

[105]. X. Zhang, G. G. Karady and S. T. Ariaratnam, "Optimal allocation of CHP-based distributed generation on urban energy distribution networks," *IEEE Trans Sustain. Energy*, vol. 5, no. 1, pp.246–253, 2014.

[106]. C. J. Dent, L. F. Ochoa and G. P. Harrison, "Network distributed

generation capacity analysis using OPF with voltage step constraints," *IEEE Trans. Power Syst*., vol. 25, no. 1, pp. 296–304, Feb. 2010.

[107]. X. Zhang ,G. G. Karady, K. R. Piratla and S. T. Ariaratnam, "Network capacity assessment of combined heat and power-based distributed generation in urban energy infra structures," *IEEE Trans. Smart Grid*, vol. 4, no. 4, pp. 2131-2138, 2013.

[108]. L. F. Ochoa, C. J. Dent and G. P. Harrison, "Distribution network capacity assessment: Variable DG and active networks*," IEEE Trans. Power Syst*., vol. 25, no. 1, pp. 87–95, Feb. 2010.

[109]. A. R. R. De Souza et al., "Sensitivity analysis to connect distributed generation," *Int. J. Electr. Power Energy Syst.*, vol. (46), pp.145–152, 2013.

[110]. D. Q. Hung, N. Mithulananthan and W. Y. Lee, "Optimal placement of dispatchable and non-dispatchable renewable DG units in distribution networks for minimizing energy loss," *Int. J. Electr. Power Energy Syst*., vol. 55, no. 1, pp. 179-186, Feb. 2014.

[111]. T. Gözel and M. H. Hocaoglu, "An analytical method for the sizing and siting of distributed generators in radial systems," *Elect. Power Comp. Sys.*, vol. 79, no. 6, pp. 912-918, 2009.

[112]. C. Wang and M. Nehrir, "Analytical approaches for optimal placement of distributed generation sources in power systems*," IEEE Trans. Power Syst.*, vol. 19, no. 4, pp. 2068-2076, Nov. 2004.

[113]. S. Kotamarty and S. Khushalani, N. Schulz, "Impact of distributed generation on distribution contingency analysis," *Elect. Power Syst. Res.*, vol. 78, no. 9, pp. 1537-1545, 2008.

[114]. K. Vinothkumar and M. P. Selvan, "Distributed generation planning: A new approach based on goal programming," *Elect. Power Comp. Sys.*, vol. 40, no. 5, pp. 497-512, Feb. 2012.

[115]. F. Ugranli and E. Karatepe "Long-term Performance Comparison of Multiple Distributed Generation Allocations Using a Clustering-based Method," *Elect. Power Comp. Sys.*, vol. 40, no. 2, pp. 195-218, Dec. 2011.

[116]. F. Rotaru, G. Chicco, G. Grigoras and G. Cartina, "Two-stage distributed

generation optimal sizing with clustering-based node selection," *Int. J. Electr. Power Energy Syst.*, vol. 40, no. 1, pp. 120-129, Sep. 2012.

[117]. P. Dehghanian, S. H. Hosseini, M. Moeini-Aghtaie and A. Arabali, "Optimal siting of DG units in power systems from a probabilistic multi-objective optimization perspective," *Int. J. Electr. Power Energy Syst.*, vol. 51, no. 1, pp. 14-26, Oct. 2013.

[118]. G. Celli, E. Ghiani, S. Mocci and F. Pilo, "A Multiobjective evolutionary algorithm for the sizing and siting of distributed generation," *IEEE Trans. Power Syst.*, vol. 20, no. 2, pp. 750-757, 2005.

[119]. W. El-khattam, Y. G. Hegazy and M.M.A. Salama, "An integrated distributed generation optimization model for distribution system planning," *IEEE Trans. Power Syst.*, vol. 20, no. 2, pp. 1158-1165, 2005.

[120]. P. S. Georgilakis and N. D. Hatziargyriou, "Optimal distributed generation placement in power distribution networks: models, methods, and future research," *IEEE Trans. Power Syst.*, vol. 28, no. 3, pp. 3420-3428, Aug. 2013.

[121]. S. Kaur, G. Kumbhar and J. Sharma, "A MINLP technique for optimal placement of multiple DG units in distribution systems," *Elect. Power Syst. Res.*, vol. 63, pp. 609-617, 2014.

[122]. L. F. Ochoa and G. P. Harrison, "Minimizing energy losses: Optimal accommodation and smart operation of renewable distributed generation," *IEEE Trans. Power Syst.*, vol. 26, no. 1, pp. 198-205, Feb. 2011.

[123]. S. Porkar *et al.*, "Optimal allocation of distributed generation using a two-stage multi-objective mixed-integer-nonlinear programming," *Eur. Trans. Electr. Power*, vol. 21, no. 1, pp. 1072-1087, Jan. 2011.

[124]. N. Khalesi, N. Rezaei and M.R. Haghifam, "DG allocation with application of dynamic programming for loss reduction and reliability improvement," *Int. J. Electr. Power Energy Syst.*, vol. 33, no. 2, pp. 288-295, Feb. 2011.

[125]. D. K. Khatod, V. Pant and J. Sharma, "Evolutionary programming based optimal placement of renewable distributed generators," *IEEE Trans. Power Syst.*, vol. 28, no. 2, pp. 683-695, May 2013.

[126]. M. F. Shaaban, Y. M. Atwa and E. F. El-Saadany, "DG allocation for benefit maximization in distribution networks," *IEEE Trans. Power Syst.*, vol. 28, no. 2, pp. 639-649, May. 2013.

[127]. A. S. A. Awad, T. H. M. El-Fouly and M. M. A. Salama, "Optimal distributed generation allocation and load shedding for improving distribution system reliability," *Elect. Power Comp. Sys.*, vol. 42, no. 6, pp. 576-584, Mar. 2014.

[128]. M. Raoofat and A. R. Malekpour "Optimal allocation of distributed generations and remote controllable switches to improve the network performance considering operation strategy of distributed generations," *Elect. Power Comp. Sys.*, vol. 39, no. 16, pp. 1809-1827, Oct. 2011.

[129]. M. F. Akorede, H. Hizam, I. Aris and M. Z. A. Ab Kadir, "Effective method for optimal allocation of distributed generation units in meshed electric power systems," *IET Gener. Trans. Dist.*, vol. 5, no. 2, pp. 276-287, Feb. 2011.

[130]. K. Vinothkumar and M. P. Selvan, "Fuzzy embedded genetic algorithm method for distributed generation planning," *Elect. Power Comp. Sys.*, vol. 39, no. 4, pp. 346-366, Feb. 2011.

[131]. J. D. Foster, A. M. Berry, N. Boland and H. Waterer, "Comparison of mixed-integer programming and genetic algorithm methods for distributed generation planning," *IEEE Trans. Power Syst.*, vol. 29, no. 2, pp. 833-843, Mar. 2014.

[132]. J. Kennedy and R. Eberhart, "A new optimizer using particle swarm theory. In Micro Machine and Human Science," *in Proc. of IEEE Int. Conf. Neural Networks*, Oct. 1995.

[133]. M. Clerc and J. Kennedy, "The particle swarm - explosion, stability and convergence in a multidimensional complex space," *IEEE Trans. Evolut. Comput.*, vol. 6, no. 1, pp. 58-73, Feb. 2002.

[134]. N. Jain, S. Singh and S. C. Srivastava, "PSO based placement of multiple wind DGs and capacitors utilizing probabilistic load flow model," *Swarm Evol. Comput.*, vol. 19, pp. 15-24, Dec. 2014.

[135]. A. M. El-Zonkoly, "Optimal placement of multi-distributed generation

units including different load models using particle swarm optimization," *IET Gener. Trans. Dist.*, vol. 5, no. 7, pp. 760-771, Jul. 2011.

[136]. A. Ameli, S. Bahrami, F. Khazaeli and M. R. Haghifam, "A multiobjective particle swarm optimization for sizing and placement of DGs from DG owner's and distribution company's viewpoints," *IEEE Trans. Power Del.*, vol. 29, no. 4, pp. 1831-1840, Aug. 2014.

[137]. N. Jain, S. Singh and S. C. Srivastava, "Planning and impact evaluation of distributed generators in Indian context using Multi-Objective Particle Swarm Optimization," *in Proc. of IEEE Int. Conf. Power and Energy Society General Meeting*, pp. 1-8, July 2011.

[138]. J. Aghaei, K. M. Muttaqi, A. Azizivahed and M. Gitizadeh, "Distribution expansion planning considering reliability and security of energy using modified particle swarm optimization algorithm," *Energy*, vol. 65, pp. 398-411, Feb. 2014.

[139]. M. Dorigo, T. Stutzle , Ant colony optimization. Cambridge, MA: MIT Press; 2004.

[140]. J. F. Gomez et al, "Ant colony system algorithm for the planning of primary distribution circuits," *IEEE Trans. Power Syst.*, vol. 19, no. 2, pp. 996-1004, 2004.

[141]. C. T. Su, C. F. Chang and J. P. Chiou, "Distribution network reconfiguration for loss reduction by ant colony search algorithm," *Elect. Power Syst. Res.*, vol. 75, no. 2, pp.190-199, Aug. 2005.

[142]. D. Karaboga, "An idea based on honey bee swarm for numerical optimization," Technical report TR06 Erciyes University, Engineering Faculty, Computer Engineering Department, 2005.

[143]. F. S. Mouti and M. Hawary, "Optimal distributed generation allocation and sizing in distribution systems via artificial bee colony algorithm," *IEEE Trans. Power Del.*, vol. 26, no. 4, pp. 2090-2101, Oct. 2011.

[144]. N. Mohandas et al, "Optimal location and sizing of real power DG units to improve the voltage stability in the distribution system using ABC algorithm united with chaos," *Int. J. Electr. Power Energy Syst.*, vol. 66, pp. 41-52, 2015.

[145]. D. R. Prabha, T. Jayabarathi, R. Umamageswari and S. Saranya, "Optimal location and sizing of distributed generation unit using intelligent water drop algorithm," *Sust. Ener. Technol. Assess.*, vol. 11, pp. 106-113, 2015.

[146]. W. Buaklee and K. Hongesombut, "Optimal DG allocation in a smart distribution grid using cuckoo search algorithm," *in Proc. of the IEEE Conference on Electrical Computer Telecomm and Information Technology*, pp. 1-6, 2013.

[147]. Z. Moravej and A. Akhlaghi, "A novel approach based on cuckoo search for DG allocation in distribution network," *Int. J. Electr. Power Energy Syst.*, vol. 44, no. 1, pp. 672-679, Jan. 2013.

[148]. T. T. Nguyen, A. V. Truong and T. A. Phung, "A novel method based on adaptive cuckoo search for optimal network reconfiguration and distributed generation allocation in distribution network," *Int. J. Elect. Power Energy Syst.*, vol. 78, pp. 801-815, June 2016.

[149]. X. S. Yang, "Firefly Algorithm, Stochastic Test Functions and Design Optimization," *Int. J. Bio-Inspir. Comput.*, vol. 2, no. 2, pp. 78-84, 2010.

[150]. M. R. Haghifam, H. Falaghi and O. P Malik, "Risk-based distributed generation placement," *IET Gener. Trans. Dist.*, vol. 2, no. 2, pp. 252-260, 2008.

[151]. P. Duc, and K. Dervis, "Intelligent optimisation techniques: genetic algorithms, tabu search, simulated annealing and neural networks," *Springer Science Business Media*, 2012.

[152]. Z. W. Geem, J. H. Kim and G. Loganathan, "A new heuristic optimization algorithm: harmony search," *Simulation*, pp. 60-68, 2001.

[153]. R. S. Rao, K. Ravindra, K. Satish and S. V. L. Narasimham, "Power loss minimization in distribution system using network reconfiguration in the presence of distributed generation," *IEEE Trans. Power Syst.*, vol. 28, no. 1, pp. 317-325, Feb. 2013.

[154]. K. Nekooei *et al.*, "An improved multi-objective harmony search for optimal placement of DGs in distribution systems," *IEEE Trans. Smart Grid*, vol. 4, no. 1, pp. 683-695, Mar. 2013.

[155]. M. Gandomkar, M. Vakilian and M. A. Ehsan, "Genetic-based tabu search

algorithm for optimal DG allocation in distribution networks," *Electr Power Components Syst.*, vol. 33, no. 12, pp. 1351-1362, 2007.

[156]. M. Gomez-Gonzalez, A. Lopez and F. Jurado, "Optimization of distributed generation systems using a new discrete PSO and OPF," *Elect. Power Syst. Res.*, vol. 84, no. 1, pp. 174-180, Mar. 2012.

[157]. Sh. Abdi and K. Afshar, "Application of IPSO-Monte Carlo for optimal distributed generation allocation and sizing," *Int. J. Electr. Power Energy Syst.*, vol. 44, no. 1, pp. 786-797, Jan. 2013.

[158]. J. D. Foster, A. M. Berry, N. Boland and H. Waterer, "Comparison of mixed-integer programming and genetic algorithm methods for distributed generation planning," *IEEE Trans. Power Syst.*, vol. 29, no. 2, pp. 833-843, Mar. 2014.

[159]. T. Jen-Hao, "A Direct Approach for Distribution System Load Flow Solution," *IEEE Trans. Power Del.*, vol. 18, no. 3, pp. 882–887, July 2003.

[160]. S. Civanlar, J. J. Grainger, H. Yin and S. S. H. Lee, "Distribution Feeder Reconfiguration for Loss Reduction*", IEEE Trans. Power Del.*, vol. 3, no. 3, pp. 1217-1223, July 1988.

[161]. W. C. Reynolds, "Flocks, herds, and schools: A distributed behavioral model," *in Proc. of the 14th Annual Conference on Computer Graphics and Interactive Techniques*, 1987.

[162]. V. H. M. Quezada, J. R. Abbad and T. G. S. Roman, "Assessment of energy distribution losses for increasing penetration of distributed generation," *IEEE Trans. Power Syst.*, vol. 21, pp. 533-540, May 2006.

[163]. M. R. Al Rashidi and M. F. Al Hajri, "Optimal planning of multiple distributed generation sources in distribution networks: A new approach," *Energy Conver. Management*, vol. 52, no. 11, pp. 3301-3308, Oct. 2011.

[164]. R. V. Rao, V. J. Savsani and D. P. Vakharia, "Teaching–learning-based optimization: A novel method for constrained mechanical design optimization problems," *Computer-Aided Design*, vol. 43, no. 3, pp. 303-315, 2011.

[165]. S. Sultana and P. K. Roy "Krill herd algorithm for optimal location of distributed generator in radial distribution system," *Appl. Soft Comput.*,

vol. 40, pp. 391-404, Mar. 2016.

[166]. A. El-Fergany “Optimal allocation of multi-type distributed generators using backtracking search optimization algorithm,” *Int. J. Elect. Power Energy Syst.*, vol. 64, pp. 1197-1205, Jan. 2015.

[167]. J. J. Liang et al. “Problem definitions and evaluation criteria for the CEC 2006 special Session on constrained real-parameter optimization,” *Technical Report*, Sept. 2006.

[168]. D. Karaboga, and B. Akay, “A comparative study of artificial bee colony algorithm,” *Applied Mathes. Comput.*, vol. 214, no. 1, pp. 108-132, 2009.

[169]. J. Vesterstrom and R. Thomsen, A comparative study of differential evolution particle swarm optimization and evolutionary algorithms on numerical benchmark problems, *IEEE Cong. Evolu. Comp.*, vol. 3, pp. 1980-1987, June 2004.

[170]. J. H. Teng and C. Y. Chang, "Backward/Forward Sweep-Based Harmonic Analysis Method for Distribution Systems," *IEEE Trans. Power Del.*, vol. 22, no. 3, pp. 1665-1672, July 2007.

[171]. H. R. Esmaeilian and R. Fadaeinedjad, “Distribution system efficiency improvement using network reconfiguration and capacitor allocation,” *Int. J. Elect. Power Energy Syst.*, vol. 64, pp. 457-68, Jan. 2015.

[172]. EPRI. (2013). Open Distribution System Simulator. Available: http://sourceforge.net/projects/electricdss/.

[173]. Distribution test feeders – distribution test feeder working group – IEEE PES distribution system analysis subcommittee. Available: http://ewh.ieee.org/soc/pes/dsacom/testfeeders/ [accessed: 09-Apr-2014].

PUBLICATIONS FROM THE WORK

Based on the research carried out, following papers have been published /submitted for publications in various journals and conferences:

a) <u>International Journals–Published:</u>

1. Manoj Kumawat, N. Gupta, N. Jain and R. C. Bansal, "Swarm-intelligence-based Optimal Planning of Distributed Generators in Distribution Network for Minimizing Energy Loss," *Electric Power Components and Systems*, vol. 45, no. 6, pp. 589–600, 2017. (Taylor & Francis, Impact Factor: 1.220) DOI: https://doi.org/10.1080/15325008.2017.1290713.

2. M. Kumawat, N. Gupta, N. Jain and R.C. Bansal, "Optimal planning of distributed energy resources in harmonics polluted distribution system," *Swarm and Evolutionary Computation*, vol. 39, pp. 99-113, 2018. (Elsevier, Impact Factor: 3.893) DOI: https://doi.org/10.1016/j.swevo.2017.09.005.

b) <u>International Conferences–Published:</u>

3. Manoj Kumawat, N. Gupta, N. Jain and R. C. Bansal, "Optimally Allocation of Distributed Generators in Three-phase Unbalanced Distribution Network, *in Proc. of 9th Int. Conf. on Applied Energy, ICAE2017 on Cardiff, United Kingdom*, pp. 749-754, August 21-24, 2017.

4. M. Kumawat, N. Gupta and N. Jain, "Analyzing the impacts of optimally allocated distributed energy resources on harmonics in radial distribution networks," *in Proc. of IEEE Int. Conf. National Power Systems Conference, Bhubaneswar*, pp. 1-6, 2016.

5. Manoj Kumawat, N. Gupta, N. Jain and D. Saxena, "Optimal Distributed Generation Placement in Power Distributed Networks: A review," *2015 in Proc. Int. Conf. on Electrical, Electronics, Signals, Communication and Optimization (EESCO), GEC Visakhapatnam*, pp. 1-6, February 24-25, 2015.

c) <u>International Journals–Under Review:</u>

6. Manoj Kumawat, N. Gupta, N. Jain and R. C. Bansal, "Jaya Algorithm Based Optimal Allocation of Distributed Energy Resources," *International Review of Electrical Engineering*.

Appendix A

The line impedance and load data of the standard radial distribution test system are given in the appendix.

A.1. Practical 16-Bus Radial Distribution Test System

The 16-bus system is small section of the practical 83-bus distribution system of Taiwan Power Company which is used in the chapter 3.

Table A.1: Load data of the 16-bus distribution system

Node	Capacitors (kVAr)	System demand	
		Active power (kW)	Reactive power (kVAr)
1	0	0	0
2	0	0	0
3	0	0	0
4	0	2000	1600
5	1100	3000	1500
6	1200	2000	800
7	0	1500	1200
8	0	4000	2700
9	1200	5000	3000
10	0	1000	900
11	600	600	100
12	3700	4500	2000
13	0	1000	900
14	1800	1000	700
15	0	1000	900
16	1800	2100	1000

Table A.2: Line data of the 16-bus distribution system

Branch	Sending Node	Receiving Node	Branch resistance (Ω)	Branch Impedance (Ω)	Ampacity (A)
1	1	2	0.0000	0.0000	0
2	1	3	0.0000	0.0000	0
3	1	4	0.3946	0.3946	500
4	4	5	0.4232	0.5819	250
5	4	6	0.4761	0.9522	250
6	6	7	0.2116	0.2486	250
7	2	8	0.5819	0.5819	500
8	8	9	0.4232	0.5819	250
9	8	10	0.5819	0.5819	250
10	9	11	0.5819	0.5819	250
11	9	12	0.4232	0.5819	250
12	3	13	0.5819	0.5819	500
13	13	14	0.4761	0.6348	250
14	13	15	0.4232	0.5819	250
15	15	16	0.2116	0.2116	250

A.2. Standard 33-Bus Radial Distribution Test System

This test distribution system and its data are referred from [48]. The nominal active and reactive loadings are 3,715 kW and 2,300 kVAr, respectively.

Table A.3: Load data of the 33-bus distribution system

Node	System demand		Node	System demand	
	Active power (kW)	Reactive power (kVAr)		Active power (kW)	Reactive power (kVAr)
1	0	0	**18**	90	40
2	100	60	**19**	90	40
3	90	40	**20**	90	40
4	120	80	**21**	90	40
5	60	30	**22**	90	40
6	60	20	**23**	90	50
7	200	100	**24**	420	200
8	200	100	**25**	420	200
9	60	20	**26**	60	25
10	60	20	**27**	60	25
11	45	30	**28**	60	20
12	60	35	**29**	120	70
13	60	35	**30**	200	600
14	120	80	**31**	150	70
15	60	10	**32**	210	100
16	60	20	**33**	60	40
17	60	20			

Table A.4: Line data of the 33-bus distribution system

Branch	Sending Node	Receiving Node	Branch resistance (Ω)	Branch Impedance (Ω)	Ampacity (A)
1	1	2	0.0922	0.0470	400
2	2	3	0.4930	0.2510	400
3	3	4	0.3661	0.1864	250
4	4	5	0.3811	0.1941	250
5	5	6	0.8190	0.7070	250
6	6	7	0.1872	0.6188	150
7	7	8	1.7117	1.2357	150
8	8	9	1.0299	0.7400	150
9	9	10	1.0440	0.7400	150
10	10	11	0.1967	0.0651	150
11	11	12	0.3744	0.1237	150
12	12	13	1.4680	1.1549	150
13	13	14	0.5416	0.7129	150
14	14	15	0.5909	0.5260	150
15	15	16	0.7462	0.5449	150
16	16	17	1.2889	1.7210	150
17	17	18	0.7320	0.5739	150
18	2	19	0.1640	0.1564	150
19	19	20	1.5042	1.3555	250
20	20	21	0.4095	0.4784	250

Table A.4: Line data of the 33-bus distribution system (Continued…)

Branch	Sending Node	Receiving Node	Branch resistance (Ω)	Branch Impedance (Ω)	Ampacity (A)
21	21	22	0.7089	0.9373	250
22	3	23	0.4512	0.3084	150
23	23	24	0.8980	0.7091	250
24	24	25	0.8959	0.7010	250
25	6	26	0.2031	0.1034	250
26	26	27	0.2842	0.1447	250
27	27	28	1.0589	0.9338	250
28	28	29	0.8043	0.7006	250
29	29	30	0.5074	0.2585	250
30	30	31	0.9745	0.9629	250
31	31	32	0.3105	0.3619	150
32	32	33	0.3411	0.5302	150

A.3. Standard 69-Bus Radial Distribution Test System

This test distribution system and its data are referred from [48]. The nominal active and reactive loadings are 3.8 MW and 2.69 MVAr, respectively.

Table A.5: Load data of the 69-bus distribution system

Node	System demand		Node	System demand	
	Active power (kW)	Reactive power (kVAr)		Active power (kW)	Reactive power (kVAr)
1	0	0	**26**	14	10
2	0	0	**27**	14	10
3	0	0	**28**	26	19
4	0	0	**29**	26	19
5	0	0	**30**	0	0
6	3	2	**31**	0	0
7	40	30	**32**	0	0
8	75	54	**33**	14	10
9	30	22	**34**	20	14
10	28	19	**35**	6	4
11	145	104	**36**	26	19
12	145	104	**37**	26	19
13	8	6	**38**	0	0
14	8	6	**39**	24	17
15	0	0	**40**	24	17
16	46	30	**41**	1	1
17	60	35	**42**	0	0
18	60	35	**43**	6	4
19	0	0	**44**	0	0
20	1	1	**45**	39	26
21	114	81	**46**	39	26
22	5	4	**47**	0	0
23	0	0	**48**	79	56
24	28	20	**49**	385	275
25	0	0	**50**	384	275

Table A.5: Load data of the 69-bus distribution system (Continued…)

Node	System demand		Node	System demand	
	Active power (kW)	Reactive power (kVAr)		Active power (kW)	Reactive power (kVAr)
51	41	28	**61**	1244	888
52	4	3	**62**	32	23
53	4	4	**63**	0	0
54	26	19	**64**	227	162
55	24	17	**65**	59	42
56	0	0	**66**	18	13
57	0	0	**67**	18	13
58	0	0	**68**	28	20
59	100	72	**69**	28	20
60	0	0			

Table A.6: Line data of the 69-bus distribution system

Branch	Sending Node	Receiving Node	Branch resistance (Ω)	Branch Impedance (Ω)	Ampacity (A)
1	1	2	0.0005	0.0012	400
2	2	3	0.0005	0.0012	400
3	3	4	0.0015	0.0036	400
4	4	5	0.0251	0.0294	400
5	5	6	0.366	0.1864	400
6	6	7	0.3811	0.1941	400
7	7	8	0.0922	0.047	400
8	8	9	0.0493	0.0251	400
9	9	10	0.819	0.2707	400
10	10	11	0.1872	0.0691	200
11	11	12	0.7114	0.2351	200
12	12	13	1.03	0.34	200
13	13	14	1.044	0.345	200
14	14	15	1.058	0.3496	200
15	15	16	0.1966	0.065	200
16	16	17	0.3744	0.1238	200
17	17	18	0.0047	0.0016	200
18	18	19	0.3276	0.1083	200
19	19	20	0.2106	0.069	200
20	20	21	0.3416	0.1129	200
21	21	22	0.014	0.0046	200
22	22	23	0.1591	0.0526	200
23	23	24	0.3463	0.1145	200
24	24	25	0.7488	0.2745	200
25	25	26	0.3089	0.1021	200
26	26	27	0.1732	0.0572	200
27	3	28	0.0044	0.0108	200
28	28	29	0.064	0.1565	200
29	29	30	0.3978	0.1315	200
30	30	31	0.0702	0.0232	200
31	31	32	0.351	0.116	200
32	32	33	0.839	0.2816	200

Table A.6: Line data of the 69-bus distribution system (Continued…)

Branch	Sending Node	Receiving Node	Branch resistance (Ω)	Branch Impedance (Ω)	Ampacity (A)
33	33	34	1.708	0.5646	200
34	34	35	1.474	0.4673	200
35	3	36	0.0044	0.0108	200
36	36	37	0.064	0.1565	200
37	37	38	0.1053	0.123	200
38	38	39	0.0304	0.0355	200
39	39	40	0.0018	0.0021	200
40	40	41	0.7283	0.8509	200
41	41	42	0.31	0.3623	200
42	42	43	0.041	0.0478	200
43	43	44	0.0092	0.0116	200
44	44	45	0.1089	0.1373	200
45	45	46	0.0009	0.0012	200
46	4	47	0.0034	0.0084	300
47	47	48	0.0851	0.2083	300
48	48	49	0.2898	0.7091	300
49	49	50	0.0822	0.2011	300
50	8	51	0.0928	0.0473	300
51	51	52	0.3319	0.1114	200
52	9	53	0.174	0.0886	200
53	53	54	0.203	0.1034	300
54	54	55	0.2842	0.1447	300
55	55	56	0.2813	0.1433	300
56	56	57	1.59	0.5337	300
57	57	58	0.7837	0.263	300
58	58	59	0.3042	0.1006	300
59	59	60	0.3861	0.1172	300
60	60	61	0.5075	0.2585	300
61	61	62	0.0974	0.0496	300
62	62	63	0.145	0.0738	300
63	63	64	0.7105	0.3619	300
64	64	65	1.041	0.5302	300
65	11	66	0.2012	0.0611	300
66	66	67	0.0047	0.0014	200
67	12	68	0.7394	0.2444	200
68	68	69	0.0047	0.0016	200

A.4. Practical 83-Bus Taiwan Distribution Test System

An actual 11.4 kV practical radial distribution network is practical system of the Taiwan Power Company. The system contains 11 feeders with 35.10 MVA (total peak demand) and 0.8076 average power factors (lagging).

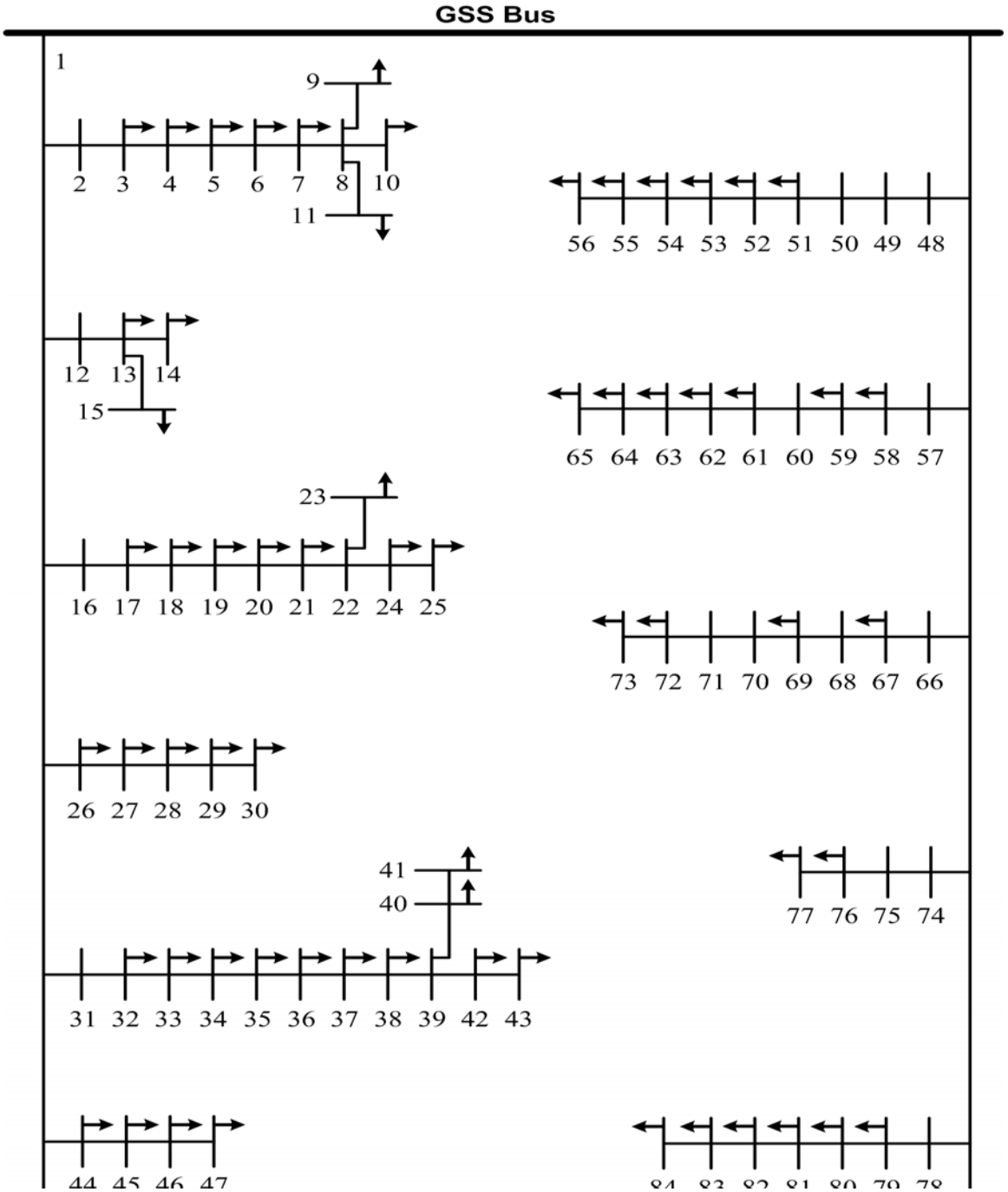

Figure A.1: 83-bus radial distribution system

Table A.7: Load data of the 83-bus distribution system

Node	System demand		Node	System demand	
	Active power (kW)	Reactive power (kVAr)		Active power (kW)	Reactive power (kVAr)
1	0	0	43	50	30
2	0	0	44	0	0
3	100	50	45	30	20
4	300	200	46	800	700

5	350	250	47	200	150
6	220	100	48	0	0
7	1100	800	49	0	0
8	400	320	50	0	0
9	300	200	51	200	160
10	300	230	52	800	600
11	300	260	53	500	300
12	0	0	54	500	350
13	1200	800	55	500	300
14	800	600	56	200	80
15	700	500	57	0	0
16	0	0	58	30	20
17	300	150	59	600	420
18	500	350	60	0	0
19	700	400	61	20	10
20	1200	1000	62	20	10
21	300	300	63	200	130
22	400	350	64	300	240
23	50	20	65	300	200
24	50	20	66	0	0
25	50	10	67	50	30
26	50	30	68	0	0
27	100	60	69	400	360
28	100	70	70	0	0
29	1800	1300	71	0	0
30	200	120	72	2000	1500
31	0	0	73	200	150
32	1800	1600	74	0	0
33	200	150	75	0	0
34	200	100	76	1200	950
35	800	600	77	300	180
36	100	60	78	0	0
37	100	60	79	400	360
38	20	10	80	2000	1300
39	20	10	81	200	140
40	20	10	82	500	360
41	20	10	83	100	30
42	200	160	84	400	360

Table A.8: Line data of the 83-bus distribution system

Branch	**Sending Node**	**Receiving Node**	**Branch resistance (Ω)**	**Branch Impedance (Ω)**	**Ampacity (A)**
1	1	2	0.1944	0.6624	500
2	2	3	0.2096	0.4304	500
3	3	4	0.2358	0.4842	500
4	4	5	0.0917	0.1883	500
5	5	6	0.2096	0.4304	500
6	6	7	0.0393	0.0807	500
7	7	8	0.0405	0.138	250
8	8	9	0.1048	0.2152	250
9	8	10	0.2358	0.4842	250

10	8	11	0.1048	0.2152	250
11	1	12	0.0786	0.1614	500
12	12	13	0.3406	0.6944	500
13	13	14	0.0262	0.0538	250
14	13	15	0.0786	0.1614	250
15	1	16	0.1134	0.3864	500
16	16	17	0.0524	0.1076	500
17	17	18	0.0524	0.1076	500
18	18	19	0.1572	0.3228	500
19	19	20	0.0393	0.0807	500
20	20	21	0.1703	0.3497	250
21	21	22	0.2358	0.4842	250
22	22	23	0.1572	0.3228	250
23	22	24	0.1965	0.4035	250
24	24	25	0.131	0.269	250
25	1	26	0.0567	0.1932	500
26	26	27	0.1048	0.2152	500
27	27	28	0.2489	0.5111	500
28	28	29	0.0486	0.1656	500
29	29	30	0.131	0.269	250
30	1	31	0.1965	0.396	500
31	31	32	0.131	0.269	500
32	32	33	0.131	0.269	250
33	33	34	0.0262	0.0538	250
34	34	35	0.1703	0.3497	250
35	35	36	0.0524	0.1076	250
36	36	37	0.4978	1.0222	250
37	37	38	0.0393	0.0807	250
38	38	39	0.0393	0.0807	250
39	1	2	0.1944	0.6624	500
40	2	3	0.2096	0.4304	500
41	3	4	0.2358	0.4842	500
42	4	5	0.0917	0.1883	500
43	5	6	0.2096	0.4304	500
44	6	7	0.0393	0.0807	500
45	7	8	0.0405	0.138	250
46	46	47	0.2358	0.4842	250
47	1	48	0.243	0.828	500
48	48	49	0.0655	0.1345	500
49	49	50	0.0655	0.1345	500
50	50	51	0.0393	0.0807	500
51	51	52	0.0786	0.1614	500
52	52	53	0.0393	0.0807	500
53	53	54	0.0786	0.1614	250
54	54	55	0.0524	0.1076	250
55	55	56	0.131	0.269	250
56	1	57	0.2268	0.7728	500
57	57	58	0.5371	1.1029	500
58	58	59	0.0524	0.1076	500
59	59	60	0.0405	0.138	250
60	60	61	0.0393	0.0807	250
61	61	62	0.0262	0.0538	250

Table A.8 Line data of the 83-bus distribution system (Continued…)

Branch	Sending Node	Receiving Node	Branch resistance (Ω)	Branch Impedance (Ω)	Ampacity (A)
62	62	63	0.1048	0.2152	250
63	63	64	0.2358	0.4842	250
64	64	65	0.0243	0.0828	250
65	1	66	0.0486	0.1656	500
66	66	67	0.1703	0.3497	500
67	67	68	0.1215	0.414	500
68	68	69	0.2187	0.7452	500
69	69	70	0.0486	0.1656	500
70	70	71	0.0729	0.2484	500
71	71	72	0.0567	0.1932	500
72	72	73	0.0262	0.0528	250
73	1	74	0.324	1.104	500
74	74	75	0.0324	0.1104	500
75	75	76	0.0567	0.1932	500
76	76	77	0.0486	0.1656	250
77	1	78	0.2511	0.8556	500
78	78	79	0.1296	0.4416	500
79	79	80	0.0486	0.1656	500
80	80	81	0.131	0.264	250
81	81	82	0.131	0.264	250
82	82	83	0.0917	0.1883	250
83	83	84	0.3144	0.6456	250

Appendix B

The line impedance, three types of load data, configurations of the overhead lines and underground cables of the practical radial three-phase distribution test system are given in the appendix.. IEEE distribution test feeder working group sub-committee of distribution system analysis committee has been developed (13-bus and 123-bus distribution system) and formulate (37-bus actual feeder in California) distribution test network which is provide the data to analysis the practical condition of the distribution system.

B.1. IEEE 13-Bus Radial Distribution Test System

The IEEE 13-bus system is a small unbalanced distribution system.

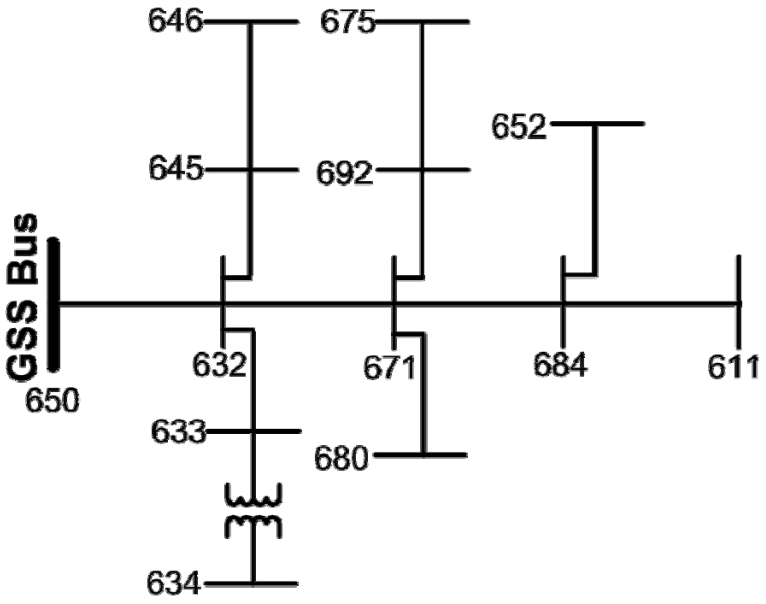

Figure B.1: 13-bus radial distribution system

Table B.1: Line segment data of IEEE 13-bus distribution system

Sending Node	Receiving Node	Length (ft.)	Configuration
632	645	500	603
632	633	500	602
633	634	0	XFM-1
645	646	300	603
650	632	2000	601
684	652	800	607
632	671	2000	601
671	684	300	604
671	680	1000	601
671	675	500	606
684	611	300	605

Table B.2: Overhead line configuration data of IEEE 13-bus distribution system

Configuration	Phasing	Phase ACSR	Neutral ACSR	Spacing ID
601	Y R B N	556,500 26/7	4/0 6/1	500
602	B R Y N	4/0 6/1	4/0 6/1	500
603	B Y N	1/0	1/0	505
604	R B N	1/0	1/0	505
605	B N	1/0	1/0	510

Table B.3: Underground line configuration data of IEEE 13-bus distribution system

Configuration	Phasing	Cable	Neutral	Spacing ID
606	R Y B N	250,000 RR, BN	None	515
607	R N	1/0 RR, TS	1/0 Cu	520

Table B.4: Capacitor data of IEEE 13-bus distribution system

Node	Phase		
	R (kVAr)	Y (kVAr)	B (kVAr)
675	200	200	200
611			100
Total	200	200	300

Table B.5: Spot load data of IEEE 13-bus distribution system

Node	Load Model	Phase-R		Phase-Y		Phase-B	
		kW	kVAr	kW	kVAr	kW	kVAr
634	Wye-PQ	160	110	120	90	120	90
645	Wye-PQ	0	0	170	125	0	0
646	Delta-Z	0	0	230	132	0	0
652	Wye-Z	128	86	0	0	0	0
671	Delta-PQ	385	220	385	220	385	220
675	Wye-PQ	485	190	68	60	290	212
692	Delta-I	0	0	0	0	170	151
611	Wye-I	0	0	0	0	170	80

Table B.6: Distributed load data of IEEE 13-bus distribution system

Node	Load Model	Phase-R		Phase-Y		Phase-B	
		kW	kVAr	kW	kVAr	kW	kVAr
632-671	Wye-PQ	17	10	66	38	117	68

Table B.7: Transformer data of IEEE 13-bus distribution system

Transformer position	Power Rating (kVA)	Voltage Rating & Connection type		Resistance (%)	Reactance (%)
		High Voltage side (kV)	Low Voltage side (kV)		
Substation	5000	115 Delta	4.16 Ground-Wye	1	8
Line	500	4.16 Ground-Wye	0.48 Ground-Wye	1.1	2

B.2. IEEE 123-Bus Radial Distribution Test System

The 123-bus system is a large unbalanced distribution system.

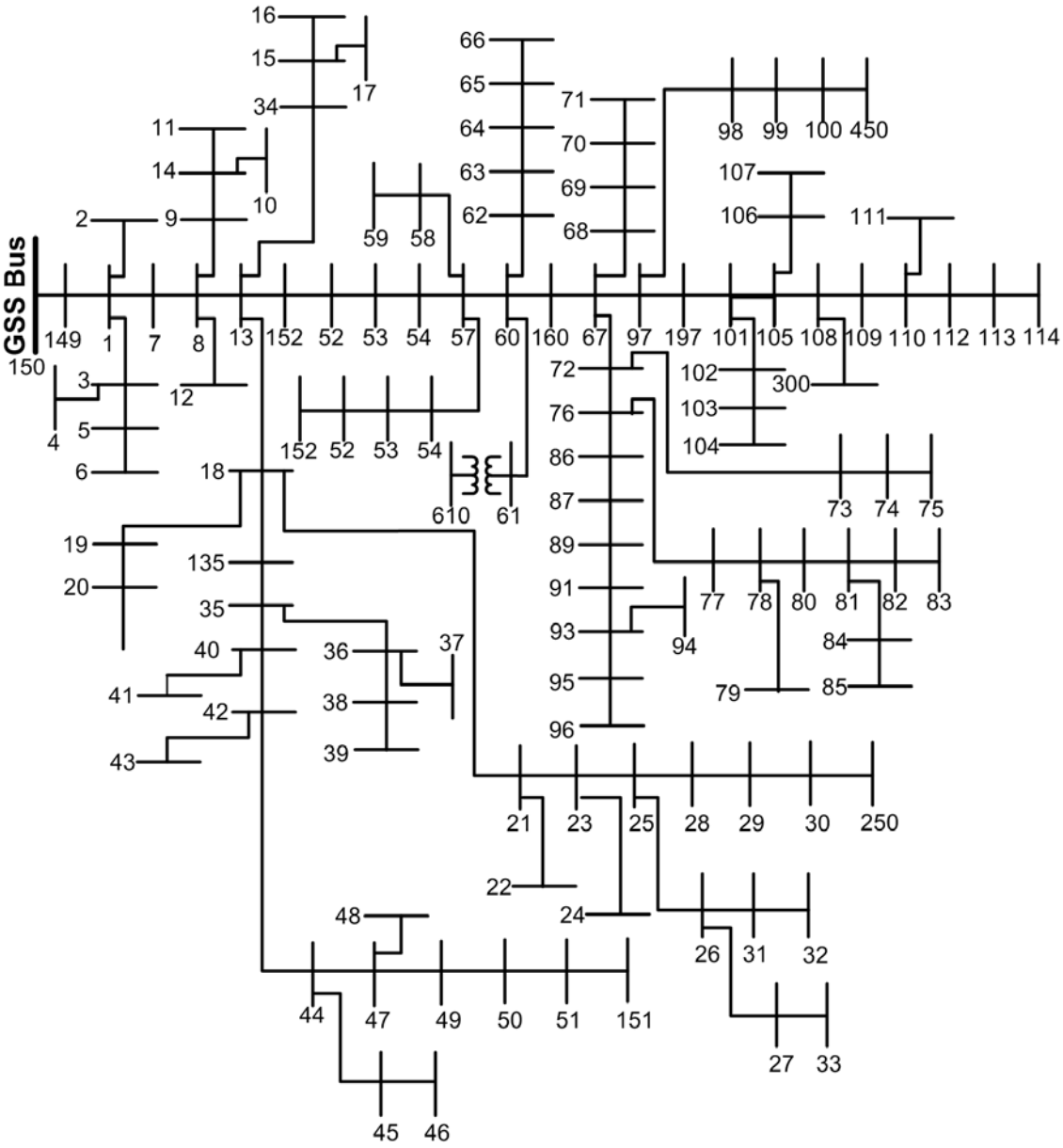

Figure B.2 123-bus radial distribution system

Table B.8: Transformer data of IEEE 123-bus distribution system

Transformer position	Power Rating (kVA)	Voltage Rating & Connection type		Resistance (%)	Reactance (%)
		High Voltage side (kV)	Low Voltage side (kV)		
Substation	5000	115 Delta	4.16 Ground-Wye	1	8
Line	150	4.16 Delta	0.48 Delta	1.27	2.72

Table B.9: Line segment data of IEEE 123-bus distribution system

Sending Node	Receiving Node	Length (ft.)	Configuration
1	2	175	10
1	3	250	11
1	7	300	1
3	4	200	11
3	5	325	11
5	6	250	11
7	8	200	1
8	12	225	10
8	9	225	9
8	13	300	1
9	14	425	9
13	34	150	11
13	18	825	2
14	11	250	9
14	10	250	9
15	16	375	11
15	17	350	11
18	19	250	9
18	21	300	2
19	20	325	9
21	22	525	10
21	23	250	2
23	24	550	11
23	25	275	2
25	26	350	7
25	28	200	2
26	27	275	7
26	31	225	11
27	33	500	9
28	29	300	2
29	30	350	2
30	250	200	2
31	32	300	11
34	15	100	11
35	36	650	8
35	40	250	1
36	37	300	9
36	38	250	10
38	39	325	10
40	41	325	11
40	42	250	1
42	43	500	10
42	44	200	1
44	45	200	9
44	47	250	1
45	46	300	9

Table B.9: Line segment data (continued…)

Sending Node	Receiving Node	Length (ft.)	Configuration
47	48	150	4
47	49	250	4
49	50	250	4
50	51	250	4
52	53	200	1
53	54	125	1
54	55	275	1
54	57	350	3
55	56	275	1
57	58	250	10
57	60	750	3
58	59	250	10
60	61	550	5
60	62	250	12
62	63	175	12
63	64	350	12
64	65	425	12
65	66	325	12
67	68	200	9
67	72	275	3
67	97	250	3
68	69	275	9
69	70	325	9
70	71	275	9
72	73	275	11
72	76	200	3
73	74	350	11
74	75	400	11
76	77	400	6
76	86	700	3
77	78	100	6
78	79	225	6
78	80	475	6
80	81	475	6
81	82	250	6
81	84	675	11
82	83	250	6
84	85	475	11
86	87	450	6
87	88	175	9
87	89	275	6
89	90	225	10
89	91	225	6
91	92	300	11
91	93	225	6

Table B.9: Line segment data (continued…)

Sending Node	Receiving Node	Length (ft.)	Configuration
93	94	275	9
93	95	300	6
95	96	200	10
97	98	275	3
98	99	550	3
99	100	300	3
100	450	800	3
101	102	225	11
101	105	275	3
102	103	325	11
103	104	700	11
105	106	225	10
105	108	325	3
106	107	575	10
108	109	450	9
108	300	1000	3
109	110	300	9
110	111	575	9
110	112	125	9
112	113	525	9
113	114	325	9
135	35	375	4
149	1	400	1
152	52	400	1
160	67	350	6
197	101	250	3
95	96	200	10
97	98	275	3
98	99	550	3
99	100	300	3
100	450	800	3
101	102	225	11
101	105	275	3
102	103	325	11
103	104	700	11
105	106	225	10
105	108	325	3
106	107	575	10
108	109	450	9
108	300	1000	3
109	110	300	9
110	111	575	9
110	112	125	9
112	113	525	9
113	114	325	9

Table B.9: Line segment data (continued…)

Sending Node	Receiving Node	Length (ft.)	Configuration
135	35	375	4
149	1	400	1
152	52	400	1
160	67	350	6
197	101	250	3

Table B.10: Overhead line configuration data of IEEE 123-bus distribution system

Configuration	Phasing	Phase ACSR	Neutral ACSR	Spacing ID
1	R Y B N	336,400 26/7	4/0 6/1	500
2	B R Y N	336,400 26/7	4/0 6/1	500
3	Y B R N	336,400 26/7	4/0 6/1	500
4	B Y R N	336,400 26/7	4/0 6/1	500
5	Y R B N	336,400 26/7	4/0 6/1	500
6	R B Y N	336,400 26/7	4/0 6/1	500
7	R B N	336,400 26/7	4/0 6/1	505
8	R Y N	336,400 26/7	4/0 6/1	505
9	R N	1/0	1/0	510
10	Y N	1/0	1/0	510
11	B N	1/0	1/0	510

Table B.11: Capacitor data of IEEE 123-bus distribution system

Node	Phasing		
	R (kVAr)	Y (kVAr)	B(kVAr)
83	200	200	200
88	50	-	-
90	-	50	-
92	-	-	50
Total	**250**	**250**	**250**

Table B.12: Underground line configuration data of IEEE 123-bus distribution system

Configuration	Phasing	Cable	Neutral	Spacing ID
12	R Y B	1/0 RR, BN	515	12

Table B.13: Spot load data of IEEE 123-bus distribution system

Node	Load Model	Phase-R		Phase-Y		Phase-B	
		kW	kVAr	kW	kVAr	kW	kVAr
1	Wye-PQ	40	20	0	0	0	0
2	Wye -PQ	0	0	20	10	0	0
4	Wye -PQ	0	0	0	0	40	20
5	Wye -I	0	0	0	0	20	10
6	Wye -Z	0	0	0	0	40	20
7	Wye -PQ	20	10	0	0	0	0
9	Wye -PQ	40	20	0	0	0	0
10	Wye -I	20	10	0	0	0	0
11	Wye -Z	40	20	0	0	0	0
12	Wye -PQ	0	0	20	10	0	0

Table B.13 Spot load data (continued…)

Node	Load Model	Phase-R		Phase-Y		Phase-B	
		kW	kVAr	kW	kVAr	kW	kVAr
16	Wye -PQ	0	0	0	0	40	20
17	Wye -PQ	0	0	0	0	20	10
19	Wye -PQ	40	20	0	0	0	0
20	Wye -I	40	20	0	0	0	0
22	Wye -Z	0	0	40	20	0	0
24	Wye -PQ	0	0	0	0	40	20
28	Wye -I	40	20	0	0	0	0
29	Wye -Z	40	20	0	0	0	0
30	Wye -PQ	0	0	0	0	40	20
31	Wye -PQ	0	0	0	0	20	10
32	Wye -PQ	0	0	0	0	20	10
33	Wye -I	40	20	0	0	0	0
34	Wye -Z	0	0	0	0	40	20
35	Wye -PQ	40	20	0	0	0	0
37	Wye -Z	40	20	0	0	0	0
38	Wye -I	0	0	20	10	0	0
39	Wye -PQ	0	0	20	10	0	0
41	Wye -PQ	0	0	0	0	20	10
42	Wye -PQ	20	10	0	0	0	0
43	Wye -Z	0	0	40	20	0	0
45	Wye -I	20	10	0	0	0	0
46	Wye -PQ	20	10	0	0	0	0
47	Wye -I	35	25	35	25	35	25
48	Wye -Z	70	50	70	50	70	50
49	Wye -PQ	35	25	70	50	35	25
50	Wye -PQ	0	0	0	0	40	20
51	Wye -PQ	20	10	0	0	0	0
52	Wye -PQ	40	20	0	0	0	0
53	Wye -PQ	40	20	0	0	0	0
55	Wye -Z	20	10	0	0	0	0
56	Wye -PQ	0	0	20	10	0	0
58	Wye -I	0	0	20	10	0	0
59	Wye -PQ	0	0	20	10	0	0
60	Wye -PQ	20	10	0	0	0	0
62	Wye -Z	0	0	0	0	40	20
63	Wye -PQ	40	20	0	0	0	0
64	Wye -I	0	0	75	35	0	0
65	Delta-Z	35	25	35	25	70	50
66	Wye -PQ	0	0	0	0	75	35
68	Wye -PQ	20	10	0	0	0	0
69	Wye -PQ	40	20	0	0	0	0
70	Wye -PQ	20	10	0	0	0	0
71	Wye -PQ	40	20	0	0	0	0
73	Wye -PQ	0	0	0	0	40	20
74	Wye -Z	0	0	0	0	40	20
75	Wye -PQ	0	0	0	0	40	20
76	Delta-I	105	80	70	50	70	50
77	Wye -PQ	0	0	40	20	0	0
79	Wye -Z	40	20	0	0	0	0

Table B.13 Spot load data (continued…)

Node	Load Model	Phase-R		Phase-Y		Phase-B	
		kW	kVAr	kW	kVAr	kW	kVAr
80	Wye -PQ	0	0	40	20	0	0
82	Wye -PQ	40	20	0	0	0	0
83	Wye -PQ	0	0	0	0	20	10
84	Wye -PQ	0	0	0	0	20	10
85	Wye -PQ	0	0	0	0	40	20
86	Wye -PQ	0	0	20	10	0	0
87	Wye -PQ	0	0	40	20	0	0
88	Wye -PQ	40	20	0	0	0	0
90	Wye -I	0	0	40	20	0	0
92	Wye -PQ	0	0	0	0	40	20
94	Wye -PQ	40	20	0	0	0	0
95	Wye -PQ	0	0	20	10	0	0
96	Wye -PQ	0	0	20	10	0	0
98	Wye -PQ	40	20	0	0	0	0
99	Wye -PQ	0	0	40	20	0	0
100	Wye -Z	0	0	0	0	40	20
102	Wye -PQ	0	0	0	0	20	10
103	Wye -PQ	0	0	0	0	40	20
104	Wye -PQ	0	0	0	0	40	20
106	Wye -PQ	0	0	40	20	0	0
107	Wye -PQ	0	0	40	20	0	0
109	Wye -PQ	40	20	0	0	0	0
111	Wye -PQ	20	10	0	0	0	0
112	Wye -I	20	10	0	0	0	0
113	Wye -Z	40	20	0	0	0	0
114	Wye -PQ	20	10	0	0	0	0

B.3. IEEE 37-Bus Radial Distribution Test System

This system is actual distribution system which is located in California.

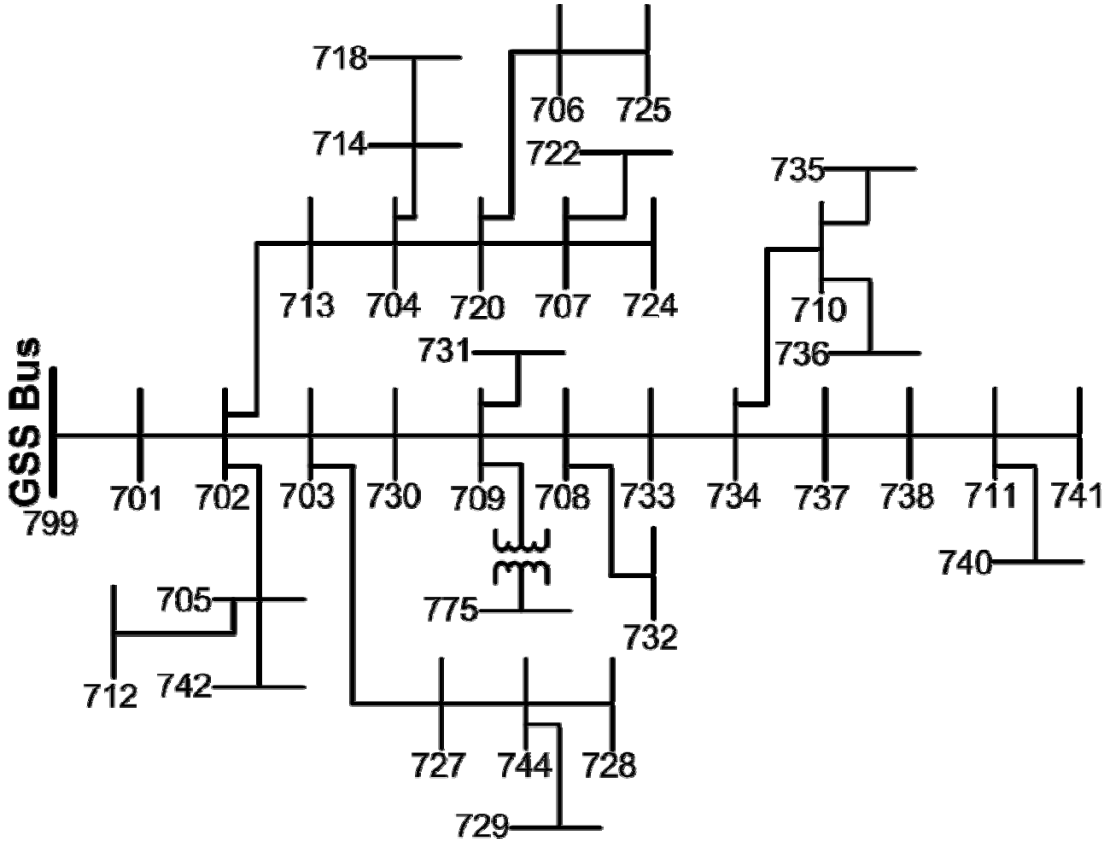

Figure B.3: 37-bus radial distribution system

Table B.14: Transformer data of IEEE 37-bus distribution system

Transformer position	Power Rating (kVA)	Voltage Rating & Connection type		Resistance (%)	Reactance (%)
		High Voltage side (kV)	Low Voltage side (kV)		
Substation	2500	230 Delta	4.8 Delta	2	8
Line	500	4.8 Delta	0.48 Delta	0.09	1.81

Table B.15: Underground line configuration data of IEEE 37-bus distribution system

Configuration	Phasing	Cable	Neutral	Spacing ID
721	R Y B	1,000,000 RR, BN	515	721
722	R Y B	500,000 RR,BN	515	722
723	R Y B	2/0 RR, BN	515	723
724	R Y B	#2 RR, BN	515	724

Table B.16 Line segment data of IEEE 37-bus distribution system

Sending Node	Receiving Node	Length (ft.)	Configuration
701	702	960	722
702	705	400	724
702	713	360	723
702	703	1320	722

Table B.16 Line segment data of IEEE 37-bus distribution system (continued…)

Sending Node	Receiving Node	Length (ft.)	Configuration
703	727	240	724
703	730	600	723
704	714	80	724
704	720	800	723
705	742	320	724
705	712	240	724
706	725	280	724
707	724	760	724
707	722	120	724
708	733	320	723
708	732	320	724
709	731	600	723
709	708	320	723
710	735	200	724
710	736	1280	724
711	741	400	723
711	740	200	724
713	704	520	723
714	718	520	724
720	707	920	724
720	706	600	723
727	744	280	723
730	709	200	723
733	734	560	723
734	737	640	723
734	710	520	724
737	738	400	723
738	711	400	723
744	728	200	724
744	729	280	724
775	709	0	XFM-1
799	701	1850	721

Table B.17: Spot load data of IEEE 37-bus distribution system

Node	Load Model	Phase-R		Phase-Y		Phase-B	
		kW	kVAr	kW	kVAr	kW	kVAr
701	Delta-PQ	140	70	140	70	350	175
712	Delta-PQ	0	0	0	0	85	40
713	Delta-PQ	0	0	0	0	85	40
714	Delta-I	17	8	21	10	0	0
718	Delta-Z	85	40	0	0	0	0
720	Delta-PQ	0	0	0	0	85	40
722	Delta-I	0	0	140	70	21	10
724	Delta-Z	0	0	42	21	0	0
725	Delta -PQ	0	0	42	21	0	0
727	Delta -PQ	0	0	0	0	42	21
728	Delta -PQ	42	21	42	21	42	21

Table B.17 Spot load data (continued…)

Node	Load Model	Phase-R		Phase-Y		Phase-B	
		kW	**kVAr**	**kW**	**kVAr**	**kW**	**kVAr**
729	Delta -I	42	21	0	0	0	0
730	Delta -Z	0	0	0	0	85	40
731	Delta -Z	0	0	85	40	0	0
732	Delta -PQ	0	0	0	0	42	21
733	Delta -I	85	40	0	0	0	0
734	Delta -PQ	0	0	0	0	42	21
735	Delta -PQ	0	0	0	0	85	40
736	Delta -Z	0	0	42	21	0	0
737	Delta -I	140	70	0	0	0	0
738	Delta -PQ	126	62	0	0	0	0
740	Delta -PQ	0	0	0	0	85	40
741	Delta -I	0	0	0	0	42	21
742	Delta -Z	8	4	85	40	0	0
744	Delta -PQ	42	21	0	0	0	0

Appendix C

The problem definition and evolution criteria of experienced constrained and unconstrained benchmark function are as:

C.1. Unconstrained Benchmark Function:

The summary of unconstrained problems are illustrated in following Table C.1

Table C.1 Summary of unconstrained benchmark function

S. No.	Function	Formulation	Evolution criteria
1.	Sphere	$\min(f)=\sum_{d_m=1}^{Dim} x_{d_m}^2$	[-100,100]
2.	Ackley	$\min(f)=-20\exp\left(-0.2\sqrt{\frac{1}{Dim}\sum_{d_m=1}^{Dim} x_{d_m}^2}\right)-\exp\left(\sqrt{\frac{1}{Dim}\sum_{d_m=1}^{Dim}\cos 2\pi x_{d_m}}\right)+20+e$	[-32, 32]
3.	Sum Squares	$\min(f)=\sum_{d_m=1}^{Dim} d_m x_{d_m}^2$	[-10,10]
4.	Beale	$\min(f)=\sum_{d_m=1}^{Dim}(1.5-x_1+x_1x_2)^2+(2.25-x_1+x_1x_2^2)^2+(2.625-x_1+x_1x_2^3)^2$	[-4.5, 4.5]
5.	Easom	$\min(f)=-\cos(x_1)\cos(x_2)\exp\left(-(x_1-\pi)^2-(x_2-\pi)^2\right)$	[-100, 100]
6.	Matyas	$\min(f)=0.26\left(x_1^2+x_2^2\right)-0.48x_1x_2$	[-10,10]
7.	Colville	$\min(f)=100\left(x_1^2-x_2\right)^2+(x_1-1)^2+(x_3-1)^2+90\left(x_3^2-x_4\right)+10.1\left((x_2-1)^2+(x_4-1)^2\right)-0.48x_1x_2+19.8(x_2-1)(x_4-1)$	[-10,10]
8.	Rosen-brock	$\min(f)=\sum_{d_m=1}^{Dim}[100(x_{d_m}^2-x_{d_m+1})^2+(1-x_{d_m})^2]$	[-30, 30]
9.	Schwefel 2.22	$\min(f)=\sum_{d_m=1}^{Dim}\left\|x_{d_m}\right\|+\prod_{d_m=1}^{Dim}\left\|x_{d_m}\right\|$	[-10, 10]
10.	Branin	$\min(f)=\left(x_2-\frac{5.1}{4\pi^2}x_1^2+\frac{5}{\pi}x_1-6\right)^2+10\left(1-\frac{1}{8\pi}\right)\cos x_1+10$	[-5,10], [0, 15]
11.	Booth	$\min(f)=\left(x_1-2x_2-7\right)^2+\left(2x_1+x_2-5\right)^2$	[-10, 10]
12.	Gold Stein-Price	$\min(f)=\left[1+(x_1+x_2+1)^2(19-14x_1+3x_1^2-14x_2+6x_1x_2+3x_2^2\right]\left[30+(2x_1-3x_2)^2(18-32x_1+12x_1^2+48x_2-36x_1x_2+27x_2^2)\right]$	[-2, 2]
13.	Griewank	$\min(f)=\frac{1}{4000}\sum_{d_m=1}^{Dim}x_{d_m}^2-\prod_{d_m=1}^{Dim}\cos\left(\frac{x_{d_m}}{\sqrt{d_m}}\right)+1$	[-600, 600]
14.	Rastrigin	$\min(f)=\sum_{d_m=1}^{Dim}\left[x_{d_m}^2-10\cos(2\pi x_{d_m})+10\right]$	[-5.12, 5.12]

15. Schwefel $\min(f) = -\sum_{d_m=1}^{Dim}\left(x_{d_m}\sin(\sqrt{|x_{d_m}|})\right)$ [-500, 500]

C.2. Constrained Benchmark Function:

The summary of experienced constrained problems is individually illustrated with their evolution criteria as follows:

C.2.1 Constrained Benchmark function 1(BF1):

The function formulation is:

$$\text{Minimize } f(\vec{x}) = 5\sum_{d_m=1}^{4} x_{d_m} - 5\sum_{d_m=1}^{4} x_{d_m}^2 - \sum_{d_m=5}^{13} x_{d_m}$$

Subjected to:

$$g1(\vec{x}) = 2x_1 + 2x_2 + x_{10} + x_{11} - 10 \le 0$$
$$g2(\vec{x}) = 2x_1 + 2x_3 + x_{10} + x_{12} - 10 \le 0$$
$$g3(\vec{x}) = 2x_2 + 2x_3 + x_{11} + x_{12} - 10 \le 0$$
$$g4(\vec{x}) = -8x_1 + x_{10} \le 0$$
$$g5(\vec{x}) = -8x_2 + x_{11} \le 0$$
$$g6(\vec{x}) = -8x_3 + x_{12} \le 0$$
$$g7(\vec{x}) = -2x_4 - x_5 + x_{10} \le 0$$
$$g8(\vec{x}) = -2x_6 - x_7 + x_{11} \le 0$$
$$g9(\vec{x}) = -2x_8 - x_9 + x_{12} \le 0$$

The evolution criteria are:

$$0 \le x_{d_m} \le 1 \qquad \forall d_m\,(d_m = 1, 2..., 9)$$
$$0 \le x_{d_m} \le 100 \qquad \forall d_m\,(d_m = 10, 11, 12)$$
$$0 \le x_{d_m} \le 1 \qquad \forall d_m\,(d_m = 13)$$

C.2.2 Constrained Benchmark function 2(BF2):

The function formulation is:

$$\text{Minimize } f(\vec{x}) = 5.3578547x_3^2 + 0.8356891x_1x_5 + 37.293239x_1 - 40792.141$$

Subjected to:

$$g1(\vec{x}) = 85.334407 + 0.0056858x_2x_5 + 0.0006262x_1x_4 - 0.0022053x_3x_5 - 92 \le 0$$
$$g2(\vec{x}) = -85.334407 - 0.0056858x_2x_5 - 0.0006262x_1x_4 + 0.0022053x_3x_5 \le 0$$
$$g3(\vec{x}) = 80.51249 + 0.0071317x_2x_5 + 0.0029955x_1x_2 + 0.0021813x_3^2 - 110 \le 0$$
$$g4(\vec{x}) = -80.51249 - 0.0071317x_2x_5 - 0.0029955x_1x_2 - 0.0021813x_3^2 + 90 \le 0$$
$$g5(\vec{x}) = 9.300961 + 0.0047026x_3x_5 + 0.0012547x_1x_3 + 0.0019085x_3x_4 - 25 \le 0$$
$$g6(\vec{x}) = -9.300961 - 0.0047026x_3x_5 - 0.0012547x_1x_3 - 0.0019085x_3x_4 + 20 \le 0$$

The evolution criteria are:

$78 \le x_{d_m} \le 102 \qquad (d_m = 1)$

$33 \le x_{d_m} \le 45 \qquad (d_m = 2)$

$27 \le x_{d_m} \le 45 \qquad \forall d_m (d_m = 3,4,5)$

C.2.3 Constrained Benchmark function 3(BF3):

The function formulation is:

$$\text{Minimize } f(\vec{x}) = (x_1 - 10)^3 + (x_2 - 20)^3$$

Subjected to:

$$g1(\vec{x}) = -(x_1 - 5)^2 - (x_2 - 5)^2 + 100 \le 0$$

$$g2(\vec{x}) = (x_1 - 6)^2 + (x_2 - 5)^2 - 82.81 \le 0$$

The evolution criteria are:

$13 \le x_{d_m} \le 100 \qquad (d_m = 1)$

$0 \le x_{d_m} \le 100 \qquad (d_m = 2)$

C.2.4 Constrained Benchmark function 4(BF4):

The function formulation is:

$$\text{Minimize } f(\vec{x}) = -\frac{\sin^3(2\pi x_1)\sin(2\pi x_2)}{x_1^3(x_1 + x_2)}$$

Subjected to:

$$g1(\vec{x}) = x_1^2 - x_2 + 1 \le 0$$

$$g2(\vec{x}) = 1 - x_1 + (x_2 - 4)^2 \le 0$$

The evolution criteria are:

$0 \le x_{d_m} \le 10 \qquad \forall d_m = 1,2$

C.2.5 Constrained Benchmark function 5(BF5):

The function formulation is:

$$\text{Minimize } f(\vec{x}) = -x_1 - x_2$$

Subjected to:

$$g1(\vec{x}) = -2x_1^4 + 8x_1^3 - 8x_1^2 + x_2 - 2 \le 0$$

$$g2(\vec{x}) = -4x_1^4 + 32x_1^3 - 88x_1^2 + 96x_1 + x_2 - 36 \le 0$$

The evolution criteria are:

$0 \le x_{d_m} \le 3 \qquad (d_m = 1)$

$0 \le x_{d_m} \le 4 \qquad (d_m = 2)$